THE INTERPLAY BETWEEN FIELD MEASUREMENTS AND SOIL BEHAVIOR FOR LEARNING SUPPORTED EXCAVATION RESPONSE

BY

ABDOLREZA OSOULI

DISSERTATION

Submitted in partial fulfillment of the requirements
for the degree of Doctor of Philosophy in Civil Engineering
in the Graduate College of the
University of Illinois at Urbana-Champaign, 2010

Urbana, Illinois

Doctoral Committee:

Associate Professor Youssef M.A. Hashash, Chair
Associate Professor James Long
Assistant Professor Scott Olson
Professor Jamshid Ghaboussi

ABSTRACT

In urban areas, estimation of ground movements due to excavation is critically important. In this thesis after a short review of currently used methods in practice for estimating excavation induced ground movements, a novel inverse analysis approach, self-learning in engineering simulation (SelfSim), is presented. SelfSim is applied to deep excavations in order to extract underlying soil behavior.

The performance of the SelfSim inverse analysis is compared to inverse analysis based on a genetic algorithm. In the SelfSim approach, soil behavior is extracted from in situ measurements without a pre-defined constitutive model. In the genetic algorithm approach, soil parameters of an existing constitutive model are identified using field measurements. The performance of both techniques in capturing soil displacements and in predicting of soil behavior associated with the Lurie Center excavation in Chicago is presented.

In order to demonstrate SelfSim's capabilities in learning soil behavior using different instrument measurements, a simulated deep excavation is analyzed. The quality of the extracted behavior is examined by deploying different instrument configurations. The instruments required to provide sufficient information for SelfSim to extract soil behavior are identified. Then, some of the findings are further demonstrated in a case study of an excavation in Taipei soft clays.

To illustrate that it is possible to learn from local experience and predict excavation performance in similar soil stratigraphy, case studies in Texas, Shanghai and Taipei are analyzed. The difficulties associated with the use of measured excavation response that is incompatible with recorded construction activity and the importance of engineering judgment in preparing measurement data for inverse analysis are highlighted.

Finally, it is shown that the 2D extracted soil behavior of excavation in Chicago clays can not provide a reasonable excavation performance for an elevated ground surface excavation in Chicago suburbs within similar soil stratigraphy. It is demonstrated that the 3D effects of excavation are captured via 3D modeling using SelfSim. At the end, the extracted soil behavior from 3D analysis is discussed and compared to extracted soil behavior from 2D analysis.

To my father, mother, sister and my

Lovely wife

ACKNOWLEDGEMENT

I would like to express my sincere gratitude and appreciation to Professor Youssef M.A. Hashash for his tremendous support and time spent with me in all past years. He has been tutoring, guiding, and encouraging me throughout my whole research. Working with Professor Hashash has been an intense and memorable learning experience both technically and personally.

I would like to extend my deep appreciation to the members of the committee: Professors Jamshid Ghaboussi, James H. Long, Scott M. Olson, for their interests and insightful advice in my research.

Special thanks are extended to all my colleagues whose thoughtful discussions contributed greatly to my education, especially Hwayeon Song, Dr. Sungmoon Jung, Dr. Camilo Marulanda, Yun-Yi Su, Dr. Tanner Blackburn, Dr. Severine Levasseur, Erfan Ghazi Nezami, Chi-Chin Tsai, Abouzar Sadrekarimi, and Nejan Huvaj. It is hard to imagine life without their friendship.

I owe the most to my lovely parents for their love, support, and understanding in the course of my Ph.D. studies. Thanks to my lovely sister, Elmira, for her continuous support.

I would especially like to thank my wife, Shadi Ansari, for her love, support, and understanding during this very demanding period of life. She has been and always will be an inspiration to me.

TABLE OF CONTENTS

CHAPTER 1 INTRODUCTION

There is a high demand for underground space in urban areas. In high density populated urban areas, there is a great concern for excessive movements induced by underground space. Therefore, it is critically important to estimate and control the magnitude and distribution of excavation-induced ground deformations.

In practice, both semi-empirical approaches (Peck 1969; Clough and O'Rourke 1990) and numerical modeling are used to estimate ground deformations due to excavation. Instruments often are installed to monitor and control the performance of excavations. If the observed performance of the excavation shows intolerable deformations changes in the design and construction procedure of excavation is made.

While engineers benefit from semi-empirical methods that are developed based on previous case studies, there is a gap between numerical modeling and learning from case histories. Constitutive models are the critical component of numerical modeling. In typical numerical modeling, an existing constitutive model for various soil and rock materials is used to represent each sublayer. These constitutive models have all been developed within the framework of nonlinear elasticity, plasticity, hypoelasticity etc. They require many model parameters that sometimes have no physical meaning. In many cases, determining these parameters requires complex laboratory tests that are not typically available in practice. Numerical models have generally been used for adjusting or calibrating soil parameters of conventional constitutive models. In most cases the calibrated material models were site-specific and could not capture material behavior within similar soil stratigraphy.

Therefore, due to difficulties associated with conventional constitutive models, a new approach for developing constitutive models and performing numerical modeling of deep excavations is used in this thesis. In this novel approach the soil constitutive model is extracted from field measurements that are the actual representation of stress-strain in an excavation.

Application of this approach is demonstrated for six case studies in this thesis. It is shown that how it is possible to incorporate numerical simulations as an integral component in the application of the observational method in geotechnical engineering.

This thesis is divided into four main topics that are discussed after a review of currently used methods for estimating excavation induced ground movements in practice and a review of development of "Self Learning in Engineering Simulations" (SelfSim): 1) comparison of two inverse analysis techniques for learning deep excavation response; 2) the interplay between field measurements and soil behavior for capturing supported excavation response; 3) case studies of prediction of excavation response using learned performance of excavations; and 4) two- and three-dimensional inverse analyses of deep excavations in Chicago clays.

1. *Comparison of two inverse analysis techniques for learning deep excavation response:* Chapter 3 describes and compares two inverse analysis approaches for an excavation project in downtown Chicago. The first approach is a parameter optimization approach based on a genetic algorithm. The second approach, self-learning in engineering simulations (SelfSim), is an inverse analysis technique that combines finite element method, continuously evolving material models, and field measurements. The optimization based on the genetic algorithm approach identifies material properties of an existing soil model, whereas the SelfSim approach extracts the underlying soil behavior unconstrained by specific assumptions of a soil constitutive model.

2. *The interplay between field measurements and soil behavior for capturing supported excavation response:* Chapter 4 demonstrates the integration of inverse analysis and instrument measurements. It is shown that how it is possible to provide information on excavation performance at locations where no instrumentation are available. In this study the relationship between various instruments typically used on an excavation project and the quality of information that can be extracted for excavation modeling is examined. A synthetically generated set of instrument measurements that include inclinometers, surface settlement points, extensometers, heave gages, piezometers and strain gauges, using an idealized soil profile are initially used. The findings are further demonstrated with a well-instrumented deep excavation case study in Taipei.

3. *Case studies of prediction of excavation response using learned performance of excavations:* Chapter 5 illustrates the performance of SelfSim inverse analysis approach, with a special focus on its ability to provide soil models based on field measurements that can predict other excavation performance in similar ground conditions

in Texas, Shanghai and Taipei. The difficulties associated with the use of measured excavation response that is incompatible with the recorded construction activity and the importance of engineering judgment in preparing measurement data for inverse analysis are discussed. In the Texas A&M full scale model wall, the limitations of inverse analysis in modeling the slippage of the wall and predicting settlements are demonstrated.

4. *Two- and three-dimensional inverse analyses of deep excavations in Chicago clays:* Chapter 6 demonstrates the performance of the extracted soil behavior using SelfSim, from 2D excavation simulation of Lurie Center in Chicago in predicting the excavation response in Ford Center excavation with similar soil stratigraphy. It is shown that due to an elevated ground surface around the Ford Center excavation site, 2D simulation can not provide a reasonable prediction of ground movements around the excavation. The numerical development required for 3D modeling of excavation using SelfSim inverse analysis is demonstrated. Then, SelfSim inverse analysis is conducted to extract the 3D behavior of Ford Center deep excavation from inclinometer measurements around the excavation. The extracted global response and soil behavior is discussed in detail.

CHAPTER 2 ESTIMATING EXCAVATION INDUCED GROUND MOVEMENTS

2.1. Introduction

In urban areas there is a continuing and increased demand for underground space. It is critically important to estimate and control the magnitude and distribution of ground movements that result from developing underground space. Since the excavation construction can influence surrounding structures, observational programs are commonly set up at an excavation site to evaluate the design assumptions, determine causes of movements, improve the construction procedure, determine the need for immediate repair, and evaluate the stability of the excavation. This thesis focuses on applying novel inverse analysis, SelfSim, in deep excavations and predicting soil movements in response to excavations.

In this chapter, Section 2.2 describes important factors needs to be considered in deep excavations. Section 2.3 summarizes related work to numerical modeling of deep excavations. Section 2.4 addresses the techniques used for deep excavation inverse analysis. Section 2.5 reviews the SelfSim inverse analysis framework. Section 2.6 explains the application of SelfSim into various geotechnical problems, and Section 2.7 discusses the outstanding issues about deep excavation.

2.2. Important design factors for deep excavations

Observational methods, introduced by Terzaghi and Peck (1948) and Peck (1969) are used in applied soil mechanics to monitor, control and learn soil behavior. Monitoring ground and support system response, recording construction activities, and learning from measured data to extract underlying soil behavior is an important component of this method. Consequently, the design of braced excavations is based for the most part on empirical procedures and precedent (Dunnicliff 1996).

Table 2-1 summarizes typical factors that influence the performance of an excavation. An adequate design has to ensure acceptable structural performance of the bracing system based on the maximum estimated forces. Section 2.2.1 describes various approaches used for stability calculations of deep excavations. Section 2.2.2 presents a

brief description of the more commonly adopted design recommendations for excavation supports. Soil displacements are generally the limiting component in design of urban excavations; therefore, predicting soil movements is usually a primary consideration. Section 2.2.3 summarizes various methods based on observed field behavior for predicting the magnitude and distribution of soil movements in response to excavation. These methods are only capable of giving approximate estimates of ground movement, and give limited insight into factors affecting their magnitude and distribution. More reliable site specific calculations can be achieved using non-linear finite element analyses that incorporate realistic constitutive models of soil behavior.

2.2.1. Stability

Limit equilibrium methods are widely used in design practice and include separate calculations of basal stability based on failure mechanisms proposed by Terzaghi (1943), and Bjerrum and Eide (1956) and overall system stability (Bishop 1955; Spencer 1967). The factor of safety against basal heave is important in estimating ground deformations of excavation and the support systems constructed in soft cohesive soils (Mana and Clough 1981). Hashash and Whittle (1996) summarized a number of alternative methods (Terzaghi 1943; Bjerrum and Eide 1956; Hashash and Whittle 1992; O'Rourke 1992) for determining the factor of safety against basal heave as provided in Table 2-2. They also compared results of parametric finite element analyses with the closed-form methods and concluded that the penetration depth of the support wall has a significant influence on the overall stability of the excavation and that failure of the soil is constrained by the presence of the wall unless structural failure of the wall occurs. It should be noted that this thesis does not deal with stability problems of deep excavations, but with pre-failure ground movements.

2.2.2. Earth pressures and support system

The support system for deep excavations consists of a retaining wall and wall supports. Sheetpiles and concrete diaphragm walls are two of the more commonly used support walls. The wall is either internally braced or anchored with tiebacks. Structural design focuses on ensuring that the support system can withstand the projected loads and can control movements within specified allowable limits.

Four important issues are often considered in the design of the support wall: (a) sufficient strength to resist estimated loads; (b) appropriate wall stiffness to limit bending and deformation; (c) appropriate embedment depth to guarantee stability; and (d) adequate embedment depth to control seepage into the excavation.

The selection of support stiffness and spacing generally relies on practical issues such as minimum spacing to accommodate construction activities. However there are design methods that recommend anticipated forces on the struts for controlling soil deformations or estimating projected loads. The most widely used method for estimating earth pressure for the design of lateral wall support is the empirical apparent earth pressure diagrams proposed by Peck (1969). These diagrams are based on field measurements of strut loads for excavations in various soil types supported by sheet piles and soldier piles and are referred to as apparent earth pressures. Figure 2-1 outlines apparent earth pressures diagrams suggested by Terzaghi et al. (1996) for excavations in both clay and sand. Despite their development based on measurements from strutted excavations, the apparent earth pressure envelopes have been widely used for estimating the earth pressure in both tieback and strutted excavations. Mueller et al. (1998) summarized the methods used for design of ground anchor walls. In general the choice of an appropriate earth pressure diagram for estimating loads for the wall support depends primarily on the tolerable wall and soil movement. Apparent earth pressures diagrams shown in Figure 2-1 are more appropriate for excavations supported using relatively flexible walls and, are not necessarily applicable to excavations using stiff walls (Hashash and Whittle 2002).

2.2.3. Ground movements

In dense populated urban environments, there is a great concern about excessive movement of the soil due to excavation. The design of the excavation support system must limit ground deformations within an allowable range. Therefore, it is critically important for both design engineers and contractors to estimate the magnitude and distribution of the ground movements caused by the excavation (Boscardin and Cording 1989). Since there is high risk of litigation over damages caused by excavation construction, the accurate estimation of ground movements is of primary concern in the design process of deep excavation in urban areas. Figure 2-2 illustrates general pattern of

ground movements' profiles as observed in typical excavations. In general, existing methods of predicting excavation performance are either based on empirical observations or numerical simulations. Empirical studies attempt to develop general relationships between observed ground movements and construction activities based on actual observations from a number of similar excavations.

Peck (1969) provided a framework for understanding the factors that control the performance of deep excavation supporting system. Peck (1969) compiled ground surface settlement data measured adjacent to temporary braced sheet pile and soldier pile walls with struts or tieback support, and summarized the data normalized by the excavation depth as shown in Figure 2-3. The figure defines three zones, each representing certain ground conditions. The data suggest that excavations within a thick layer of soft to medium clay can generate large settlements, often greater than 2% of the excavation depth adjacent to the support wall, and extend laterally up to four times the excavated depth from the wall. Hashash et al. (2008) (appendix A) studied the excavation induced ground deformations measured in Central Artery/Tunnel project in Boston and reported that for stiff walls the lateral movements can extend up to five times of excavation depth. Therefore, considering that this chart is based on data from relatively flexible support walls, the use of the results for much stiffer wall systems such as concrete diaphragm walls is not reliable.

Clough et al. (1989) and Clough and O'Rourke (1990) presented a semi-empirical method for estimating excavation deformations in soft clays. The maximum lateral deformations caused by the excavation depend on the system stiffness and the factor of safety against basal heave. The overall stiffness of the support system is typically expressed in terms of an effective stiffness of the system and is defined in Figure 2-4. They noted that when factor of safety against basal heave is less than 1.5, the system stiffness can significantly influence the soil movements. Figure 2-4 allows the estimation of maximum lateral deformation as a percentage of the depth of the excavation, once the system stiffness has been selected and the factor of safety against basal heave has been estimated. It should be noted that the factor of safety calculated as proposed by Clough et al. (1989) ignores the increase of stability due to wall embedment. Hashash et al. (2008)

showed that the results of embedment of the wall can limit the soil movements to much lower magnitudes than what is proposed in their chart.

Figure 2-5 and Figure 2-6 proposed by Clough and O'Rourke (1990) show maximum lateral wall deflection and surface settlements respectively as a function of excavation depth. These figures are commonly used as design tools to estimate maximum wall and soil movements. Hashash et al. (2008) illustrated that for Central Artery/Tunnel project the large stiffness of the supporting system and wall embedment limits the lateral deformations and surface settlements to lower magnitudes than what is proposed by Clough and O'Rourke (1990). Clough and O'Rourke (1990) also presented dimensionless settlement profiles in Figure 2-7 as a basis for estimating settlement patterns adjacent to excavations. Separate profiles were developed for sands, stiff to very hard clays and soft to medium clays. With knowledge of the maximum settlement, the dimensionless diagrams in Figure 2-7 can be used to obtain an estimate of the actual surface settlement. The figure shows that the settlement influence zone extends a distance of about three times the depth of the excavation (3H) for excavations in stiff to very hard clays and 2H for excavations in sands and soft to medium clays. However based on Hashash et al. (2008) for stiff supporting systems, the influence zone can extend up to five times of excavation depth.

Based on 10 case histories in Taipei, Taiwan, Ou et al. (1993) observed that the vertical movements of the soil behind the wall may extend to a considerable distance. For the concave settlement profile, Hsieh and Ou (1998), proposed an envelope for both soft clay and stiff clay to take into account the settlements in farther distances than 2H from the excavation, Figure 2-8.

Since empirical and semiempirical methods (Peck 1969; Clough and O'Rourke 1990; Ou et al. 1993; Bowles 1996; Hsieh and Ou 1998) have incomplete linkage between wall deflections and surface settlement and do not quantify uncertainty in the estimates of deformations, Kung et al. (2007) proposed a simplified semiempirical model for estimating maximum wall deflection, maximum surface settlement, and surface settlement profile for soft to medium clays. Kung et al. (2007) proposed a model (KJHH), that consists of three component models for predicting wall deflection, deformation ratio, and ground surface settlement profile caused by a braced excavation in soft to medium

clays. The KJHH model, developed based on thirty-three case histories of braced excavations in soft to medium clays (obtained from Taipei, Singapore, Oslo, Tokyo, and Chicago), and the results of a large number of well-calibrated FEM analyses. They also demonstrated that maximum wall deflections has to be modified by deflection reduction factor due to presence of hard stratum. The deflection reduction factor K, is related to the ratio of the depth to hard stratum, measured from the current excavation level, over the excavation width (*T*/*B)*. At smaller *T*/*B* ratios (*T*/*B*<0.4), the presence of the hard stratum has a great influence on the magnitude of the calculated maximum wall deflection, and at *T*/*B*>0.4, the influence of the hard stratum is negligible, Figure 2-9.

Measurements from model tests have been another tool to investigate ground movements. Mueller (2000) performed model tests at the University of Illinois on a solder pile wall with tie-backs in sand and measured surface settlement and lateral wall displacements for different construction stages. Mueller (2000) also reported results of analysis using theory of beam on elastic foundation (BOEF). In this approach soil is idealized by linear springs with certain assumptions regarding soil stiffness.

The above-mentioned empirical and semiempirical correlations estimate ground movements and support loads on the basis of soil type, workmanship, system stiffness and the factor of safety against basal heave. These variables correspond to a small number of the possible factors affecting the performance of deep excavations. Obtaining relationships for the other factors using empirical data is a complex task since capturing the effects caused by a single factor requires a significant number of case histories. Accessing and analyzing such a large number of case studies is extremely difficult; therefore, many have resorted to performing complementary numerical analyses that are capable of modeling actual constructions.

2.3. Numerical models

In recent years, numerical simulations have become much more common for the analysis of excavations in urban environments. Numerical models are used to predict induced ground deformations due to excavation (Morgenstern and Eisenstein 1970; Wong 1970; Clough and Duncan 1971; Clough and Tsui 1974; Clough and Mana 1976; Mana and Clough 1981; Finno and Harahap 1991; Hashash 1992; Hashash and Whittle 1993; Hsi and Small 1993; Whittle et al. 1993; Whittle and Hashash 1994; Ng et al. 1995;

Hashash and Whittle 1996; Ou et al. 1996; Ou et al. 2000; Potts and Zdravkovic 2001; Hashash and Whittle 2002; Ukritchon et al. 2003; Finno and Calvello 2005; Finno and Roboski 2005; Kung et al. 2007; Ou et al. 2008; Kung et al. 2009).

Finite element predictions contain uncertainties related to soil properties, support system details, and construction procedures. Although many factors such as limited information about the construction sequence (Clough and O'Rourke 1990); limited site investigation (Hashash and Whittle 1996); inappropriate representation of the soil constitutive behavior (Finno and Harahap 1991) limit the application of excavation simulations, they are still very useful tools to predict excavation performance.

In practice generally plane strain two-dimensional (2D) analysis is conducted to assess wall and ground movements in the center of each side of the excavation. This simplifying assumption sometimes is not consistent with actual excavation. In more complex analysis that the behavior of corner or shorter side of the excavations is concerned, the analyses apply axisymmetric assumption. To date, due to high cost of computational and time constraints, the full three-dimensional (3D) analyses have been rarely applied in practice. A number of studies have been conducted to describe the 3D modeling of deep strutted excavations in a variety of soil conditions (St-John 1975; Ou et al. 1996; Ou and Shiau 1998; Zhang et al. 1999; Moormann and Katzenbach 2002; Finno and Roboski 2005; Zdravkovic et al. 2005; Ou et al. 2008).

Ou et al. (1996) proposed a nonlinear, three- dimensional finite element technique for modeling deep excavations. They analyzed the effect of the existence of corner effect on the deflection behavior of an excavation in soft to medium clayey subsoil stratum. By performing a series of parametric studies, a tentative relationship was developed for estimating three-dimensional maximum wall deflection of an excavation based on two-dimensional finite element results. The proposed technique was explored in detail for TNEC excavation case study by Ou et al. (2000).

Finno et al. (2007) conducted 150 finite element simulations to define the effects of excavation geometry, i.e., length, width, and depth of excavation, wall system stiffness, and factor of safety against basal heave on the three-dimensional ground movements caused by excavation through clays. The results of the analyses were represented by the plane strain ratio (PSR), defined as the maximum movement in the

center of an excavation wall computed by three-dimensional analyses normalized by that computed by a plane strain simulation. Results of their analysis showed that the value of PSR is affected by (1) the ratios of the length of wall to the excavation depth (*L*/*He)*; (2) the plan dimensions of the excavation, *L*/*B*, with *L* being the side where movements are computed, (3) the wall system stiffness ($EI/\gamma_w h^4$) as defined by Clough et al.(1989); and (4) the factor of safety against basal heave. Of these factors, the *L*/*He* ratio was the most influential for the range of parameters considered. When *L*/*He* is greater than 6, the PSR is equal to one and results of plane strain simulations yield the same displacements in the center of an excavation as those computed by a 3D simulation.

2.4. Inverse analysis approach

Inverse analyses have been applied to geotechnical problems for several decades (Sakurai and Takahashi 1969; Cividini and Rossi 1983; Gioda and Sakurai 1987; Hashash et al. 2006). These techniques allow engineers to evaluate numerically performance of geotechnical structures by a quantifiable observational method. Inverse analyses have been used to identify soil parameters from laboratory or insitu tests (Anandarajah and Agarwal 1991; Zentar et al. 2001; Samarajiva et al. 2005), performance data from excavation support systems (Ou and Tang 1994; Hashash and Whittle 1996; Calvello and Finno 2004), excavation of tunnels in rock (Sakurai and Takahashi 1969; Gens et al. 1996; Gioda and Locatelli 1999), and embankment construction on soft soils (Arai et al. 1986; Honjo et al. 1994).

The common application of numerical modeling is “back calculation”, in which the simulated model is adjusted to agree with measured values. This approach is primarily a linear process with ad hoc loops as follows (

Figure 2-10):

1) Problem definition and model idealization: The problem is defined and the objective of the simulation is determined. For excavations, model simulation is used to estimate anticipated ground deformations.

2) Material property, in situ and laboratory testing: The material properties are determined either in the lab or in the field.

3) Material constitutive behavior, model and property choices: A material constitutive model that best represents the stress-strain behavior of the soil is selected based on information gained in Step 2.

4) Boundary value problem solution: A finite element or finite difference analysis program is used with selected soil model. The model computes anticipated ground deformations including lateral wall displacement and surface settlement.

5) Comparison to measured field behavior: Computed and measured ground deformations are compared during construction. The most common field measurements are lateral wall deflections and surface settlements. If a significant discrepancy between the computed results and the actual measurements exist, often an ad hoc loop of adjusting model properties (back to Step 3), re-analysis (Step 4) and matching of field measurements (Step 5) is performed.

6) Analysis of future excavations/stages: The constitutive model is then used to compute deformations due to additional excavation stages or for similar excavations.

This approach to the solution of boundary value problems is not always successful in capturing measured field behavior due to various factors including the lack of sufficient knowledge of soil behavior under complex shearing modes experienced in the field (Hashash et al. 2006).

It is desirable for a numerical model to learn from precedent represented by field observations. Learning from precedent represents a classic inverse analysis problem aimed in part at interpreting the soil and stress response implied by field observations. For example, during an excavation, the measured lateral wall deformations and surface settlements are a result of complex shearing of the surrounding soil, and therefore the observed deformations contain rich information on the stress–strain response of the soil. Therefore, data collected from the instruments can be used in inverse analyses after construction (Hsi and Small 1993; Whittle et al. 1993; Ng and Lings 1995; Jan et al. 2002; Finno and Calvello 2005; Marulanda 2005; Hashash et al. 2006). Field measurements of deep excavations have also been reported in the literature (O'Rourke et al. 1976; O'Rourke 1981; Finno et al. 1989; Finno and Harahap 1991; Ou and Tang 1994; Whittle and Hashash 1994; Ou and Wu 1996; Briaud and Lim 1997; Lee et al. 1998; Ou et al. 1998; Weatherby et al. 1998; Briaud and Lim 1999; Koutsoftas et al. 2000; Ou et al.

2000; Calvello and Finno 2004; Finno and Calvello 2005; Finno and Roboski 2005; Liu et al. 2005; Wang et al. 2005; Su et al. 2006; Hashash and Song 2008; Rechea et al. 2008; Levasseur et al. 2008c).

Ad hoc methods are often used to solve this inverse problem whereby soil model parameters are adjusted in order to more closely match numerical model calculations with field observations. In many cases the ad hoc approaches for model update are not sufficiently general. A simulation that is adjusted to fit results of a given excavation site may not provide a good estimate of response at another excavation site with a different support configuration. It is worth noting that learning from precedent in this thesis excludes issues related to problems associated with construction quality, and is instead focused on observed behavior that can be associated with well defined construction activity.

2.4.1. Optimization techniques

Optimization techniques (Gioda and Sakurai 1987; Ou and Tang 1994; Ledesma et al. 1996; Pal et al. 1996; Zentar et al. 2001; Calvello and Finno 2004; Samarajiva et al. 2005; Levasseur et al. 2008; Levasseur et al. 2009a) are used as an alternative to ad hoc methods for solving the inverse problem and for learning from precedent. Given a numerical model, unknown properties of the material constitutive model are systematically adjusted to minimize the error between numerical model calculations and observed response. However, the number and type of input parameters to be optimized depends upon many factors, including the characteristics of the selected soil model, how the model parameters are combined within the element stiffness matrix in a finite element formulation, the site stratigraphy, the number and type of observations available, the characteristics of the simulated system, and computational time issues. Calvello and Finno (2004) deployed a computer code UCODE (Poeter and Hill 1998) and Hardening-Soil (H-S) model in back analysis of supported excavations. Their results showed that the accuracy of back-figuring the observed excavation-induced wall deflection is satisfactory.

Tang and Kung (2009) used a nonlinear optimization technique (NOT) incorporating the auxiliary techniques to enhance the convergence and stability of the optimization analysis for supported excavations. The developed NOT was used for the back analysis of excavation to back-figure soil parameters based on observed

deformations. Only wall deflection was used and no other excavation induced deformation (e.g. settlements) was explored in their study. Since many factors such as soil stiffness and small-strain non-linearity of soil behavior is difficult to represent in conventional soil models, the back-figured parameters are generally different than real parameters and the back-figured parameters regarded as the equivalent parameters.

In another related study, Levasseur et al. (2008 a; 2008b) proposed the genetic algorithm as a new optimization method for geotechnical inverse analyses and soil parameter identification. This method was applied to reproduce the horizontal displacement of the wall and was compared to other optimization techniques that are based on gradient algorithm for Lurie Center case study in downtown Chicago (Rechea et al. 2008). They concluded that since gradient algorithm assumes the solution of the inverse problem is unique, and in the field of geotechnics there are a number of uncertainties associated with in situ measurements, its use is problematic. However, they recommended genetic algorithm which identifies a set of approximate solution is more relevant for deep excavation simulations.

Overall, optimization techniques provide a powerful tool for model calibration using field measurement, though they have some limitations (Hashash et al. 2006):

1) The techniques are unable to overcome inherent limitations in the selected material constitutive model such as the inability to capture small strain nonlinearity essential to representing the distribution of deformations around an excavation;

2) It is possible that several combinations of material model properties may lead to similar estimates of deformations, leading to nonconvergence or nonuniqueness in the solution.

3) Current modeling approaches are not always able to interpret and thus fully benefit from the rich soil stress–strain data implied by field observations which results in limited integration of numerical modeling with the observational approach.

2.4.2. The autoprogressive training algorithm

The field of constitutive relations has recently been extended beyond classical elastoplastic theories to include artificial neural network (ANN) concepts. The learning potential of NN material models has been realized using an innovative analysis technique known as autoprogressive training (Ghaboussi et al. 1998). This technique allows the

numerical model, for the first time, to extract the material constitutive relationship from structural systems by using the measurements of loads and displacements.

A NN material model is used in the analysis, and is continuously updated based on the rich field of stress-strain pairs obtained from the boundary value problem. This technique has been applied to modeling of composites (Ghaboussi et al. 1998; Haj-Ali et al. 2001), frictional triaxial tests (Sidarta and Ghaboussi 1998; Fu et al. 2007; Fu et al. 2007; Hashash et al. 2008), and nonuniform material tests (Ghaboussi and Sidarta 1998; Shin and Pande 2000; Pande and Shin 2002).

Given that complex stress-strains paths are generated around a braced excavation, it is argued that the rich constitutive information embedded in the global system behavior can be directly identified from appropriate number of instruments. The autoprogressive training algorithm provides a unique approach to extract rich sets of stress strain data from field observations.

The algorithm requires two complementary sets of measured boundary conditions, whereby each includes either forces or displacements at the boundaries. Using an incremental non-linear finite element analysis, the two sets of boundaries are alternatively imposed for each load/construction stage. The analyses produce complementary pairs of stresses and strains that are used in training the NN material model. The procedure is repeated until an acceptable match is obtained between the numerical analysis and the measured data. The resulting NN material model can then be used in the analysis of new boundary value problems.

2.5. SelfSim inverse analysis framework

Hashash et al. (2003; 2006) introduced a robust inverse analysis approach, self-learning simulations (SelfSim), to extract soil behavior by using wall deformations and surface settlements measurements. SelfSim is a software analyses framework that can be applied to a wide range of engineering problems, including excavations as shown in Figure 2-11. In a typical excavation problem, wall deformations and surface settlements are measured at selected excavation stages (Step 1). At a given excavation stage, the soil is excavated to a known depth and struts or another form of lateral supports (e.g., tiebacks) are placed to support the excavation wall. The measured deformations and the corresponding known excavation stage represent complementary sets of field

observations. A numerical model is developed to simulate the construction sequence. ABAQUS (2005) is used as finite element engine for this method. The soil response is represented using a NN based material constitutive model. Initially the soil response is unknown and the NN soil model is pretrained using stress–strain data that reflect linear elastic response over a limited strain range. Additional available soil behavior information, such as that from laboratory tests, can be used in this initialization process (Hashash et al. 2006).

In Step 2a of SelfSim a finite-element (FE) analysis using the current NN soil model is performed simulating soil removal and support installation corresponding to a given excavation stage. The FE analysis computes stresses and strains throughout the soil in addition to wall and ground deformations based on equilibrium considerations. Most likely, the computed deformations will not match measured deformations. SelfSim stipulates that due to equilibrium considerations and the use of correct boundary forces due to soil removal, the corresponding computed stress field provides an acceptable approximation of the actual stress field experienced by the soil. The computed strain field is considered to be a poor approximation of the actual strain field due to the discrepancy between computed and measured deformations. In Step 2b of SelfSim a parallel FE analysis using the same NN soil model is performed in which the lateral wall deflections and surface settlements are imposed as additional displacement boundary conditions. The soil is also removed to reflect the current excavation stage (Hashash et al. 2006).

The stress field from Step 2a and the strain field from Step 2b are extracted to form stress–strain pairs that approximate the soil constitutive response and are used to retrain the NN soil model. The analyses of Step 2 and the subsequent NN model training are referred to as a SelfSim learning cycle. The analyses of Step 2 are repeated using the updated NN soil model and a new set of stress–strain data are extracted for retraining of the NN soil model in additional SelfSim learning cycles. The solution converges when the analysis of Step 2a provides the correct ground deformation, i.e., analyses of Steps 2a and 2b provide similar results. Several SelfSim learning cycles are performed for each construction stage. The SelfSim learning cycles are performed sequentially for all available construction stages. This results in a single SelfSim learning pass. SelfSim learning passes are repeated until the computed and measured displacements match.

The resulting NN constitutive model can be used in the analysis of other types of excavations in similar ground conditions or a later excavation stages as illustrated in Step 3. The predictive capability of the developed NN soil model is limited to the stress–strain levels extracted during SelfSim learning. The predictive capability of the model can be extended by: (1) additional SelfSim learning using other available excavation case histories; (2) using additional laboratory test data; and (3) using conventional constitutive model at stress and strain levels outside those extracted from SelfSim learning (Hashash et al. 2006).

The SelfSim analyses presented by Hashash et al. (2006) use lateral wall deflections and surface settlement measurements to capture excavation response and extract soil behavior. However, SelfSim framework is not limited to these two types of measurements and can benefit from other measurements. Marulanda (2005) concluded that additional instruments can potentially be used to develop a more reliable extracted soil behavior.

The proposed framework "SelfSim" represents a major departure from conventional methods for development and calibration of numerical models using laboratory measurements and field observations in which such calibration is limited by the capabilities and complexity of the material constitutive model. The SelfSim framework in conjunction with a NN soil constitutive model is also distinctly different from more common uses of neural networks in geotechnical engineering including deep excavations (Goh 1996; Kiefa 1998; Jan et al. 2002) in which NN are used as simple function approximators or to perform tasks where regression analysis will be sufficient. Within SelfSim, the NN constitutive model can continuously evolve as additional field observations become available. SelfSim opens new ways to systematically incorporate field observations of excavation performance into numerical simulations.

2.6. Application of SelfSim in Geotechnical problems

SelfSim has been applied in broad range of geotechnical problems such as numerical modeling of laboratory tests, seismic site response analyses, and deep excavations.

Fu (2007) applied SelfSim learning in to two simulated laboratory test, a triaxial compression shear test with frictional loading platens, and a triaxial torsional shear test

with frictional ends. Fu et al. (2007) demonstrated that SelfSim usefully extracts the diverse stress-strain behavior from within the specimens. The extracted NN based constitutive model was used in the forward prediction of the load-settlement behavior of a simulated strip footing. Fu et al. (2007) demonstrate that it is possible to extract non-uniform stress and strain states from global measurements of load and displacement. Laboratory test imposing non-uniform conditions on tested soil specimen can then be used in conjunction with the SelfSim framework to interpret a wide range of soil stress strain behavior. For further exploration of SelfSim application, Hashash et al. (2008) employed SelfSim to interpret Racci sand drained shear behavior. The sand specimens in three different relative densities were tested under three different confining pressures in a triaxial cell with frictional loading platens. SelfSim framework used to extract stress behavior from within each specimen using load and displacement measurements. The extracted behaviors from different tests were combined into a single NN material model. The extracted stress strain provided insight into sand behavior under more general loading modes.

Tsai (2007) integrated site response analysis and field measurements from downhole arrays. Tsai and Hashash (2006; 2008) illustrated that SelfSim framework is able to gradually capture the measured response while simultaneously extracting the underlying soil behavior. The resulting soil model, used in a site response analysis, provides correct ground response. Tsai and Hashash (2009) demonstrated that the extracted cyclic soil behavior can be further enhanced using additional field measurements. The algorithm was verified with four synthetic vertical array recordings and also applied to Lotung and La Cienaga vertical array recordings. The extracted soil behavior was compared with laboratory measurements and was used to assess influence of number of cycles and loading rate on soil behavior.

The feasibility of extracting soil behavior from "field measurements" obtained from simulated excavations using SelfSim was illustrated by Marulanda (2005). The "field" measurements of lateral wall deflections and surface settlements were generated synthetically using a FE model of a braced excavation. The target soil behavior was represented using two plasticity-based soil models: (a) the Modified Cam Clay (MCC) model (Roscoe and Burland 1968), and (b) the MIT-E3 model (Whittle 1987). After

using surface settlements and lateral wall deflections, the results showed that the NN material model learned sufficient features of soil behavior, in this case represented by MCC or MIT-E3, to reproduce the global response of the excavation.

Since a NN material model allows learning and/or evolving from field observations and case histories, learning from precedent which is an essential part of civil and geotechnical engineering for developing empirical design methods, was explored using SelfSim framework by Marulanda (2005). Marulanda (2005) used SelfSim to extract soil behavior from three simulated excavation case histories with similar soil stratigraphy to develop "local experience". Then the extracted soil behavior was used to predict the behavior of a new fourth excavation that is distinct from the case studies used for SelfSim learning. The predicted wall deflections and surfaces settlements matched reasonably well with the target measurements generated by MIT-E3 model. This exercise with synthetic data demonstrated that through SelfSim it was possible to incorporate knowledge gained from precedent in a predictive numerical analysis, and anticipate more accurate assessment of ground response in deep excavations. However, this exercise was conducted only with synthetic data by Marulanda (2005) and never was tested for deep excavation case studies.

SelfSim framework was also examined in using instrumentation programs to extract soil behavior by Marulanda (2005). Seven configurations in simulated excavations with synthetic measurements generated by MIT-E3 were used in SelfSim framework to extract soil behavior. The extracted soil model was used to compute wall deformations and surface settlements (Marulanda 2005). The main important conclusions was that lateral wall deflection as the only boundary condition imposed during SelfSim learning does not provide sufficient constraints to correctly compute the surface settlements. Using an additional inclinometer farther away from the excavation provided enough information to capture surface settlements. While this conclusion was critically important, the study had some limitations: 1) The study was focused on prediction of wall deformations and surface settlements and not other instrument measurements around the excavation; 2) The number of configurations were insufficient to make a general conclusion regarding the effect of different instrument lay outs on extracted soil behavior;

3) Only synthetic data in simulated excavations were used in the study and the applications of the findings needed further exploration in excavation case studies.

2.7. Outstanding issues about deep excavations

The previous studies about deep excavations left some questions that motivated this study:

1. *How can the accuracy of the extracted soil behavior in prediction be improved during SelfSim learning?* It is desirable to maximize the richness and diversity of the extracted stress-strain database to enhance the performance of the extracted material model. Various combinations of measurements can be used in SelfSim to extract the soil behavior. Marulanda (2005) studied only a few combinations of instrument layout for synthetic excavations. It is desirable in a systematic study to investigate the effect of using different instruments on learning soil behavior.
2. *Learning from local experience?* In a given urban area, case histories of excavation performance are available and could be used to develop "local experience" in cases with similar stratigraphy. Marulanda (2005) showed that SelfSim can be used to extract soil behavior from three simulated excavation case histories and then the extracted soil model can be used to predict the behavior of a fourth excavation. However, this approach was not validated using field case histories.
3. *Learning of 3-D excavation response?* The analyses presented in Marulanda (2005) simplify what is truly a three-dimensional response as a two dimensional model. The plane strain assumption and the idealization of the field measurements for a two dimensional analysis is a practical necessity in view of the substantial additional computational effort involved in performing multiple three dimensional, non-linear analyses needed for SelfSim. This simplification results in the loss of information on 3-D soil response, therefore the information gained from a three dimensional analysis is expected to provide a much richer and a more general stress-strain data set.

In the following chapters these questions are addressed and discussed in details by using numerical analysis and case histories.

2.8. Summary

The deformation behavior of a braced excavation may be affected by a large number of factors such as the excavation with and depth, wall stiffness, strut spacing, prestress, depth to an underlying hard stratum, soil stiffness, strength distribution, dewatering operation, soil consolidation, creep, and workmanship. Nonlinear finite element analysis provide a comprehensive framework that can be use to evaluate excavation performance including the design of the wall and support system, prediction of ground movements and the effects of construction activities. Inverse analysis approaches are commonly used to compute excavation response. The optimization technique, whereby the designer adjusts various constitutive model properties to achieve a better match of ground surface does not overcome the inherent limitation of constitutive models. These adjustments lack a systematic approach and are rarely useful for modeling similar problems. While engineers continuously learn from case histories and field behavior, the current approaches to numerical simulations do not fully benefit from direct measurements of field behavior. SelfSim inverse analysis is a powerful solution to learn from precedents and enhance the design of deep excavations in future. The instrumentation layout effect on extracted soil model from excavations needs further studies. The capability of SelfSim in predicting excavation response in new excavations while learning from previous local experience needs further consideration. The SelfSim framework needs to be tested using measurements of excavation case studies.

Table 2-1 Factors cited by Mana and Clough (1981) that influence excavation performance

Design	*Site*	*Construction*
- Depth and width of excavation - Support spacing - Stiffness of support - Stiffness of the wall	- Soil Properties - Existing structures and utilities - Transient loads during and after construction	- Method and sequence of construction - Duration of construction

Table 2-2 Summary of closed-form calculations of base stability for soft to medium soils after Hashash and Whittle (1996)

Reference	Capacity Factors			Avg. Depths for S_u		Notes
	N_c	N^*	n	S_{ub}	S_{uu}	
Terzaghi (1943)	5.7	0	1	$H + B/(2\sqrt{2})$	$(H/2)$	--
Bjerrum and Eide (1956)	5.7 to 6.2	0	0	$H + B/(2\sqrt{2})$	--	N_c function of H/B
O'Rourke (1992)	5.7 to 6.2	$\sqrt{2}\alpha M_y \pi^2/[B(L+h-H)]$		$H + B/(2\sqrt{2})$	--	
Hashash and Whittle (1992)	$(2+\pi)$ f	$(B/4) f \gamma_b (S_{uDDS}/\sigma'_{vo})$		H	$(H/2)$	Values of f from Davis and Booker (1973)

General Equation: $FS = \{N_c S_{ub} + N^*/H[\gamma - n\sqrt{2}(S_{uu}/B]\}$

Note: α=end condition factor, B= excavation width, f=stability calculation factor, h=average vertical support spacing, H=depth of excavation, N_c=bearing capacity factor as a function of H/B, N^*=stability calculation factor in general equation, n=stability calculation factor in general equation, S_{ub}=depth averaged shear strengths, S_{uDSS}=undrained shear strength from direct shear test, γ_b=soil total unit at base of excavation.

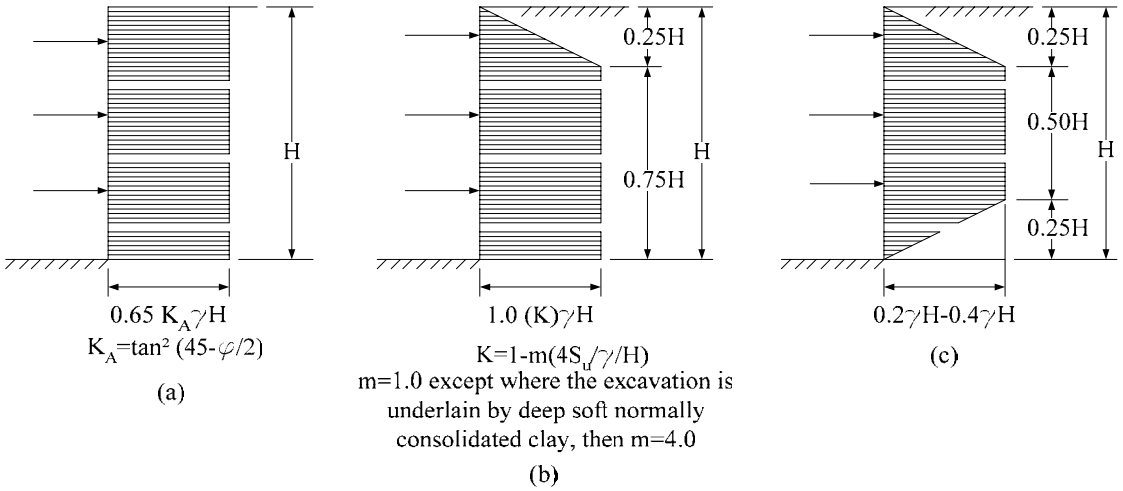

Figure 2-1 Suggested apparent earth-pressure diagram for design of struts in open cuts in (a) Sand (b) soft to medium clay and (c) stiff-fissured clays, after Terzaghi et al. (1996)

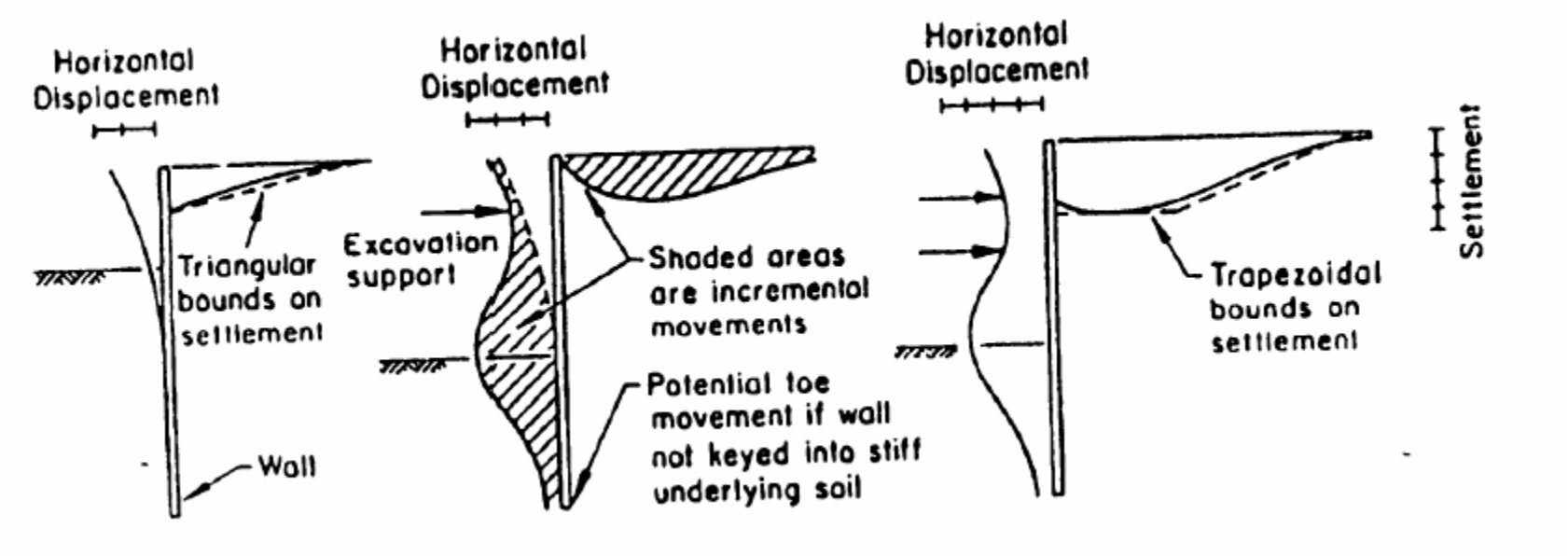

Figure 2-2 Typical profiles of movements, after Clough and O'Rourke (1990)

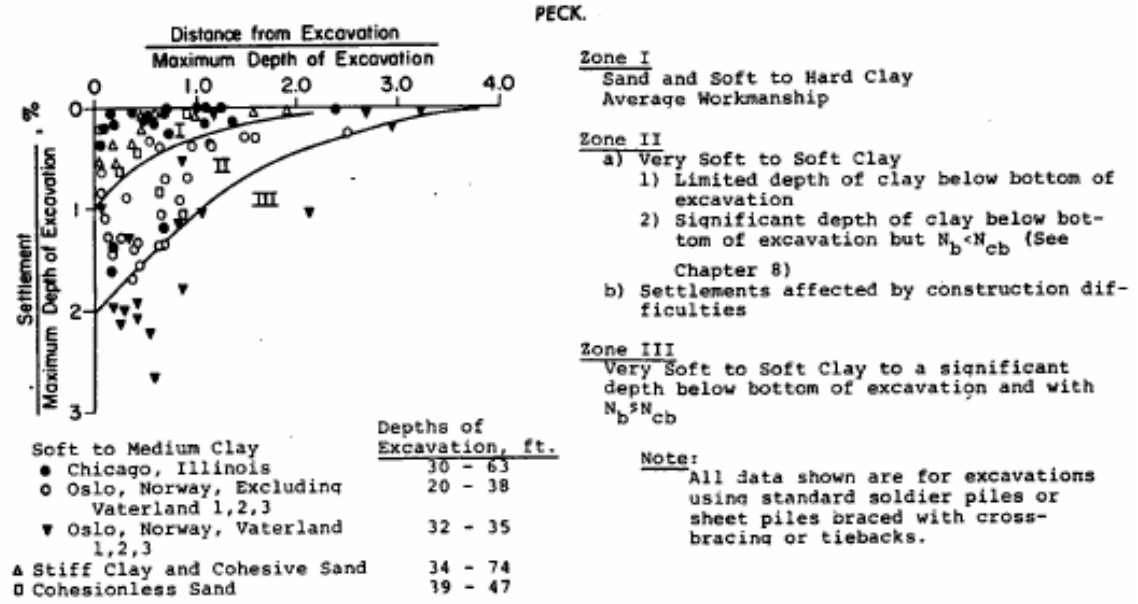

Figure 2-3 Summary of settlements adjacent to open cuts in various soils, as function of distance from edge of excavation, after Peck (1969)

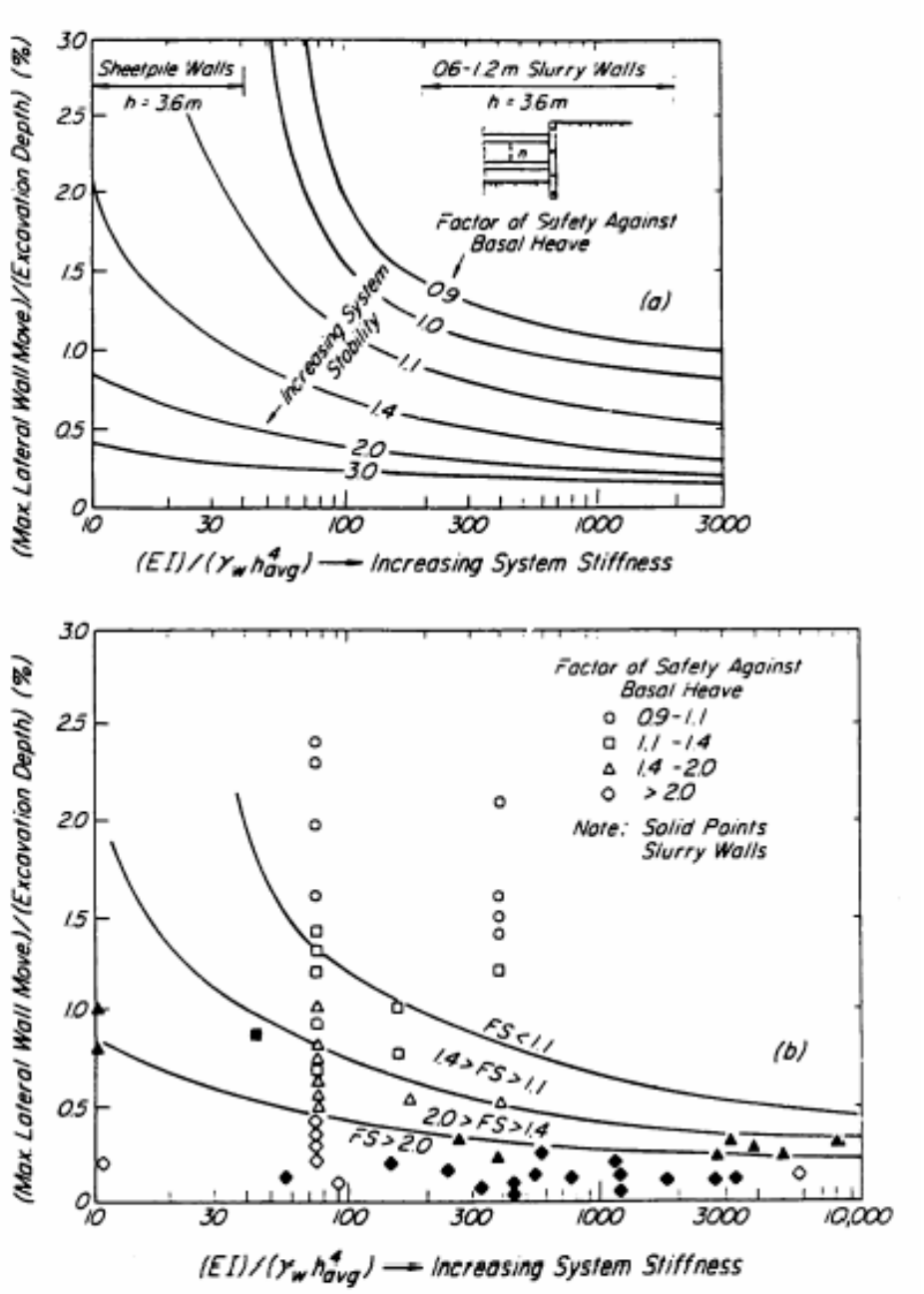

Figure 2-4 Maximum lateral wall movements and ground surface settlements for support systems in clay for different values of factor of safety against basal heave. (a) Calculated by FEM analyses, (b) Comparison with Field Measurements, after Clough et al. (1989)

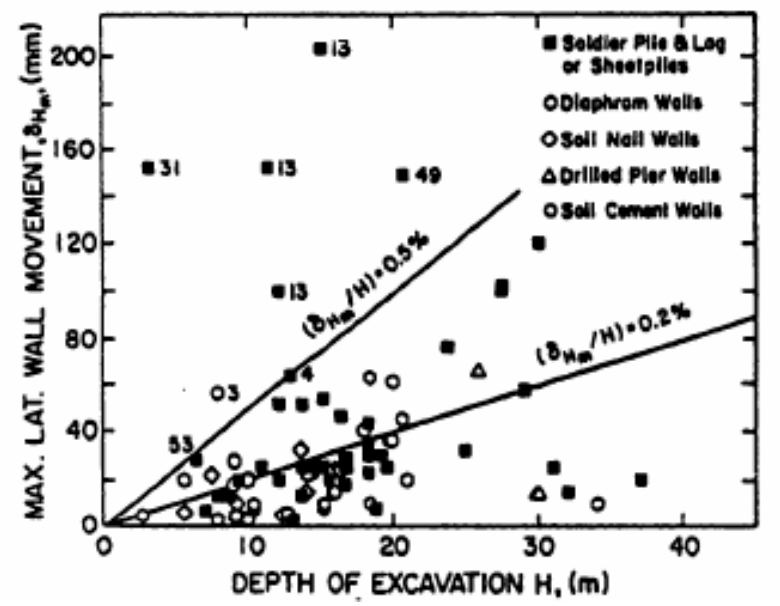

Figure 2-5 Observed maximum lateral movements for in-situ walls in stiff clays, residual soils and sands, after Clough and O'Rourke (1990)

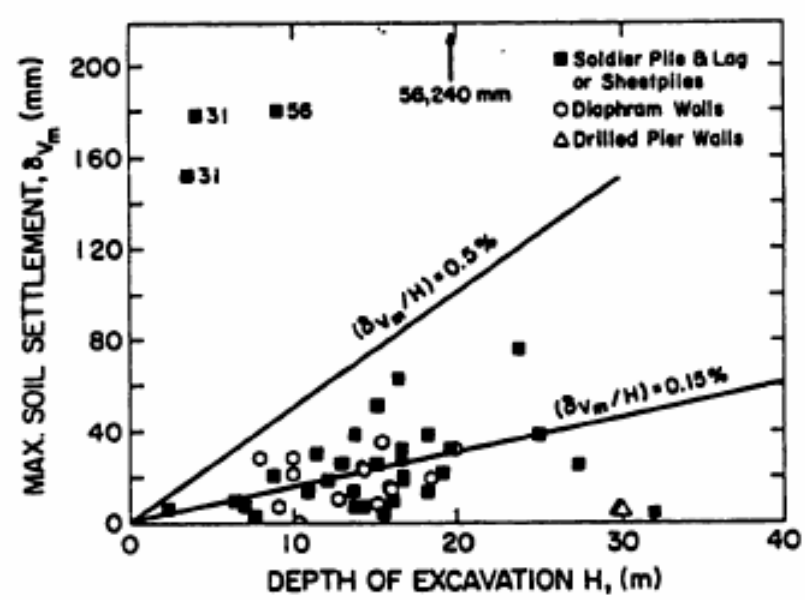

Figure 2-6 Observed maximum soil settlements in the soil retained by in-situ walls, after Clough and O'Rourke (1990)

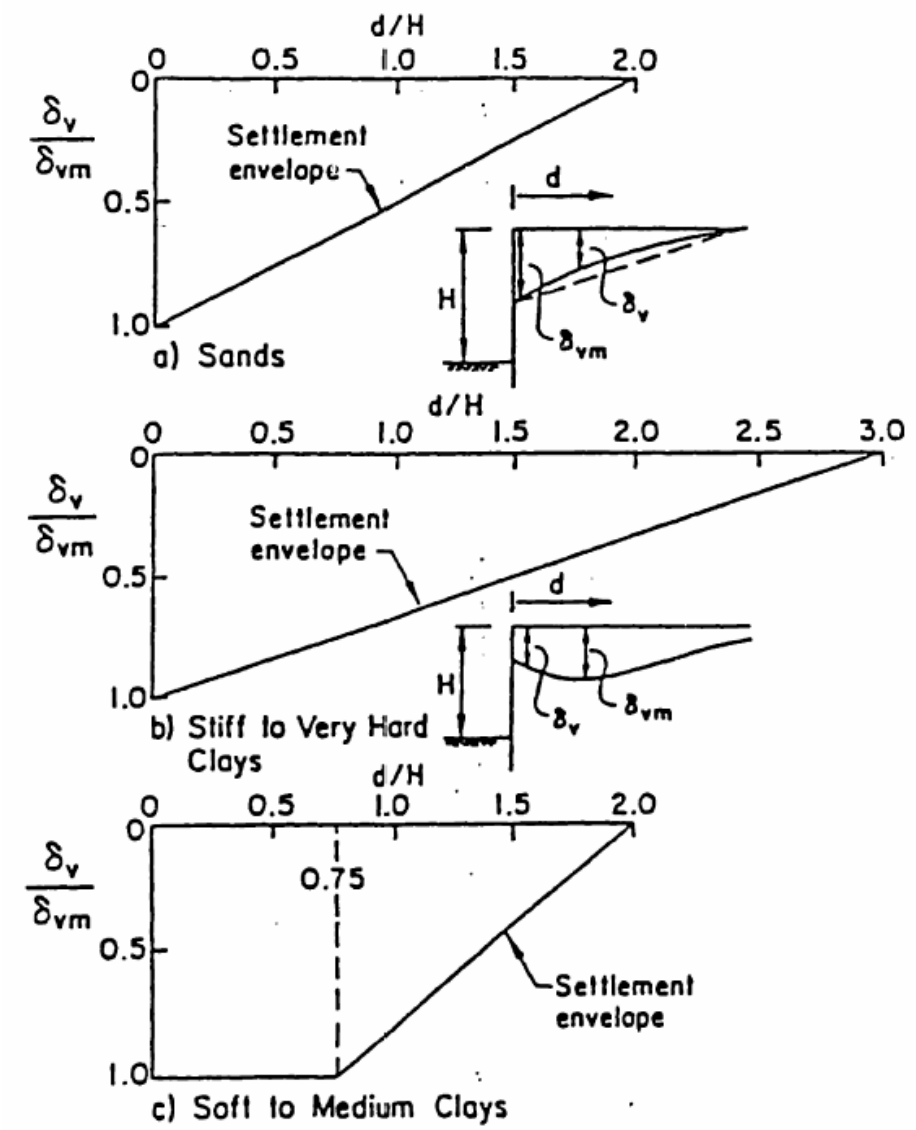

Figure 2-7 Dimensionless settlement profiles recommended for estimating the distribution of settlement adjacent to excavation, after Clough and O'Rourke (1990)

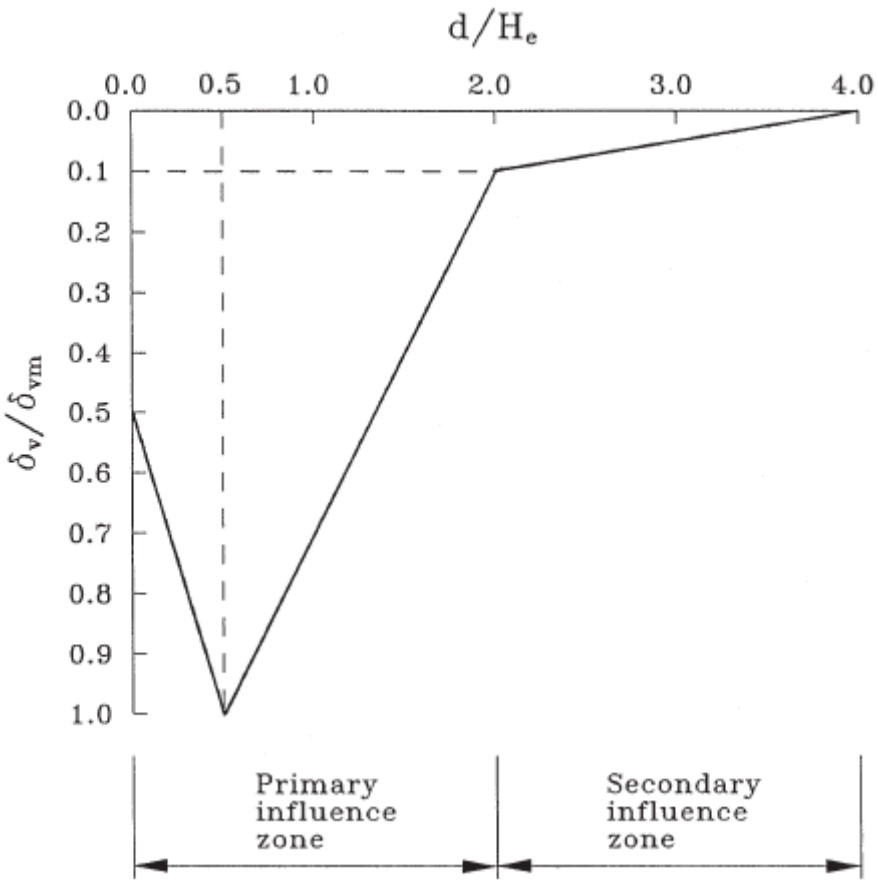

Figure 2-8 The proposed method for predicting concave settlement profile, after Hsieh and Ou (1998)

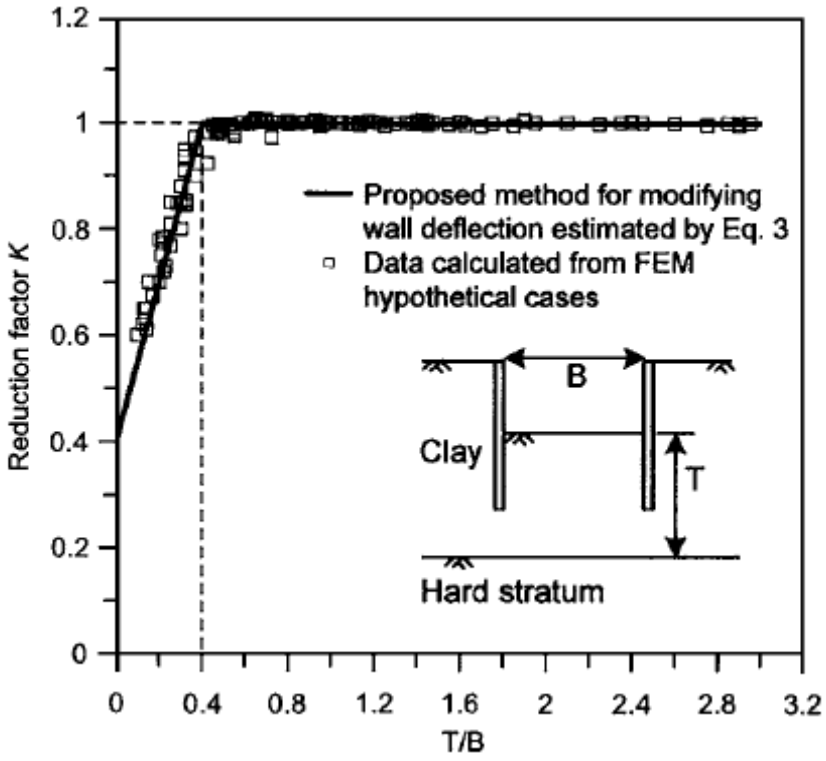

Figure 2-9 Effect of the hard stratum on the computed wall deflection, after Kung et al. (2007)

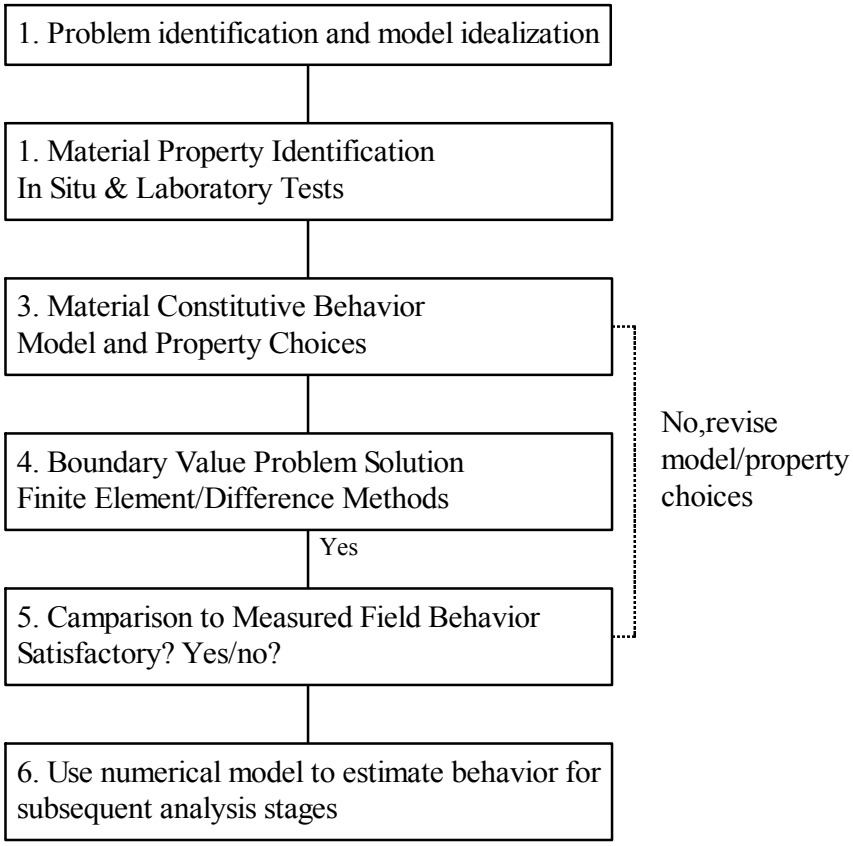

Figure 2-10 Common approach to modeling of geomechanics problems, after Marulanda (2005)

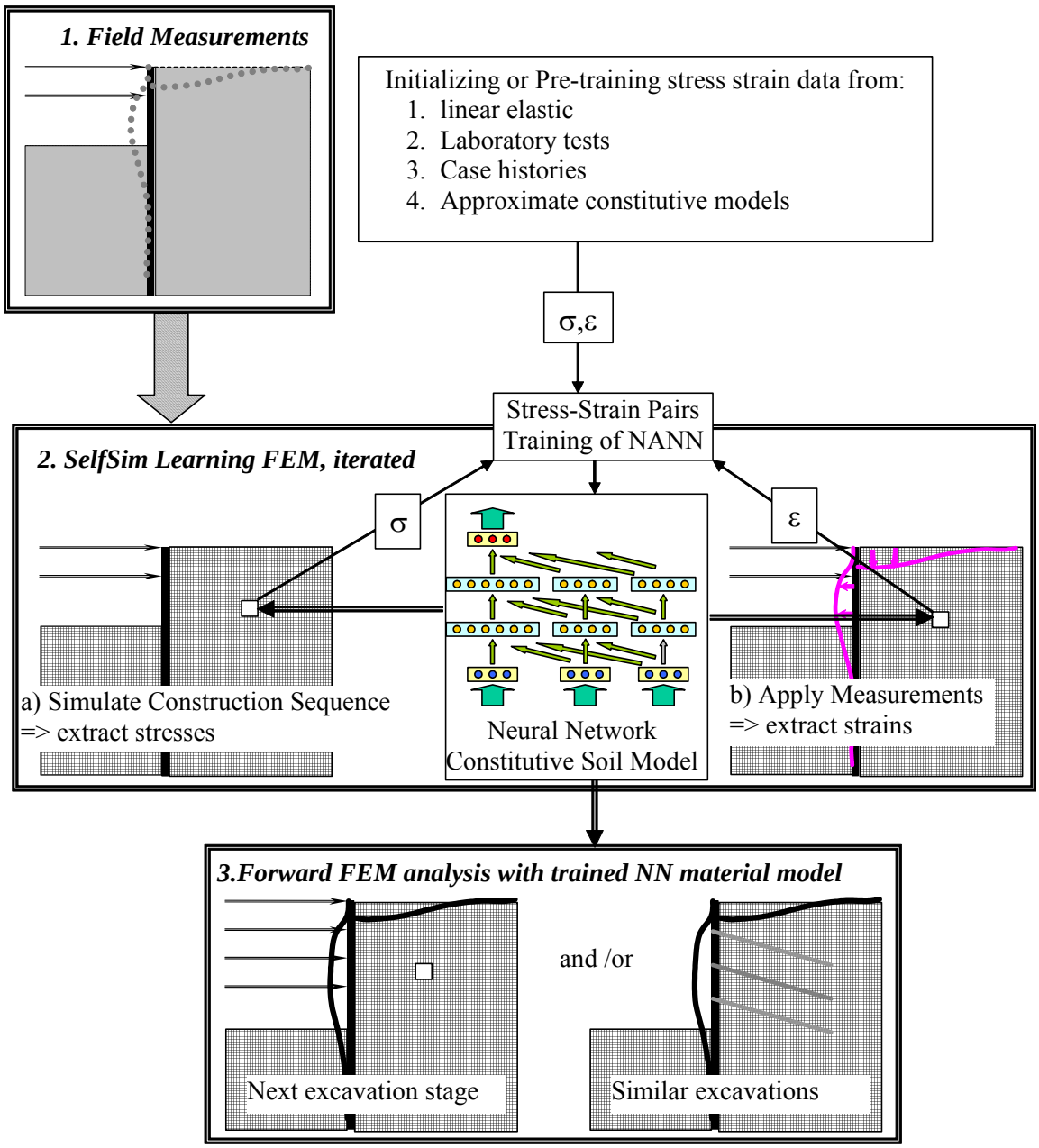

Figure 2-11 Application self-learning simulations to deep excavation problems, after Hashash et al. (2006)

CHAPTER 3 COMPARISON OF TWO INVERSE ANALYSIS TECHNIQUES FOR LEARNING DEEP EXCAVATION RESPONSE: PARAMETER OPTIMIZATION USING GENETIC ALGORITHM AND EVOLUTIONARY BEHAVIOR LEARNING VIA SELFSIM

3.1. Introduction

In this chapter the performance of two inverse analysis techniques in capturing observed performance of a deep excavation in downtown Chicago are compared. The first method is based on a Genetic Algorithm (GA) optimization method. Its goal is to identify soil parameters of a constitutive model from in situ measurements. The second method is based on Artificial Neural Networks (ANN). Its goal is to extract soil behavior from experimental data without a pre-defined constitutive model. Both inverse analysis techniques and their application to a deep excavation in downtown Chicago are described in the following sections. Each method has been presented in previous studies as very efficient methods to solve excavation inverse analysis problem (Hashash et al. 2006; Levasseur et al. 2009a; Levasseur et al. 2009b). This chapter compares the performance of both techniques in capturing soil displacements and in predicting of soil behavior (stress path) in Lurie Center excavation in Chicago, IL, USA.

3.2. Inverse analysis techniques

3.2.1. System identification: error minimization and Genetic Algorithms

The proposed identification method is used to study the soil behavior in Lurie Center deep excavation, based on the inverse analysis theory introduced by Tarantola (1987). This method establishes a suitable identification method to adapt itself to different kinds of geotechnical structures.

The inverse analysis is based on a genetic algorithm optimization process (GA) used to identify soil parameters. This method is well known as a robust and efficient approach to solve complex problems (Goldberg 1989). Genetic algorithm can find the best solution of the problem even with a flat or noisy error function (Levasseur et al.

2008). This optimization process also provides information on the existence of correlations between parameters. Moreover, as geotechnical studies are perturbed by modeling errors or in situ measurement uncertainties, rather than only one exact solution, several approximate solutions exist for the inverse problem. Levasseur et al. (2009a; 2009b) have shown that a genetic algorithm in combination with a statistical analysis like principal component analysis is able to identify many of these approximated solutions of the inverse analysis problem. The main drawback of this method is the high calculation cost. For instance for an excavation problem requiring identification of three soil model parameter, it takes about two days with an office computer. It is necessary to perform many finite element calculations at the beginning of the optimization process to have a good estimation of the error function in the search space. This sweep, which is essential for the genetic algorithm, makes this method computationally expensive (Levasseur 2007).

The application of this method in excavation problems is shown in Figure 3-1. Trial values of the unknown soil model parameters are used as input values in a finite element code to simulate the excavation problem. PLAXIS (2002) is used as the finite element engine in this study. The computed lateral wall deflections and surface settlements are compared to measured values. If the discrepancy between measured and computed results is not in acceptable range, then through Genetic Algorithm (GA) the input soil model parameters are optimized. This process is repeated until a good match between computed and measured soil behavior is observed. Then the identified solution sets are interpreted through statistical approach, Principal Component Analysis (PCA).

Identification method:

Error function

The discrepancy between the measured behavior and the modeled one is expressed by a scalar error function, F_{err} in the sense of the least square method as introduced by Levasseur et al. (2008):

$$F_{err} = \left(\frac{1}{N} \sum_{i=1}^{N} \frac{\left(Ue_i - Un_i\right)^2}{\Delta U_i^2} \right)^{1/2} \quad (1)$$

where N is the number of measurement points, Ue_i the i^{th} measured value, Un_i the corresponding value of the numerical calculation and $1/\Delta U_i$ the weight of the discrepancy between Ue_i and Un_i. $1/\Delta U_i$ is equal to the experimental uncertainty of the i^{th} measurement point.

Genetic algorithm

Genetic algorithms are inspired by Darwin's theory of evolution and are used in this study to solve the optimization problem. The main outline of the algorithm, adapted for excavation problems by Levasseur (2007) and summarized below, is based on the studies of Goldberg (1989) and Renders (1994).

Each soil parameter that will be optimized is binary encoded and represents a gene. In this study the primary deviatoric modulus E^{ref}_{50} represents a gene. The concatenation of several genes forms an individual. For instance if two E^{ref}_{50} of two soil layers are identified in genetic algorithm, the concatenation of encoded two E^{ref}_{50} is called an individual which is defined by vector p. A group of N_i individuals represents a population of the i^{th} generation.

A scalar error function $F_{err}(p)$ is defined for each set of N_p unknown parameters, noted as a vector p. The minimization problem is solved in the N_p-dimension space restricted to a maximum and minimum value for each component of vector p.

The main stages of the genetic algorithm are shown in Figure 3-1. In case that the F_{err} for wall deformations and surface settlements exceeds the stop criteria, an evolutionary process using successively selection, reproduction and mutation of soil model parameters of interest (in this study E^{ref}_{50}) is begun to generate new sets of soil model parameters (Levasseur et al. 2008). The new sets of soil model parameters are used in a forward analysis to compute deformations. This process is repeated until conditions of convergence are satisfied: Either the average of the error function on the parent part of the population is less than a given error or its standard deviation becomes small enough. Finite element analysis needs to be conducted for generating each new population. More details of the analysis can be found in Levasseur (2007) and Levasseur et al.(2008; 2009a; 2009b)

Principal Component Analysis

After optimum soil model parameters based on minimal value of the scalar error function are identified by GA, an analysis is conducted to evaluate solution sets. Therefore, Principal Component Analysis (PCA) is used to provide a representation of the solution sets identified by GA to make the comparison between several optimizations easier. The principal component analysis is a factorial analysis method which defines main orientation of a set of under-study soil parameters, which in this study are E^{ref}_{50} of soil layers in the research space. This orientation can be used to interpret the parameter sensitivities or to find correlations between parameters. By using PCA statistical analysis, from a discrete set of solution sets identified by GA, a continuous space of solution sets is estimated. As a result an ellipsoid bounding the sought after solution set can be deduced from the principal component analysis. The area included in the ellipsoid is a first order approximation of the set of solutions identified by the GA optimization (Levasseur et al. 2009b).

3.2.2. SelfSim Learning inverse analysis

SelfSim framework application to Lurie deep excavation is illustrated in Figure 3-2. Wall deformations and surface settlements are measured during excavations stages (Step 1). In Step 2a of SelfSim, a finite-element (FE) analysis is conducted to simulate soil removal and tieback installation for a given excavation stage in Lurie Center excavation using the current NN soil model. In Step 2b of SelfSim a parallel FE analysis using the same NN soil model is performed whereby displacement boundary conditions such as wall deflection and surface settlements are imposed. The extracted stress field from Step 2a and the extracted strain field from Step 2b form stress–strain pairs representing soil constitutive model and are used to retrain the NN soil model. The solution converges when the analysis of Step 2a and 2b provide similar results. This process is continued until the computed displacements match the measured values.

3.3. Lurie Center excavation case study

3.3.1. Geometry and instrument locations

The excavation for the Lurie Research Center was approximately 82 m by 69 m and depth of 13 m (Finno and Roboski 2005). The site was heavily instrumented to monitor the ground movements resulting from the excavation. Plan view and instrument locations are shown in Figure 3-3. The support system, typical soil profile at the site and element locations for stress paths plots are shown in Figure 3-4. The element locations were chosen close to inclinometer locations to have a better understanding of the soil displacement and soil behavior simultaneously. The support system consisted of a sheet pile wall with three levels of tiebacks. The soil profile from the top consists of fill layer, lake sand layer, and soft to stiff silty clay layers.

Results from inclinometer LR1 were not used in the analyses due to proximity of the Prentice Pavilion building to this instrument location. Results from inclinometers LR3 and LR4 were not used in the analyses because of the presence of an existing, pile supported pedestrian tunnel in left north corner of the site. Inclinometer LR2 was damaged during the construction. Corner effects influenced the results of inclinometer LR5, and hence were not amenable to plane strain simulations. Therefore inclinometer measurements obtained from LR6 and LR8 were employed in GA and SelfSim inverse analyses.

The finite element model associated with Lurie Center deep excavation problem is a 2D plane strain model. To avoid 3D stiffening effect of the corners and the variability of measurements around the excavation, average data of inclinometers installed around the excavation sides (i.e LR6 and LR8) were used as measurements for inverse analysis. Settlement data are also used for both inverse analyses. The settlement data correspond to average vertical displacements measured in proximity to selected inclinometers around the excavation. The excavation sequence was idealized into seven stages as shown in Figure 3-5.

The response of clayey layers was assumed to be undrained during excavation. The excavation was simulated down to El. -7.3 m.

3.3.2. Learning global excavation response using optimization approach based on GA

In the optimization approach based on GA, each soil layer is modeled by the constitutive Hardening Soil model of PLAXIS (Brinkgreve 2003). For volumetric hardening, an elliptical yield function is used and an associated flow rule is assumed. For shear hardening, a yield function of hyperbolic type and a non-associated flow rule that incorporates a dilation angle is employed. The field observations used in the optimization analysis are selected from inclinometers measurements and surface settlements at stage 7 of the excavation.

Since the stiffness of stiff clay is different around the excavation (Calvello 2002) and the primary deviatoric modulus E_{50}^{ref} in the soft to medium clay and the stiff clay layers, are the most influential parameters on the behavior of the excavation (Finno and Calvello 2005), E_{50}^{ref} of the soft to medium clay and stiff clay layers are identified by GA approach. The E_{50}^{ref} of fill layer is also identified, because surface settlements are used in the inverse analysis. The other Hardening Soil model parameters for Chicago clays are kept fixed as shown in Table 3-1.

The range of $(E^{ref}_{50})_{fill}$, $(E^{ref}_{50})_{med}$, and $(E^{ref}_{50})_{stiff}$ values is assumed to be in the following intervals:

$$3000 \leq (E^{ref}_{50})_{fill} \leq 35000 \text{ kPa}$$
$$3000 \leq (E^{ref}_{50})_{medium\ clay} \leq 35000 \text{ kPa}$$
$$40000 \leq (E^{ref}_{50})_{stiff\ clay} \leq 200000 \text{ kPa}$$

These intervals define the boundaries of the research space for GA optimization. The increment changes of the parameters in this research spaces are as following: $\Delta(E^{ref}_{50})_{med} = \Delta(E^{ref}_{50})_{fill} = 500$ kPa and $\Delta(E^{ref}_{50})_{stiff} = 2500$ kPa. According to this research space and measured deformations of the excavation, a solution set is identified by GA as shown in Figure 3-6. The convergence for this analysis takes about 2 days with an office computer. From this set, an ellipsoid is estimated by PCA, Figure 3-6. The ellipsoid characterizes the solution set. Figure 3-6 shows that the ellipsoid is elongated in the directions of (E^{ref}_{50}) stiff clay and (E^{ref}_{50}) fill, which implies the model is more sensitive to the medium clay modulus, $(E^{ref}_{50})_{med}$, than to moduli of fill and stiff clay layer. In this set, the optimal parameter values estimated by GA are as follows:

$(E^{ref}_{50})_{fill}$ = 28000 kPa

$(E^{ref}_{50})_{medium\ clay}$ = 5500 kPa

$(E^{ref}_{50})_{stiff\ clay}$ = 172500 kPa

Figure 3-7 shows that these parameter values reproduce the horizontal displacements measured by the inclinometers as well as the observed settlements for stage 7 of the excavation reasonably well.

3.3.3. Learning of global excavation response using SelfSim learning approach

SelfSim is applied to the Lurie Research Center whereby lateral soil movements in proximity to the wall and surface settlements corresponding to the known construction stages for all stages of the excavation are used as boundary conditions for SelfSim learning. The inclinometers were located 5 ft behind the sheetpile wall, and therefore the lateral deflections used during SelfSim learning are applied in the finite element analysis at the same location for all elevations. Each soil layer is modeled with a different NN soil model.

Prior to any learning, initial soil constitutive models using the NN base module were developed to represent linear elastic response within a small strain range of 0.1%. This analysis underestimates lateral wall deformations and surface settlements, but gives a qualitatively reasonable deformed shape. Several SelfSim learning cycles are conducted at each excavation stage. After a few passes of SelfSim learning, the calculated deformations match reasonably with the measured values.

Figure 3-8 shows the deformations after 12 SelfSim learning passes (Hashash et al. 2006). This SelfSim learning takes about few hours with an office computer. The computed deformations using soil models extracted through SelfSim learning are similar to the field measurements, although there are some noticeable discrepancies in the initial two stages between the computed and the measured soil movements. One possible reason for these differences is the large measured surface settlement associated with the behavior of the pavement material and/or near-surface fill. These relatively large surface settlements at the early stages were likely caused by cyclic motions induced by the vibratory hammer used to install the sheeting, and thus are not considered in the learning process.

3.3.4. Comparison of global excavation response

Comparison of computed lateral deformations and surface settlement from GA and SelfSim for the stage 7 of excavation are shown in Figure 3-9. Since both analyses used the inclinometer measurement of the stage 7 of excavation, computed lateral deformation of SelfSim and genetic algorithm match reasonably with the measurements.

Although the settlement profile was also used in GA optimization analysis, it appears that the Hardening-Soil model used in the FE model is not capable of reproducing the settlement profile behind the wall, neither in magnitude nor in shape. The Hardening-Soil model version used in this study does not have small strain non-linearity and thus could not represent the stiffness variation over the range of strain levels that diminishes with further distance from the wall. Therefore, the computed surface settlements do not perfectly match with the measured values.

The ratio of area under wall deflection divided by the area under settlement profile for measured, SelfSim result, and GA based optimization is 1.9, 1.6, and 1.3, respectively. Therefore, based on volume calculation of the area under wall deflection and settlement profile, closer match of SelfSim and Measured values is reconfirmed.

Since SelfSim in not preconstrained to the limitation of conventional constitutive models, it can capture the settlements more reasonably. SelfSim can also provide computed deformations in intermediate stages of excavation.

3.3.5. Comparison of extracted soil behavior after GA and SelfSim learning

The stress paths for selected elements, shown in Figure 3-4, are compared in Figure 3-10. It is observed that stress paths in the clay layers primarily are elastic. This confirms Finno and Calvello (2005) conclusions that the primary deviatoric modulus E_{ref}^{50} have the most influence on the behavior of an excavation through the compressible clays in Chicago.

The stress paths before and after SelfSim learning are illustrated in Figure 3-11. The NN soil model evolved from reflecting linear elastic soil response, such that it is able to learn relevant soil behavior, including small strain nonlinearity, essential to compute the shape of the settlement trough. The stress paths for the top soft layers are more non-linear than the bottom layers. The comparison of Figure 3-10 and Figure 3-11 shows that in unloading condition (i.e. element E), the extracted soil behavior from both analyses is

closer to an elastic response. For elements located in retained soil (i.e. element A, B, C, D), the mean stress extracted from SelfSim analysis is decreasing with shearing during the excavation steps. The SelfSim extracted stress paths demonstrate a nonlinear response for all clay layers and the sand layer. The SelfSim analysis shows that elements A, B and C undergo shearing almost identical to the Plane Strain Active (PSA) mode. Element A and B in the retained soil reach a peak strength and undergo some strain softening afterwards. However the mean stress during excavation from GA analysis is constant for all layers other than the sand layer. Therefore the stress paths from GA analysis for all clay layers show qualitatively an elastic behavior.

Figure 3-12 shows the comparison of stress paths after using genetic algorithm and SelfSim learning for the lake sand layer. The friction angle envelope is shown in this figure. Under plane strain conditions, the out-of-plane component of strain is equal to zero. This constraint reduces the degree of freedom that individual soil particles can move in relation to one another, thus increasing geometric influence (Terzaghi et al. 1996) . Therefore the triaxial friction angle is converted to plane strain friction angles as indicated in Table 3-1. Both analyses show a nonlinear stress path for lake sand layer. SelfSim analysis is not using any predefined stress strain relationship, nevertheless the stress paths for SelfSim analysis shows that it is consistent with the friction angle line.

Figure 3-13 shows the comparison of stress paths using genetic algorithm and SelfSim learning for clay layers. For simplicity in SelfSim learning the coefficient of earth pressure at-rest is constant through the soil layers, but in genetic algorithm the coefficient of earth pressure is varied through the soil layers. Genetic algorithm analysis shows an elastic stress path for all clay layers. The stress paths obtained after SelfSim learning for clay layers show a distinct nonlinear soil behavior. This observation can explain why the surface settlement predictions in genetic algorithm are not as accurate as settlement predictions in SelfSim. Since the small strain non linearity of soil is reasonably captured with SelfSim learning approach, the surface settlement match with the measured values (Hashash et al. 2006; Song et al. 2007). The stress path for all clay layers particularly element B which is in soft/med clay layer shows that they are consistent with friction angle envelope.

Both GA and SelfSim could reproduce the wall deformations reasonably well; however comparison of stress paths show that SelfSim approach could extract the underlying soil behavior more reasonably than hardening soil model used in the GA optimization approach. The outcome would differ if a different material constitutive model is used in the GA approach

SelfSim learning is based on soil horizontal displacement measurements and settlements which permit the capture of the soil non linear behavior. However, this method is independent of any constitutive model. In contrast, GA optimization is based on the calibration of an existing soil constitutive model on soil horizontal displacement measurements and settlements. This method permits the use of well known conventional geotechnical models (often used in engineering) from which some of parameters can be evaluated independently through an optimization. However, the choice of the constitutive model mainly influences the final soil behavior in GA optimization. SelfSim allows for the discovery of new material behavior while GA optimization assists engineers in use of existing material models through a better selection of material model parameters.

3.4. Summary

Field data are integrated with numerical models to simulate complex geotechnical problems. Inverse analysis techniques are powerful numerical tools to evaluate performance of geotechnical structures and extract soil behavior. Two inverse analysis methods are evaluated using data measured at the Lurie Center case study in Chicago. Optimized parameters found from the GA approach and the learned constitutive responses from SelfSim formed the basis of simulations that could reasonably compute deformations observed during the excavation for the Lurie Center. Unlike GA analysis in which the soil model has to be preconstrained to specific model (in this study soil hardening model), SelfSim analysis is able to produce continuously evolving material models that can learn new material behavior. This capability allows SelfSim to capture the underlying soil behavior learning measurements at different construction stages. Optimization based on genetic algorithm could predict the inclinometer measurements very well, but the stress paths for this method show linear elastic behavior for clay layers, a feature of the hardening soil model and the undrained simulation. On the other hand SelfSim is able to capture nonlinearity of soil behavior. This feature explains why the

ANN model is able to compute settlement profile reasonably well. The computational demands of both methods vary, though they require skilled users. SelfSim allows for the discovery of new material behavior while GA optimization assists engineers in use of existing material models through a better selection of material model parameters.

Hardening soil Parameters	Fill layer	Lake Sand layer	Soft to medium clay layer	Stiff clay layer	Hard clay layer
Type	Drained	Drained	Undrained	Undrained	Undrained
E_{50}^{ref} (kPa)	*Studied Parameter*	48000	*Studied Parameter*	*Studied Parameter*	$\left(1.5 \cdot E_{50}^{ref}\right)_{Stiff}$
E_{oed}^{ref} (kPa)	13500 *	48000 *	$0.7 \cdot E_{50}^{ref}$ *	$0.7 \cdot E_{50}^{ref}$ *	$0.7 \cdot E_{50}^{ref}$ *
E_{ur}^{ref} (kPa)	40500 *	144000 *	$3 \cdot E_{50}^{ref}$ *	$3 \cdot E_{50}^{ref}$ *	$3 \cdot E_{50}^{ref}$ *
Power coefficient m	0.5	0.5	0.8 *	0.85 *	0.6
p^{ref} (kPa)	100 *	100 *	100 *	100 *	100 *
Cohesion c (kPa)	19	0.2 *	0.2 *	0.2 *	0.2 *
Friction angle φ (º)****	30	35 ***	26 *	32 *	35 ***
Dilatancy angle ψ (º)	2	5 *	0 *	0 *	0 *
ν_{ur} -poison ratio unloading/reloading	0.2 *	0.2 *	0.2 *	0.2 *	0.2 *
OCR	1 **	1.1 **	1.4 **	1.5 **	2.5 **

* (Calvello and Finno 2004)
** (Chung and Finno 1992)
*** (Finno and Calvello 2005)
**** The converted friction angles of lake sand, soft to medium clay, stiff clay and hard clay for plain strain condition are considered 40, 30, 36, and 39 degrees respectively. (Ladd and Edgers 1972; Terzaghi et al. 1996; Pestana et al. 2002)

Table 3-1 Hardening soil parameters for each soil layers of the Lurie Center

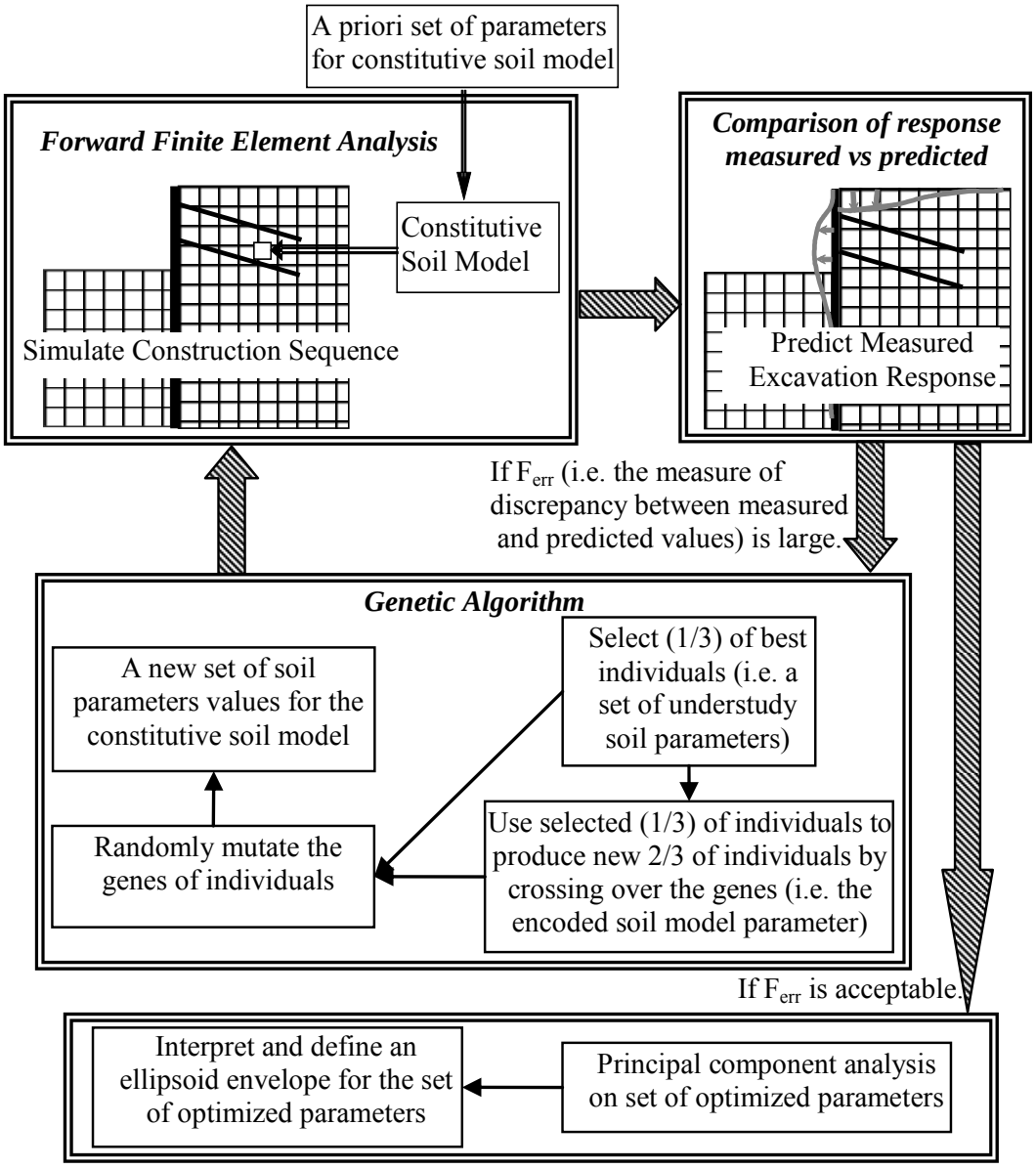

Figure 3-1 Application of GA optimization to deep excavation problems

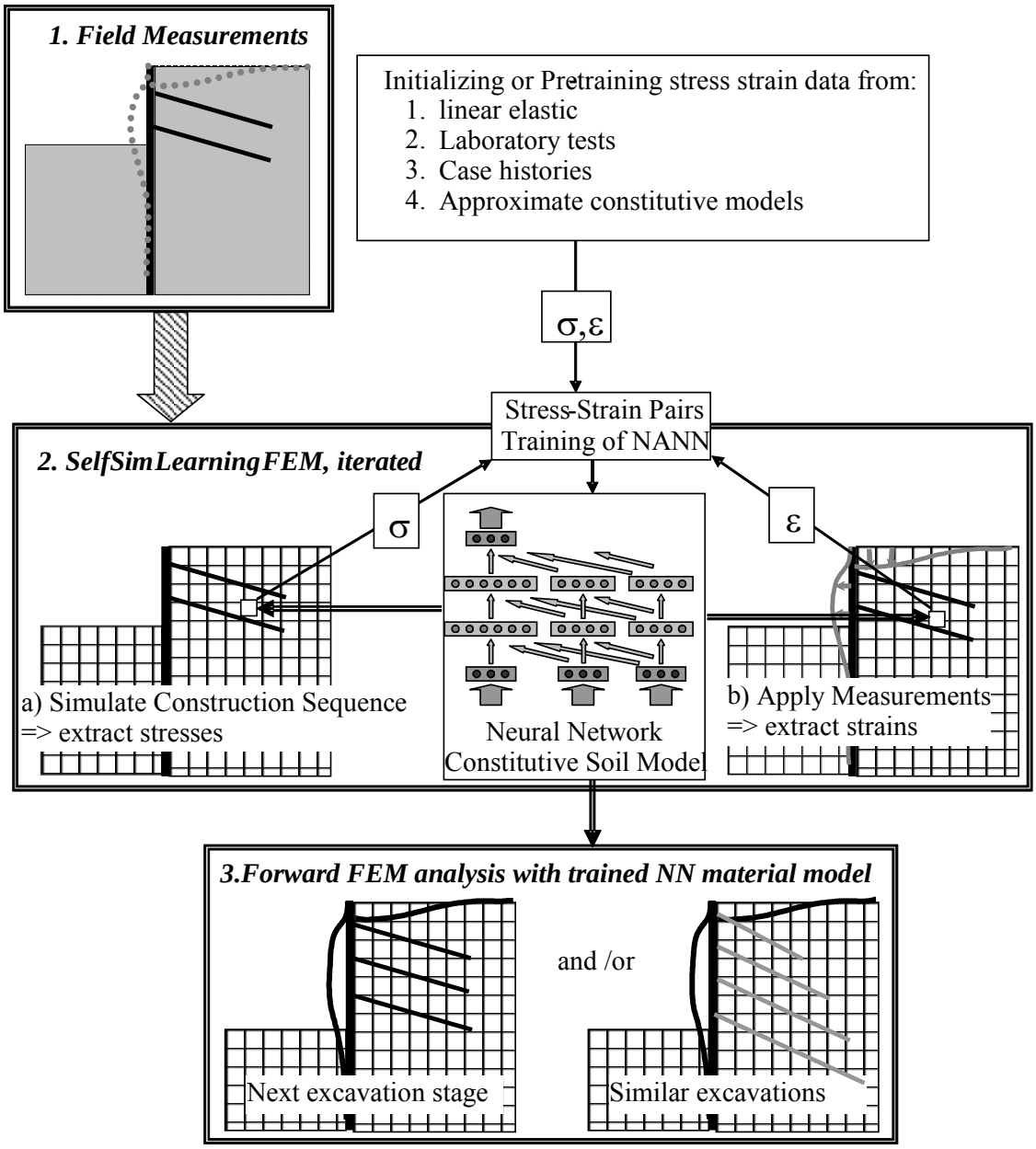

Figure 3-2 Application of self-learning simulations to Lurie deep excavation

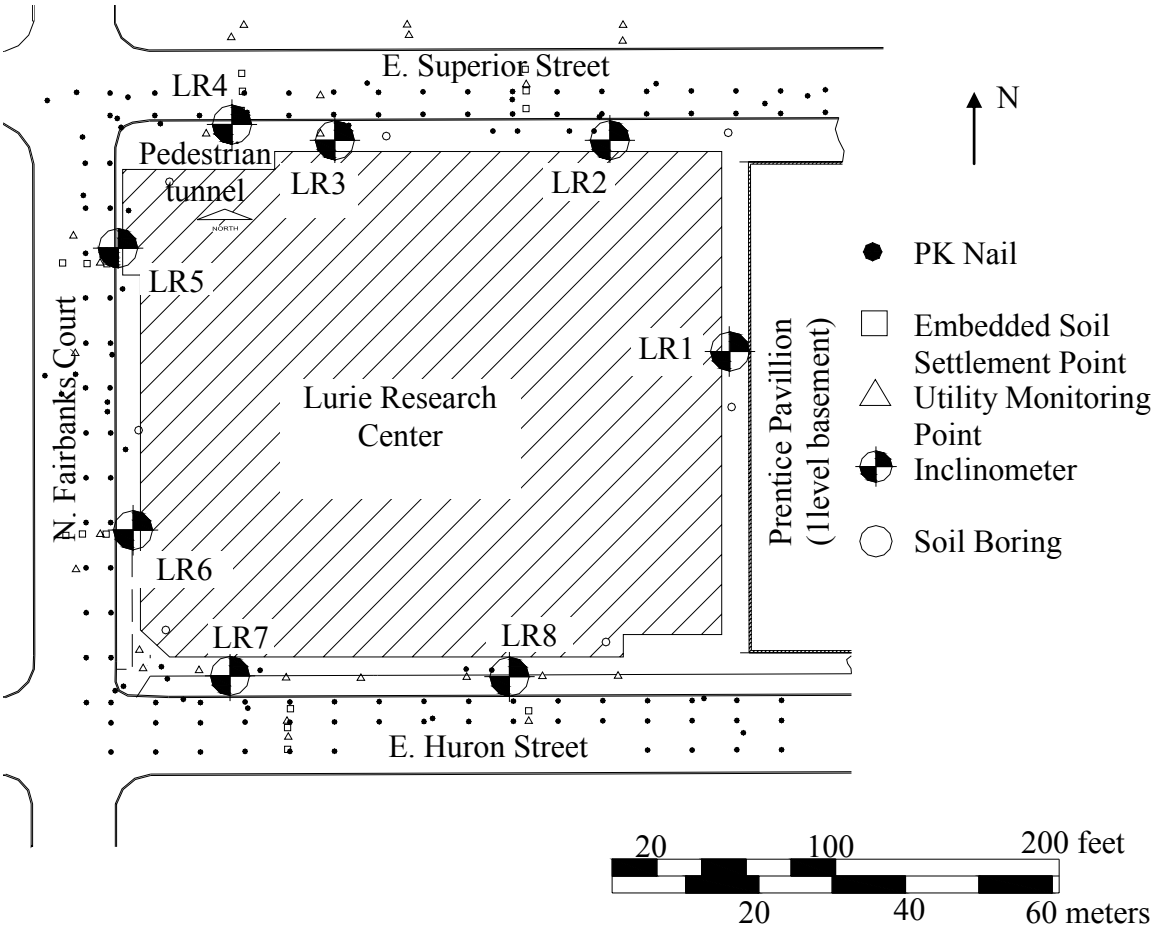

Figure 3-3 Plan view and instrument locations of Lurie Center excavation

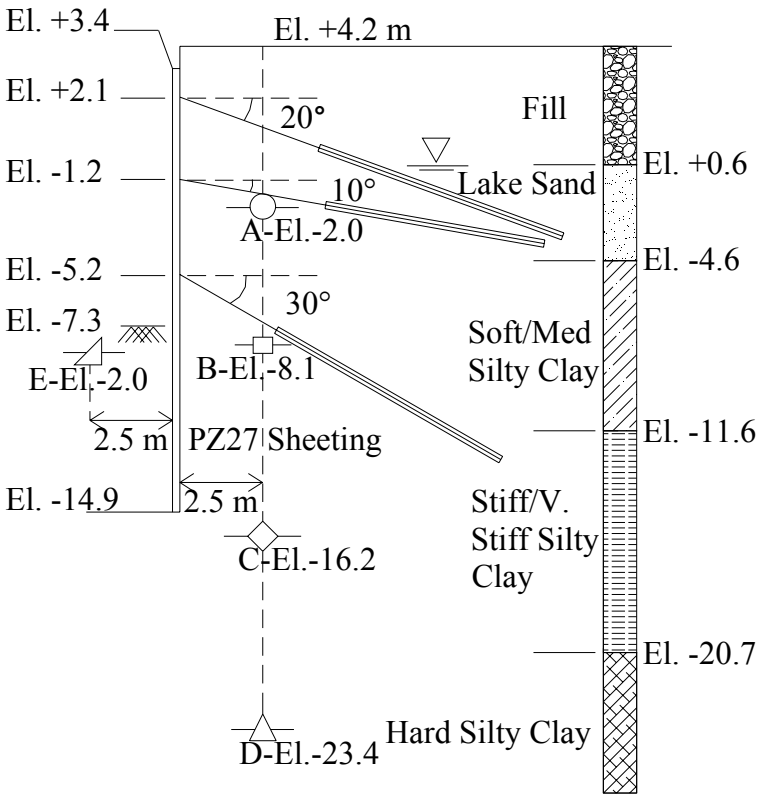

Figure 3-4 Cross section of the wall, soil layers and location of elements for extracted stress paths

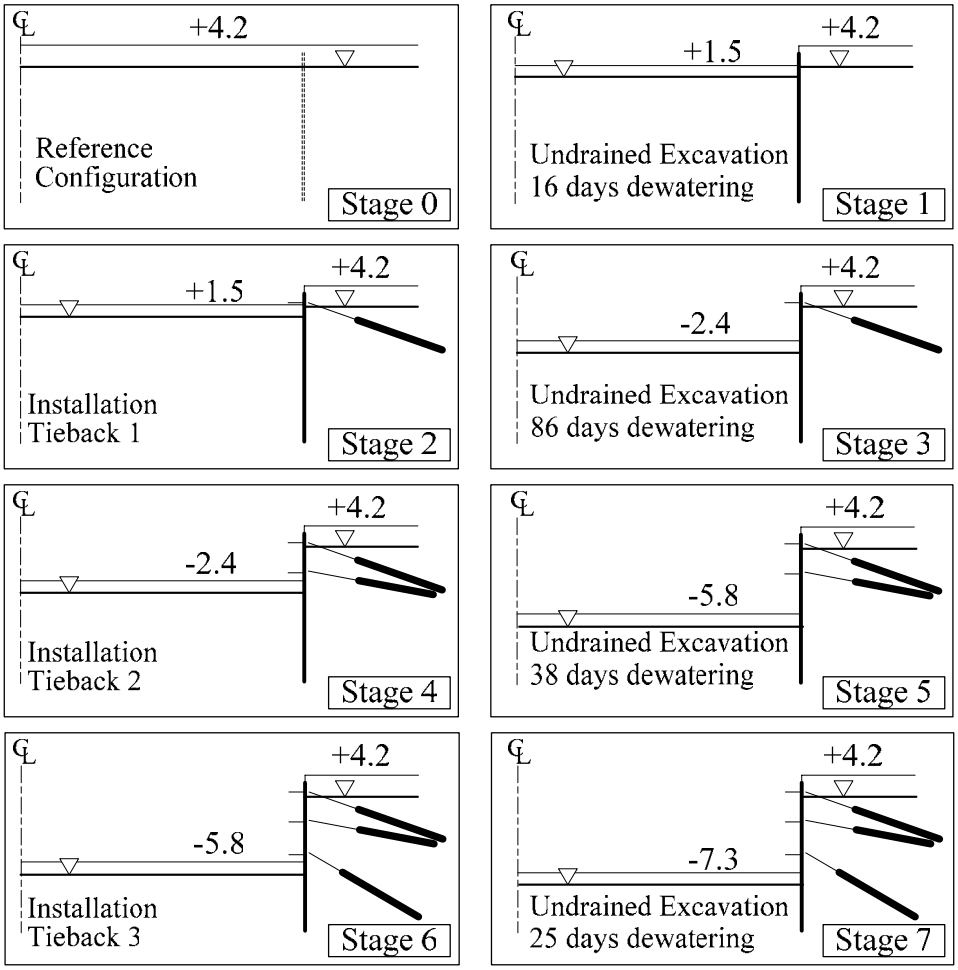

Figure 3-5 Construction sequence of Lurie Center excavation site

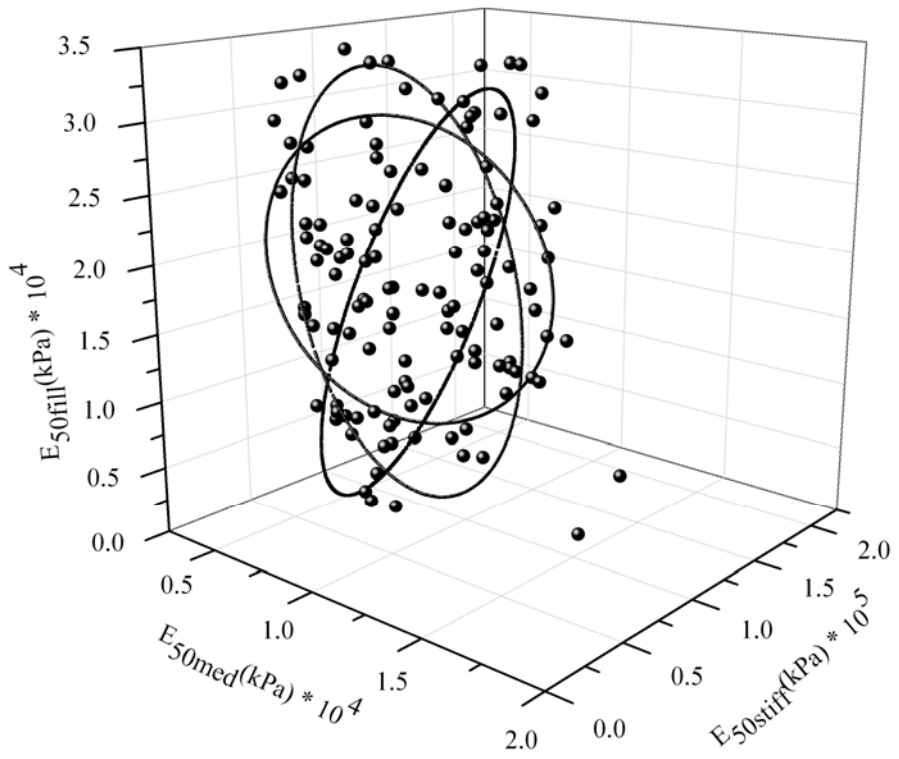

Figure 3-6 Solution set identified by GA and estimated ellipsoid using wall deformation and surface settlements

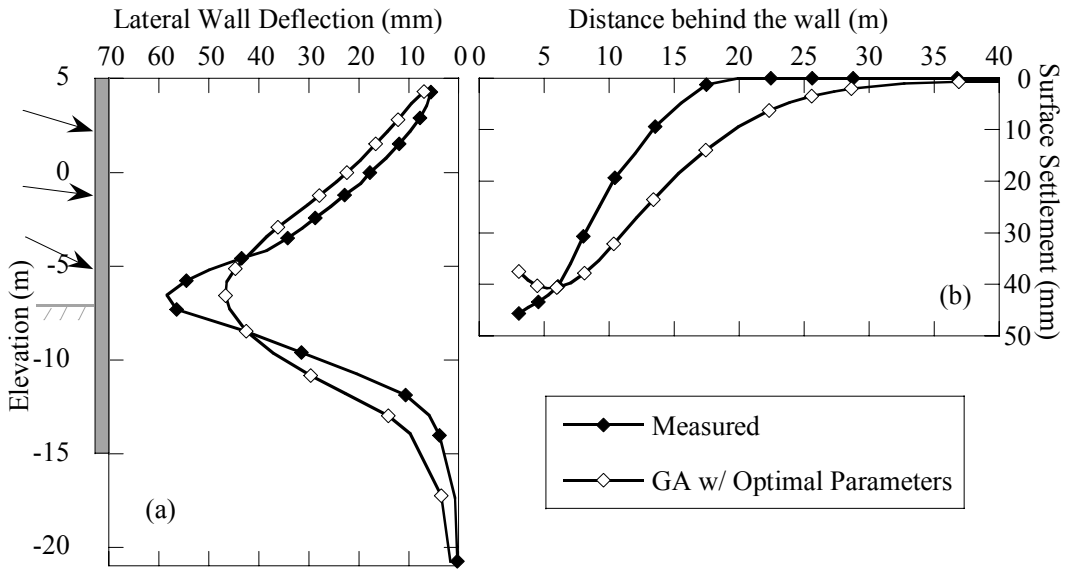

Figure 3-7 Comparison of computed (a) lateral wall deformation and (b) surface settlement using GA method with optimal parameter values

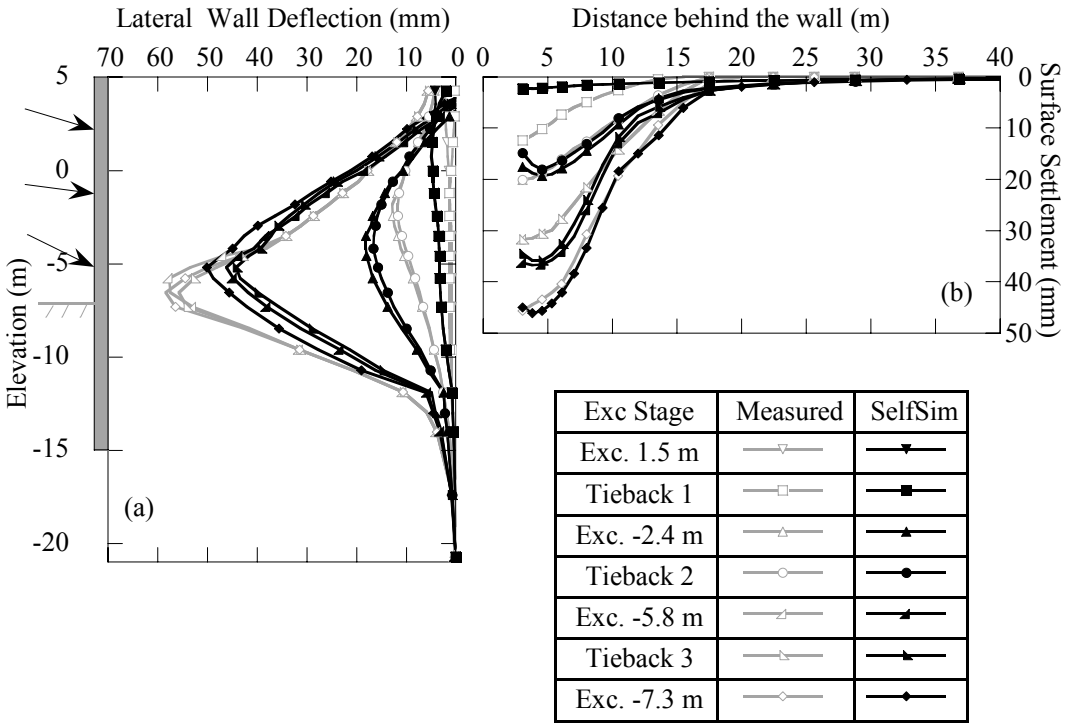

Figure 3-8 Computed (a) lateral wall deformations and (b) surface settlements after 12 passes of SelfSim learning

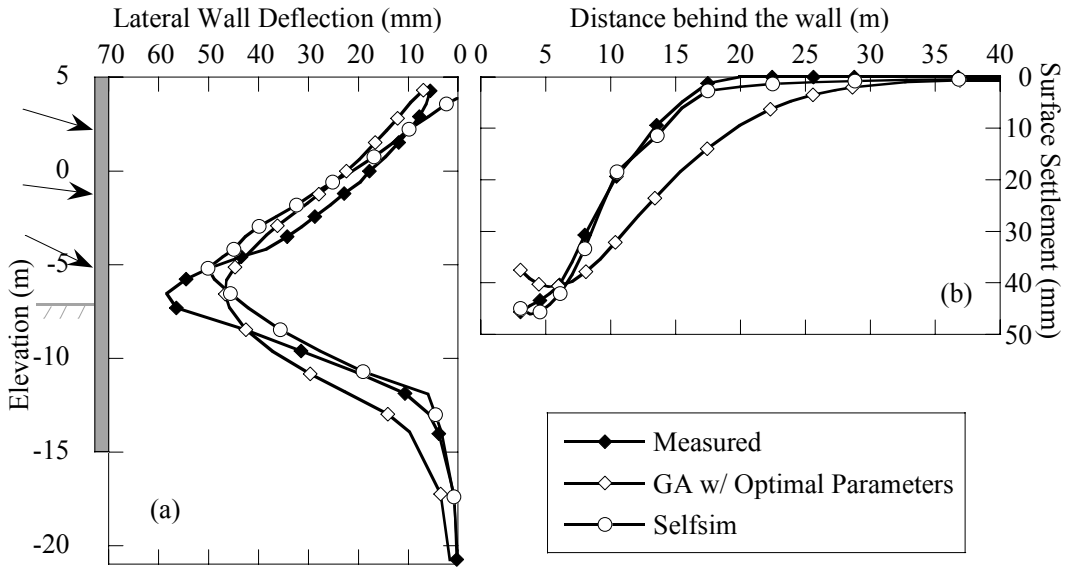

Figure 3-9 Comparison of computed (a) lateral wall deformation and (b) surface settlement using GA and SelfSim for the stage 7 of excavation

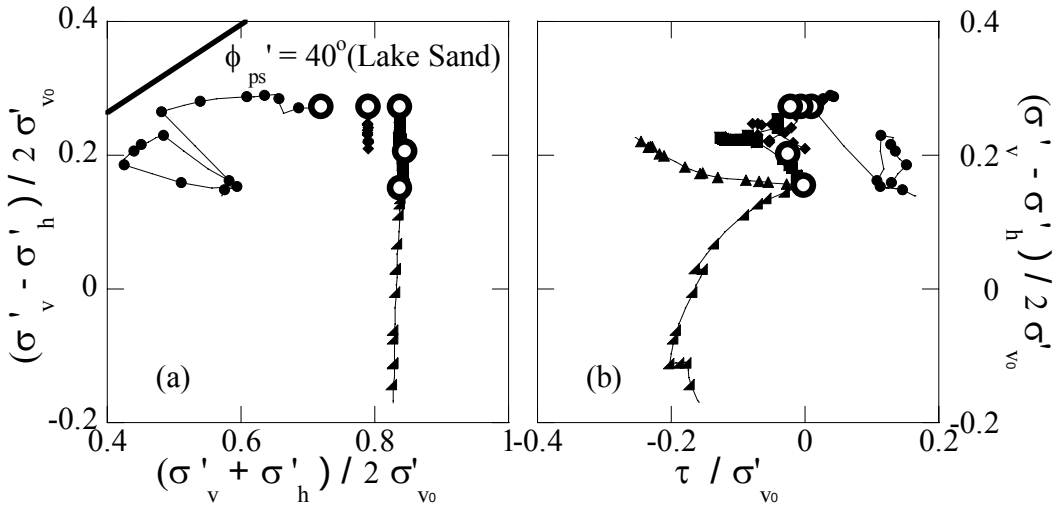

	GA w/Opt	Soil Layer
A	—●—	Lake Sand
B	—■—	Soft/Med Silty Clay
C	—◆—	Stiff/V.Stiff Silty Clay
D	—▲—	Hard Silty Clay
E	—◀—	Soft/Med. Silty Clay

Figure 3-10 Normalized stress paths of (a) p'-q, and (b) τ-q for elements A, B, C, D, E after using GA analysis method with optimal parameter values

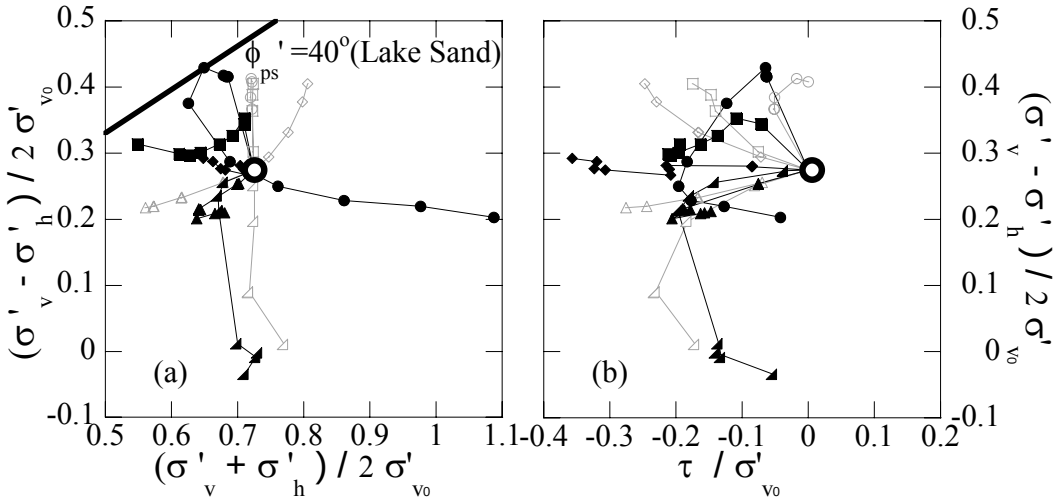

	Prelearning	SelfSim	Soil Layer
A			Lake Sand
B			Soft/Med Silty Clay
C			Stiff/V.Stiff Silty Clay
D			Hard Silty Clay
E			Soft/Med Silty Clay

Figure 3-11 Normalized stress paths of (a) p'-q, and (b) τ-q for elements A, B, C, D, E before and after SelfSim learning

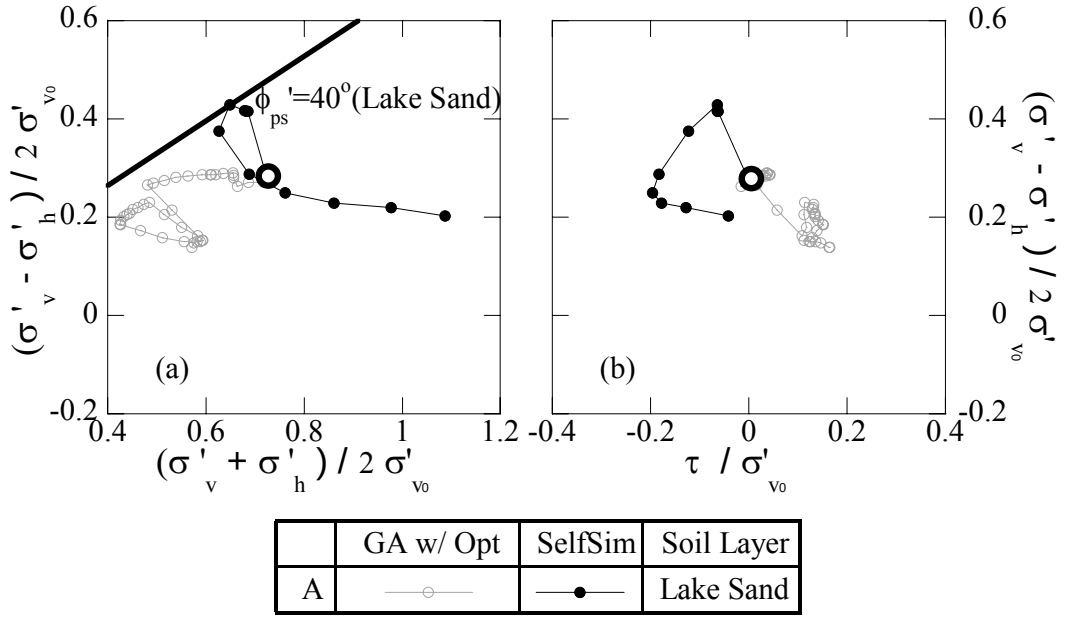

Figure 3-12 Normalized stress paths comparison of (a) p'-q, and (b) τ-q for element A after using GA with optimal parameter values and SelfSim in lake sand layer

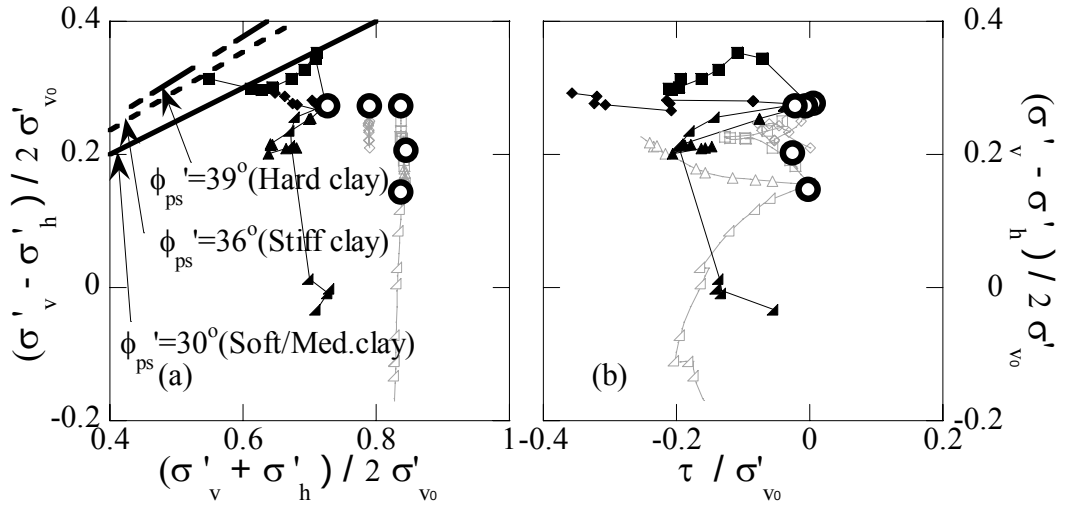

	GA w/ Opt	SelfSim	Soil Layer
B			Soft/Med Silty Clay
C			Stiff/V.Stiff Silty Clay
D			Hard Silty Clay
E			Soft/Med Silty Clay

Figure 3-13 Normalized stress paths comparison of (a) p'-q, and (b) τ-q for elements B, C, D, E after using GA with optimal parameter values and SelfSim in clay layers

CHAPTER 4 THE INTERPLAY BETWEEN FIELD MEASUREMENTS AND SOIL BEHAVIOR FOR CAPTURING SUPPORTED EXCAVATION RESPONSE

4.1. Introduction

Although installing instruments at an excavation site is an important element to control and monitor the soil behavior, there are several limitations to field monitoring: 1) the instruments are installed at discrete locations around the excavation site and cannot provide a complete picture of ground response everywhere around the site; 2) the number of installed instruments is limited since their installation, maintenance, and data collection can be costly; and 3) instruments can be damaged or become inaccessible due to construction activities. On the other hand numerical models, if reliable, can present a complete picture of gound response to excavation inexpensively. However the successful use of numerical simulations is highly dependent on the constitutive model chosen to represent soil behavior.

Inverse analysis techniques are used to improve or calibrate soil models and enhance the ability of the numerical analysis to estimate excavation performance. In this chapter the use of SelfSim inverse analysis and numerical modeling as a tool to complement instrumentation measurement to develop a more complete estimate of excavation performance at a given construction stage is explored, Figure 4-1. It is common to use field measurements from one excavation project to improve a numerical model to predict performance at later excavation stages or performance of nearby excavations. Self-learning inverse analysis framework, (SelfSim), introduced by Hashash et al. (2006) is used to extract soil behavior from instrument measurements. It is demonstrated that the extracted soil model can be used to predict the excavation response elsewhere around the excavation. Thus numerical modeling and inverse analysis would provide information on performance in areas where no instrumentation is available, i.e. fill-in-the-gaps.

The study explores: 1) the inter-relationship between instrument type and location and the quality of extracted soil behavior; 2) the potential redundancy in the extracted soil behavior information from different instruments; and 3) the best deployment of

instruments so that a more complete picture of excavation performance is known. These finding are especially valuable should some instruments at the site be damaged or become inaccessible or when budget constraints limit the number of instruments that can be deployed.

A simulated excavation is used to examine the effect of inclinometer locations, piezometers, extensometers, heave gauges, and strut loads on the quality of extracted soil behavior using synthetically measured excavation performance. Some of the findings are then illustrated using a well instrumented deep excavation case history in Taipei, Taiwan.

4.2. SelfSim-learning simulations of deep excavations

SelfSim framework application to excavation problems in this chapter is illustrated in Figure 4-1 (Hashash et al. 2003; Hashash et al. 2006; Hashash 2007; Song et al. 2007). The deformations of the excavation are measured at selected excavation stages (Step 1). A NN based constitutive model is used to simulate the soil response. Initially the soil response is unknown and the NN soil model is pre-trained using stress–strain data that reflect linear elastic response over a limited strain range. In Step 2a of SelfSim a finite-element (FE) analysis using the current NN soil model is performed simulating construction sequences (i.e. soil removal and support installation). In Step 2b of SelfSim a parallel FE analysis using the same NN soil model is performed in which field measurements are imposed as additional displacement boundary conditions. The stress field from Step 2a and the strain field from Step 2b are extracted to form stress–strain pairs that approximate the soil constitutive response and are used to retrain the NN soil model. The solution converges when the analysis of Step 2a provides the correct ground deformation, i.e., analyses of Steps 2a and 2b provide similar results.

The resulting NN constitutive model can be used in the analysis of other types of excavations in similar ground conditions or a later excavation stage. Alternately the extracted constitutive model can be used in an FE analysis to provide a more complete estimate of excavation behavior at a given excavation stage in areas where no instruments are available as illustrated in Figure 4-1.

4.3. Relationship between instrumentation layout and extracted soil behavior via a simulated excavation

Marulanda and Hashash (2007) and Song et al. (2007) employed SelfSim inverse analysis framework to show a strong relationship between instrumentation layout for a few instruments and the quality of extracted soil behavior. In this section an extensive numerical study is presented for an idealized braced excavation in soft soil to examine the relationship between various instruments typically used on an excavation project and the quality of information that can be extracted for excavation modeling. The field measurements are generated synthetically using a coupled pore-water pressure-effective stress FE model of the braced excavation whereby soil behavior is represented using the MIT-E3 effective stress soil model (Hashash 1992) to represent Boston Blue Clay behavior. The MIT-E3 model (Whittle and Kavvadas 1994) simulates important features of soil behavior including anisotropic stress–strain–strength relationship, small strain nonlinearity, and hysteretic response upon load reversal.

Inclinometers, surface settlement points, extensometer, piezometer, strain gauges, and heave gauge are placed at selected locations within the excavation site, Figure 4-2. The 15-m deep excavation which has an equivalent 0.9-m thick concrete wall is supported by 2.5 m spacing struts. The cross section of the excavation, instrument locations and construction sequence are shown in Figure 4-2 as well. In this model excavation, the assumed soil profile includes a very deep 50-m soft clay (OCR=1.3) layer. The ground water table is 2.5 m below the ground surface.

The SelfSim inverse analysis framework is used to extract the underlying soil behavior using several combinations of instrument measurements and to examine instrumentation layout effect on the extracted soil behavior. The instrumentation layouts employed are: 1) wall deformations only; 2) wall deformations and surface settlements; 3) wall deformations and lateral deflections from inclinometers at various distances from the wall; 4) wall deformations, surface settlements, and strut loads; 5) wall deformations, lateral deflection from inclinometer I4 shown in Figure 4-2, and strut loads, 6) wall deformation, surface settlements, and pore water pressures; and 7) all instruments shown in Figure 4-2 except strut loads.

Two indices are used to evaluate the learned instrument response and extracted soil behavior as they were used by Marulanda and Hashash (2007). For all instrument readings, $M_{La,}$ which is the measured limits of agreement (Bland and Altman 1986), measures the agreement between the computed deformations and their corresponding measured values. The differences between measured and computed response are calculated. Then, the mean and the standard deviation are computed for these differences to estimate the limits of agreement defined by Bland and Altman (1986). The limits of agreement are defined by the mean of the differences ($\overline{d}$) plus or minus two standard deviations ($2s$):

$$L_a^{+} = \overline{d} + 2s$$
$$L_a^{-} = \overline{d} - 2s \qquad (1)$$

L_a^+ and L_a^- are the upper and lower limits of the absolute value of the differences between measured and computed response, whereby 95% of differences lie between these limits (Bland and Altman 1986). The magnitude of the interval from L_a^+ to L_a^- is referred here as the M_{La}:

$$M_{La} = (L_a^{+}) - (L_a^{-}) \qquad (2)$$

A small value for M_{La} represents better agreement between the measured and computed values.

For a measure of quality of extracted soil behavior, the differences of stress-strain response between the correct behavior (soil behavior is known in the simulated excavation) and extracted behavior are quantified using the concordance correlation coefficient (CCC) presented by Lin (1989). The CCC ranges from -1 to 1, where 1, -1 and zero mean perfect agreement, perfect reverse agreement, no agreement, respectively. The CCC is estimated using the mean ($\overline{Y}_j$), variance ($S_j{}^2$) and covariance ($S^2{}_{ij}$) of the stresses and strains as follows:

$$CCC = \frac{2S_{12}}{S_1^2 + S_2^2 + (\overline{Y}_1 - \overline{Y}_2)^2} \qquad (3)$$

Where

$$\overline{Y}_j = \frac{1}{n}\sum_{i=1}^{n} Y_{ij}$$

$$S_j^2 = \sum_{i=1}^{n} (Y_{ij} - \overline{Y}_j)^2,\ j = 1,2 \qquad (4)$$

and

$$S_{ij}^2 = \frac{1}{n}\sum_{i=1}^{n} (Y_{i1} - \overline{Y}_1)(Y_{i2} - \overline{Y}_2)$$

In particular, Y_1 and S_1 correspond to the mean and the variance of computed values of stresses or strains, and Y_2 and S_2 correspond to the mean and the variance of measured values of stresses or strains. S_{12} is the covariance between computed and measured values. For CCC values the suffixes of 11, 22, and 12, reflect the horizontal, vertical, and shear components of stresses (σ) and strains (ε). Although CCC is a good measure for the purpose of comparison between extracted soil behaviors in this study, it is worth mentioning that it is not sufficiently illustrating the difference of extracted soil behavior for each individual element.

4.3.1. Learning from measurement of inclinometer in the wall (I1) and surface settlements points

In a typical excavation, measurement of wall deformations is considered to be of utmost importance. SelfSim learning is conducted using lateral wall deflection (I1) measurements only and the extracted soil model is then used in an FE simulation to compute the excavation behavior. Figure 4-3 shows that the model captures wall deflections (I1) very well but does not provide a very good match for surface settlement (not used in SelfSim learning). Figure 4-3 shows that the lateral movements of I2 and I3 are captured reasonably well, and the lateral movements of I4 are slightly overestimated, but the vertical movement of E1 is underestimated. Therefore, using wall deformations is important, but does not provide sufficient information for learning global excavation behavior.

SelfSim learning is then conducted with measurements of wall deflections (I1) and surface settlement points and the extracted soil model is used in an FE simulation to compute the excavation response. Figure 4-4 shows that the model is able to reproduce both learned measurements well. The lateral movements of I2 and I3 are captured

reasonably well. The lateral movements of I4 and vertical deformations of E1 have improved, however they do not match well the measured values. The vertical movements of H1 are slightly underestimated. Therefore the extracted soil behavior through SelfSim inverse analysis using measurements of inclinometer in the wall (I1) and surface settlement points contains enough information about the soil behavior to provide a reasonable estimate of the overall excavation behavior.

4.3.2. Learning from inclinometer measurements at different locations behind the wall

SelfSim learning is conducted using measurements of I1 (inclinometer in the wall) or surface settlements points and I3 or I4 (see Figure 4-2) to evaluate the effect of inclinometer location on extracting the excavation behavior.

Figure 4-5 shows the computed surface settlement, wall deformation, lateral movement of I2, I3, I4, vertical movement of E1 and vertical movement of H1 after SelfSim learning with measurement of inclinometer in the wall (I1) and inclinometer I3. The lateral deformations of I1 and I3 (used in learning) match the measurements. Comparison of Figure 4-5 and Figure 4-3 also shows that the computed surface settlements (which were not used in learning) are improved by using an inclinometer at distance from the wall. However the lateral deformation of inclinometer I4 is overestimated and the vertical movements of E1 and H1 are underestimated.

Figure 4-6 shows the extracted excavation behavior after learning with measurement of inclinometer in the wall (I1) and inclinometer I4. The lateral deformations of inclinometer I1 and I4 match well the measured values. The computed surface settlements (which were not used in learning) are significantly improved compared to the computed settlements in Figure 4-3 and Figure 4-5.

SelfSim learning was also conducted using surface settlements measurements with lateral deformations of inclinometers I3 and I4. The computed lateral deflections of inclinometers I1, I2, I3, and I4 and vertical movements of E1 and H1 and surface settlements do not match well with the measured values. It appears that lateral deformations of an inclinometer in close proximity to the wall have important information that cannot be replaced by the surface settlement points or even inclinometers at some distance from the wall.

Figure 4-7 provides a quantitative measure, M_{La}, of the quality of predicted response for surface settlements, I1, I2, I3, I4, E1 and H1 after learning with selected instruments. Lower M_{La} values imply better match with the observations. The prediction of excavation behavior using measurements of lateral movements of the wall and inclinometers at farther distances from the wall (i.e. I3 and I4) is improved compared to the case where only wall deformations are used in SelfSim learning. Using an inclinometer which is farther away from the excavation in addition to the deformations of the wall provides valuable information about small strain non-linearity of the soil and therefore, lowers M_{La} values. This figure also shows that the M_{La} value for settlements predictions of the case whereby wall deformation and inclinometer I3 or I4 are used in SelfSim learning is close to M_{La} value for the case where wall deformations and surface settlements are used in SelfSim learning. So it appears that inclinometers at some distance from the wall provide redundant measurements that can be used to obtain surface settlement estimates especially when settlement points are damaged and are no longer accessible. The closer the inclinometer is to the wall, the better the extracted behavior is. By locating the inclinometer at greater distances from the wall (SS+I3 & SS+I4), the ability to predict measurements at other locations within the excavation deteriorates significantly.

Figure 4-8 shows similar trends for the extracted soil behavior (as CCC approaches 1, the extracted behavior approaches the correct behavior) which is quite poor for SS+I3 & SS+I4 cases, and acceptable for I1+I3 and I1+I4. In all the cases that wall deformations are used in SelfSim learning, the stresses and strain are reasonably matched with the correct values.

4.3.3. Learning from strut loads, piezometers, and all instruments

Strut loads

SelfSim learning is conducted with measurements of inclinometer in the wall (I1), surface settlements points and strut loads to evaluate the strut load (SL) effects on extracted soil behavior, Figure 4-9. Overall the resulting estimates for I1, I2, I3, E1 and SS are similar to those from the case where wall deformations (I1) and surface

settlements used in SelfSim learning (Figure 4-4). The computed lateral movements of I4 and vertical movements of H1 have improved.

SelfSim learning is conducted using lateral deformations of the wall, inclinometer I4, and strut loads to include both effect of strut load and inclinometer at a distance from the wall, Figure 4-10. The lateral deformations of I1 through I4, and vertical movement of E1 match reasonably well with the measured deformations. The extracted settlement profile (which was not used in learning) is slightly underestimated (for the last excavation stage), but is, nevertheless, reasonable. The extracted vertical deformation of the heave gauge (H1) is overestimated.

Piezometers

SelfSim learning is conducted with measurements of inclinometer in the wall (I1), surface settlements points and piezometer line (P1), Figure 4-11. Compared to Figure 4-4, whereby wall deformations and surface settlements used, the computed lateral movements of I1, I2, I3 and vertical movements of H1 still match reasonably well with the measured values. However, the computed lateral movements of I4 at stage 6 and vertical movements of E1 have deteriorated. The computed pore water pressures at other locations improved and they are close to the measured values. Therefore, in case studies where pore water pressures are needed, it is beneficial to use pore water pressure measurement in SelfSim learning.

All instruments except strut loads

SelfSim learning is conducted using a total of 7 instruments. Learning is conducted gradually by introducing one instrument at a time: inclinometer in the wall (I1), then surface settlements points, then inclinometer 2 (I2), then inclinometer 3 (I3), then inclinometer 4 (I4), then extensometer 1 (E1), then heave gauge 1 (H1), and then piezometer line 1 (P1) (See the locations in Figure 4-2).

Figure 4-12 shows the computed surface settlement, wall deformation, lateral movement of I2, I3, I4, vertical movement of E1 and H1 after SelfSim learning. The lateral deformations of I1, I2 and I3, vertical movements of E1 and H1 and surface settlements match with measured values. The computed lateral deformations of inclinometers I3 and I4 and vertical movements of E1 in stages 5 & 6 are not as smooth

as the other stages indicating instability in the results. It appears that the use of so many instruments over constrains the problem leading to numerical instability.

Figure 4-13 shows M_{La} values for analyses whereby four different combinations of instruments were used in SelfSim learning. The analyses where strut loads are used in the learning process have low M_{La} values, therefore it appears that strut loads provide important information to evaluate the overall excavation response. The comparison also shows that in cases where the settlement profile is no longer accessible, learning from inclinometers at the wall and some distance away from the wall along with strut loads can extract a model that predicts the overall excavation behavior reasonably well. The pore water pressures do not appear to provide additional information that significantly enhances the quality of computed excavation response. As expected, the use of multiple instruments improves the predicted behavior.

Figure 4-14 shows the comparison of M_{La} values for strut loads. The results show that the model that uses the strut loads in learning process improves significantly the computed strut loads in FE analysis. However, the model that uses all the instruments except strut loads does not predict strut load well.

Figure 4-15 provides CCC values, which is a measure of the accuracy of the extracted soil behavior for extracted stresses and strains. The use of strut loads greatly improves the extracted strains and shows a significantly better match with the measured soil behavior compared to other instrument combinations. This comparison demonstrates that the strut load data is of major importance for the reliable prediction of ground response and can provide information that compensate for other missing instruments.

4.4. TNEC deep excavation case study

The utility of inclinometers at some distance from the excavation wall in estimating ground surface settlements is evaluated using a well instrumented excavation case history in Taipei. The Taipei National Enterprise Center (TNEC) is an 18-story building with five basement levels using top-down construction techniques. In the top-down excavation method concrete floor slabs are used to support the wall. Longer periods of times are required between two subsequent excavation levels leading to the dissipation of pore-water pressure which may have a significant influence on the movements of the wall and soil (Ou et al. 1998).

The site has slightly irregular plan view and occupies an area of about 3500 m^2, as shown in Figure 4-16 and the excavation is 19.7-m deep. Installed instrumentation includes earth pressure cells on the wall, rebar stress meters on the reinforcement cage, piezometers, inclinometers, heave gauges and settlement gauges.

A cross section of the excavation is shown in Figure 4-18. The excavation site consists of six layers of alternating silty clay and silty sand deposits overlying a thick gravel formation. The first and second layers consist of a 5.6-m-thick silty clay (CL) layer and a 2.4-m-thick silty sand (SM) layer, respectively. The third layer is a 25-m-thick silty clay (CL), and it is mainly this layer that affects the excavation behavior. The hydraulic conductivity (k) from one-dimensional consolidation tests is around $4x10^{-6}$cm/s. The fourth layer is a 4-m-thick medium dense fine sand and silty clay. The fifth layer is an 8-m-thick medium to dense silt or silty sand. A gravel formation is located 45 m below the ground surface. Prior to excavation the ground water table was 2 m below the ground surface. A 90-cm-thick and 35-m-deep diaphragm wall was used as the earth-retaining structure.

The TNEC site was excavated down to 19.7 m in seven main stages. Because of a shift observed in measured wall deformations after the fifth stage of the excavation, the measurements of sixth and seventh stages were not used in SelfSim inverse analysis. Therefore in this study the excavation site was modeled with five excavation stages down to a depth of 15.2 m depth, as indicated in Figure 4-19.

4.4.1. SelfSim learning using wall deformations only

A set of SelfSim learning analyses was conducted using wall deformation measurements only. Separate NN material models are assigned for the various soil formations. Prior to any learning, the (NN) material models are trained to reproduce linear elastic behavior. Computed deformations prior to learning are shown in Figure 4-20. The computed deformations differ significantly from and are less than the measured values.

Five SelfSim learning passes are performed using wall deformations only, down to third excavation stage. The SelfSim analysis could not progress beyond this excavation stage using wall deformations only and failed. This might be due to a limitation in the information contained in these additional stages. Figure 4-21 shows plots of computed

and predicted deformations of the ground surface, wall and inclinometers SI-1, SI-2, SI-3 and SI-4. The computed deformations for the first three stages have improved significantly compared to those shown in Figure 4-20. Since SelfSim does not provide a reasonable prediction outside of the learned stress-strain ranges, the predicted lateral wall deflections in the fourth and fifth excavation stages are underestimated. While the deformations of the wall, inclinometer SI-1 and SI-2 match reasonably with the measurements down to the third excavation stage, the surface settlement and deformations of inclinometers farther away from the excavation site (i.e. SI-3, and SI-4) differ from the measured values.

4.4.2. SelfSim learning using wall deformations and an inclinometer farther away

An inclinometer measurement SI-4, 22 m away from the excavation wall is added to the wall deformation measurements as part of further SelfSim learning down to fifth excavation stage.

Figure 4-22 shows the measured and predicted deformations of the excavation after six additional learning passes. The computed lateral deformations of wall (I-1) and inclinometer SI-4 are in close agreement with the measured values. The predicted deformations of inclinometers SI-1, SI-2 behind the wall match reasonably with the actual measurements. The predicted settlement profile has also significantly improved compared to the predictions in Figure 4-21 even though it was not used in learning. This confirms earlier finding that an inclinometer at some distance from the excavation wall has important information about small strain nonlinearity of the soil behavior and the estimate of surface settlements.

Comparison of measured and computed pore pressures for piezometer lines P1, P2 and SP (shown in Figure 4-18) are illustrated in Figure 4-23. The comparison shows the computed pore pressures match reasonably at different depths of the soil profile with the measured values. In Figure 4-24 measured and computed earth pressures are shown for the stage 3 and stage 5 of the excavation. The predicted and measured earth pressures for the stages 1 down to stage 4 match reasonably both in retained soil behind the wall and the passive side in front of the wall. The predicted as well as measured earth pressures are started from at rest condition and they become closer to active and passive conditions for retained soil and passive zone in front of the wall, respectively. The earth

pressures for the stage five of the excavation in the passive zone in front of the wall are underestimated.

The SelfSim learning was conducting using instruments along main observation section shown in Figure 4-16. The extracted soil model is then used in a numerical analysis to compute deformations at excavation sections at I-2 and I-3 (Figure 4-16). Figure 4-25 and Figure 4-26 show the comparison of measured and computed wall deformation for inclinometer I-2 and I-3 using the model developed from main observation section prior to any learning, after learning with wall deformation only (I-1) down to third stage of the excavation, and after learning with wall deformation (I-1) and inclinometer SI-4 in 22m away from the excavation down to fifth stage of excavation. The wall deflections are underestimated by using the developed model from prior learning. By using the developed model after learning with the wall deformations only(I-1), the predicted lateral wall deformations of I-2 and I-3 are in reasonable agreement with the measured values down to third stage. By using the developed model after learning wall deformations (I-1) and inclinometer SI-4 the predicted wall deformations for inclinometers I-2 and I-3 are improved and they are in reasonable agreement down to fifth stage of the excavation.

4.5. Summary

The relationship between field instrumentation and excavation response has always been recognized. This chapter presented a study that explored the relationship between field instrumentation selection and the quality of learned excavation response facilitated by a unique inverse analysis framework, SelfSim. This study shows:

1. Integrating the proposed inverse analysis framework with a field instrumentation program for deep excavation can be used to supplement physical measurements and provide reliable estimates of deformations and loads elsewhere around the excavation. This finding can assist engineers on projects whereby cost and space constraints as well as damage to instruments during construction limit the number of available instrument measurements.

The integration of the inverse analysis with the remaining measurements can help fill-in-the-gap otherwise unavailable information.

2. Wall deformations and surface settlements provide essential information for learning of overall excavation behavior. An inclinometer placed within or in close proximity to the wall is essential.

3. Additional inclinometers placed farther back from the wall provide supplementary information that can be used to complement prediction of surface settlements if that information becomes unavailable at certain excavation stages. The finding is confirmed using the TNEC excavation case study. This is a useful and practical finding as surface settlement points can be easily lost in a heavily trafficked urban environment.

4. Strut loads and (by analogy), tieback loads provide valuable information to extract soil behavior and enhance the overall quality of estimated ground response. Therefore, measurement of bracing loads is recommended.

5. Other instruments such as heave gauges, extensometers, and piezometers provide useful measurements in order to monitor construction and verify design assumptions; though it appears in the simulated excavation study that they are less critical for overall learning of excavation behavior.

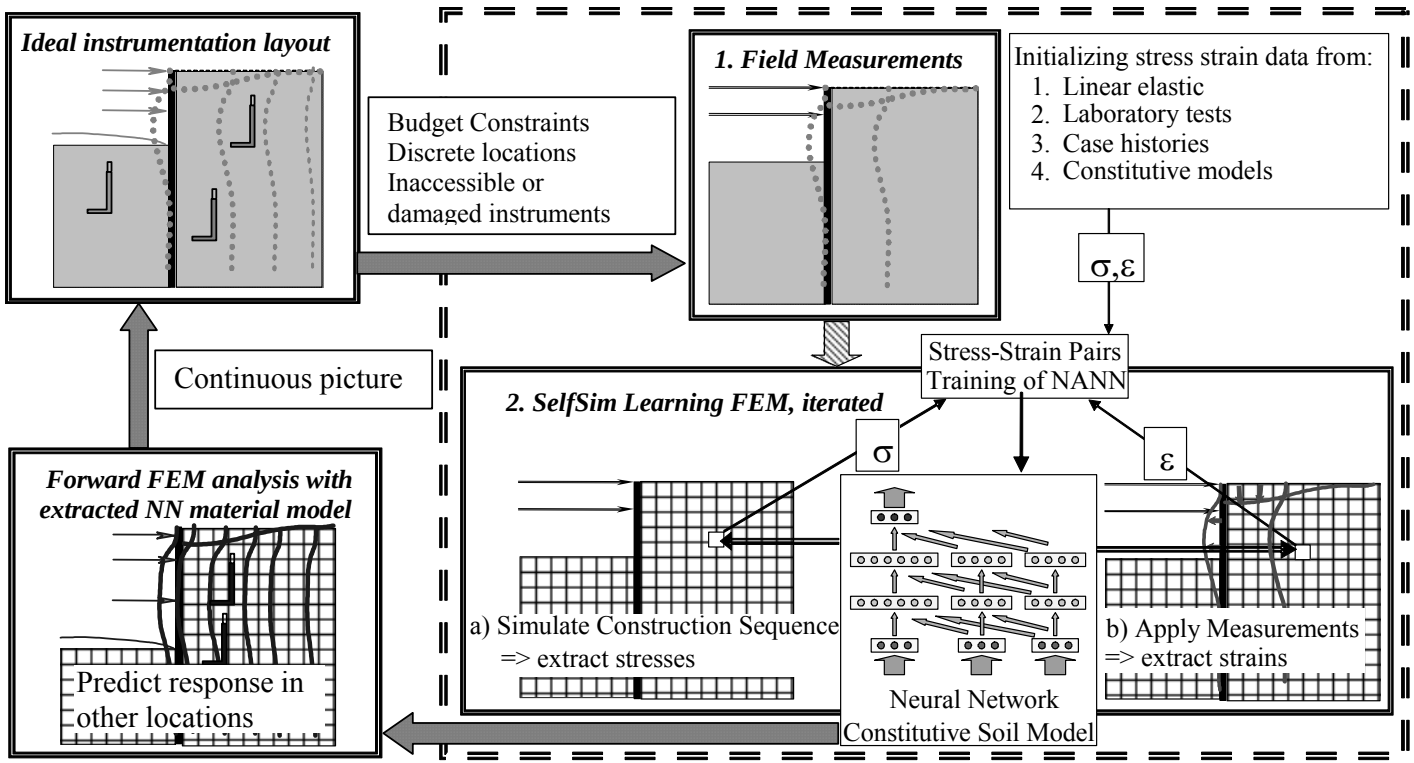

Figure 4-1 Application of Self-learning simulations to deep excavation problems

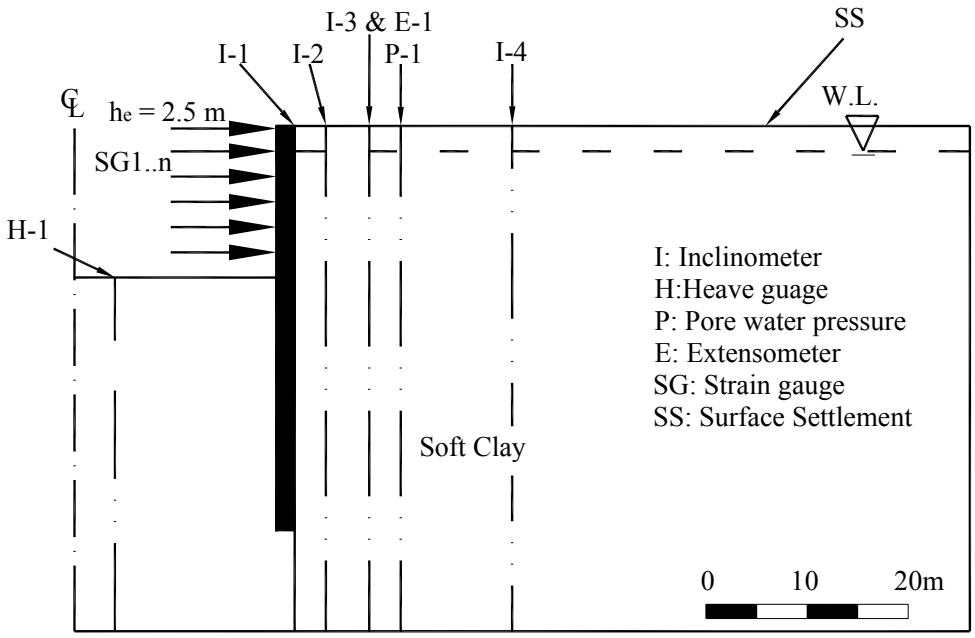

Excavation stages	Excavation activity
Stage 1	2.5 m Excavation
Stage 2	5.0 m Excavation, Installation of struts at 1st and 2nd levels
Stage 3	7.5 m Excavation, Installation of struts at 3rd level
Stage 4	10.0 m Excavation, Installation of struts at 4th level
Stage 5	12.5 m Excavation, Installation of struts at 5th level
Stage 6	15.0 m Excavation, Installation of struts at 6th level

Figure 4-2 Dimensions of the excavation, instrument locations and construction sequence

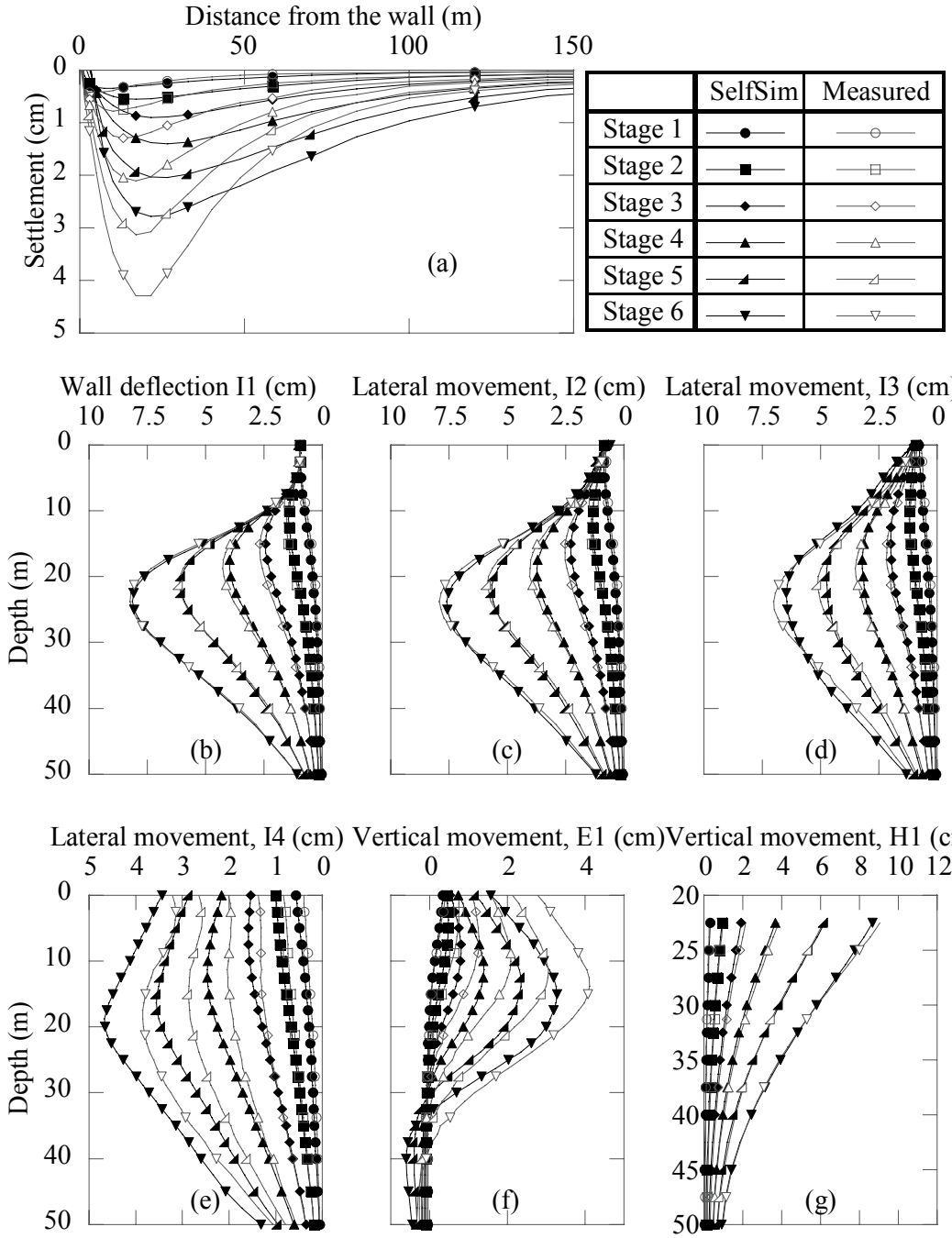

Figure 4-3 Computed response of (a) surface settlements , (b), wall deflections at I1 (c) lateral movement at I2, (d) lateral movement at I3, (e) lateral movement at I4, (f) vertical movement at E1, and (g) vertical movement at H1 after SelfSim learning with measurements from inclinometer in the wall (I1) only.

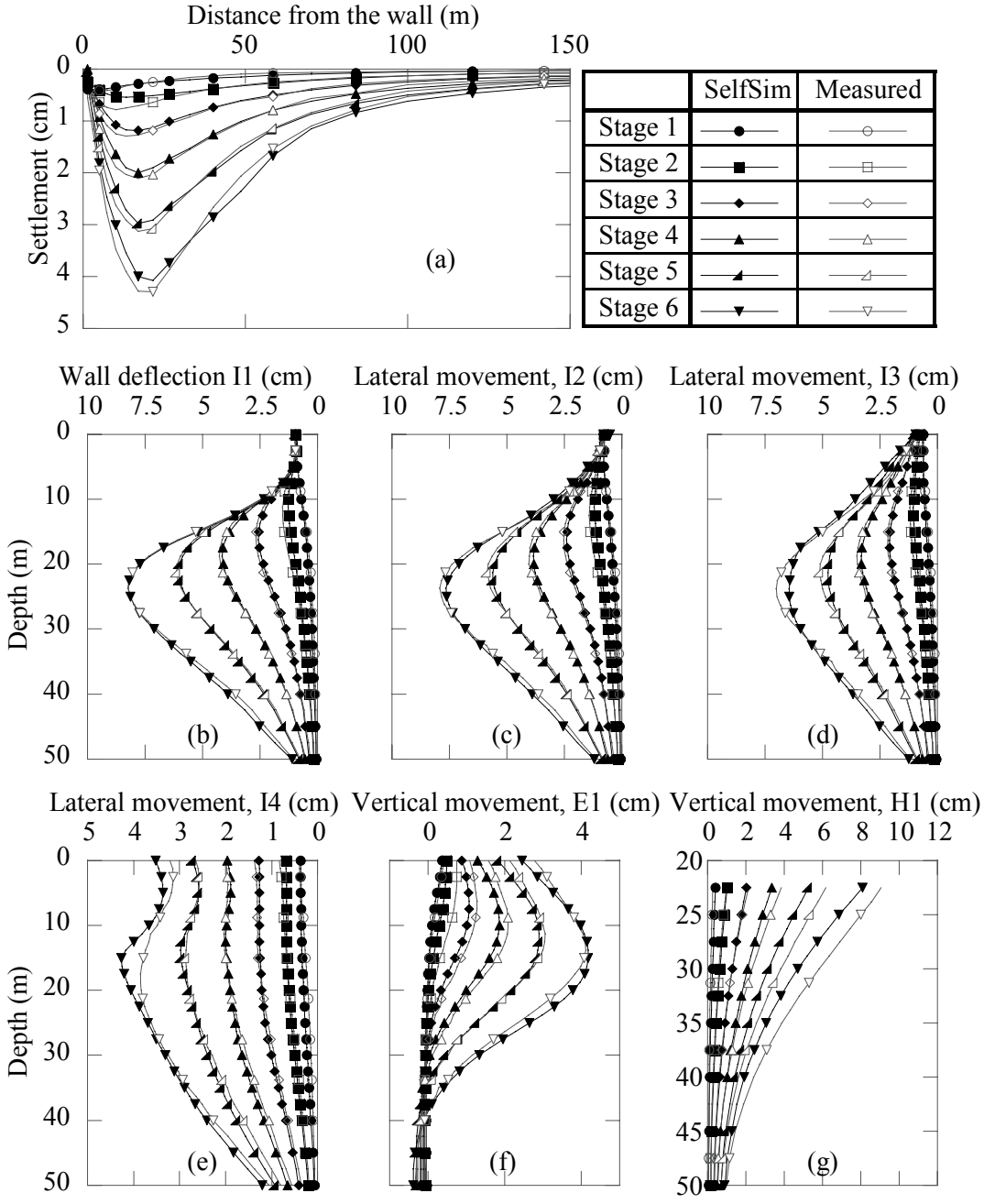

Figure 4-4 Computed response of (a) surface settlements , (b), wall deflections at I1 (c) lateral movement at I2, (d) lateral movement at I3, (e) lateral movement at I4, (f) vertical movement at E1, and (g) vertical movement at H1 after SelfSim learning with measurements from inclinometer in the wall (I1) and surface settlement points.

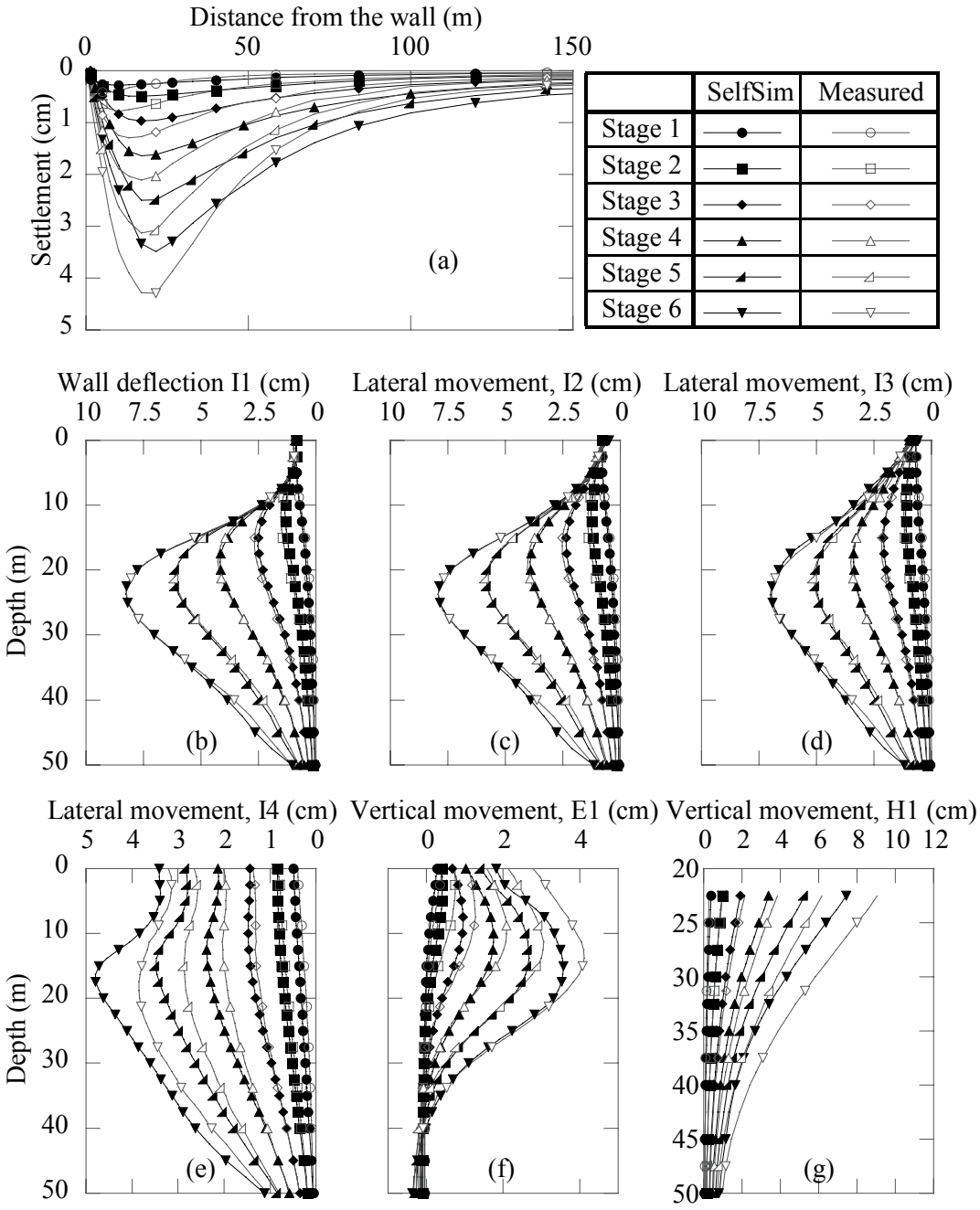

Figure 4-5 Computed response of (a) surface settlements , (b), wall deflections at I1 (c) lateral movement at I2, (d) lateral movement at I3, (e) lateral movement at I4, (f) vertical movement at E1, and (g) vertical movement at H1 after SelfSim learning with measurements of inclinometer in the wall (I1) and I3.

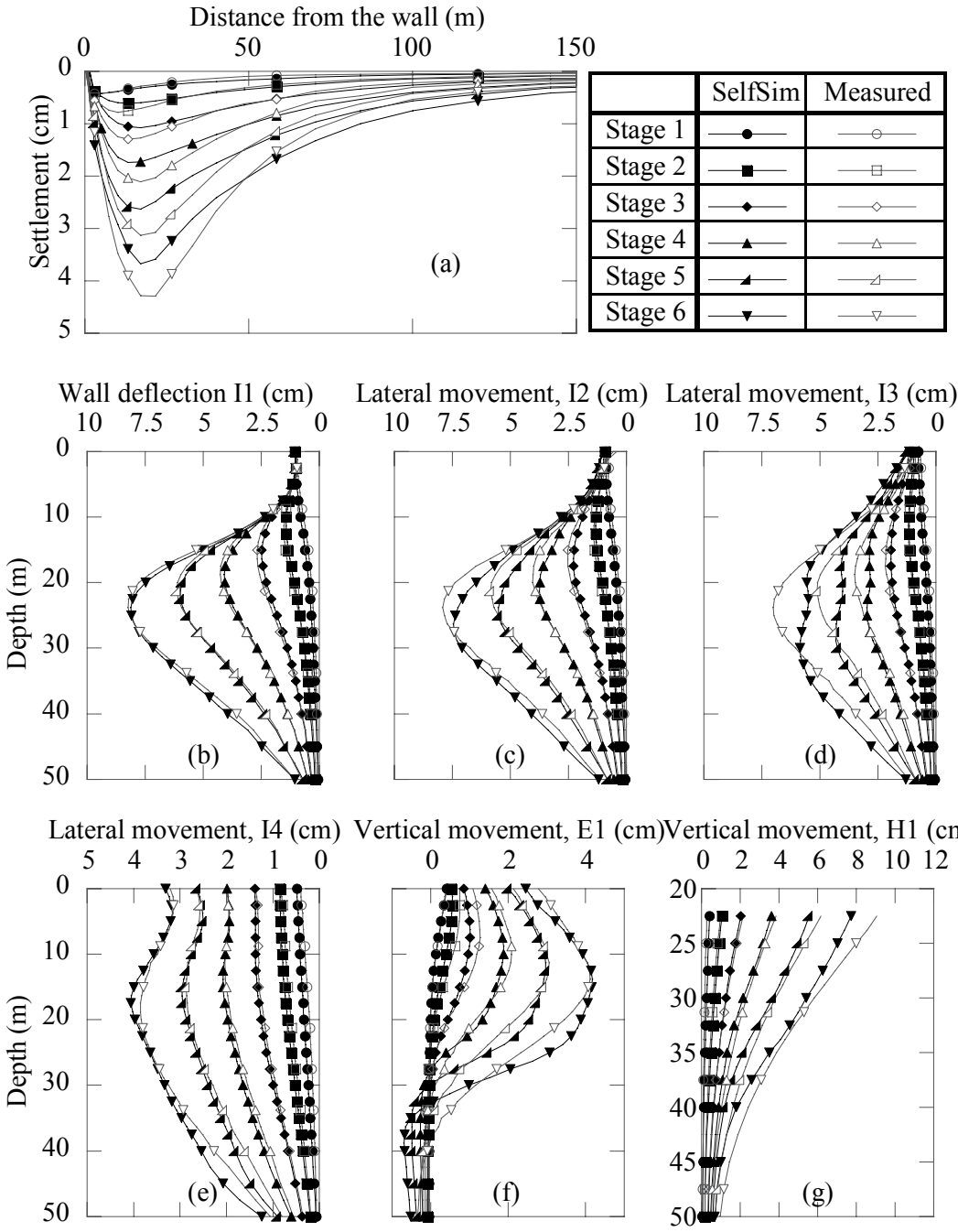

Figure 4-6 Computed response of (a) surface settlements , (b), wall deflections at I1 (c) lateral movement at I2, (d) lateral movement at I3, (e) lateral movement at I4, (f) vertical movement at E1, and (g) vertical movement at H1 after SelfSim learning with measurements of inclinometer in the wall (I1) and I4.

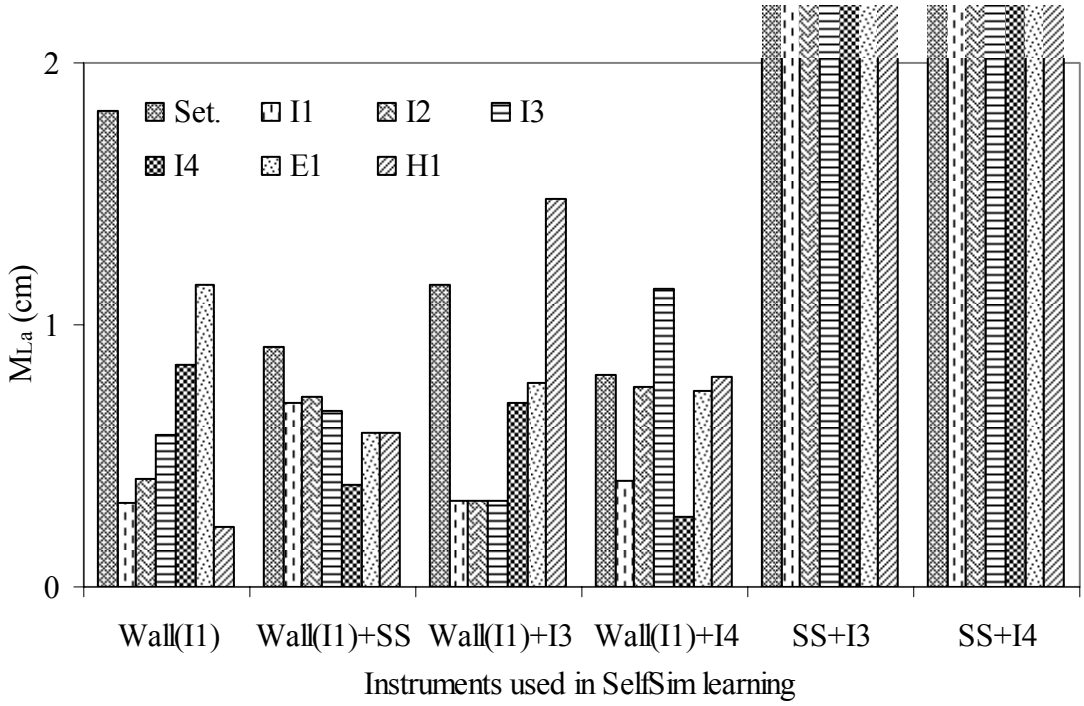

Figure 4-7 Comparison of M_{La} values for computed deformations after SelfSim learning with combination of measurements of inclinometer in the wall (I1) and surface settlements with inclinometer measurements behind the wall (i.e. I3, I4).

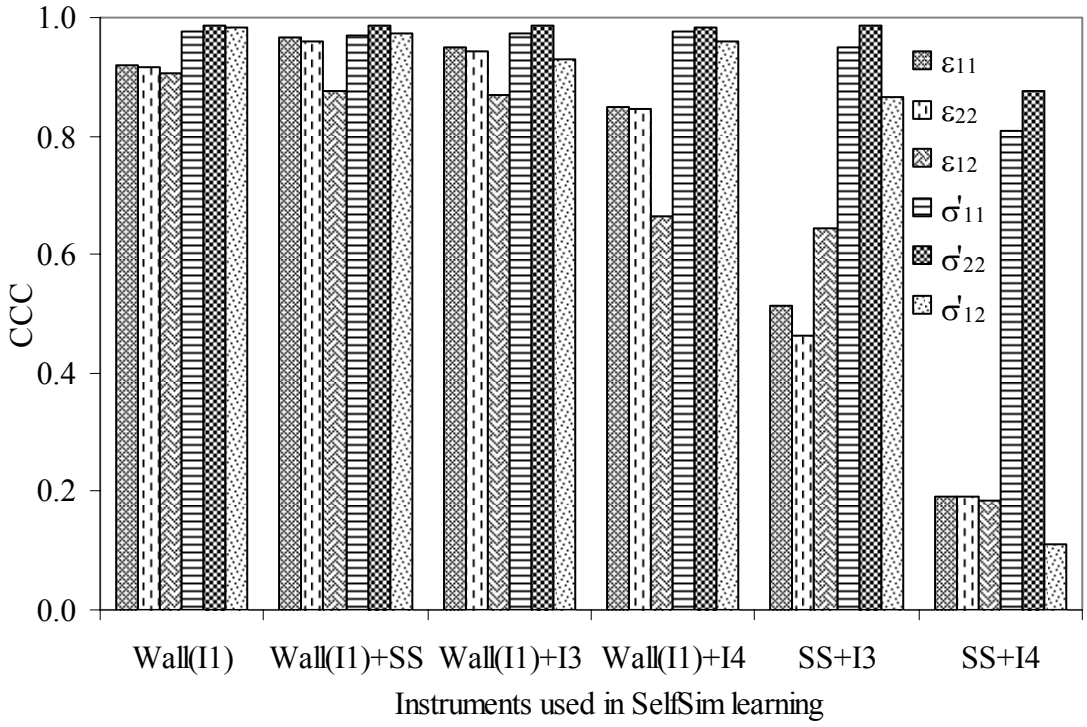

Figure 4-8 Comparison of CCC values for soil behavior after learning with combination of measurements of inclinometer in the wall (I1) and surface settlements with inclinometer measurements behind the wall (i.e. I3, I4).

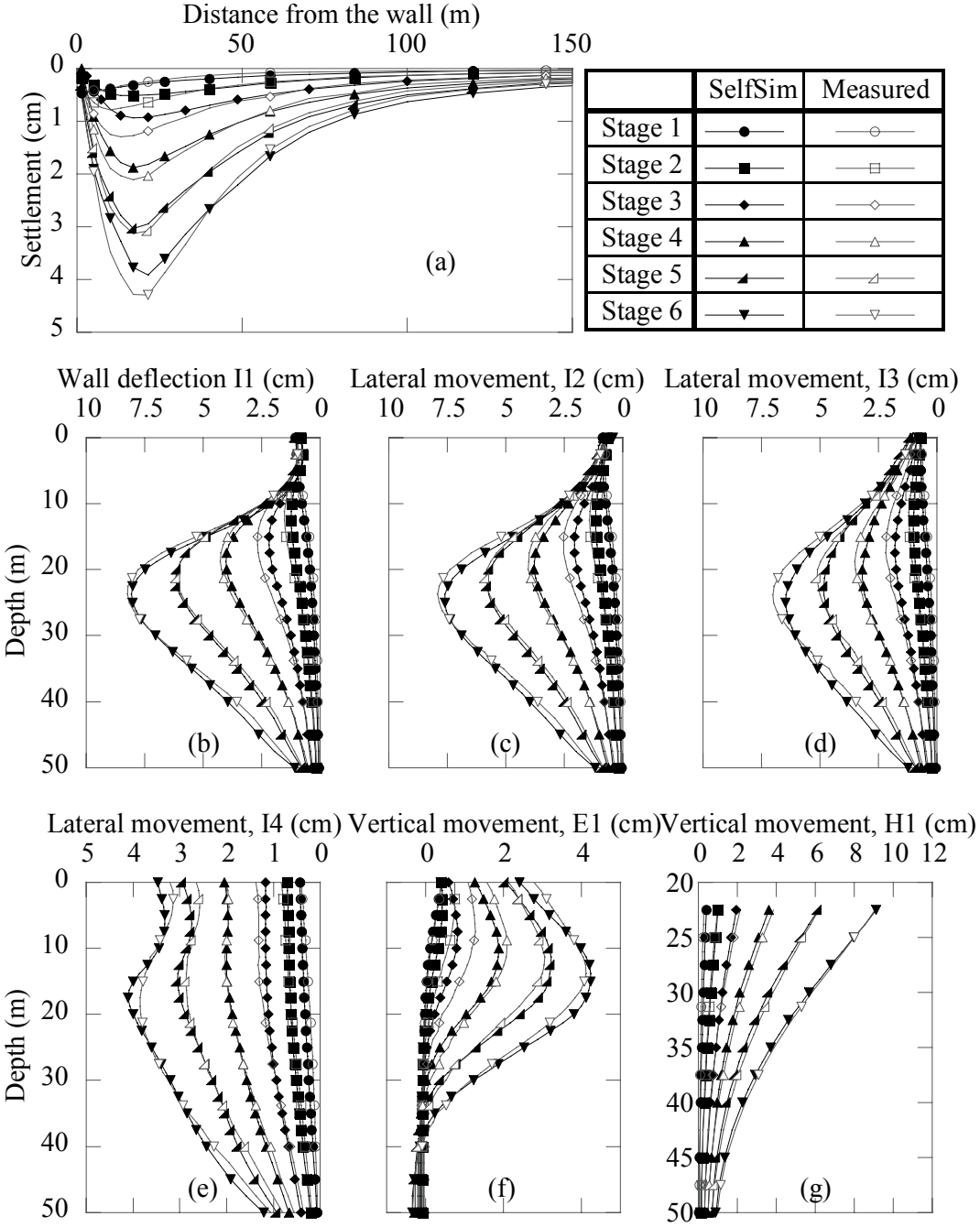

Figure 4-9 Computed response of (a) surface settlements , (b), wall deflections at I1 (c) lateral movement at I2, (d) lateral movement at I3, (e) lateral movement at I4, (f) vertical movement at E1, and (g) vertical movement at H1 after SelfSim learning with measurements of inclinometer in the wall (I1), surface settlements, and strut loads.

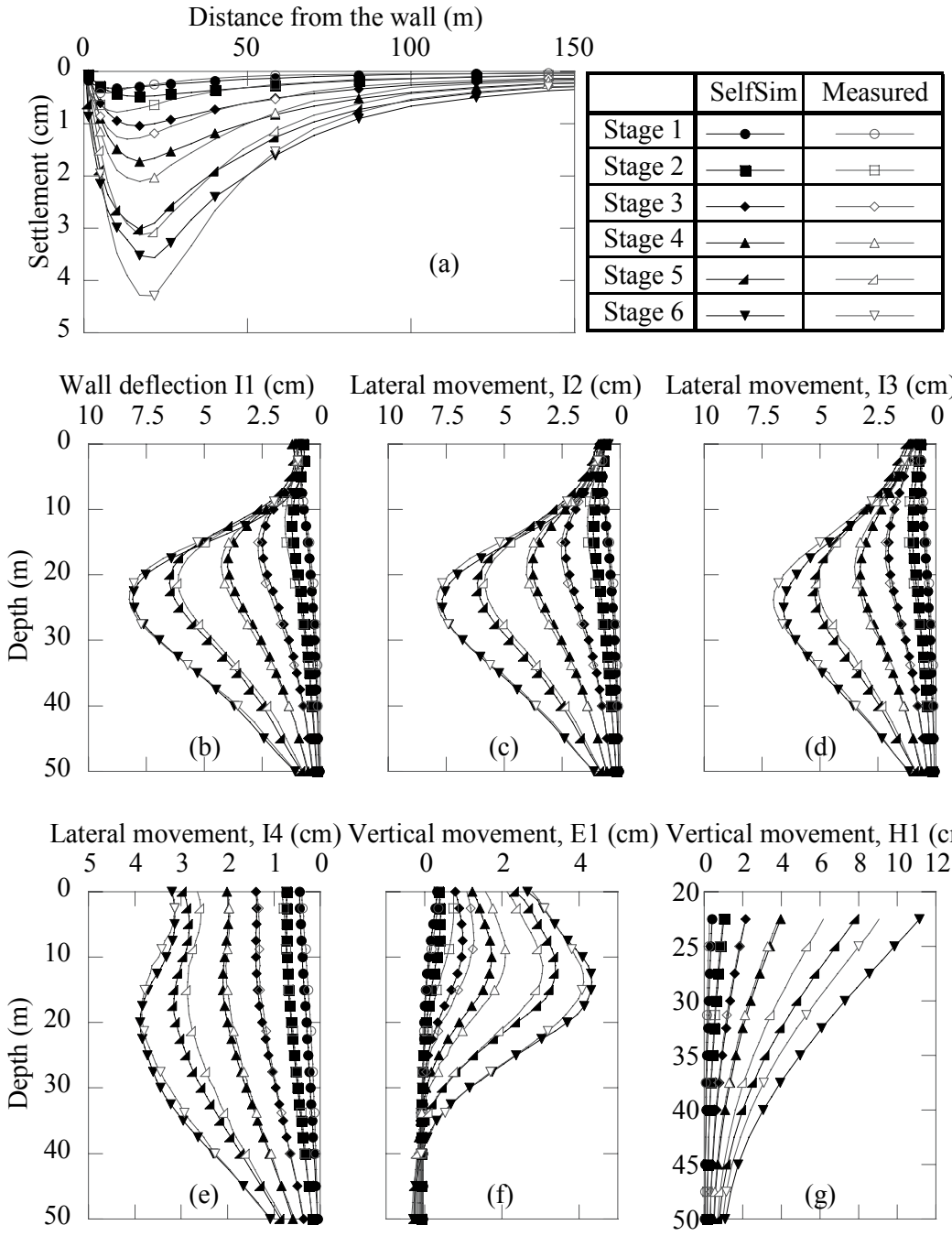

Figure 4-10 Computed response of (a) surface settlements , (b), wall deflections at I1 (c) lateral movement at I2, (d) lateral movement at I3, (e) lateral movement at I4, (f) vertical movement at E1, and (g) vertical movement at H1 after SelfSim learning with measurements of inclinometer in the wall (I1), inclinometer I4, and strut loads.

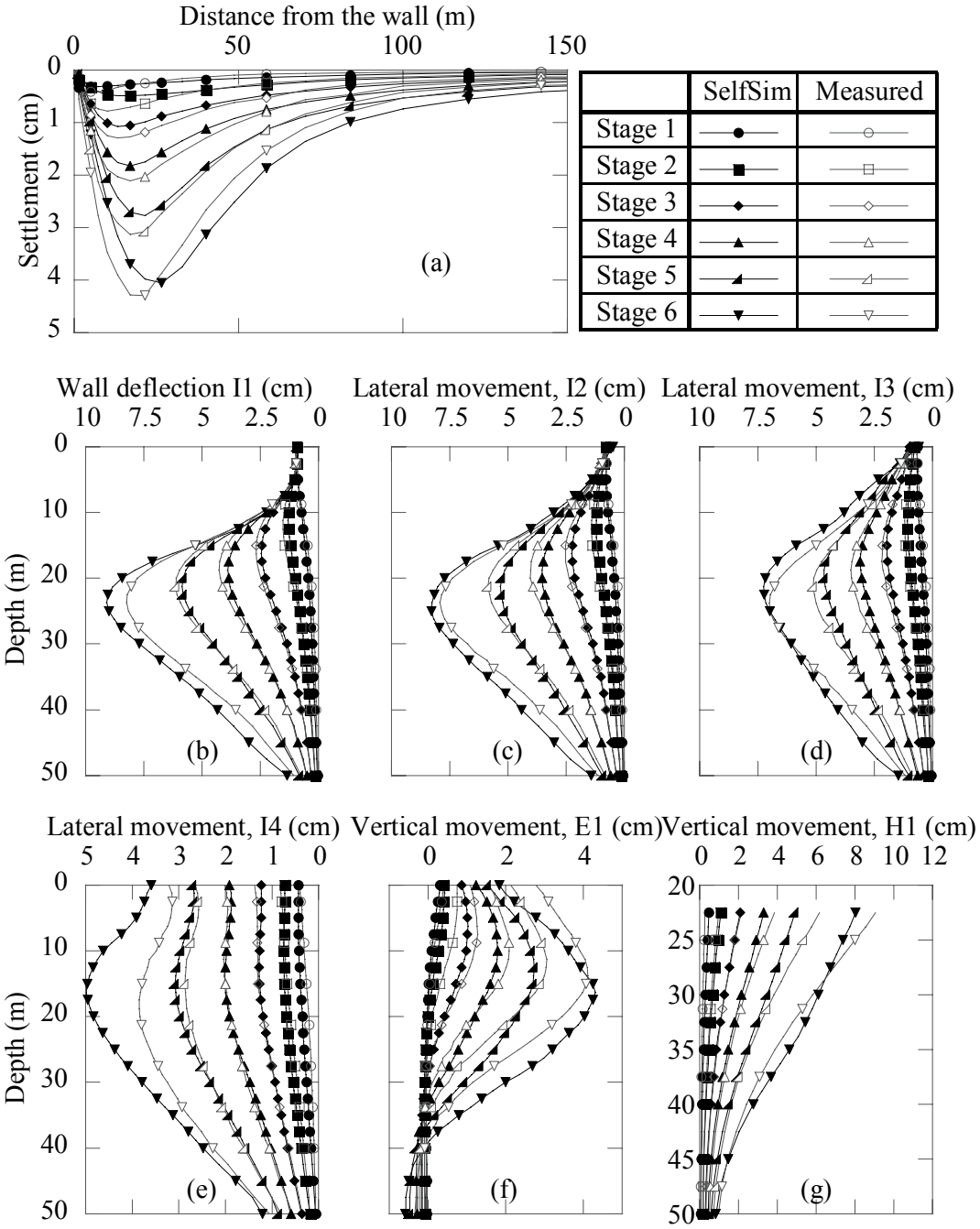

Figure 4-11 Computed response of (a) surface settlements , (b), wall deflections at I1 (c) lateral movement at I2, (d) lateral movement at I3, (e) lateral movement at I4, (f) vertical movement at E1, and (g) vertical movement at H1 after SelfSim learning with measurements of inclinometer in the wall (I1), surface settlements and pore pressures at P1.

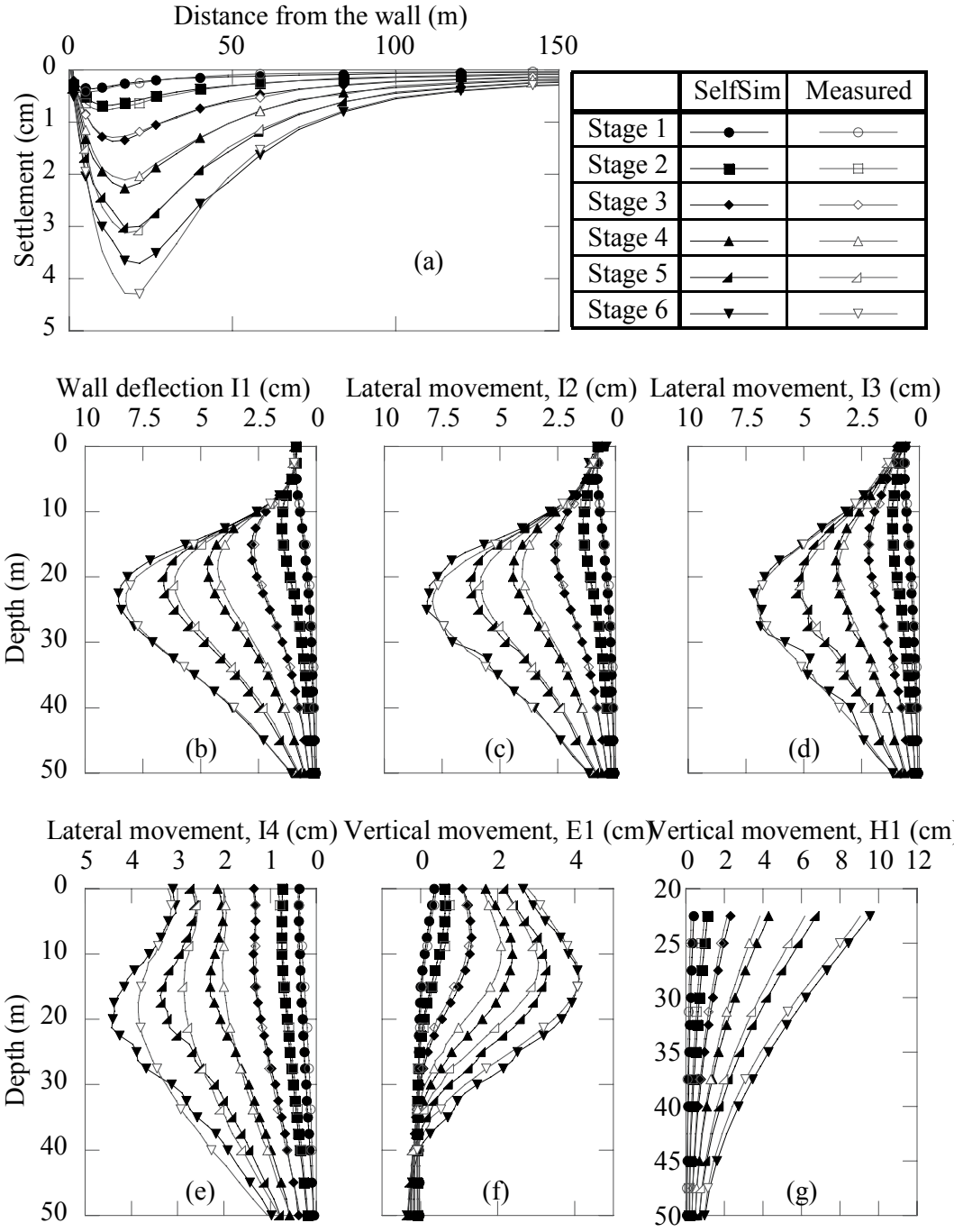

Figure 4-12 Computed response of (a) surface settlements , (b), wall deflections at I1 (c) lateral movement at I2, (d) lateral movement at I3, (e) lateral movement at I4, (f) vertical movement at E1, and (g) vertical movement at H1 after SelfSim learning with measurements of inclinometer in the wall (I1), surface settlements, I2, I3, I4, E1, H1, P1.

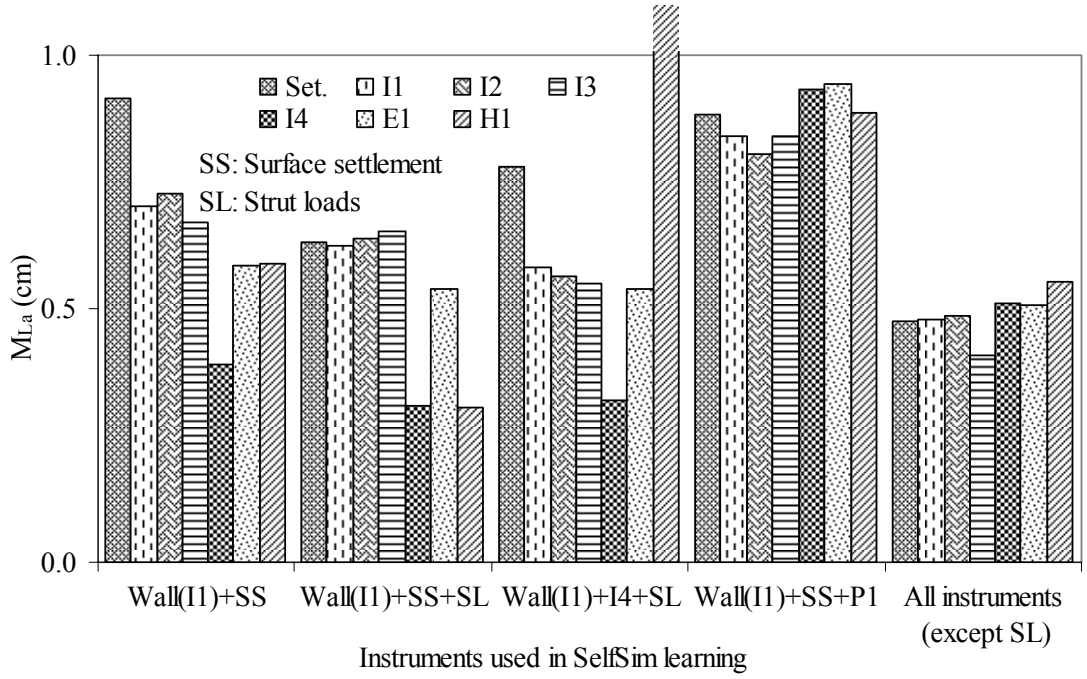

Figure 4-13 Comparison of M_{La} values for computed deformations after learning with measurements of inclinometer in the wall (I1) and surface settlement points; measurements of inclinometer in the wall (I1), surface settlement points, and strut loads; measurement of inclinometer in the wall (I1), inclinometer I4, and strut loads; measurements of inclinometer in the wall (I1), surface settlement points, and piezometer P1; all instruments except strut loads;

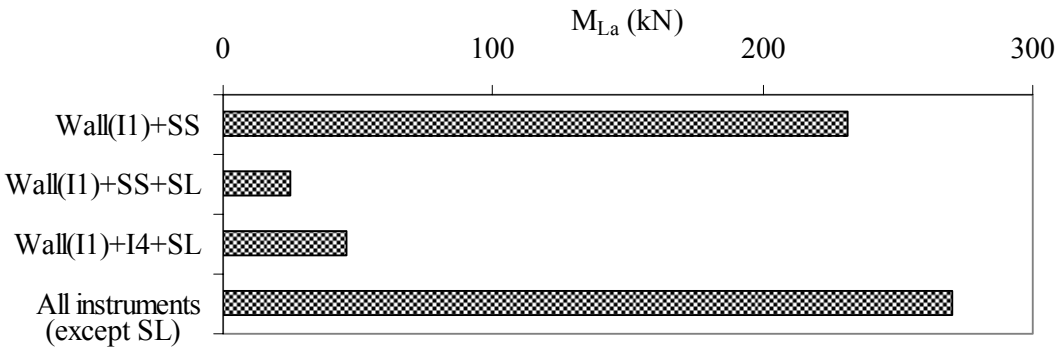

Figure 4-14 Comparison of M_{La} values for computed strut loads by using and not using strut loads in SelfSim learning.

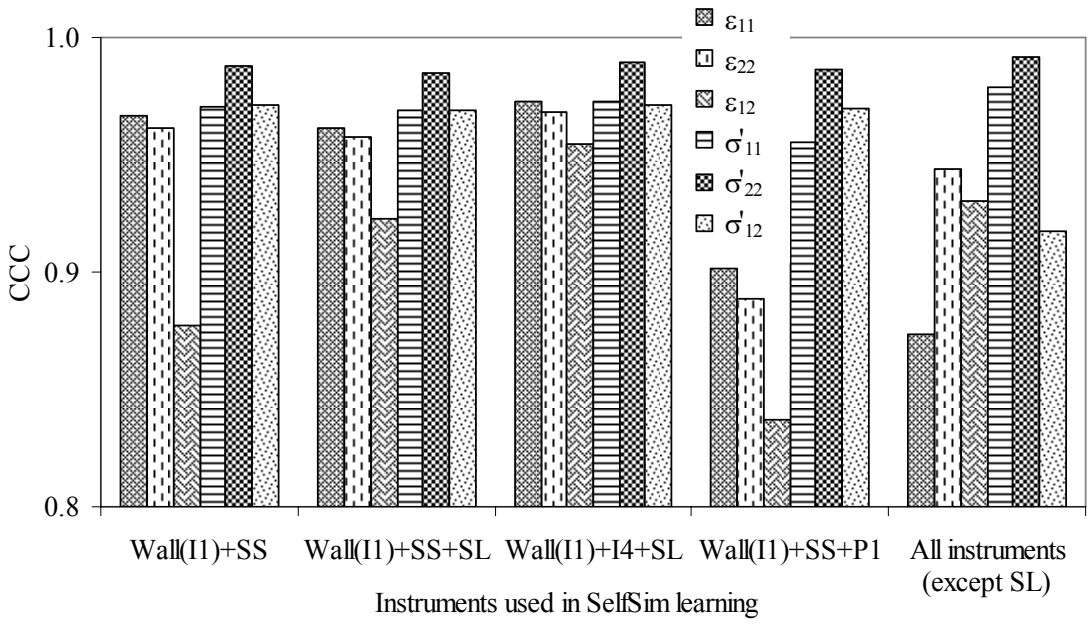

Figure 4-15 Comparison of CCC values for soil behavior after learning with measurements of inclinometer in the wall (I1) and surface settlement points; measurements of inclinometer in the wall (I1), surface settlement points, and piezometer P1; all instruments except strut loads; measurements of inclinometer in the wall (I1), surface settlement points, and strut loads; measurement of inclinometer in the wall (I1), inclinometer I4, and strut loads.

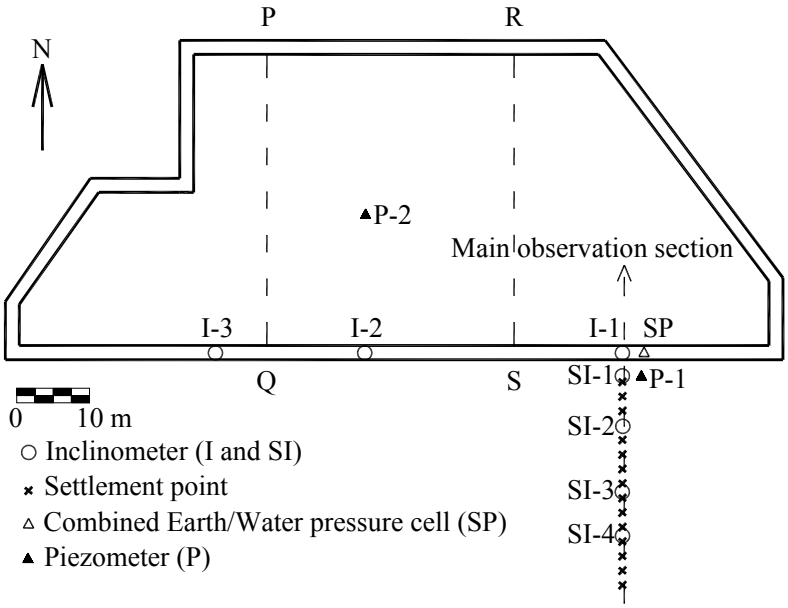

Figure 4-16 TNEC plan view and instrument locations, modified after Ou et al. (1998)

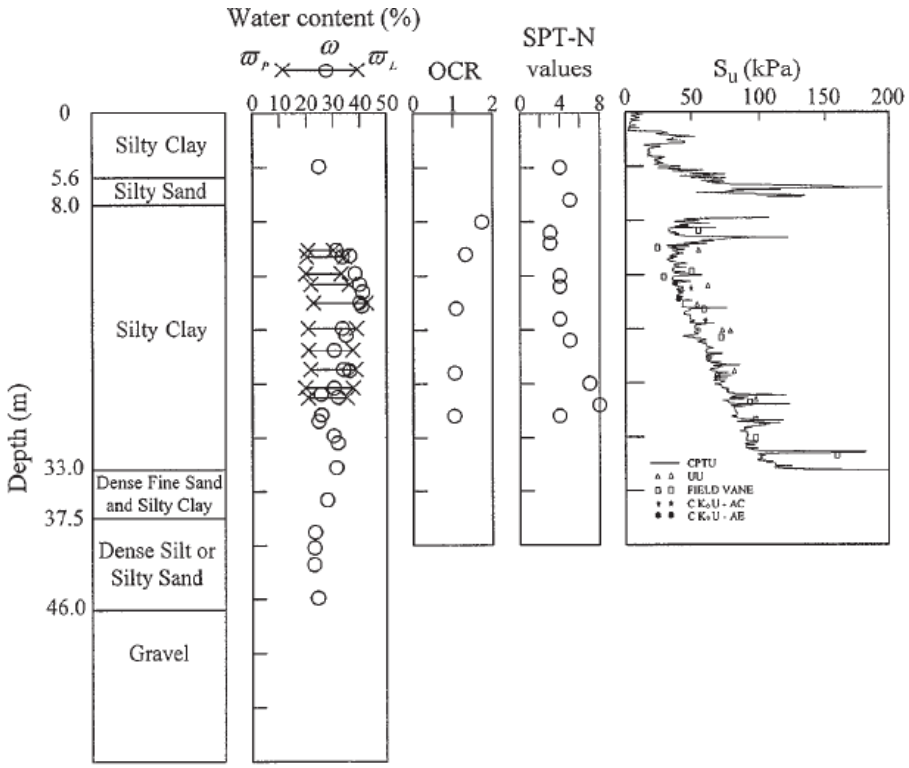

Figure 4-17 Subsurface ground conditions and soil properties, after Ou et al. (2000)

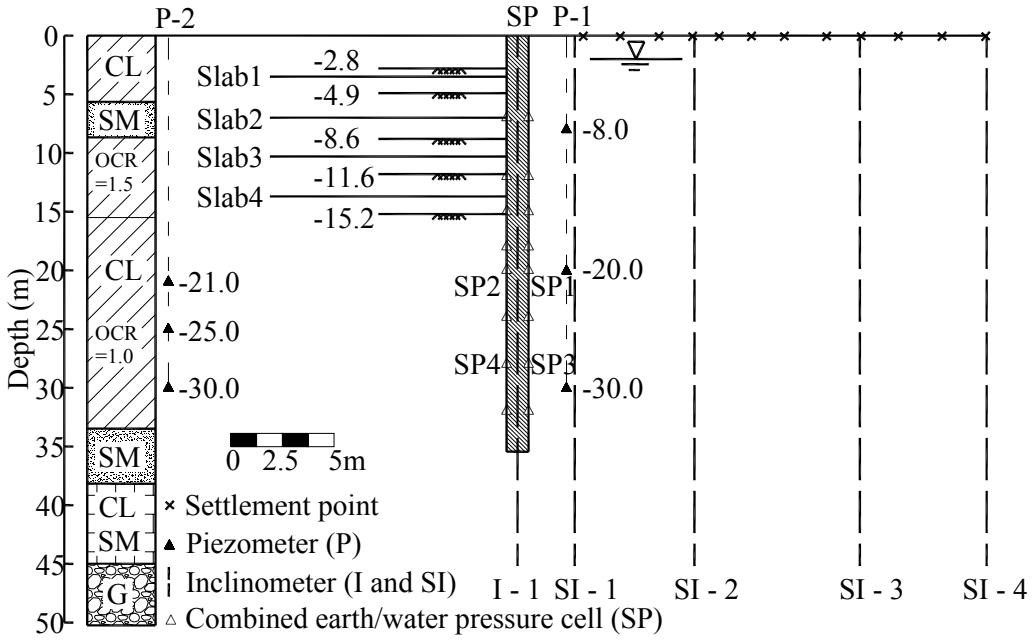

Figure 4-18 Excavation section view, modified after Ou et al. (1998)

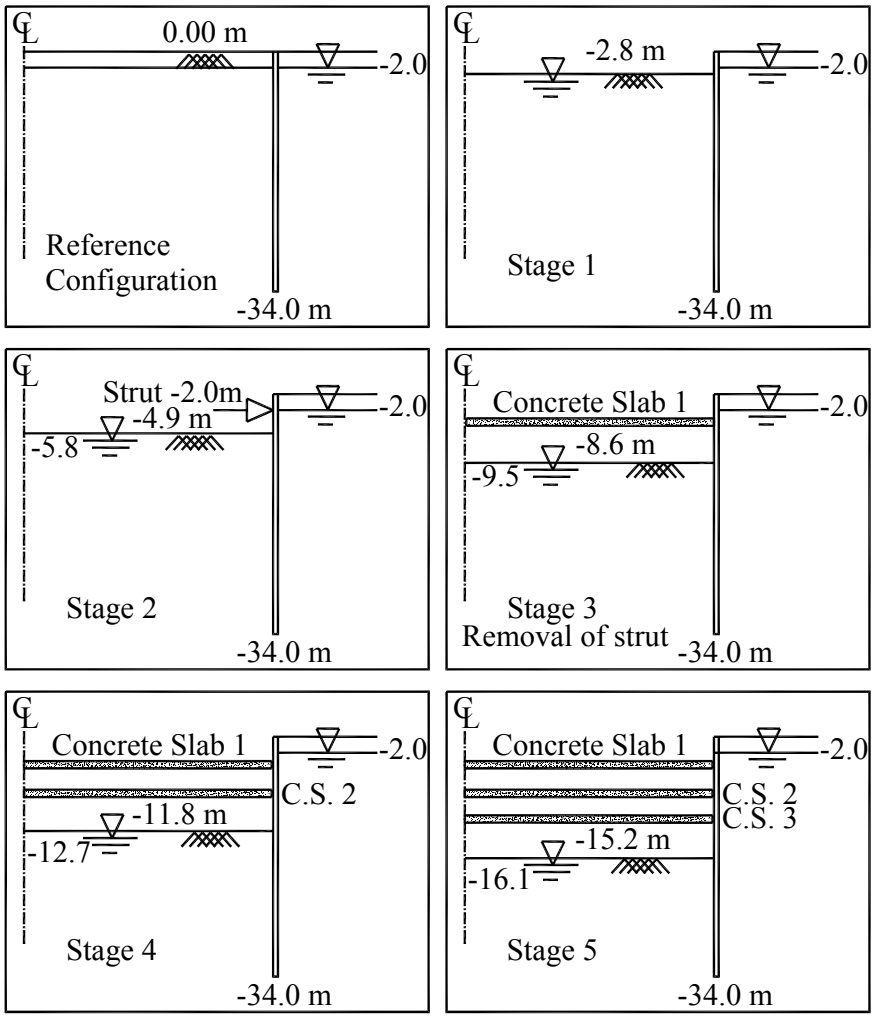

Figure 4-19 Excavation sequence in TNEC project

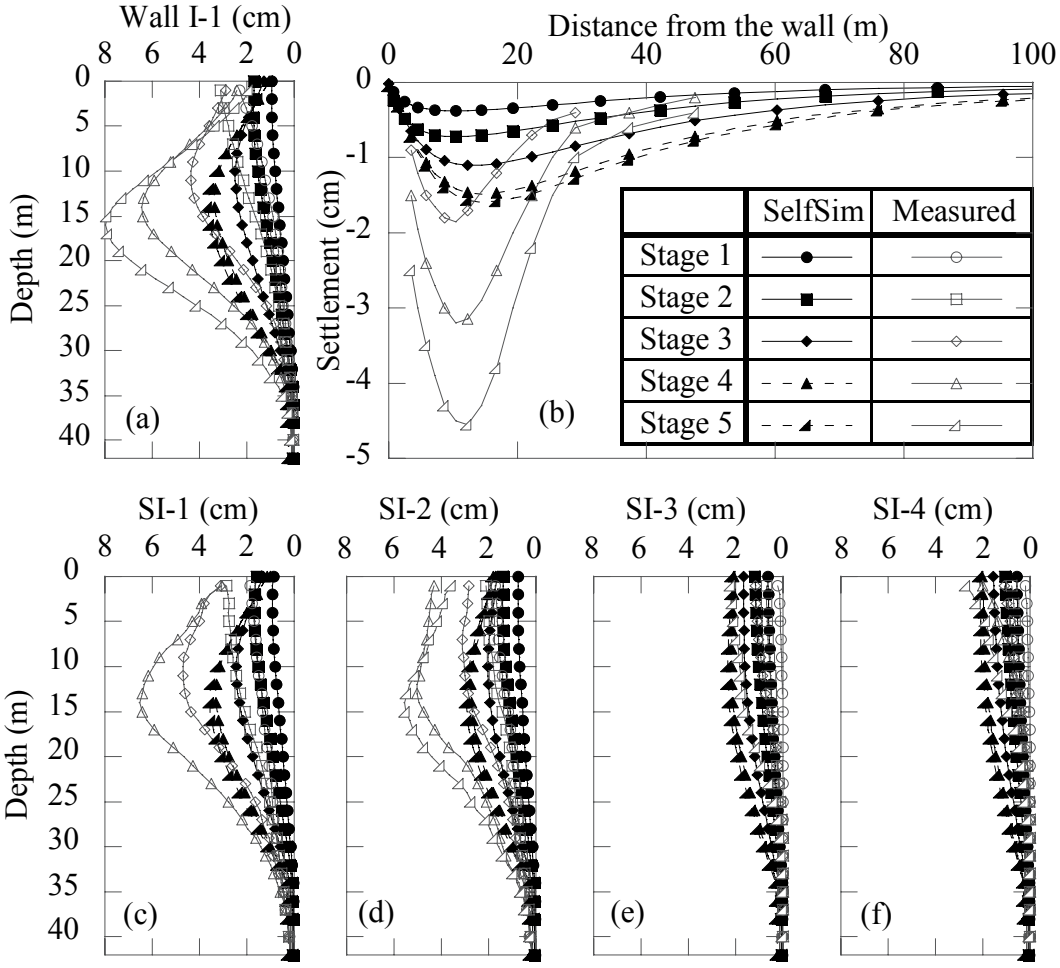

Figure 4-20 Computed response of (a) wall deflections, (b) surface settlements, (c) lateral movement at SI-1, (d) lateral movement at SI-2, (e) lateral movement at SI-3, (f) lateral movement at SI-4 prior to SelfSim learning, TNEC excavation.

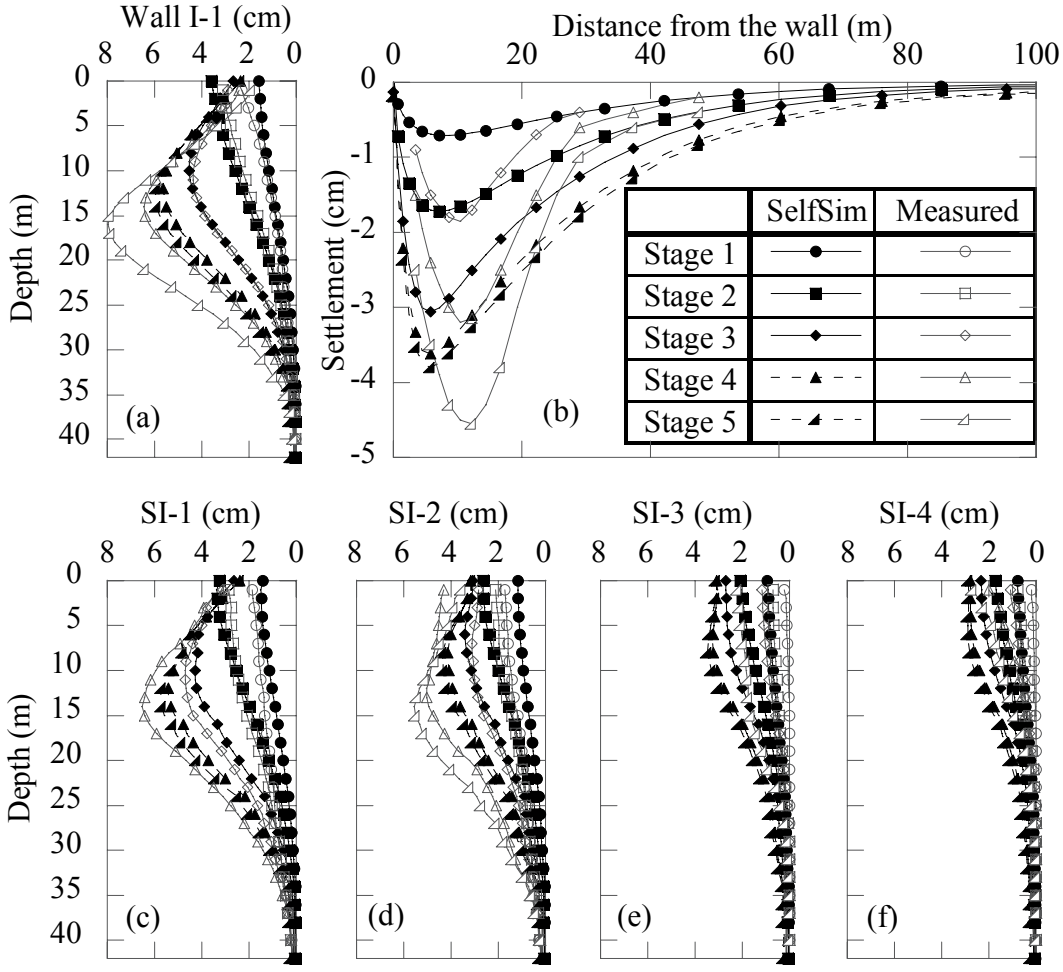

Figure 4-21 Computed response of (a) wall deflections, (b) surface settlements, (c) lateral movement at SI-1, (d) lateral movement at SI-2, (e) lateral movement at SI-3, (f) lateral movement at SI-4 after 5 passes of SelfSim learning with wall deformations (I-1) only down to third excavation stage, TNEC excavation.

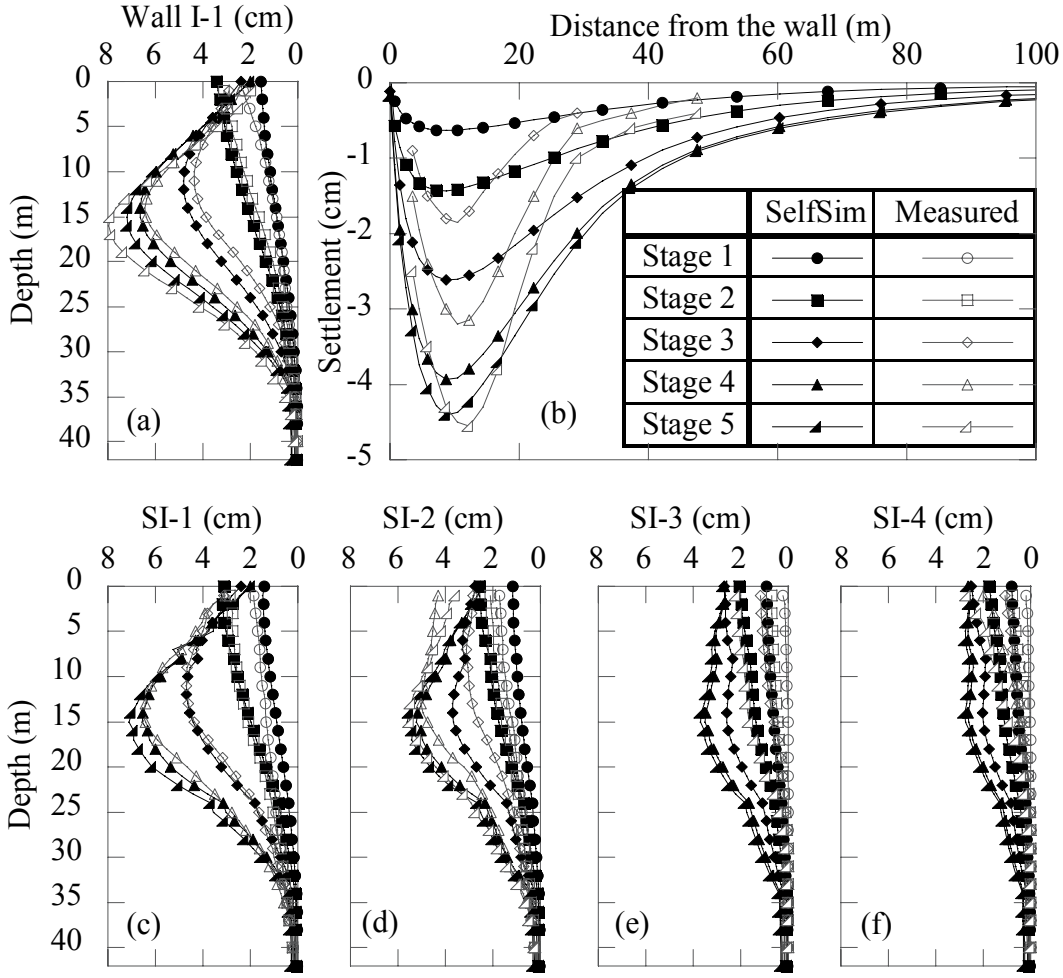

Figure 4-22 Computed response of (a) wall deflections, (b) surface settlements, (c) lateral movement at SI-1, (d) lateral movement at SI-2, (e) lateral movement at SI-3, (f) lateral movement at SI-4 after 6 passes of SelfSim learning with wall deformations (I-1) and inclinometer SI-4 at 22 m distance from the wall, down to fifth stage of the excavation using the database of SelfSim learning with wall deformations only down to third stage of excavation, TNEC excavation.

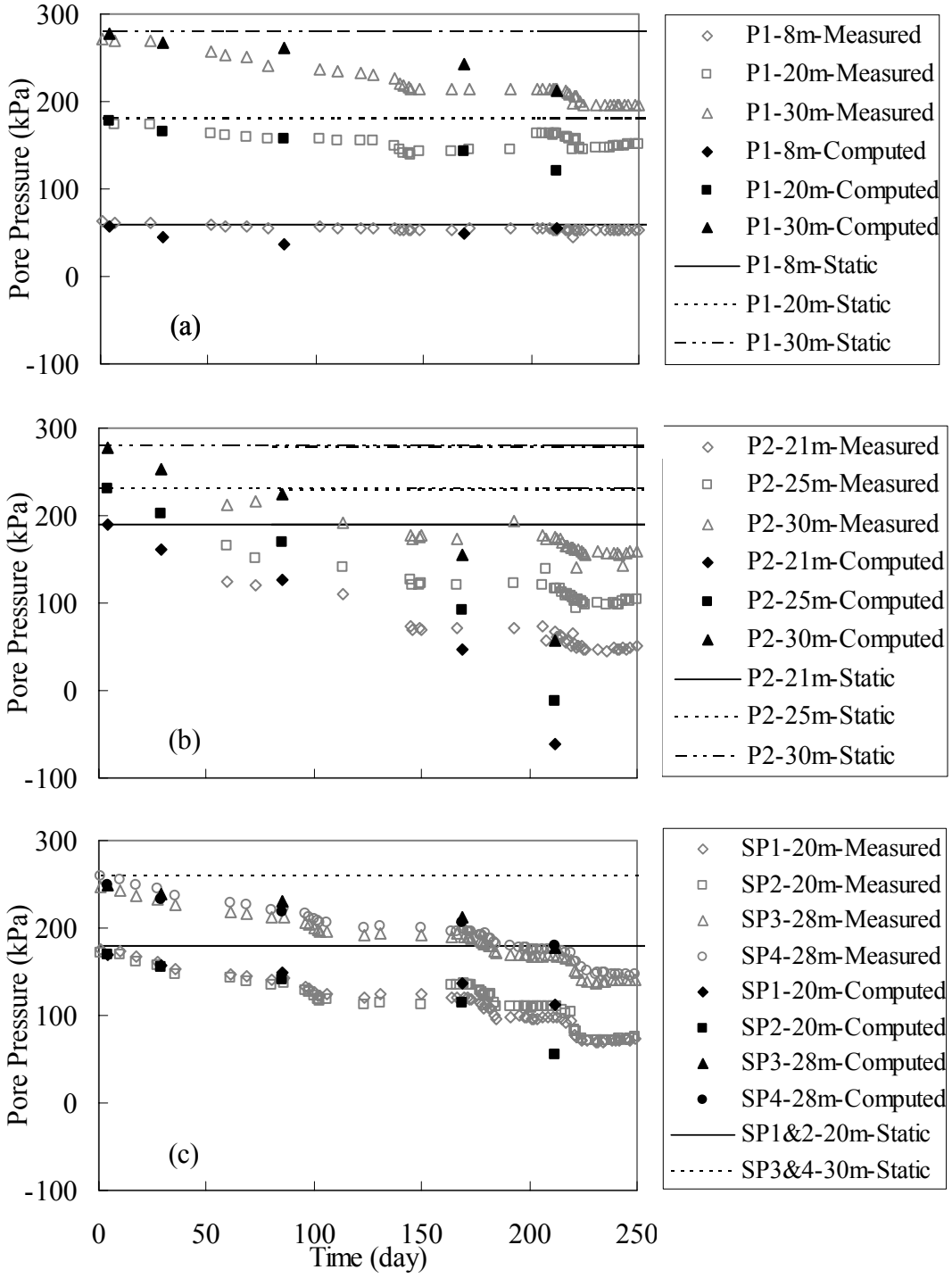

Figure 4-23 Comparison of measured and computed pore pressures after learning with wall deformations (I-1) and inclinometer SI-4 for piezometers a) P1, b) P2 and c) SP1, SP2, SP3, and SP4, TNEC excavation.

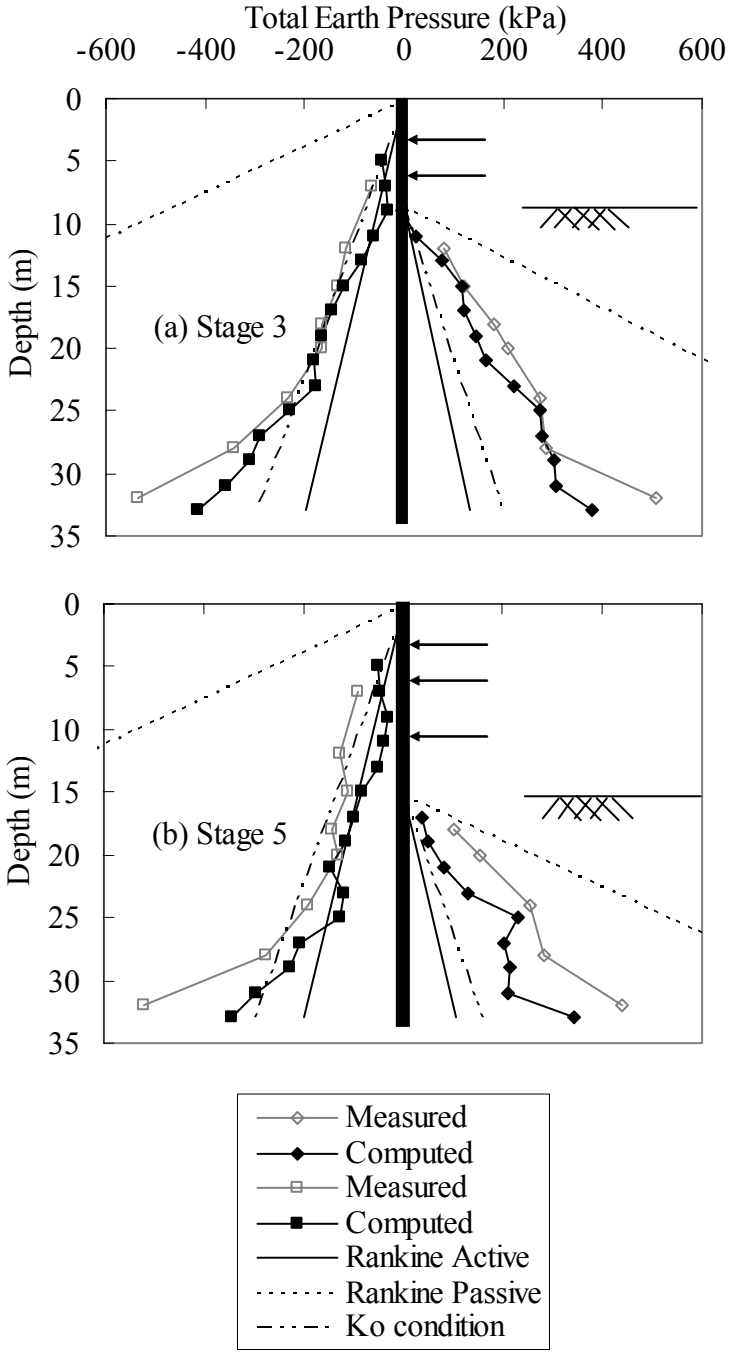

Figure 4-24 Comparison of measured and computed earth pressures after learning with wall deformations (I-1) and inclinometer SI-4 for earth pressures at the wall for a) stage 3, and b) stage 5 of the excavation, TNEC excavation.

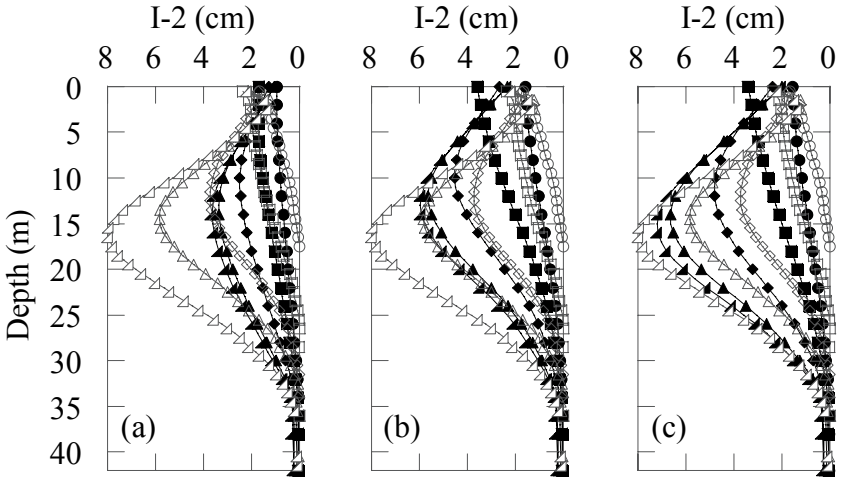

Figure 4-25 Comparison of measured and computed wall deformations of I-2 after a) prelearning, b) learning with wall deformations only (I-1), and c) learning with wall deformations (I-1) and inclinometer SI-4, TNEC excavation (For legend see Figure 4-22).

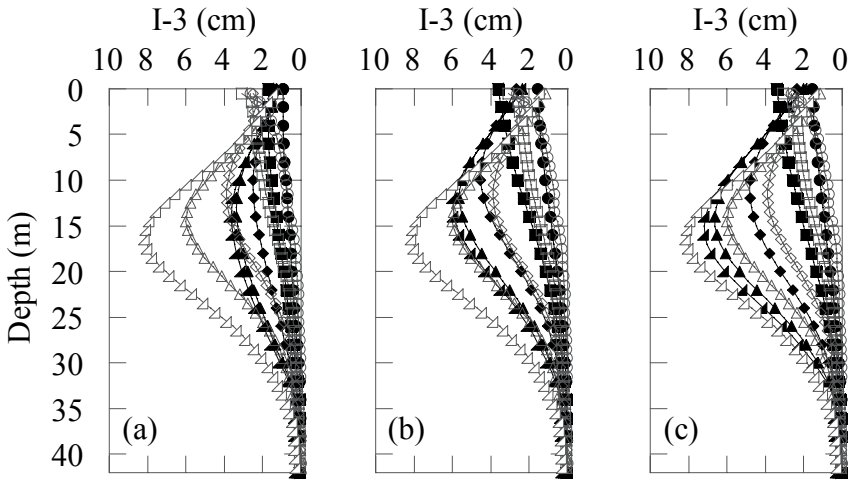

Figure 4-26 Comparison of measured and computed wall deformations of I-3 after a) prelearning, b) learning with wall deformations only (I-1), and c) learning with wall deformations (I-1) and inclinometer SI-4, TNEC excavation (For legend see Figure 4-22).

CHAPTER 5 CASE STUDIES OF PREDICTION OF EXCAVATION RESPONSE USING LEARNED PERFORMANCE OF EXCAVATIONS

5.1. Introduction

In many major urban areas, there are a number of well document excavation case histories that are used by engineers as the precedent to estimate performance of new excavations in similar soil stratigraphy. Learning from precedent represents a classic inverse analysis problem aimed in part at interpreting the soil and stress response implied by field observations. For instance, Calvello and Finno (2004) optimized the Hardening-Soil (H-S) model (Schanz et al. 1999) for four layers of Chicago glacial clays initially using results from triaxial test. Since the developed model could not predict the wall lateral deformations of a subway station excavation in Chicago, they had to recalibrate the model using inclinometer data that recorded the lateral displacements. Finno and Calvello (2005) used the inclinometer at stage 1 of excavation to recalibrate the H-S model and could predict the measured lateral deflections for later stages reasonably well. Their study was limited to prediction of lateral wall deflections. While parameter optimization approaches are very powerful, they are constrained by prior assumptions regarding the material constitutive model and thus unable to learn new material behavior.

Hashash et al. (2006) demonstrated SelfSim learning capacity and the ability to extract soil material behavior using numerically simulated excavation case histories. The extracted soil model provided a reasonable prediction of excavation performance in a new excavation site, Figure 5-1.

Three different simulated case histories were developed within a fictitious urban area where the geologic profile is similar but not identical at all three sites. The subsurface profiles assumed for the three simulated case histories had slight variations in properties (different overconsolidation ratios OCRs) and strata thickness. SelfSim learning was conducted using measurements of inclinometer at the wall and surface settlements behind the wall from all three cases. Then the extracted soil model was used in a new excavation in the hypothetical urban area to predict the ground movements. Afterward, synthetic measurements that were not used in SelfSim learning were obtained from the simulated excavation and compared to the predictions. The lateral wall

deflections and surface settlements of a new case study were predicted reasonably well. This finding demonstrated that it is possible to predict excavation performance of a new case study after learning soil behavior from previous case studies that have similar soil stratigraphy. However, the findings of Hashash et al. (2006) are limited to simulated excavations using synthetic measurements.

In this chapter, the performance of SelfSim learning is demonstrated using excavations in Texas, Shanghai and Taiwan. At each of these locations an instrumented excavation is used in learning of the relevant underlying soil behavior. The learned soil behavior is then used in a numerical analysis to predict the performance of another excavation in similar stratigraphy that was not used in the learning process.

5.2. Full scale model wall in sandy soils at University of Texas A&M

5.2.1. Site description

The Texas A&M full scale model wall was constructed and tested as a part of research performed to improve the design of permanent ground anchor walls for highway applications (Weatherby et al. 1998). A 7.5-m-high, instrumented, full-scale, tiedback, H-beam and wood lagging wall was constructed in an alluvial sand deposit to study various aspects of the behavior of anchored walls. Figure 5-2 shows the location of the site at Texas A&M University Riverside campus.

The schematic of plan view, instrument locations and elevation view of the Texas A&M site are shown in Figure 5-3. The wall which is supported by pressure-injected ground anchors has two sections. Up to soldier beam number 12 the piles have lighter sections, (HP8x36, HP6x25), and therefore two levels of tiebacks are used. For soldier beam numbers 13 to 22 a single tieback level was used, because of the larger pile sections (HP10x57, HP12x53, HP10x42). Soldier beams 7 to 10 in the two levels of tieback section and soldier beams 13 to 16 in the single tieback level section are instrumented with inclinometers and surface settlement points, Figure 5-3. There are 6 inclinometers in the retained soil. Inclinometers I-1, I-2 and I-3 are in the two-level tieback section of the wall and located behind soldier beam 10 at distances of 0.7m, 1.5m, and 4.5m from the wall, respectively. The corresponding surface settlement points for these inclinometers are located behind soldier beam 9. Inclinometers I-4, I-5, and I-6 are in the single tieback

level section of the wall behind the soldier beam 14 at distances of 0.7m, 1.5m, and 4.5m from the wall, respectively. The corresponding surface settlement points for these inclinometers are located behind soldier beam 15.

The cross sections of the wall with soil stratigraphy are shown in Figure 5-4. The soil profile consists of fill overlying loose clayey sand followed by medium dense clean sand, and medium dense clayey sand. The fill is composed of silty and clayey sand, which was placed in 15 to 22 cm lifts and compacted with two passes of a fully loaded rubber tire pan scraper. The water table is at El. -7.0 m. The friction angle was estimated to be between 30 to 32 degree using the correlation developed by Trofimenkov (1974) for loose clayey sand and medium dense sand layers at this site (Weatherby et al. 1998). The relative densities of the layers vary from 40 to 60 percent.

SelfSim learning is conducted using inclinometers measurements from the two-level tieback section. The extracted soil models are used in a finite element analysis to predict the excavation performance in single tieback section of the wall.

5.2.2. Learning soil behavior from two-level tieback section of the wall

Figure 5-5 summarizes the construction activities affecting the wall in the two-level tieback section of the wall. The excavation induced deformations are available at stages 2, 4, and 7 for two-level tieback section.

The full scale model wall is simulated using solid element with a bending stiffness equivalent to that of the soldier-pile wall. The tiebacks are simulated by elastic spring elements. The soil profile in the analyses consists of four representative layers for fill, loose clayey sand, medium dense clean sand and medium dense clayey sand.

Although the Texas A&M excavation was not constructed symmetrically, it is modeled as a 2D symmetric excavation with large half width of 20m to minimize the effect of this assumed symmetry. The model dimensions are 85m and 18m in horizontal and vertical dimensions, respectively. Individual soil layer are represented separately via corresponding NN based material models.

Prior to any SelfSim learning, initial NN based soil constitutive models are pre-trained to represent linear elastic response within a very small strain range. The initial Young's moduli used for pre-training are deliberately chosen large to produce small

excavation-induced deformations. Figure 5-6 shows the computed deformations prior to SelfSim learning. The surface settlements and lateral deflections of I-1, I-2, and I-3 are underestimated. In the last stage of full scale model wall construction (i.e. 122nd day), the soldier beam piles appears to have settled/slipped. The measured subsurface settlement behind the wall reflects this observation, Figure 5-6a. The slippage of the wall induced large settlements behind the wall and is not represented in the inverse analysis. Various instrument combinations are used in SelfSim learning to explore the extent of learning and the ability to predict excavation response.

Learning soil behavior using wall deformations (I-1) only

Figure 5-7 shows the results of forward analysis after SelfSim learning from wall deformations (I-1) only. The computed response of the wall (I-1) provides a reasonable match to measured values, but the lateral movements at I-2 and I-3 and vertical movements of settlement points are underestimated for Stage 7. Surface settlements near the wall which are affected by wall slippage are underpredicted. It is worth noting that measured wall deflections for I-2 Stage 7 exceed those for I-1 Stage 7. This behavior is unexpected and likely due to spatial variability of measurement. However this measured data is inconsistent from the 2-D inverse analysis point of view as it provides contradictory information. Therefore I-2 is not used in learning.

Learning soil behavior using wall deformations (I-1) and inclinometer measurements at I-3

SelfSim learning is conducted using wall deformations (I-1) and lateral deflections of the inclinometer I-3 in order to improve the learned behavior. Figure 5-8 shows the computed excavation response. The computed lateral deformations of I-3, particularly in stage 7, have improved in comparison to Figure 5-7.

Learning soil behavior using wall deformations (I-1), inclinometer measurements at I-3 and tieback loads

Final SelfSim learning analysis is conducted using the wall deformations (I-1), lateral movements of inclinometer I-3, and tieback loads to capture the change in lateral

deformations of the wall after tieback installation. Figure 5-9 shows the computed excavation response. The computed lateral movements of the wall (I-1) and inclinometer I-3 improved compared to the results in Figure 5-7 and Figure 5-8. It is observed using tieback loads provide important information that enhances the model to capture reasonably the measured deformations in inclinometer I-3, noticeably for the stage 7.

Figure 5-10 shows the comparison of measured and computed tieback loads. The computed tieback loads after learning with wall deformations (I-1), lateral deflections at inclinometer I-3 and tieback loads are in more agreement with the measured loads. When only wall deformations or wall deformations and lateral deformations at inclinometer I-3 are used in SelfSim learning, the computed tieback loads are overestimated. Nevertheless, the computed loads are improved by using both wall deformations (I-1) and lateral deflections of inclinometer I-3 compared to the case where wall deformations (I-1) only are used.

5.2.3. Predicting excavation response in one-level tieback section of the wall

The developed models from the SelfSim learning of the two-level tieback section are used to predict the soil behavior in one-level tieback section of the wall. The wall length and excavation depth are the same as those for the two-level tieback section (Figure 5-4), but larger soldier beams sections are used. Figure 5-11 shows the construction sequence for one-level tieback section of the wall.

Figure 5-12 shows the predicted excavation performance for the one-level tieback section using the developed model after SelfSim learning with wall deformations (I-1) only of two-level tieback section. Since heavier soldier beams are used in one-level tieback section, the deformations are generally less than the two-level tieback section. It is observed that the lateral deflections of inclinometer I-4, I-5 and I-6 are slightly overpredicted for all excavation stages. The results show that for all inclinometers, the deep seated deflections are overpredicted.

Figure 5-13 shows the predicted and measured surface settlements and lateral deformations of inclinometer I-4, I-5, and I-6 after SelfSim learning with wall deformations (I-1) and lateral deflections of inclinometer I-3 from the two-level tieback section. The prediction improved in comparison to Figure 5-12. However the deflections

for the inclinometer I-5 and I-6 at stage 6, particularly in lower elevations are still overpredicted.

Figure 5-14 shows the predicted excavation response using the developed model after SelfSim learning with wall deformations (I-1), lateral deflections of I-3 and tieback loads of two-level tieback section. The predicted lateral deformations of inclinometers I-4, I-5 and I-6 are in good agreement with measured values. Similar to the two-level tieback section of the wall, the slippage of the wall induced large surface settlements behind the wall in single tieback level section. Therefore, the surface settlements near the wall which are affected by wall slippage are not modeled in this simulation and are under-predicted.

Figure 5-15 compares measured and predicted tieback loads in one-level tieback section of the wall. The predicted tieback loads using developed model after SelfSim learning with wall deformations (I-1), lateral deflections of I-3 and tieback loads of two-level section of the wall are in reasonable agreement with measured values, for one out of the three construction stages. The predicted tieback loads using developed model after SelfSim learning with wall deformations (I-1) only or wall deformations (I-1) and lateral deflections of I-3 consistently overestimate the measured loads.

This case study demonstrates that the lateral deformations at the wall and at distances from the wall in the single tieback level section can be predicted using the soil model extracted from field observations in the two-level tieback section of the wall. However, the surface settlements are not predicted reasonable due to the wall slippage effect which caused large settlements behind the wall and was not simulated in the inverse analysis.

5.3. Bottom-up excavation in soft clays of a metro station in Shanghai

5.3.1. Site description

The Yishan Road metro station, located in southwest Shanghai, is a 15.5 m deep excavation with 17.4 m width and 335 m length in Shanghai soft clays at Pearl II metro line (Liu et al. 2005). The site is instrumented to monitor wall deflections, total earth pressures at the wall, pore-water pressures, and vertical ground movements. Figure 5-16

shows the plan view of Yishan Road metro station and instrument locations along the project line. The ground water table is at about 1 m below the ground level.

Figure 5-17 shows the soil stratigraphy and typical cross section of the excavation site. The site is underlain by thick, relatively soft to stiff clay deposits. The uppermost clay layer appeared to be desiccated and it has lower water content but higher shear strength than those of the underlying marine deposits (i.e., soft to medium stiff clay). The shear strength and compressive modulus profiles were obtained from in situ vane shear tests and oedometer tests at stress ranges from 100 to 200 kPa, respectively. The permeability of shallow sedimentary marine soft silty and marine medium clays was 10^{-8} and 10^{-9} m/s, respectively. Generally the water content of each soil lies close to the liquid limit and the soils have a relatively high void ratio and hence high compressibility (Liu et al. 2005).

The Yishan Road metro station excavation was supported by a 0.6 m thick concrete diaphragm wall. The wall length between Panels 27 and 35 was 28 m and in the remaining panels were 28 and 34 m at the north and south sides of the station, respectively. The deeper wall in the south was placed to minimize the effects of the station excavation on adjacent light-rail line running parallel to the wall about 20-30 m away. Prior to the main excavation, the soil at depths between 8.6 and 10.6 m and between 16.6 and 19.6 m below the ground surface was treated by compaction grouting at the passive zone of the excavation with 3 m spacing after the construction of the diaphragm wall. Since the compaction grouting was discontinuous, the inclinometer deflections showed that the grouting was ineffective. The excavation was conducted from two ends towards the center of the station.

Reinforced concrete struts of 800 mm width and 1200 mm depth were installed at -1.2 m depth at 6 m horizontal spacing and pre-stressed steel pipes of 609 mm in diameter (external) and 16 mm in thickness were used at other levels at 3 m horizontal spacing to support the diaphragm wall. Each pre-stressed strut was periodically adjusted to maintain the pre-stress to not less than 0.7 times the estimated total vertical stress (Liu et al. 2005). Prior to excavation to -12.5m, a 0.6 m thick reinforced concrete middle slab was constructed except for the section between Panels 27 and 35. After construction of

middle slab, 60 days were allowed for curing the concrete. Based on Liu et al. (2005) no significant creep effect could be identified over the 60 days curing of the middle slab.

Large lateral wall deflections were measured from excavation depth of 12.5 to 15.5 m, which was not consistent with reported construction activities. This was probably because of the relatively shorter wall or insufficient application of pre-stress (Liu et al. 2005). Therefore, the metro station excavation was simulated down to 12.5 m excavation depth. Based on the support system configuration and construction activities, three clusters are defined to perform forward analysis,

Figure 5-16. In cluster 1 the wall length for north and south walls of the excavation is 28 m. The middle slab was not used in this cluster. In cluster 2 the middle slab and wall length of 34 m are used to simulate excavation. In cluster 3 the middle slab and wall length of 28 m are used to simulate the excavation.

The construction sequence and wall length of excavation for clusters 1, 2, and 3 are illustrated in Figure 5-18. SelfSim learning is conducted using measurements of inclinometer I05, inclinometer I06, and settlements CJ04 in cluster 1 to extract the underlying soil behavior. The measured deflections of inclinometers in the first stage were not reported, hence the measurements of stages two to five are used for SelfSim learning. The extracted model is used to predict the instrument measurements in clusters 2 and 3 along the metro station, shown in Figure 5-16.

In order for the inverse analysis algorithm to work well, it is essential that field measurements used are compatible with reported and idealized construction sequence. Figure 5-19 shows the reported measurements of inclinometers in Yishan Road station for inclinometer I05 & I06, and surface settlements CJ04 (Cluster 1, Figure 5-16). Inclinometer data of I05 and I06 are similar. Inclinometer I05 shows outward movements into the retained soil that cannot be explained by the idealized construction sequence shown in Figure 5-18. This movement might be due to excessive pre-stressing of the bracing and pauses difficulty for inverse analysis as the pre-stressing load is not known. Therefore a slight adjustment is made to these deformations to eliminate the slight outward movement of the wall. A continuous surface settlement profile is also developed from the reported measurements at discrete points. Without these adjustments, the inverse analysis algorithm experienced significant difficulties because the original data would

indicate that the wall at the top moved into the soil due to soil removal which is physically not plausible. The adjusted measurements for inclinometer and settlements are referred to by proposed measurements label in Figure 5-19.

5.3.2. Learning soil behavior from measurements in cluster 1

The support wall for the deep excavation is simulated using solid elements with a bending stiffness equivalent to that of 0.6 m thick concrete diaphragm wall. The soil profile in the analyses is represented with five NN material models to represent layers: (1) for top fill layer, (2) for medium clay, soft silty clay, and soft to medium clay between depths of 2 m and 15 m, (3) for medium clays between depths of 15 m and 18 m, (4) for stiff clays between depths of 18 m and 23 m, and (5) for stiff silty clays at depths lower than 23 m. Shanghai deep excavation is modeled as 2D symmetric excavation with half width of 8.7m. The model dimensions are 130 m and 70m in horizontal and vertical directions, respectively.

Prior to any SelfSim learning all soil constitutive models are pre-trained to represent linear elastic response within a very small strain range. The initial Young's modulus used for pre-training is deliberately chosen large to produce small excavation-induced deformations. Computed deformations prior to SelfSim learning are shown in Figure 5-20. The computed deformations significantly underestimate the proposed measurements.

SelfSim learning is then conducted using proposed measured wall deformations of inclinometer I05 & I06 and surface settlement points CJ04 (for locations see cluster 1 in Figure 5-16). Computed and proposed measured deformations of the excavation after six passes of SelfSim learning are shown in Figure 5-21. The computed deformations improved significantly in comparison to results shown in Figure 5-20. The difference between measured and computed deformations except for wall movements in the fifth stage of excavation, are generally less than 2 mm, which indicates a reasonable match. The lateral deformations in the fifth stage are underestimated.

The predicted pore water pressures at different depth at location PA1, located in cluster 1, is shown in Figure 5-22. No pore water pressure data was used in SelfSim learning. The trends of predicted dissipation of pore pressures are in general agreement with measured values for PA1.

5.3.3. Predicting excavation response in clusters 2 and 3

The developed soil models after SelfSim learning with measured wall deformations and surface settlements in Cluster 1 are used to predict excavation behavior in Clusters 2 and 3 shown in Figure 5-16.

Prediction for Cluster 2

The predicted wall deformations of I03 and I09, and surface settlements CJ02 and CJ05 in cluster 2 are shown in Figure 5-23. The lateral deformations of I03 and I09 are less than the measured deflections of I05 and I06 due to use of middle slabs. The predicted deformations of the wall for inclinometers I03 and I09 in stages 3 and 4 are in reasonable agreement with the measured deflections. The wall deflections and surface settlement for stage 5 are underestimated. It is unclear why a sudden increase in measured settlements occurred between Stage 4 & 5 which cannot be explained by the known construction sequence. It is possible that an unrecorded deviation from the construction sequence caused this sudden increase.

The predicted pore water pressures at PA2, cluster 2, at different depths is shown in Figure 5-24. There is a general agreement between measured and predicted porewater pressures.

The comparison of predicted and measured earth pressures for PA2 is shown in Figure 5-25. Based on Liu et al. (2005) since the initial earth pressures are not consistent with K_0 pressure and Rankine's active earth pressure, the measured absolute values are not very reliable. Therefore, only the trend of the measured and predicted values should be considered. In the upper 15 m, the measured earth pressure coefficient is slightly larger than the K_0 at-rest condition for stages 2, 3, 4, and 5. For the depths more than 15 m from the ground surface, the measured earth pressure coefficient is less than K_0 at-rest condition. The predicted earth pressure for second stage is close to K_0 at-rest condition. As the excavation proceeds, the predicted earth pressure coefficient becomes smaller than K_0 at-rest value.

Prediction for Cluster 3

The predicted wall deformations of I04 and surface settlements CJ06 in cluster 3 are shown in Figure 5-26. The lateral wall deflections for stage 3, 4, and 5 of the excavation match reasonably with the measured values. The settlements also are in

reasonable agreement with measured values for stage 3, 4 and 5. Compared to surface settlements CJ02 and CJ05 (Figure 5-23), there are no large settlement measurements for stage 5 of surface settlements CJ06.

5.4. Excavation in Taipei silty clays

Two excavation sites in Taipei, shown in Figure 5-27, are employed in the inverse analysis and prediction exercise. The Taipei National Enterprise Center (TNEC) and Formosa deep excavation sites are about 2 kilometers apart. Inclinometer measurements from TNEC excavation are used in SelfSim inverse analysis to extract the underlying soil behavior. The extracted soil models are then used in a numerical analysis to predict the performance of Formosa deep excavation.

5.4.1. Site description

TNEC excavation case study

The Taipei National Enterprise Center (TNEC) is an 18-story building with five basement levels using top-down construction techniques (Ou et al. 1998). The site has slightly irregular plan view and occupies an area of about 3500 m^2, as shown in Figure 5-28. The excavation depth is 19.7-m deep. The excavation site was extensively instrumented using earth pressure cells on the wall, rebar stress meters on the reinforcement cage, piezometers, inclinometers, heave gauges and settlement gauges.

A cross section of the excavation is shown in Figure 5-29. The excavation site consists of six layers of alternating silty clay and silty sand deposits overlying a thick gravel formation. The first and second layers consist of silty clay (CL) layer and silty sand (SM) layer, respectively. The third layer is a 26-m-thick silty clay (CL), and it is mainly this layer that affects the excavation behavior. The fourth and fifth layers are medium dense fine sand and silty clay mixed with silty sand, respectively. A gravel formation is located 45 m below the ground surface. Prior to excavation the ground water table was 2 m below the ground surface. A 90-cm-thick and 35-m-deep diaphragm wall was used as the earth-retaining structure. The construction sequence of TNEC excavation is shown in Figure 5-30. The excavation is modeled in five excavation stages down to depth of 15.2 m depth.

Formosa excavation case study

Formosa is an 18.45m deep excavation case study in Taipei. Figure 5-31 shows the plan view of the project and instrument locations (i.e. inclinometer and surface settlement points). The cross section of the wall and soil layers is shown in Figure 5-32. The soil profile is a typical soil profile of Taipei and consists of mainly clayey layers at the top 26 meters. Underneath the clay layer is a combination of silty sand and clayey silt followed by a gravel layer (Ou et al. 1993). The excavation is supported by a 31 m length and 0.8 m thickness diaphragm wall and the struts are in 3m spacing. The ground water table is 2 m below the ground surface.

The 18.45 m excavation was conducted in 7 stages. The measured inclinometers for the last two stages show a shift after installation of struts. Therefore, the excavation is modeled down to fifth stage of the excavation (i.e. 13.2 m). The construction sequence of the excavation is shown in Figure 5-33.

5.4.2. Learning soil behavior from measurements of TNEC excavation, Taipei

The support wall for the TNEC excavation is simulated using solid elements with a bending stiffness equivalent to that of a 90-cm-thick concrete diaphragm wall. The soil profile is represented with four NN material models to represent layers: (1) for top 6 m silty clay and 2 m silty sand (NN1-TNEC), (2) for silty clays between depths of 8 m and 16 m (NN2-TNEC), (3) for silty clays between depths of 16m and 24m (NN3-TNEC), and (4) for silty clays between depths of 24m and 34m (NN4-TNEC). Elastic material model with Young modulus of E = 16.6 MPa is assigned for the depths lower than 34m. TNEC excavation is modeled as 2D symmetric excavation with a half width of 25m. The model dimensions are 170m and 70m in horizontal and vertical dimensions, respectively.

Prior to any SelfSim learning all NN soil constitutive models are pre-trained to represent linear elastic response within a very small strain range. The initial Young's modulus used for pre-training is sufficiently large to produce small excavation-induced deformations. A set of SelfSim learning analyses was conducted using wall deformation measurements (I-1) only. SelfSim learning failed beyond stage three of the excavation. This might be due to a limitation in the information contained in these additional stages. Therefore, an inclinometer measurements SI-4, 22 m away from the excavation wall is

added to the wall deformation measurements as part of further SelfSim learning down to fifth excavation stage. Figure 5-34 shows the measured and predicted wall deformations, lateral deflections of inclinometer SI-4 and surface settlements after six passes of SelfSim learning. The computed lateral deformations of wall (I-1) and inclinometer SI-4 are in close agreement with the measured values. The settlements (not used in SelfSim learning) are also predicted reasonably.

5.4.3. Predicting the excavation response in Formosa excavation, Taipei

The developed soil models after SelfSim learning with wall deformations of inclinometer I-1 and SI-4 from Taipei National Enterprise Center (TNEC) building in Taipei are used to predict the wall deflections and surface settlements in Formosa excavation.

The support wall for Formosa deep excavation is simulated using solid elements with a bending stiffness equivalent to that of 0.8-m-thick diaphragm wall. The soil profile in the analysis is represented with three extracted NN material models from TNEC excavation. The represented soil layers are as followings: (1) NN1-TNEC soil model for top 1 m fill, (2) NN2-TNEC soil model for clays between depth of 1m and 12m, (3) NN3-TNEC soil model of TNEC for clays between depth of 12m and 26m. Elastic material model with Young's modulus of E = 16.6 MPa is used for the depths lower than 26m. The Formosa deep excavation is modeled as a 2D symmetric excavation with half width of 15m. The model dimensions are 120m and 70m in horizontal and vertical dimensions, respectively.

Figure 5-35 shows the predicted and measured deformations of inclinometers and settlement points. The predicted wall deformations reasonably match with the measured values. The surface settlements are also reasonably predicted up to 10 m from the wall. The surface settlements are slightly overestimated at farther distances from the wall. It should be emphasized that no measurements from Formosa excavation case study were used in SelfSim learning and the computed values are pure predictions.

TNEC and Formosa case studies show a successful application of SelfSim learning whereby extracted soil behavior from a case study in Taipei provides a reasonable prediction of wall deformations and surface settlements in another case study with similar soil stratigraphy.

5.5. Summary

This chapter demonstrated that inverse analysis can be a suitable approach to predict the excavation performance in urban area after learning from precedent case histories or local experience.

The chapter highlighted the importance of having reliable measurements that can be clearly related to specific construction activities (cause and effect). Therefore it is not sufficient to rely on measurements of quantities such as deformations and pressures, but there is a need to develop a detailed record of construction.

The extracted soil behavior from two-level tieback section of the wall in Texas A&M case study in sandy soil could predict reasonable wall deformations and lateral deformations in distances from the wall in one-level tieback section of the wall. The extracted soil behavior from instrument measurements in cluster 1 of Yishan Road metro station case study provide a reasonable prediction of wall deformations and surface settlements in clusters 2 and 3 along the 335 m length of the station. Predicted pore water pressures are in agreement with the measured values. Use of extracted soil behavior from TNEC project to predict the excavation behavior in Formosa case study in soft clays of Taipei shows a successful implication of SelfSim framework whereby excavation performance can be predicted after learning from precedent.

In the future, the proposed inverse analysis approach can be used with available measurements to develop numerical models with "local experience". Available excavation performance data sets can be used to develop area-specific soil models (e.g. San Francisco Bay Mud, Boston Blue Clay). The developed soil models can be used to provide acceptable predictions of excavation-induced ground deformations for new excavations constructed in these locals.

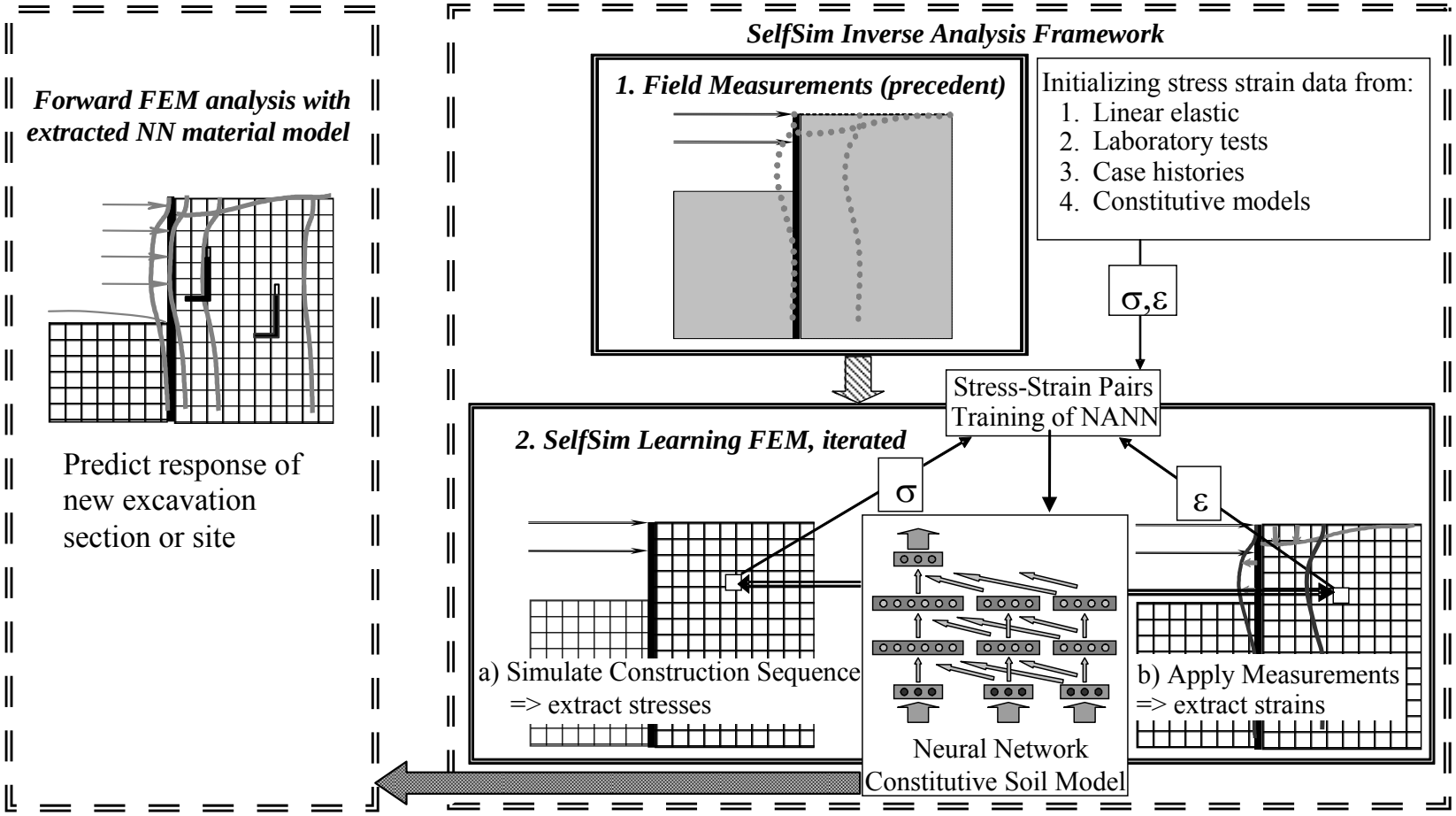

Figure 5-1 Application of SelfSim inverse analysis framework to predict ground response at a new excavation section or site.

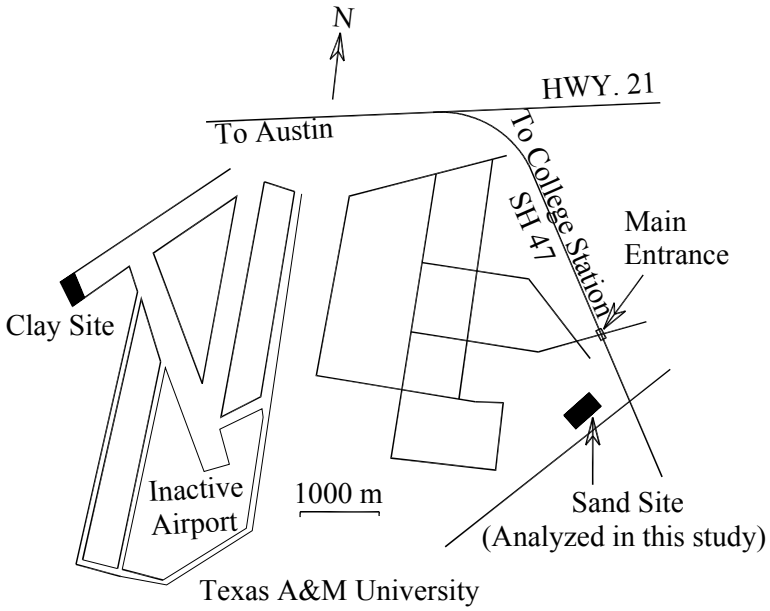

Figure 5-2 Location of sandy site at Texas A&M University (Benoit and Lutenegger 2000)

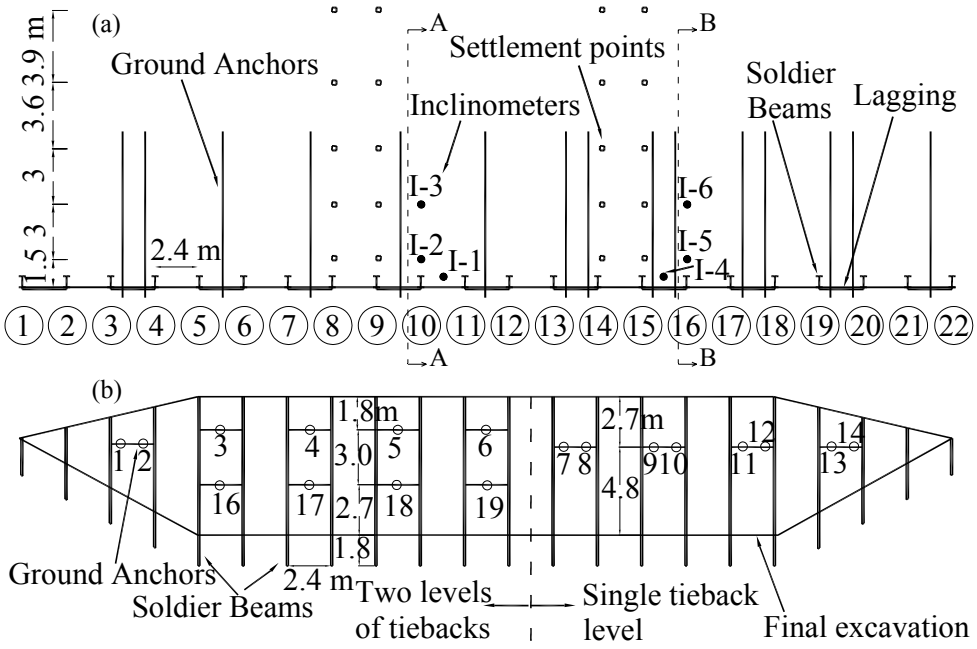

Figure 5-3 Schematic of Texas A&M University full scale model excavation site showing a) plan view and instrument locations, b) elevation view of the wall, inclinometer labels introduced in this study, modified after Weatherby et al. (1998)

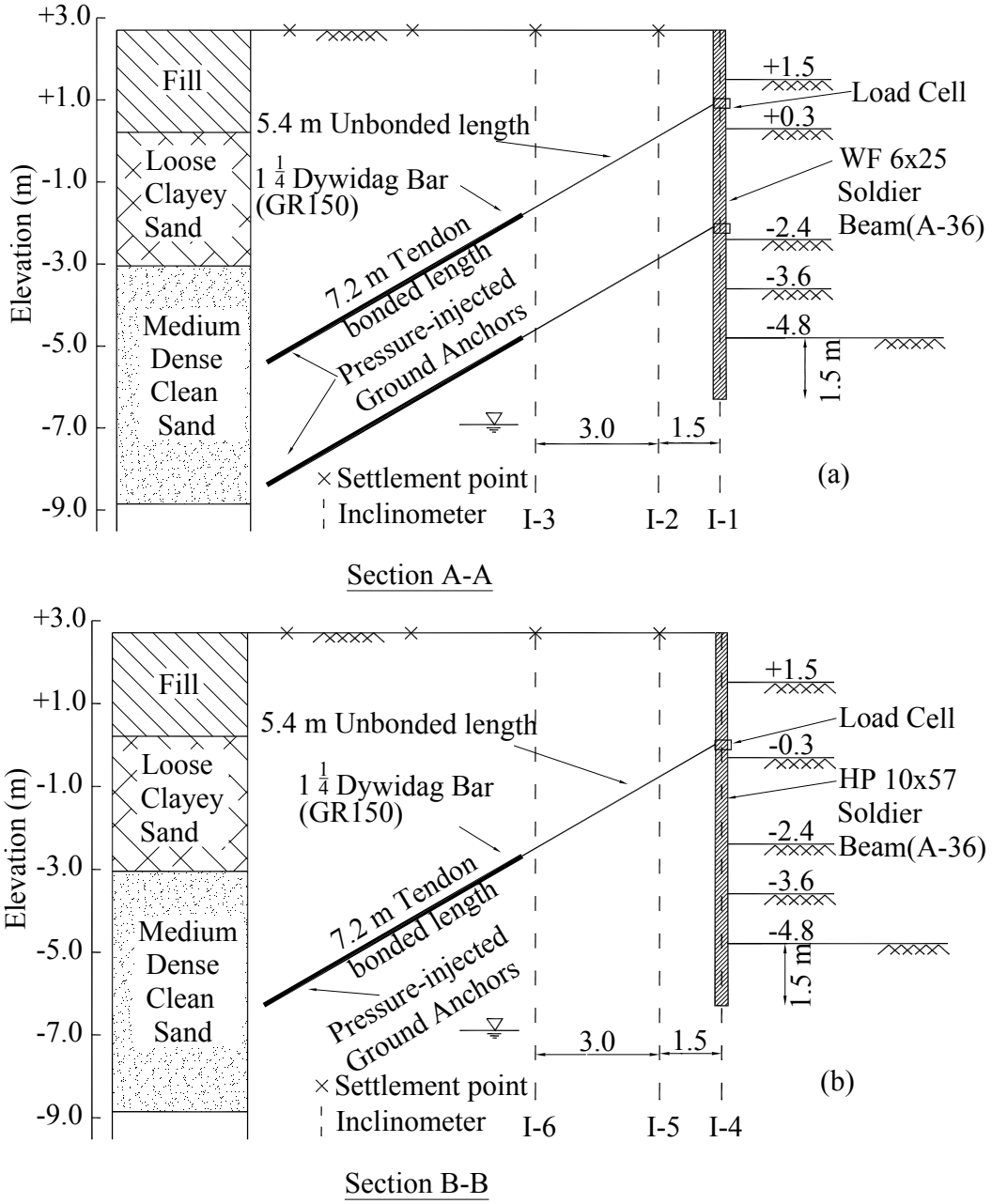

Figure 5-4 Sections of the Texas A&M University full scale model wall: a) two level tieback, b) one level tieback, modified after Weatherby et al. (1998)

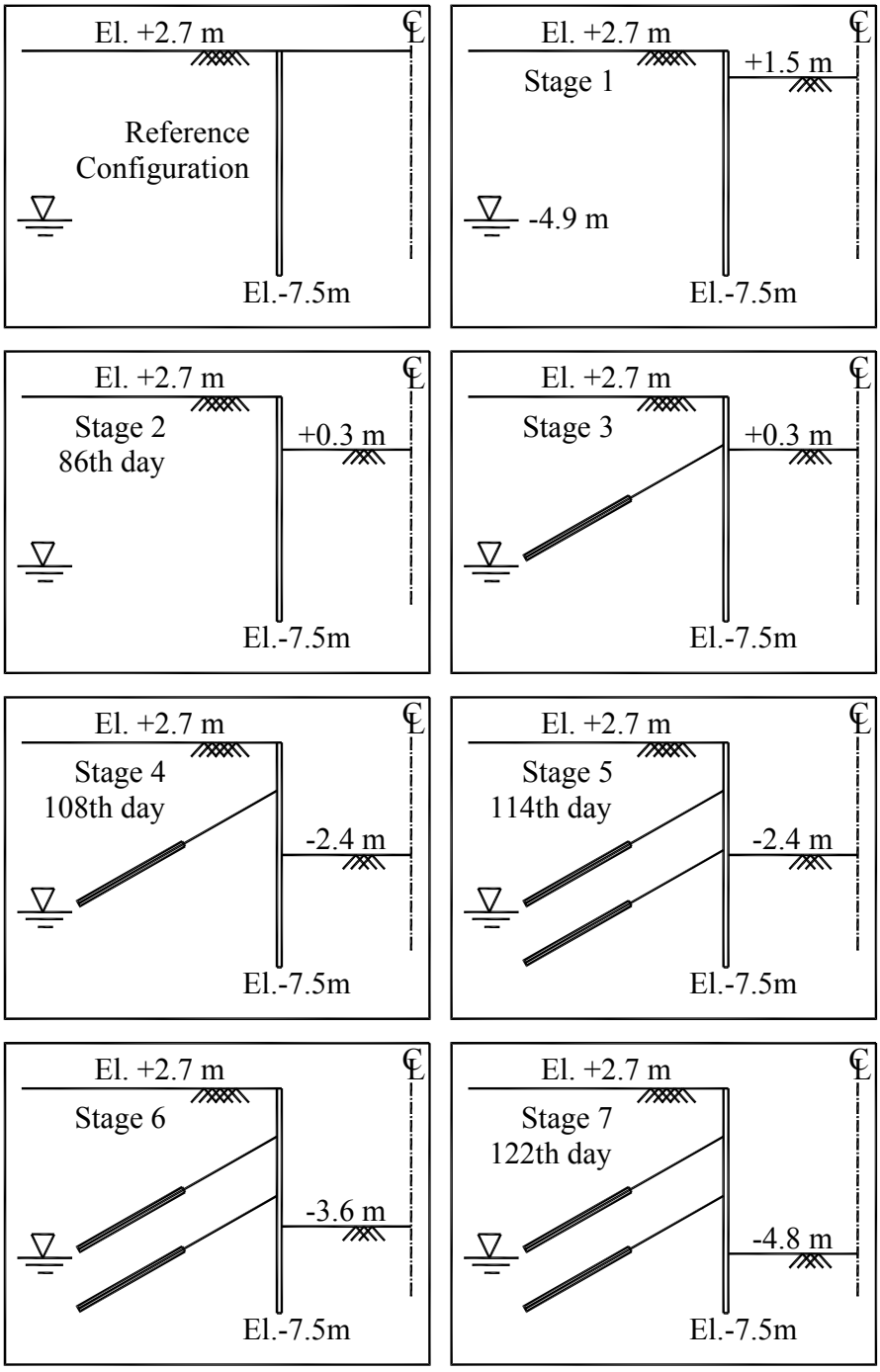

Figure 5-5 Construction sequence for two level tieback section of the Texas A&M University full scale model wall

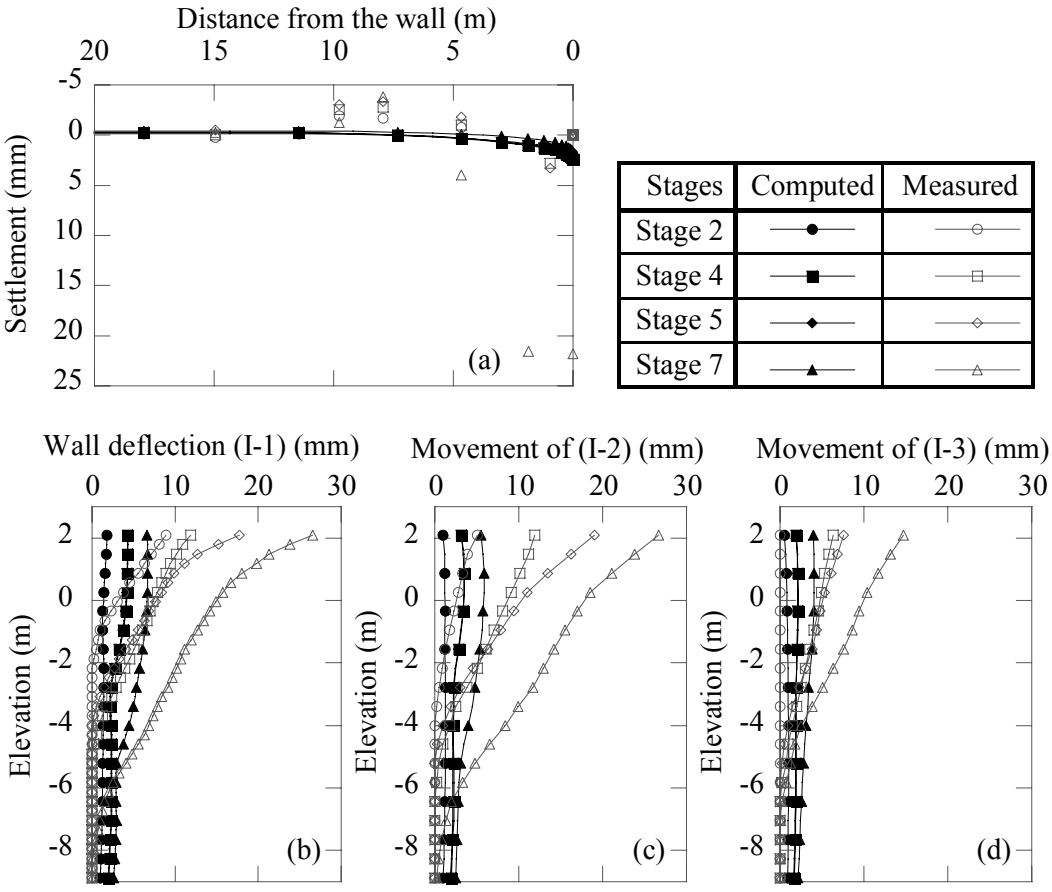

Figure 5-6 Computed response in two anchor section, Texas A&M excavation, prior to SelfSim learning.

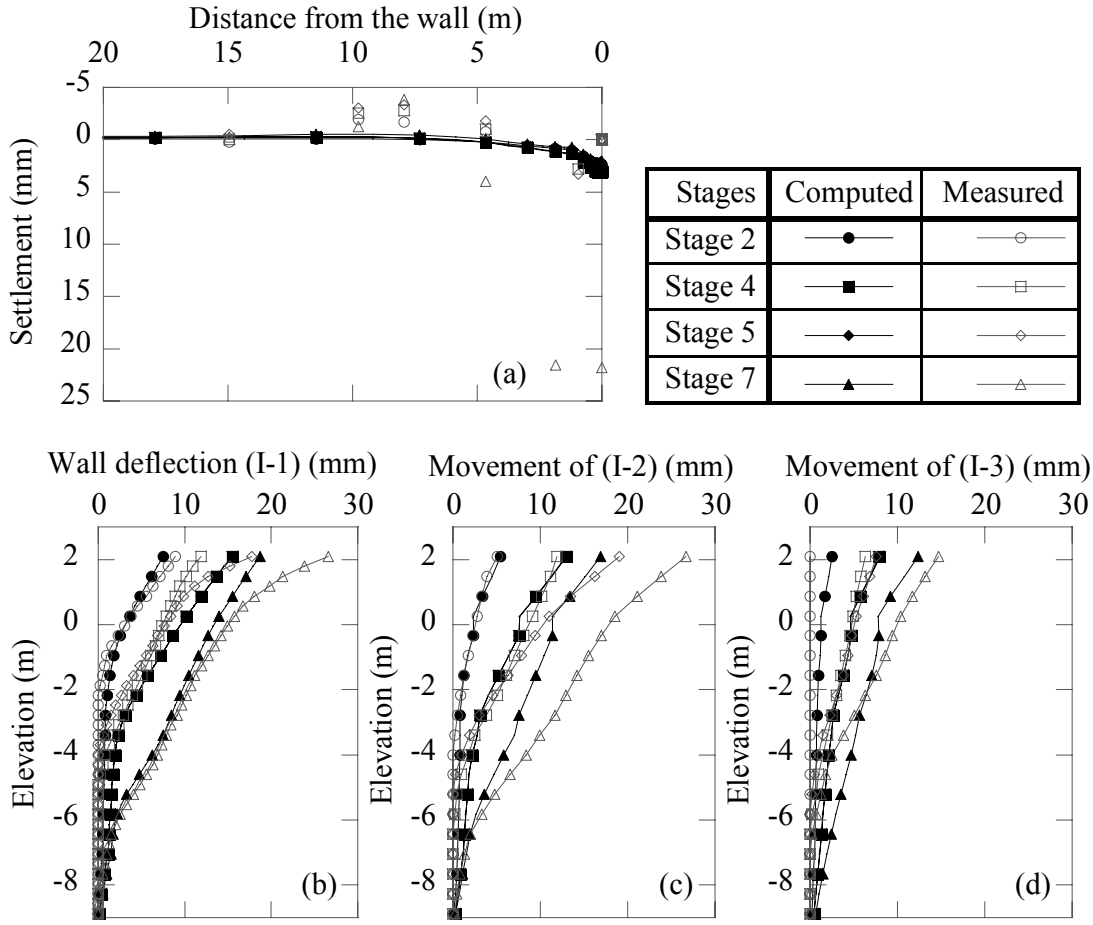

Figure 5-7 Computed response, two anchor section, Texas A& M excavation, after six passes of SelfSim learning with wall deformations (I-1) only

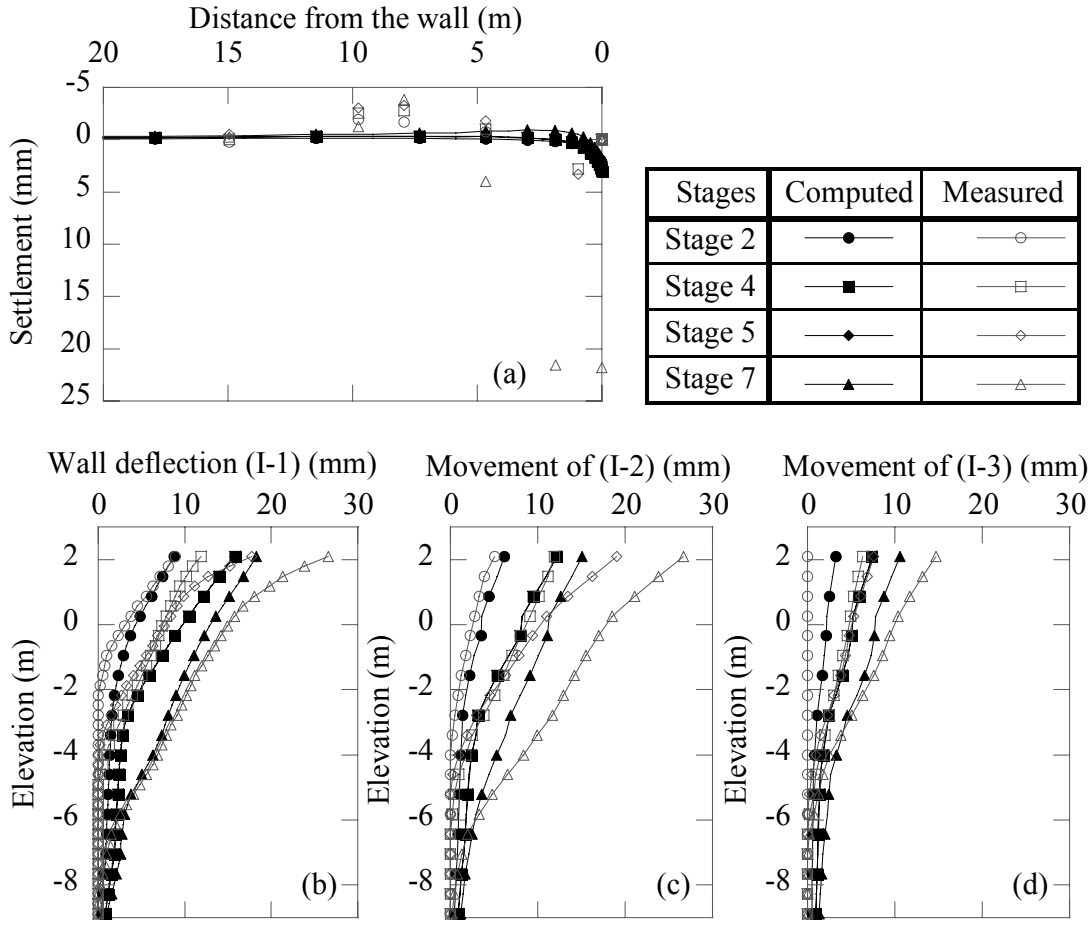

Figure 5-8 Computed response, two anchor section, Texas A& M excavation, after six passes of SelfSim learning with wall deformations (I-1), and lateral movements of inclinometer I-3.

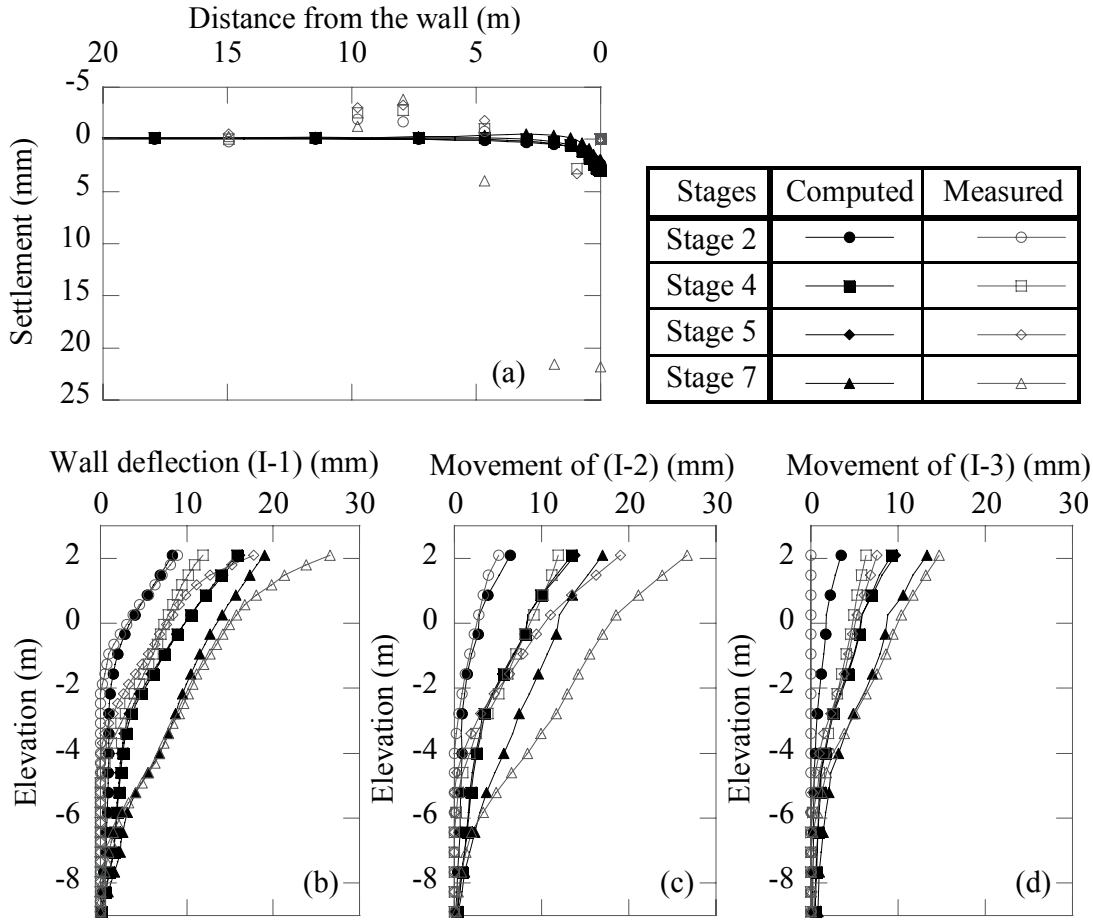

Figure 5-9 Computed response, two anchor section, Texas A& M excavation, after six passes of SelfSim learning with wall deformations (I-1), lateral movements of inclinometer I-3, and tieback loads.

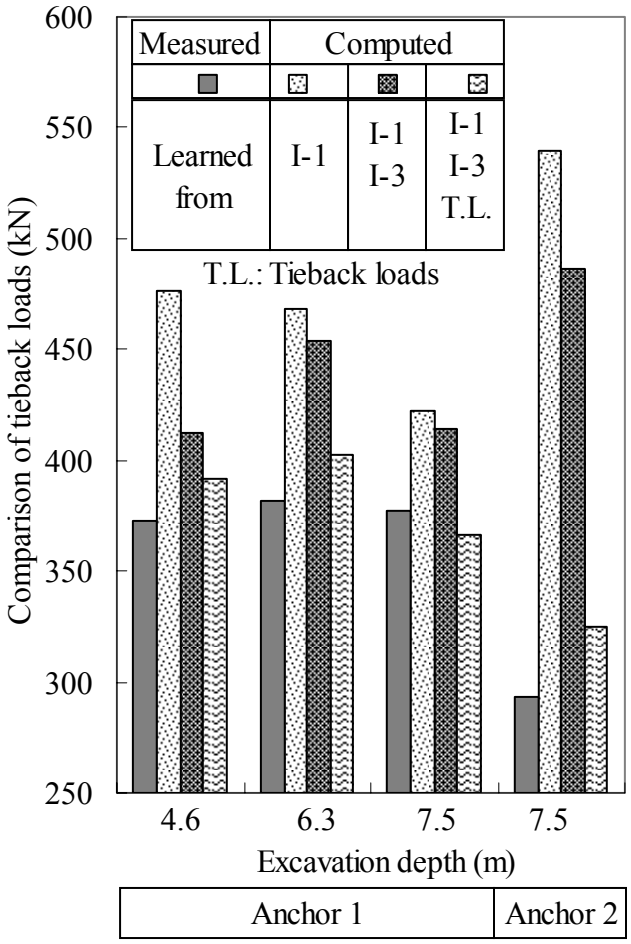

Figure 5-10 Comparison of measured and computed tieback loads in two-level tieback section of the wall, Texas A&M excavation

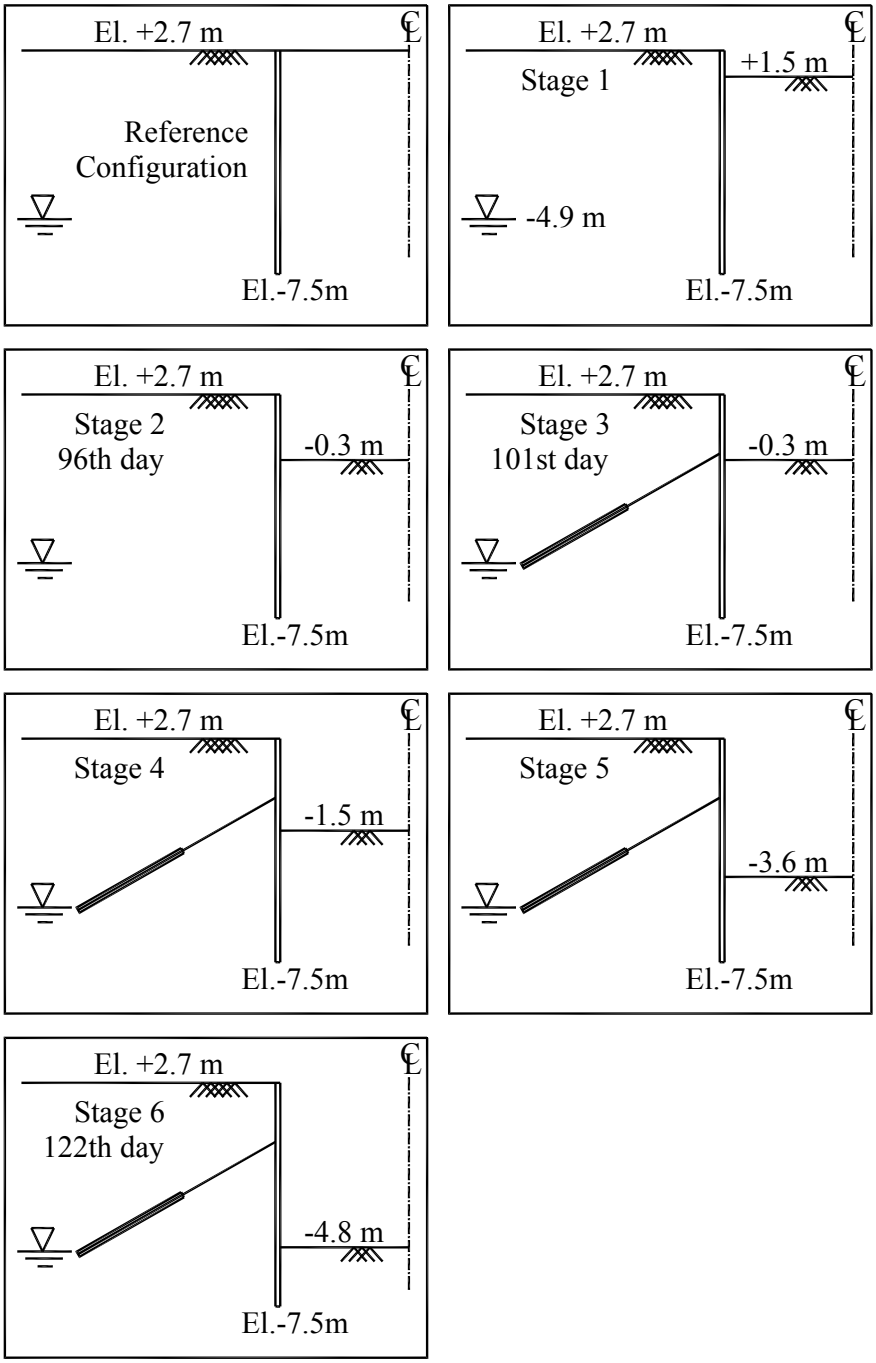

Figure 5-11 Construction sequence for single tieback section of the wall, Texas A& M excavation

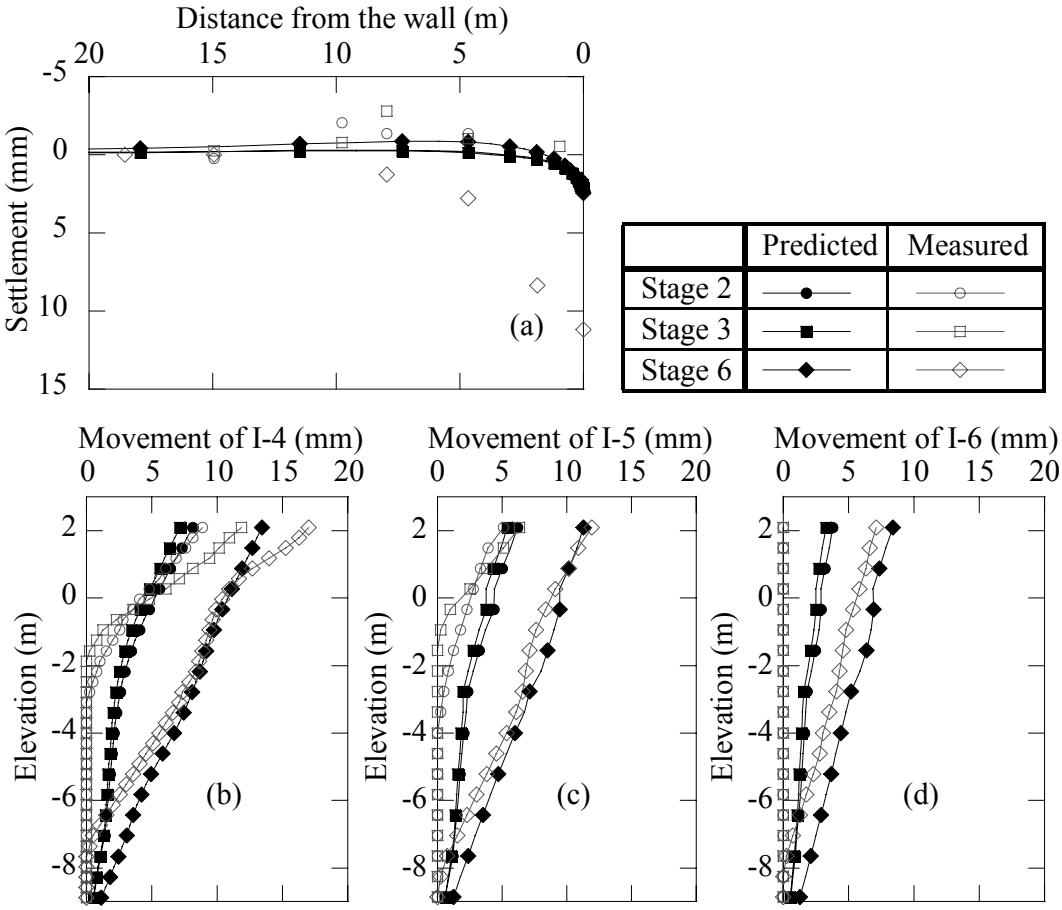

Figure 5-12 Predicted excavation response in single tieback level section, Texas A& M excavation, using developed model from learning wall deflections (I-1) only.

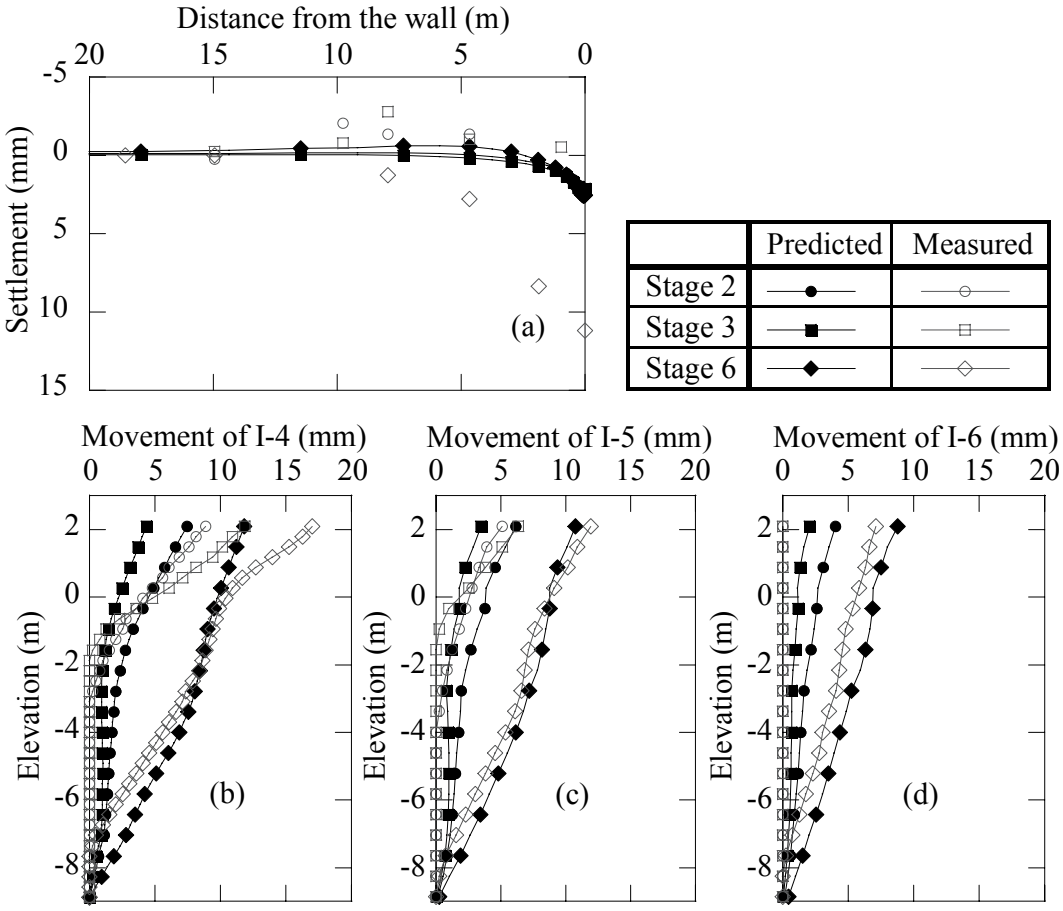

Figure 5-13 Predicted excavation response in single tieback level section, Texas A& M excavation, using developed model from learning wall deflections (I-1), and lateral movements of inclinometer I-3 in two-level tieback section of the wall.

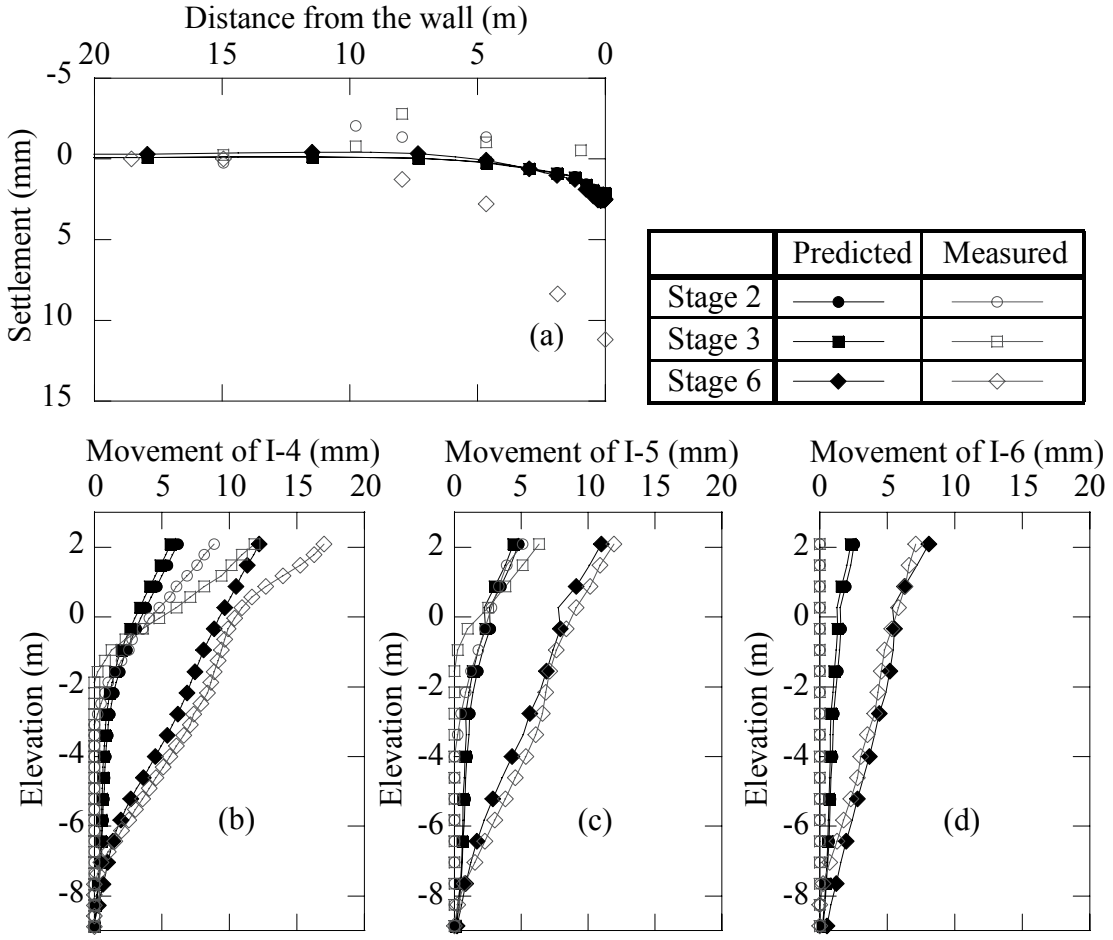

Figure 5-14 Predicted excavation response in single tieback level section, Texas A& M excavation, using developed model from learning wall deflections (I-1), lateral movements of inclinometer I-3 and tieback loads in two-level tieback section of the wall.

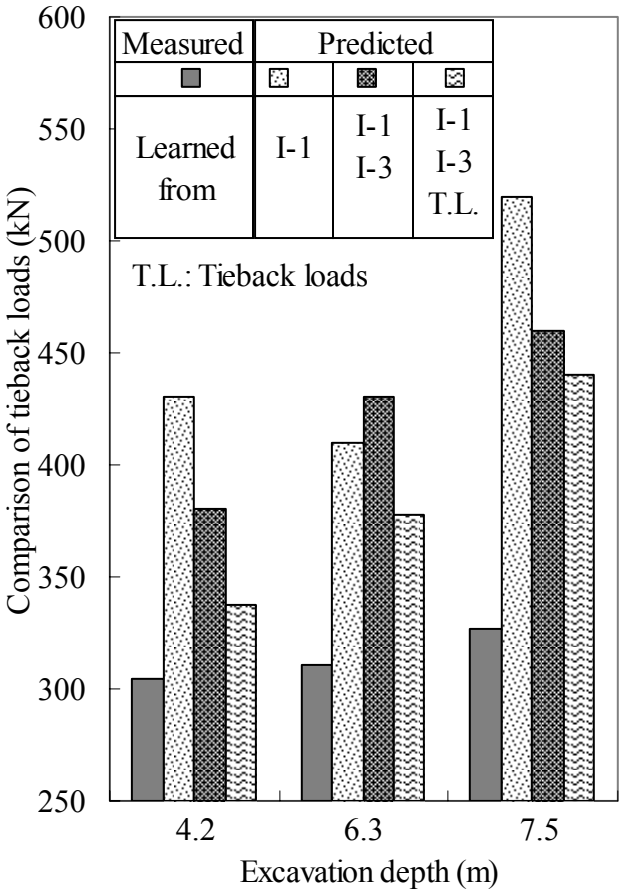

Figure 5-15 Comparison of measured and predicted tieback loads in single tieback level section of the wall, Texas A&M excavation

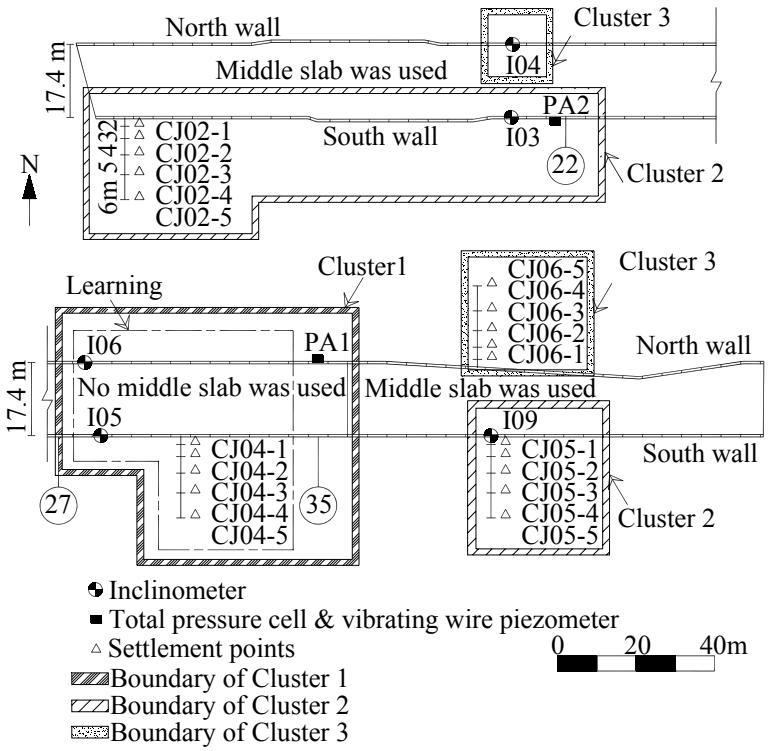

Note: These were the only instruments used in this study.

Figure 5-16 Plan view of Yishan road metro station and instrument locations, Shanghai excavation, modified after Liu et al. (2005)

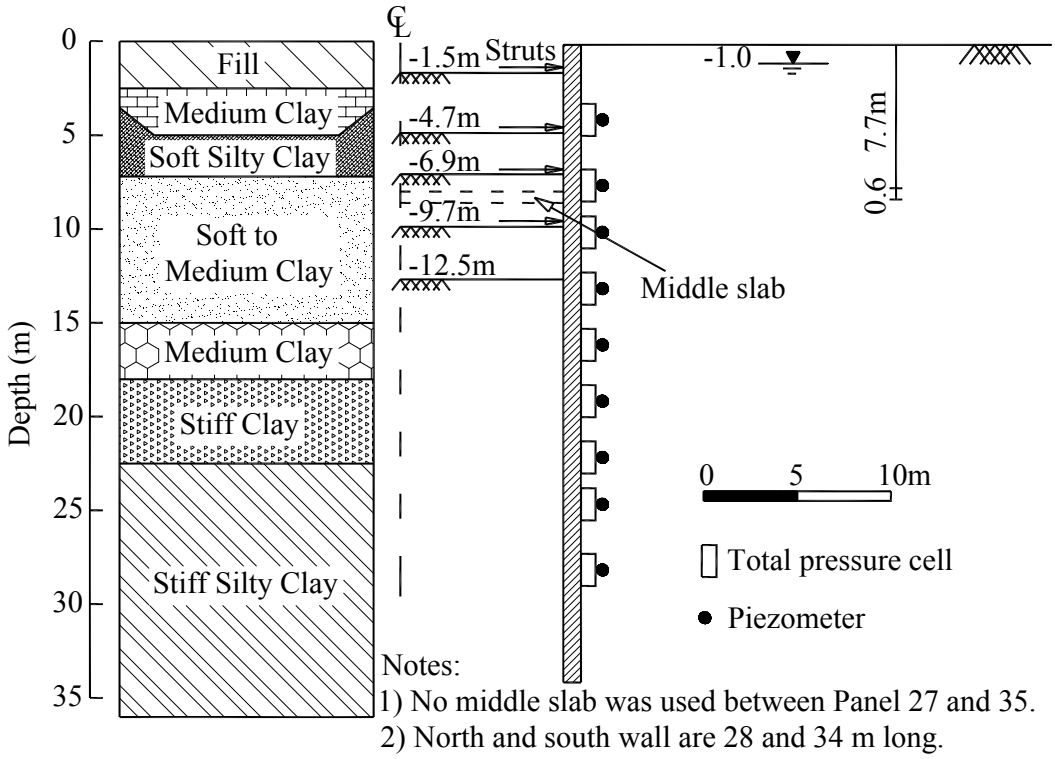

Figure 5-17 Typical cross section of the Yishan road metro station, Shanghai excavation, modified after Liu et al. (2005)

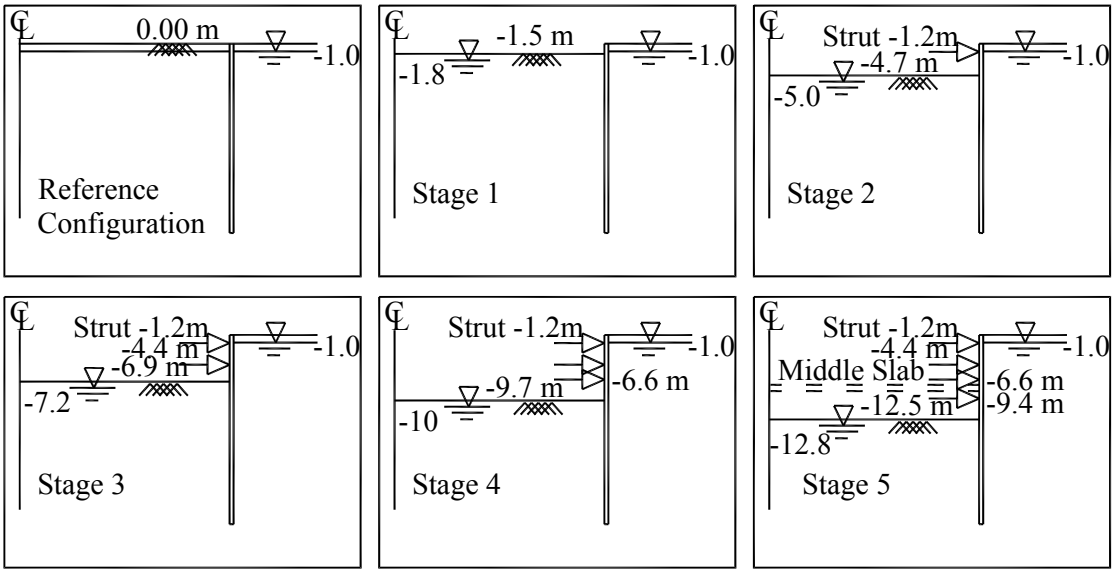

Cluster	Instruments	Middle Slab	Wall length	
			North	South
1	I05, I06, CJ04, PA1	No	28m	28m
2	I09, CJ05, I03, CJ02, PA2	Yes	----	34m
3	I04, CJ06	Yes	28m	----

Figure 5-18 Construction sequence for different clusters, Shanghai excavation

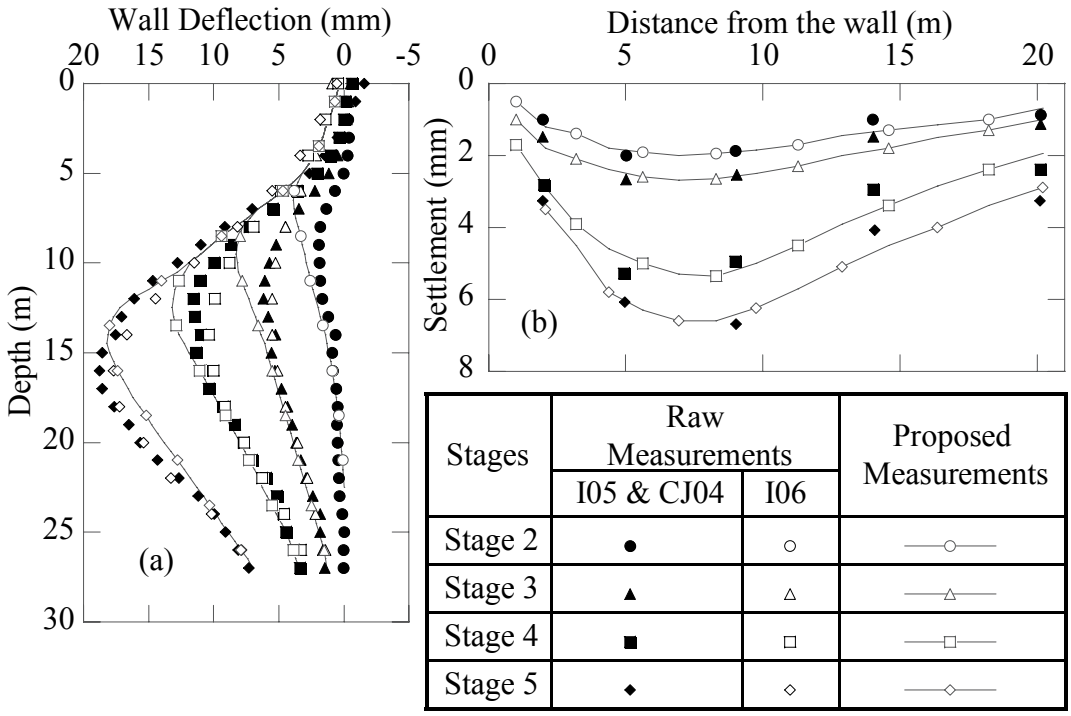

Figure 5-19 Original and proposed measurements for inverse analysis for a) lateral wall deflections of I05 & I06, and b) surface settlements CJ04, Shanghai excavation

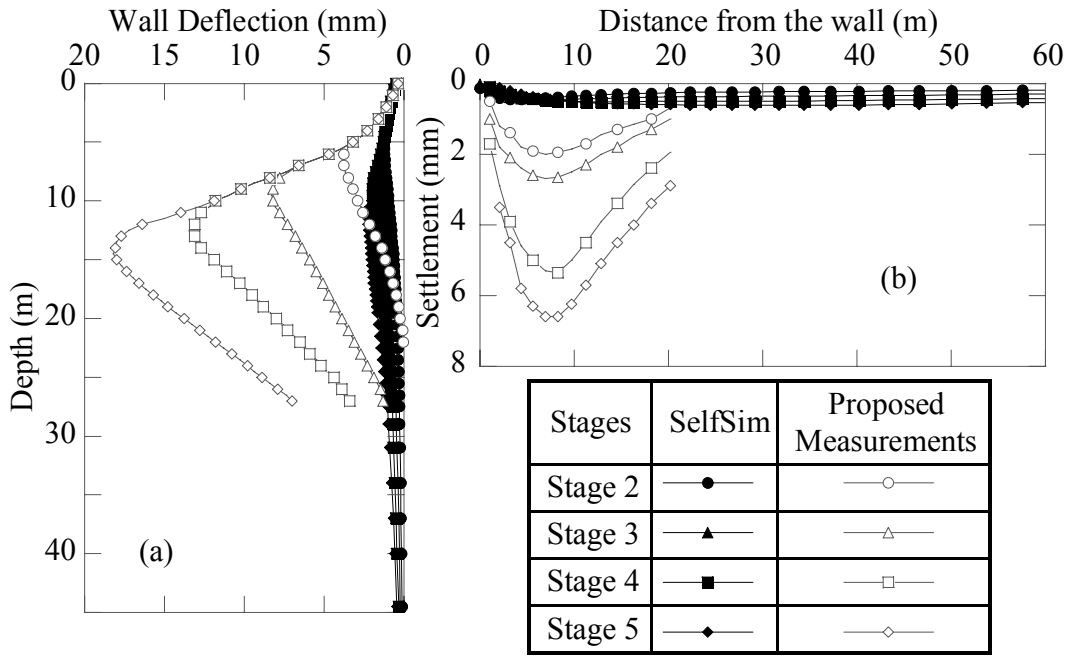

Figure 5-20 Computed deformations in Cluster 1 prior to SelfSim learning; a) wall deformations, and b) surface settlements, Shanghai excavation

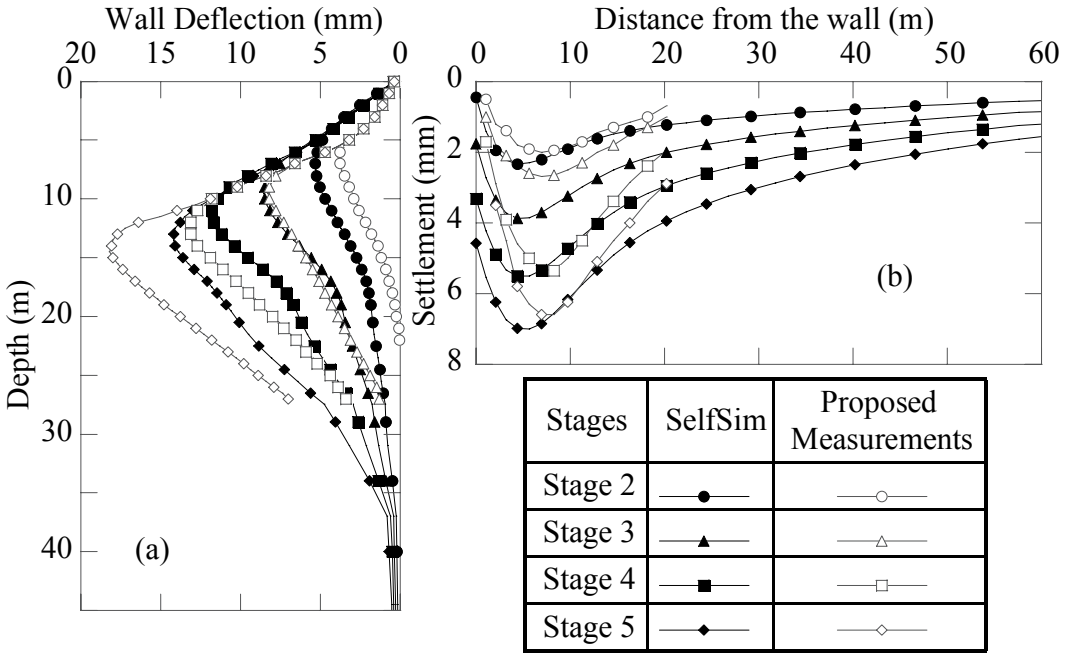

Figure 5-21 Computed deformations in Cluster 1 after six passes of SelfSim learning with Cluster 1 measured deformations; a) wall deformations, and b) surface settlements, Shanghai excavation

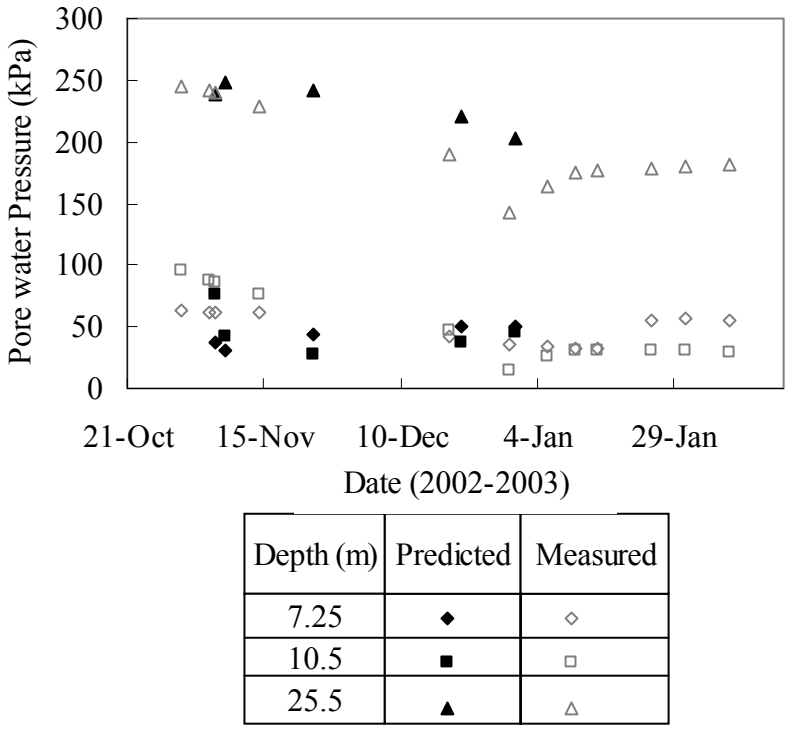

Figure 5-22 Comparison of predicted and measured pore water pressures for PA1 in cluster 1, Shanghai excavation

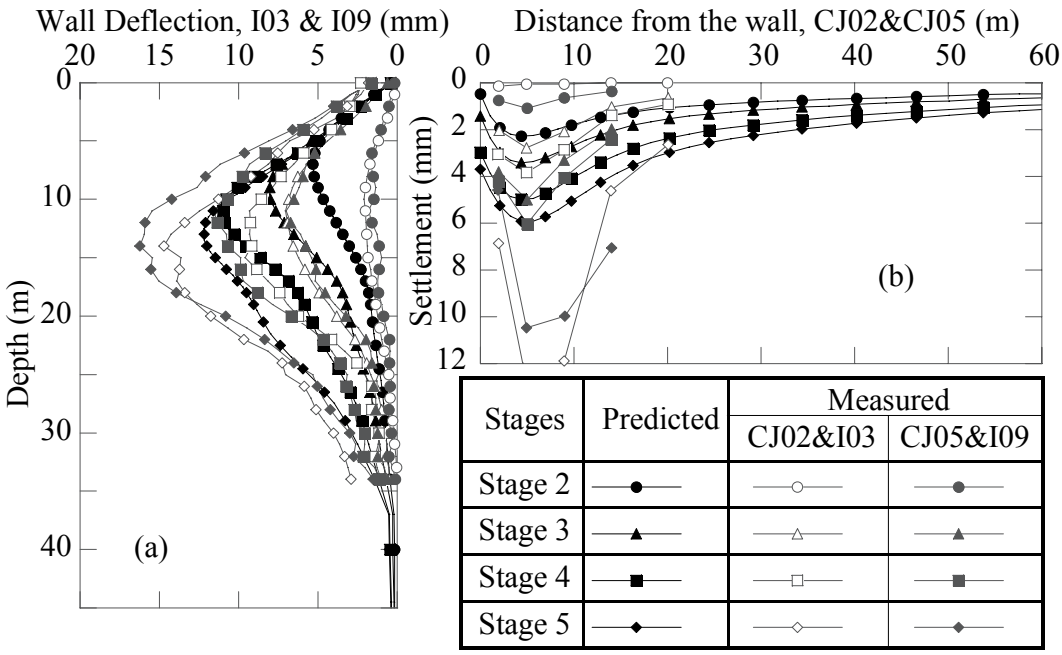

Figure 5-23 Predicted deformations in cluster 2 after six passes of SelfSim learning with Cluster 1 deformations; a) wall deformations (I03 and I09) and b) surface settlement CJ02 and CJ05, (middle slab was used), Shanghai excavation

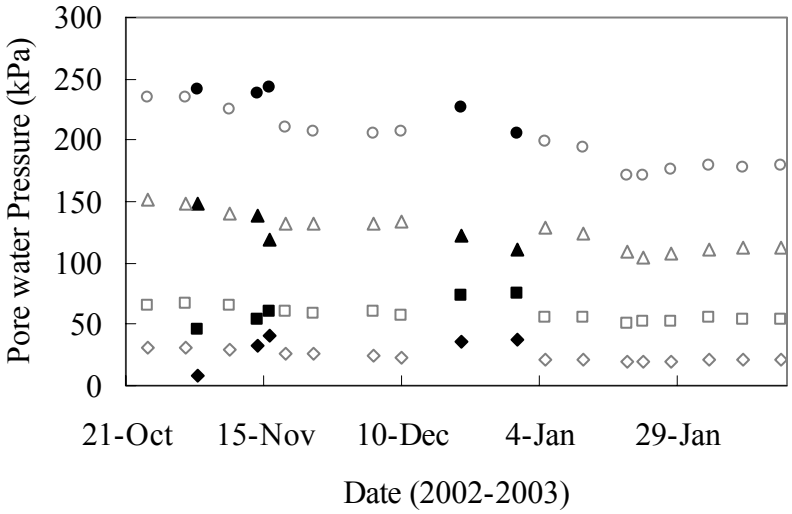

Depth (m)	Predicted	Measured
4	◆	◇
7.5	■	□
16	▲	△
24.5	●	○

Figure 5-24 Comparison of predicted and measured pore water pressures for PA2 in cluster 2, Shanghai excavation

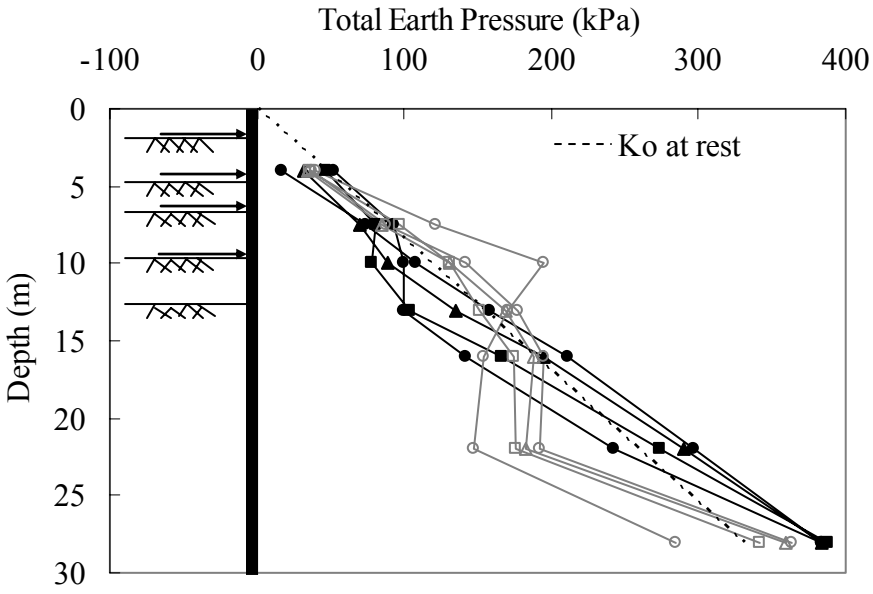

Figure 5-25 Comparison of predicted and measured earth pressures for PA2 (for legend see Figure 5-20)

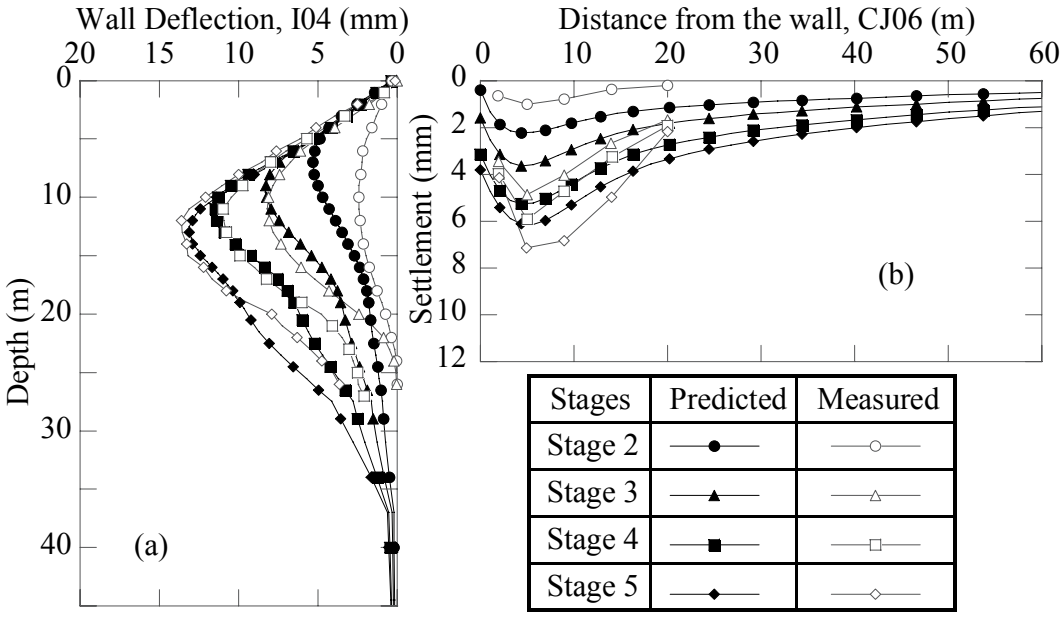

Figure 5-26 Predicted deformations in cluster 3 after six passes of SelfSim learning with cluster 1 deformations; a) wall deformations (I04) and b) surface settlement CJ06, (middle slab was used), Shanghai excavation

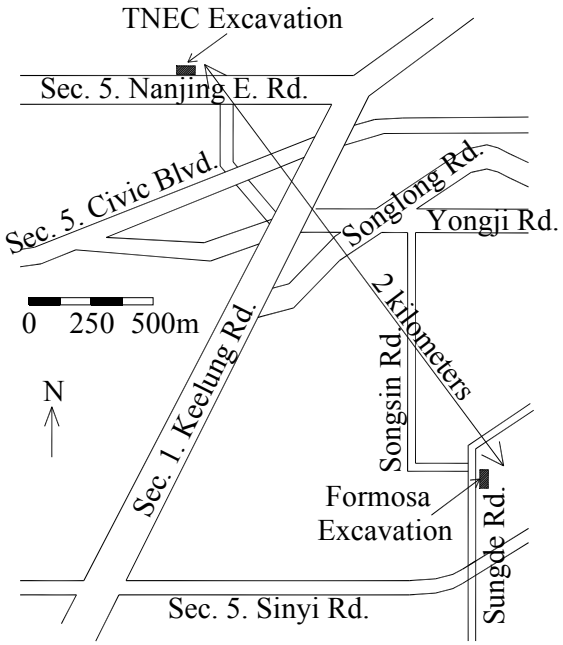

Figure 5-27 The location of TNEC and Formosa excavation site in Taipei

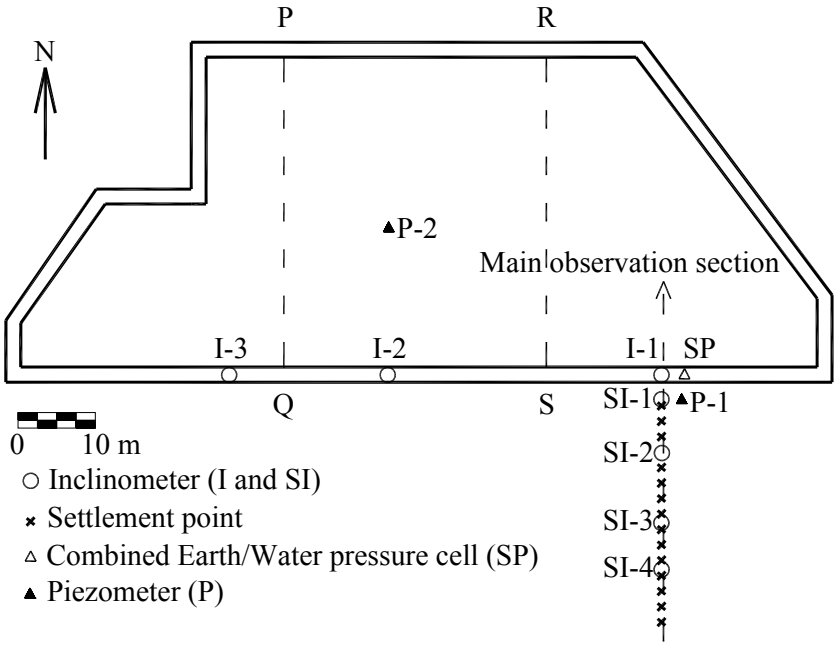

Figure 5-28 Plan view and instrument locations in TNEC excavation, modified after Ou et al. (1998)

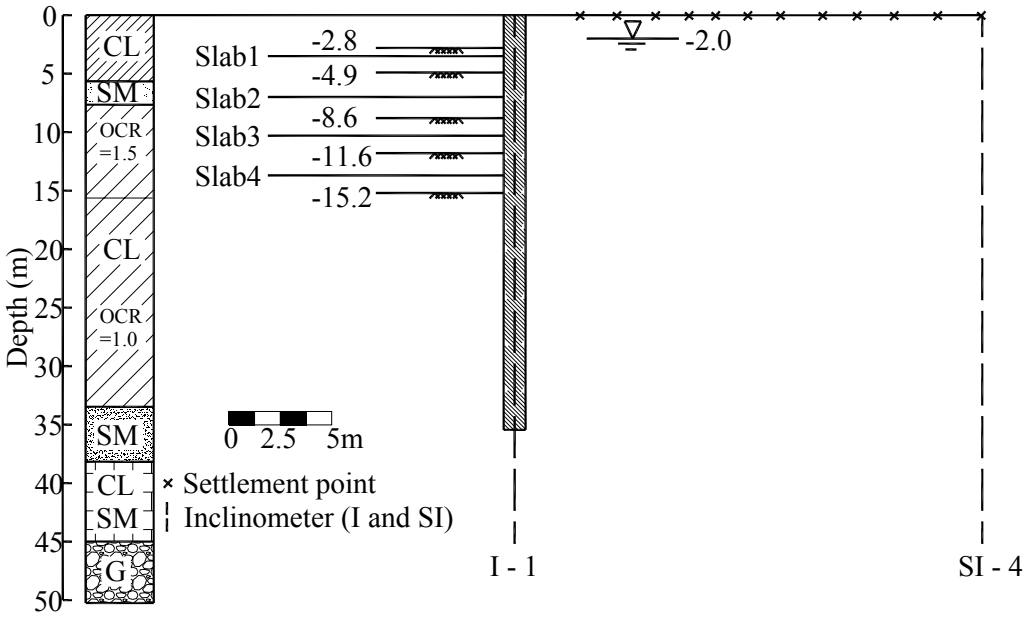

Figure 5-29 Excavation section view of TNEC excavation, modified after Ou et al. (1998)

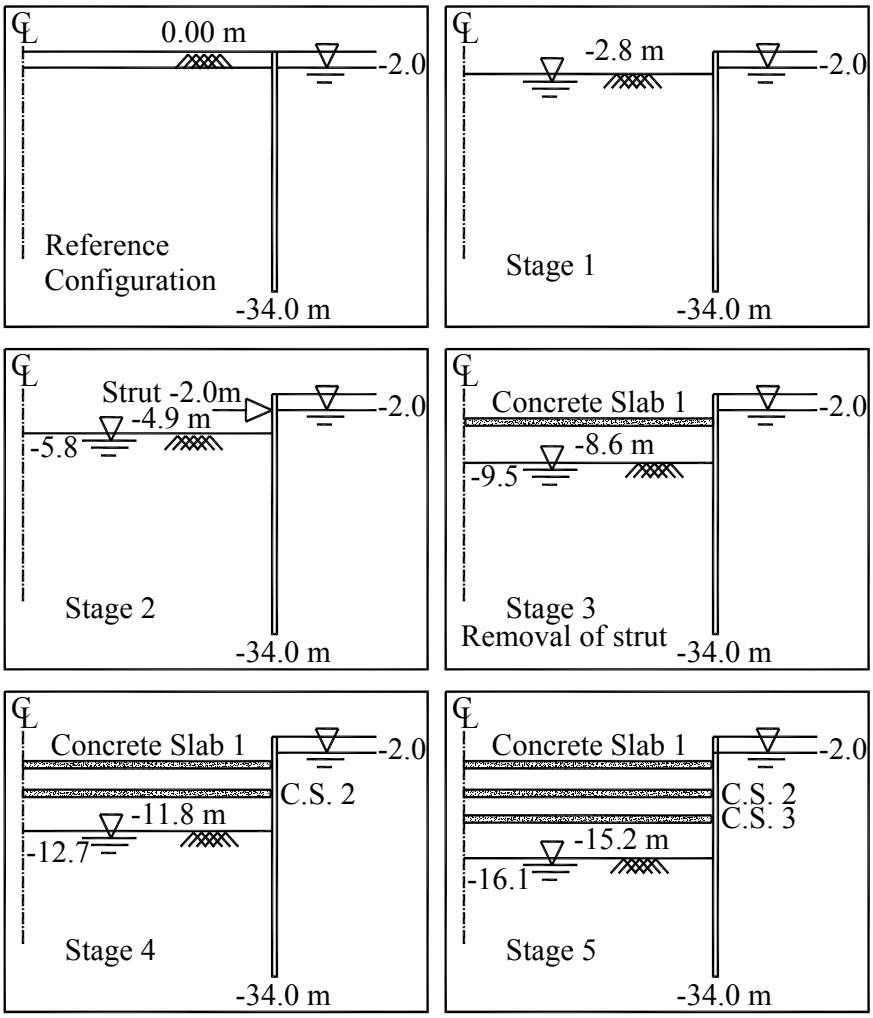

Figure 5-30 Excavation sequence in TNEC project in Taipei

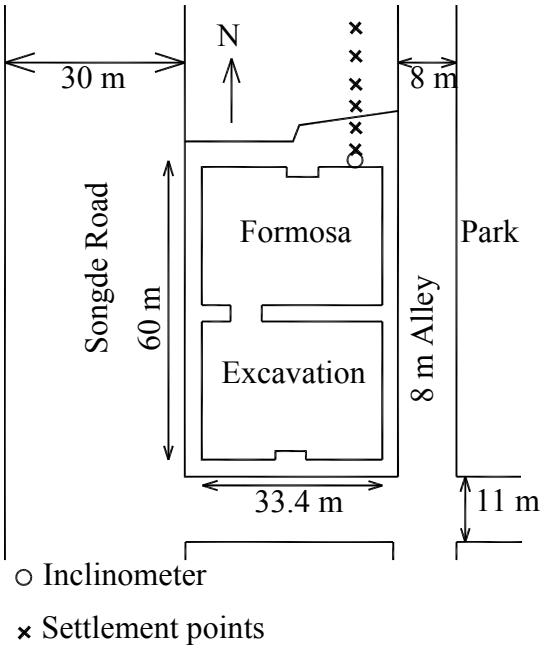

Figure 5-31 Plan view of Formosa excavation and instrument locations

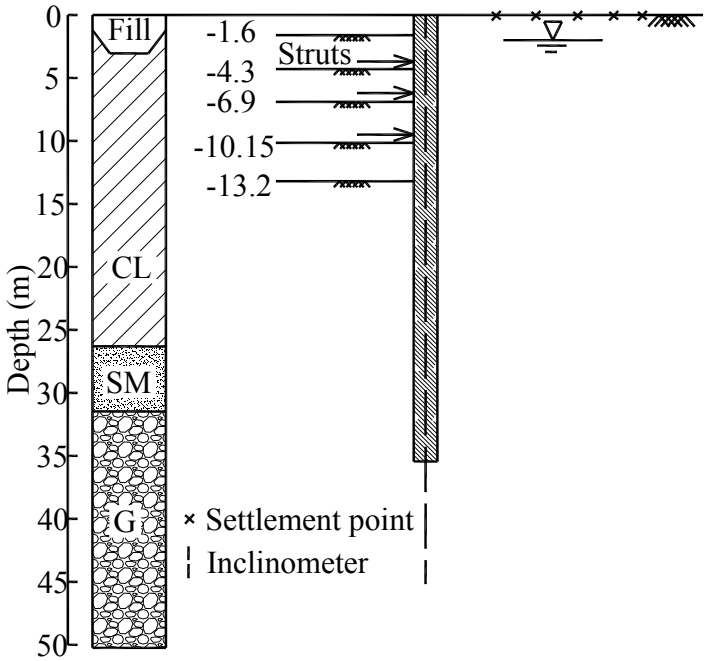

Figure 5-32 Cross section of the wall and soil layers in Formosa excavation

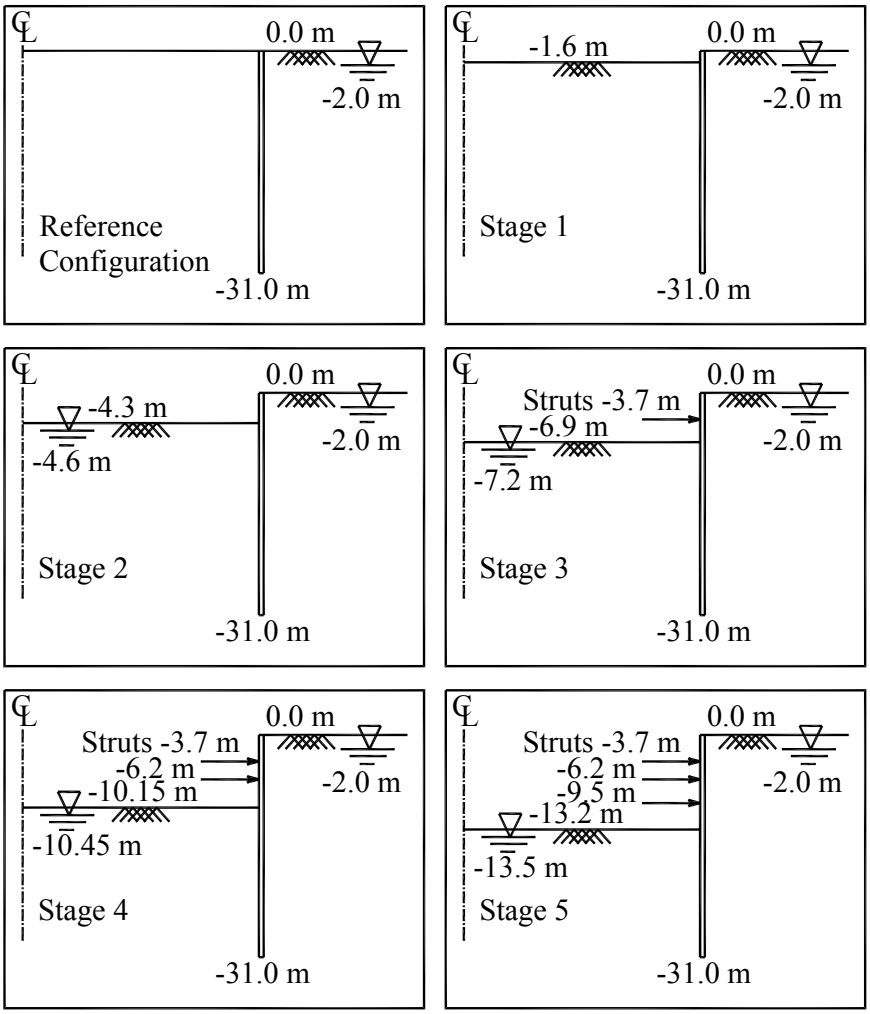

Figure 5-33 Construction sequence of Formosa excavation

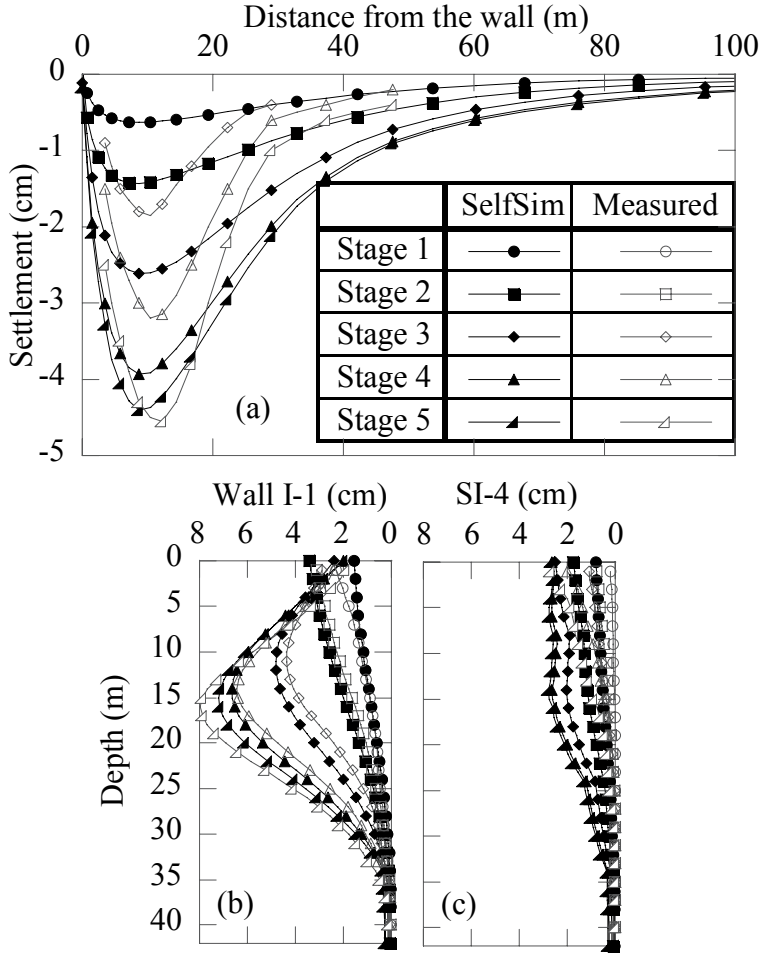

Figure 5-34 Computed response after six passes of SelfSim learning with wall deformations (I-1) and inclinometer SI-4 at 22 m distance from the wall, down to fifth stage of the excavation using the database of SelfSim learning with wall deformations only down to stage 3 for (a) surface settlements, (b) wall deflections (I-1), (c) lateral movement at SI-4 in TNEC excavation.

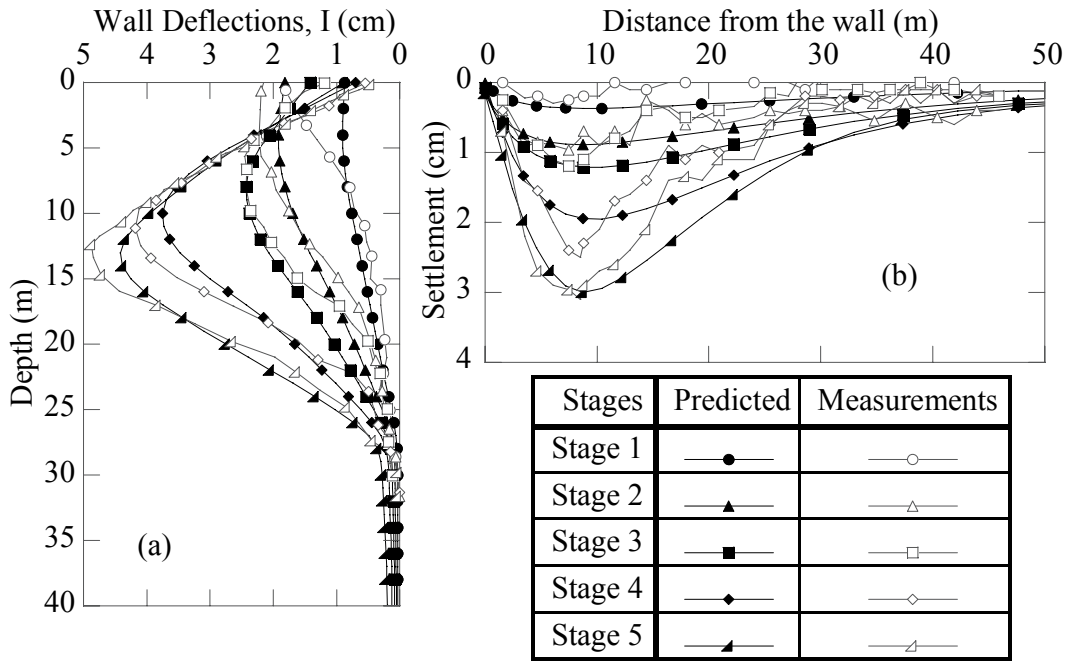

Figure 5-35 Predicted and measured excavation response for a) lateral wall deflections, b) surface settlements in Formosa excavation

CHAPTER 6 TWO AND THREE-DIMENSIONAL INVERSE ANALYSES OF DEEP EXCAVATIONS IN CHICAGO CLAYS

6.1. Introduction

Estimate and control of ground movements induced by deep excavations are critically important in urban areas. During excavations instruments are installed to monitor ground response and to verify design assumptions. In practice, a number of empirical and semi-empirical methods are used to estimate ground deformations (Peck 1969; Clough and O'Rourke 1990; Kung et al. 2007).

Numerical methods have also been used to estimate ground movements (Wong 1970; Clough and Tsui 1974; Mana and Clough 1981; Finno and Harahap 1991; Hsi and Small 1993; Whittle et al. 1993; Hashash and Whittle 2002; Finno and Calvello 2005). Generally plane strain two-dimensional (2D) analysis is conducted to assess wall and ground movements in the center of each side of the excavation. This simplifying assumption is sometimes inconsistent with the measured excavation behavior in the field. To date, due to high cost of computational cost and time constraints, the full three-dimensional (3D) analyses have been infrequently applied in practice. A number of 3D simulation studies have been conducted to describe the 3D effects in deep strutted excavations in a variety of soil conditions (St-John 1975; Ou et al. 1996; Ou and Shiau 1998; Zhang et al. 1999; Moormann and Katzenbach 2002; Finno and Roboski 2005; Zdravkovic et al. 2005; Ou et al. 2008).

Ou et al. (1996) proposed a relationship for estimating three-dimensional maximum wall deflection of an excavation based on two-dimensional finite element results. The proposed technique was explored in detail for Taipei National Enterprise Center (TNEC) excavation by Ou et al. (2000). Finno et al. (2007), conducted 150 finite element simulations to define the effects of excavation geometry, i.e., length, width, and depth of excavation, wall system stiffness, and factor of safety against basal heave on the three-dimensional ground movements caused by excavations in clays. The results of the analyses were represented by the plane strain ratio (PSR), defined as the maximum movement in the center of an excavation wall computed by three-dimensional analyses normalized by that computed from a plane strain simulation. Results of their analysis

showed that the ratio of the wall length to the excavation depth is the most influential factor.

Finno and Roboski (2005) analyzed the measured 3D reposne of Lurie Center excavation in Chicago clays and proposed a closed form solution to estimate the settlements that developed parallel to the support walls at the Lurie Center excavation. The settlements can be estimated by a complimentary error function, given a maximum movement, and depth and length of excavation.

Inverse analyses have been applied to several geotechnical problems (Sakurai and Takahashi 1969; Cividini and Rossi 1983; Gioda and Sakurai 1987; Hashash et al. 2006). Inverse analyses have been used to identify soil parameters from laboratory or insitu tests (Anandarajah and Agarwal 1991; Zentar et al. 2001; Samarajiva et al. 2005), performance data from excavation support systems (Ou and Tang 1994; Hashash and Whittle 1996; Calvello and Finno 2004), excavation of tunnels in rock (Sakurai and Takahashi 1969; Gens et al. 1996; Gioda and Locatelli 1999), and embankment construction on soft soils (Arai et al. 1986; Honjo et al. 1994).

The common application of numerical modeling is “back calculation”, in which the simulated model is adjusted to agree with measured values. This approach is primarily a linear process with ad hoc loops. This approach to the solution of boundary value problems is not always successful in capturing measured field behavior due to various factors including the lack of sufficient knowledge of soil behavior under complex shearing modes experienced in the field (Hashash et al. 2006).

Optimization techniques (Gioda and Sakurai 1987; Ou and Tang 1994; Ledesma et al. 1996; Pal et al. 1996; Zentar et al. 2001; Calvello and Finno 2004; Samarajiva et al. 2005; Levasseur et al. 2008; Levasseur et al. 2008 a) are used as an alternative to ad hoc methods for solving the inverse problem and for learning from precedent. Given a numerical model, unknown properties of the material constitutive model are systematically adjusted to minimize the error between numerical model calculations and observed response. Calvello and Finno (2004) deployed a computer code UCODE (Poeter and Hill 1998) and Hardening-Soil (H-S) model in back analysis of supported excavations. Their results showed that the accuracy of back-figuring the observed excavation-induced wall deflection is satisfactory. Tang and Kung (2009) used a

nonlinear optimization technique (NOT) incorporating the auxiliary techniques to enhance the convergence and stability of the optimization analysis for supported excavations. Since many factors such as soil stiffness and small-strain non-linearity of soil behavior is difficult to be represented by the conventional soil models, the back-figured parameters are generally away from real parameters and the back-figured parameters regarded as the equivalent parameters.

In another related study, Levasseur et al. (2008 a; 2008b) proposed the genetic algorithm as a new optimization method for geotechnical inverse analyses and soil parameter identification. This method was applied to reproduce the horizontal displacement of the wall and was compared to other optimization techniques that are based on gradient algorithm for Lurie Center case study in downtown Chicago (Rechea et al. 2008). They concluded that since gradient algorithm assumes the solution of the inverse problem is unique, and in the field of geotechnics there are a number of uncertainties associated with in situ measurements, its use is problematic. Overall, the inherent limitations of constitutive models used in optimization techniques, and non uniqueness of solution sets, results in limited integration of numerical modeling with observational approach.

However, Hashash et al. (2003; 2006) recently introduced a robust inverse analysis approach, self-learning simulations (SelfSim), to extract soil behavior by using wall deformations and surface settlements measurements.

SelfSim is an inverse analysis framework that implements and extends autoprogressive algorithm proposed by Ghaboussi et al. (1998). The filed measurements are used to extract soil behavior through the use of a continuously evolving neural network (NN) material model. Two complementary numerical analyses are performed for each excavation stage. In the first analysis the force boundary condition is applied to extract stresses. The computed strains most likely do not match with field strains in this analysis. In the second analysis the displacement boundary conditions are applied to extract strains. The computed stresses most likely do not match with field stresses. The extracted stress-strain pairs from analysis a and b are used to re-train the NN material model until the two analyses give similar results (Hashash et al. 2006; Marulanda and Hashash 2007), Figure 6-1.

Hashash et al. (2006) demonstrated SelfSim learning capacity and the ability to predict performance of a new excavation using numerically simulated excavation case histories. Song et al. (2007) demonstrated that besides wall deformations, inclinometers placed at further distances back of the wall, and strut loads are useful measurements that can improve learning soil behavior. While the SelfSim framework has been applied to several clayey excavation sites (Hashash et al. 2006), Osouli and Hashash (2008) conducted SelfSim to extract sandy soil behavior from excavation measurements of a full scale model wall at Texas A&M supported by a two-level tieback section. The SelfSim approach has also been used to predict excavation-induced ground movements in several case studies . Two dimensional analyses were used in all the previous application of SelfSim framework.

In this chapter, SelfSim learning inverse analysis approach introduced by Hashash et al. (2006) for 2-D excavation analyses is extended to learn excavation response in 3D analysis. The geographic location of the two sites is shown in Figure 6-2. SelfSim is used to extract the Chicago clay and sand layers behavior from Lurie Center excavation in a 2D analysis. The extracted soil behavior is used to predict the wall deformations and surface settlements in Ford Center deep excavation, in Evanston, IL. Since the different ground elevation around the excavation site imposes 3D effects, the incapability of 2D analysis is highlighted. The numerical development in order to simulate the excavation in 3D via SelfSim inverse analysis is demonstrated. The SelfSim inverse analysis in three-dimensional simulation is used to learn the Ford Center deep excavation measured response. The quality of the learned global response and extracted soil behavior is discussed in detail.

6.2. Site description

6.2.1. Lurie center

The excavation for the Lurie Research center was approximately 82 by 69 m and depth of 13m (Finno and Roboski 2005). The site was heavily instrumented to monitor the ground movements resulting from the excavation. The support system and typical soil profile at the site are shown in Figure 6-3. The support system consisted of a sheet pile

wall with three levels of tiebacks. The soil profile consists of fill layer at the top, lake sand layer, and soft to stiff silty clay at the bottom. Much of the subsoil in the Chicago area consists of fairly distinct strata deposited during the advances and retreat of glaciers during the Wisconsin Stage and are identified as clay strata. In order of deposition they are Park Ridge, Deerfield, and Blodgett (Chung and Finno 1992). The Park Ridge, Deerfield, and Blodgett are ice margin silty clay deposits which have different water contents and strength parameters. The stiff crust above Blodgett layer is desiccated clay caused by drop on the level of Chicago Lake.

The excavation sequence was idealized in seven stages down to elevation -7.3. The average inclinometer measurements obtained from LR6 and LR8 and surface settlements were deployed in SelfSim learning analysis.

6.2.2. Ford Center engineering design center

The Ford Motor Company Engineering Design Center is a five-story building founded on drilled caissons with two-level basement (Blackburn 2005). The 9.1 m depth excavation is supported by sheet pile walls and two levels of bracing. Due to closeness of excavation site to the Tech building and cautious about any damage to Tech building, several instruments are placed around the site: inclinometers on 3 sides of the excavation, tiltmeters affixed to columns in Tech building, optical surveying of the ground surface and sheet pile wall, and strain gauges on struts (Blackburn 2005). The plan view of the site and instrument locations are shown in Figure 6-4. Two inclinometers (i.e. I-1 and I-2) were installed in north side of the excavation. Inclinometer I-3 and I-4 were installed in east and west side of the excavation, respectively. Eight settlement points were monitored for this excavation. Settlement point P1 and P2 were in farther distance from the excavation as reference points. Settlement point P3 and P4 were on top of the sheet pile wall. Settlement point P5 was located on a concrete block in 2.5 m from the sheet pile wall. The other three settlement points (i.e. P6, P7, and P8) were located on ground surface. The excavation support system includes XZ85 section sheet pile walls supported by two levels of internal bracing, which are 0.61m-diameter pipes. In each corner of the excavation six struts in two levels supported the sheet pile walls, Figure 6-4. Two levels of walers in elevations +1.5 m and -1 m were installed around the excavation. The eastward and southward cross sections of the excavation are shown in Figure 6-5 and

Figure 6-6, respectively. Three locations in each side of the excavation are selected to show the stress paths and are indicated by S-1 to S-9. The stress paths for fill, soft clay, and medium clay layers are demonstrated for each location.

The Soil profile in Evanston area, similar to Chicago's, consists of fill, sand and clay layers overlay limestone bedrock. Figure 6-7 shows comparison of soil profiles in Evanston and Chicago. As it is observed, the Ford Center excavation site is located on a compressible clay layer which is up to 17-m thickness in some areas.

6.3. Learning of 2D global excavation response from Lurie Center using SelfSim

Hashash et al. (2006) applied SelfSim to the Lurie Research Center. All lateral soil movements in proximity to the wall and surface settlements corresponding to the known construction stages are used as boundary conditions for SelfSim learning by Hashash et al. (2006). The inclinometers were located 5 ft behind the sheetpile wall, and therefore the lateral deflections used during SelfSim learning were applied in the finite element analysis at the same location for all elevations. The soil profile in the analyses was represented with four NN material models to represent layers: (1) top fill layer (NN1-Lurie), (2) lake sand layer (NN2-Lurie), (3) soft to medium silty clay layer (NN3-Lurie), (4) stiff to very stiff silty clays (NN4-Lurie). Lurie deep excavation was modeled as 2D symmetric excavation with half width of 25m. The model dimensions were 150 m and 22m in horizontal and vertical directions, respectively.

Prior to any SelfSim learning all soil constitutive models were pre-trained to represent linear elastic response within a very small strain range. The initial Young's modulus used for pre-training was deliberately chosen large to produce small excavation-induced deformations. This analysis underestimated lateral wall deformations and surface settlements, but gives a qualitatively reasonable deformed shape. Several SelfSim learning cycles were conducted at each excavation stage. After a few passes of SelfSim learning the calculated deformations reasonably match with the measurements in all excavation stages.

Figure 6-8 shows the deformations after 12 SelfSim learning passes (Hashash et al. 2006). Overall, the computed deformations using soil models extracted through SelfSim learning are similar to the field measurements, although there are some

noticeable discrepancies in the initial two stages between the computed and the measured soil movements. One possible reason for these differences is the large measured surface settlement associated with the behavior of the pavement material and/or near-surface fill. The soil models extracted by Hashash et al. (2006) from Lurie Center are used to predict the excavation response in Ford Center excavation.

6.4. Predicting 2D excavation response in Ford Center using Lurie Center extracted soil models

Due to the similarity in soil profile of Ford Center in Evanston and Lurie center in downtown Chicago, the extracted soil model from Lurie Center is used to predict the inclinometer measurements and surface settlements in Ford center excavation. Construction sequence of the excavation in 2D analyses in six main stages is shown in Figure 6-9.

The soil profile in the analysis is represented with three extracted NN material models from Lurie Center excavation. The represented soil layers are as followings: (1) NN1-Lurie soil model for fill/sand/silt layer, (2) NN3-Lurie soil model for crust clay, soft clay, and medium clay, (4) NN4-Lurie soil model for stiff silty clay. The Ford Center deep excavation is modeled as a 2D symmetric excavation with half width of 20m. The model dimensions are 120m in horizontal dimension. The vertical dimension of the model is 22m.

Figure 6-10 shows the measured and predicted vertical movements of surface settlements points and lateral movements of inclinometers I-1, I-2, I-3 and I-5. The settlements for all stages are underestimated. The lateral deflections of I-1, I-2, I-5 are overpredicted by two orders of magnitude. The lateral deflections of I-3 are predicted in the same order of magnitude. The large deflections measured by inclinometer I-3, are most likely due to the close proximity of the inclinometer to the wall and the reduced system stiffness caused by the pop out constructed for elevator pit in east part of excavation (Blackburn 2005).

Although the Tech building foundation load could have an effect on the measured data and could be considered as a source of disagreement between the computed and target values, further analysis by considering its effect did not improve the predicted results.

In addition since the Tech building is a two-story building with a basement level, the consolidation of clays due to loads of building could not change the stiffness of clay layers significantly. Therefore it is less likely that the different stiffness of clay layers be the source of discrepancy between predicted and measured deflections values.

6.5. Extracted soil behavior in 2D analysis

Figure 6-11 shows the normalized stress paths for elements in middle of fill/sand/silt, soft clay and medium clay layers for locations S-1 in the north side of excavation; see the S-1 location in Figure 6-4. The location of elements in each soil layer is shown in Figure 6-5 and Figure 6-6. The fill/sand/silt layer undergoes shearing almost identical to Plane Strain Active (PSA) mode and it reaches peak shear strength. The stress paths for clay layers show a change in the direction of shear plane. The soft clay shows a drained type of behavior , which does not seam reasonable. The stress path for stiff clay demonstrates a shearing behavior almost identical to Place Strain Passive (PSP) mode.

Figure 6-12 shows the normalized stress paths for elements in middle of fill/sand/silt, soft clay and medium clay for locations S-5 in the west side of excavation; see the S-5 location in Figure 6-4. The sand, soft clay and medium clay layers demonstrate a drained type of behavior. A change in the direction of the principal stresses for fill/sand/silt and clay layers is observed.

Figure 6-13 shows the normalized stress paths for elements in middle of fill/sand/silt, soft clay and medium clay for locations S-3 in the east side of excavation; see the S-3 location in Figure 6-4. Similar to S-5 stress paths, the fill/sand/silt, soft clay and medium clay layers demonstrate a drained type of behavior with a rotation in the direction of principal stresses.

The different elevation of more than a couple of meters among different sides of the excavation has a great influence on the behavior of the excavation. The elevations of surrounding sides of the excavation are shown in Figure 6-5 and Figure 6-6. Since the excavation site is not a flat area, the 2D plain strain assumption to model this excavation will not capture the true behavior of excavation. Therefore, 3D modeling of the Ford Center is an inevitable task.

6.6. Three-dimensional construction monitoring of Ford Center deep excavation

Ford Center deep excavation was monitored with instruments and extensive number of as-built digital photos from prior to sheet pile wall installation to the end of the excavation. In addition a relatively new technology, three-dimensional laser scanning (3DLS) that utilizes LIDAR (Light Detection and Ranging), was used to produce accurate 3-D representations of soil surface and construction activities as shown in Figure 6-14. Through 3DLS process, thirteen scans of whole excavation at approximately one week intervals became available for Ford Center excavation which is shown in Figure 6-15. The scans and photos are used to define the 3D construction sequences in SelfSim inverse analysis.

6.7. Numerical development of 3D simulation: Brick element deleting scheme

Since all the analyses that have been conducted by SelfSim in deep excavations are either in 1D or 2D framework (Marulanda 2005; Hashash et al. 2006; Song et al. 2007; Osouli and Hashash 2008), the SelfSim analysis in 3D for Ford Center is an extension of SelfSim application to 3D geotechnical problems.

A Finite Element Model can be generated and updated more accurately using 3D laser scanning result. The terrain meshes obtained from 3DLS contain most of the basic geometric information, including the shape, height, and location of the excavated ground surface. To use this information in numerical modeling of deep excavation problems this image should be converted to 3D finite element meshes.

The procedure for a 3DLS image of a given excavation stage is presented in Figure 6-16. The scanned image of the excavation stage on March 12th is presented in Figure 6-16(a). The points are important data in the scanned image that represents the surface of ground. The point data is extracted from the image as illustrated in Figure 6-16(b).

In order to model this excavation stage an initial FE model of the geometry before excavation is developed using a FE preprocessor, shown in Figure 6-16(c). At this stage, user can define the dimensions and size of the elements, and also the density of the mesh in a certain area. This initial model is used as a base model throughout all the excavation stages. Then after, the 3D point data, shown in Figure 6-16(b) is compared with the node and element information of the FE model. Those elements in the base model that are

located above the point data from the scanning are deleted. As a result, the remained elements represent the geometry of the excavation site at this given excavation stage, Figure 6-16d.

Using this procedure, separate FE meshes are generated for each excavation stages used in the FE analysis. To combine them into one input, Element Change option in ABAQUS is utilized. For instance, Figure 6-17(a) is FE mesh of the excavation stage on March 12th, and Figure 6-17(d) is on April 14th. The elements in those two models are compared with each other. Based on the comparison a set of elements that should be deleted (Figure 6-17(b)) and a set of elements that should be added (Figure 6-17(c)) are detected. The whole procedure is automated using C++.

Figure 6-18 illustrates the initial FE mesh of Ford Center. Elastic analyses with several different sets of dimensions are performed to decide the final dimension. The chosen model dimensions are 200m by 200m in horizontal direction. The vertical dimension of the model is 22m. Total of 11572 elements are used with the highest density of elements near the excavation site. The density of elements in the mesh is decreasing by distance from the site to reduce the computational cost.

Due to high computational costs associated with 3D modeling the construction sequence of the excavation are selected carefully to minimize the number of excavation stages without compromising the accuracy of the problem. Therefore, besides the reference ground surface Feb 18th (Figure 6-19(b)), four stages of excavation on March 12th (Figure 6-19(c)), April 14th (Figure 6-19(d)), and May 7th (Figure 6-19(e)), are selected from thirteen available scans shown in Figure 6-15 as construction stages for 3D simulation. Figure 6-19 illustrates the FE mesh which was built using a brick element deleting scheme for selected excavation stages. The elevation difference around the excavation site before the excavation is also observed in the model in Figure 6-19(a). Walers and struts are implemented with bar elements using the transformed section area reported by Blackburn (2005). The elastic material with properties of steel is used for the bar elements.

6.8. Learning 3D behavior of Ford Center excavation using SelfSim in 3D analysis

Inclinometers I-1, I-2, I-3 and I-4 with different configuration are used in SelfSim learning to extract the soil behavior. Since the settlement points P3 and P4 are located on

the sheet pile wall, and settlement point P5 is located on a concrete block in vicinity of excavation, the reliable soil settlement measurements are limited to three points P6, P7, and P8. Therefore, settlements measurements are not used in SelfSim learning analyses.

The soil profile in the analyses is represented with five NN material models to represent layers: (1) top fill/sand/silt layer, (2) lake sand layer, (3) soft silty clay layer, (4) medium silty clay layer, and (5) stiff to very stiff silty clays.

Prior to any SelfSim learning all soil constitutive models are pre-trained to represent linear elastic response within a very small strain range. The initial Young's modulus used for pre-training is deliberately chosen large to produce small excavation-induced deformations. Figure 6-20 shows this analysis underestimates lateral deformations of inclinometer I-1, I-2, I-3, and I-5 and surface settlements.

Figure 6-21 shows the computed and measured lateral deflections and settlements after five passes of SelfSim learning using inclinometers I-5 only. The deflections of inclinometer I-5 improved in comparison to that of Figure 6-20. However the inclinometer measurements of I-1, I-2, and I-3 and surface settlements are underestimated. One inclinometer measurement in the west side of the excavation is not providing sufficient information about the excavation behavior in north and east side of the excavation.

Then the measurement of inclinometer I-1 is added to SelfSim learning analysis. Figure 6-22 shows the computed and measured lateral deflections and settlements after five passes of SelfSim learning using inclinometers I-5 and I-1. Computed lateral deflections of I-5 are slightly improved. The computed lateral deflections of inclinometer I-1 improved significantly. By providing measurement of inclinometer I-1, the results improve significantly in predicting lateral deformations of inclinometer I-2. The lateral deflections of I-3 and surface settlements are underestimated.

In the next SelfSim analysis inclinometer I-2 is added to inclinometers I-1 and I-5 using the database of previous analysis whereby inclinometers I-1 and I-5 used for SelfSim learning. Figure 6-23 shows the computed and measured lateral deflections and settlements after five passes of SelfSim learning using inclinometers I-5, I-1, and I-2. The computed lateral deformations of inclinometers I-1 and I-2 slightly improved. The computed lateral deflections of inclinometers I-5 and I-3 and surface settlements

remained unchanged in comparison to Figure 6-22. Since inclinometers I-1 and I-2 are in the same side of the excavation, the learned behavior does not change significantly from the configuration whereby the inclinometers I5 and I1 were used.

SelfSim learning analysis continued by adding inclinometer I-3 to inclinometers I-5, I-1, and I-2. The measurements of inclinometer I-3 show large deflections. Most likely the inclinometer was affected by the construction of elevator pop out in proximity to its location. Therefore by introducing the inclinometer I-3 the computed deflections of inclinometers I-5, I-1, and I-2 shifted to larger values.

The settlement contours around the excavation are shown in Figure 6-24. In each excavation stage, except than stage 4, the elevation of the ground surface inside excavation is lower in the proximity to the east wall than the walls in other sides of the excavation. Therefore, the predicted settlements are larger in east side than the other sides of the excavation.

In Figure 6-25 the predicted settlements in parallel distances of 4.7, 10, and 17 m from the east wall are compared to the settlements computed with the closed form solution proposed by Finno and Roboski (2005). Based on this solution the settlements can be estimated by a complimentary error function, given a maximum movement, and depth and length of excavation. The settlements calculated by Finno and Roboski (2005) method, slightly over predict the settlements computed by SelfSim. However both methods show a symmetry behavior in east side of the excavation.

Figure 6-26, Figure 6-27, and Figure 6-28 show the comparison of two methods in estimating the settlements trough in the retained soil in 10 m distance from the wall and parallel to the north, west, and south wall. The settlements calculated by Finno and Roboski (2005) predict a symmetric settlement trough, while a non symmetric settlement profile is predicted by SelfSim 3D analysis. The 3D effect imposed by elevated ground surface is not compatible with the symmetric assumption.

6.9. Extracted soil behavior in 3D analysis

Figure 6-29 shows the normalized stress paths for elements in middle of fill/sand/silt, soft clay and medium clay layers for locations S-2, S-1 and S-7 in the north side of excavation; see the element locations in Figure 6-4. In element S-2 the fill/sand/silt layer undergoes shearing almost identical to the Plane Strain Passive (PSP)

mode. However the clay layers show a behavior close to Plane Strain Active (PSA) mode. The stress paths for clay layers are consistent with friction angle envelope. In element S-1, the fill/sand/silt layer undergoes PSA mode and shows strain softening. The clay layers show a behavior almost identical to PSA mode. In element S-7, while the fill/sand/silt layer demonstrates a behavior close to PSA mode of shear, the clayey layers show PSP mode of shear. Although SelfSim analysis is not using any predefined stress strain relationship, the stress paths for fill/sand/silt layer is consistent with the friction angle line. The clay layers for this element show an elastic response.

Figure 6-30 shows the normalized stress paths for elements in middle of fill/sand/silt, soft clay and medium clay for locations S-5, S-8 and S-9 in the west side of excavation; see the element locations in Figure 6-4. In element S-5, the fill/sand/silt and clay layers undergo shearing almost identical to PSA mode of shear. However the clay layers show an elastic response. The medium clay layers show a rotation in direction of principal stresses. In element S-8, the fill/sand/silt and soft clay layer undergo shearing close to PSA mode. In element S-9, the fill/sand/silt and soft clay layer demonstrate a PSA mode of shear.

Figure 6-31 shows the normalized stress paths for elements in middle of fill/sand/silt, soft clay and medium clay for locations S-10, S-4 and S-11 in the south side of excavation; see the element locations in Figure 6-4. In element S-10, the fill/sand/silt layer reaches the peak shear strength. The clay layers experience slight shearing due to be in proximity to corner of the excavation. In element S-4, while the sand layer experience PSP mode of shear, the clay layers undergo PSA mode of shear. A change in the direction shear plane is observed for sand and soft clay layers. In element S-11, the fill/sand/silt and clay layers undergo shear almost identical to PSP mode of shear.

Figure 6-32 shows the normalized stress paths for elements in middle of fill/sand/silt, soft clay and medium clay for locations S-12, S-13 and S-3 in the east side of excavation; see the element locations in Figure 6-4. In element S-12, while the fill/sand/silt layers undergoes shear identical to PSP mode of shear. In element S-13, the fill/sand/silt layer demonstrates PSP mode of shear and the clay layers has a similar behavior to PSA mode of shear. In element S-3 the sand and soft clay layers undergo shear similar to PSP and PSA mode of shear, respectively. Due to proximity of element

S-12 and S-3 to the wall, the stress paths demonstrated for medium clay layer do not show fully undrained behavior.

Although all 12 selected elements show undrained soil behavior for medium clay layer, the extracted soil behavior of medium clay layer for elements S-9, S-12, and S3 shows stress paths that are not representative of undrained type of soil behavior. This may be due to two reasons: 1) the element locations are in proximity to the wall, and therefore the excessive pore water pressures are dissipated more quickly; 2) the excavation period, which started in February and ended in May 2004, is long enough so that some of the excess pore water pressure is dissipated during the construction period.

6.10. Summary

The extracted soil models from Lurie Center excavation in downtown Chicago has been used to predict excavation performance in Ford Center excavation in Evanston, IL. Although both sites have similar soil stratigraphy, the lateral deflections are overestimated by two orders of magnitude. The settlement profile is underestimated. The uneven ground surface around the excavation in Ford Center imposes a 3D effect on excavation performance. Therefore a 3D analysis was conducted to overcome the limitations plane strain assumption in 2D analysis. Brick element technique was developed to simulate excavation stages which were recorded by LIDAR scanning technique during the excavation. The extracted soil models from 3D SelfSim analysis in Ford Center can provide a reasonable lateral deflections induced by excavation around the site. The 3D analysis provides a more reasonable soil behavior than 2D analysis.

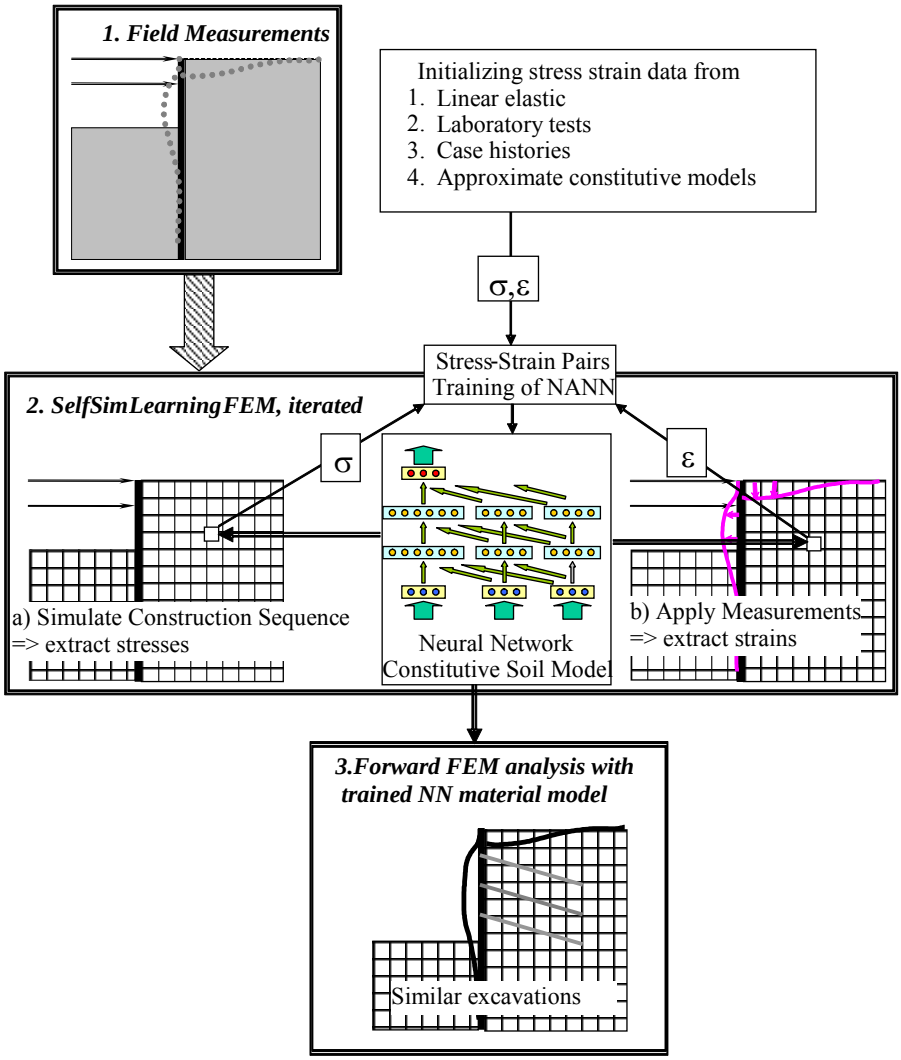

Figure 6-1 Application of self-learning simulations to deep excavation problems

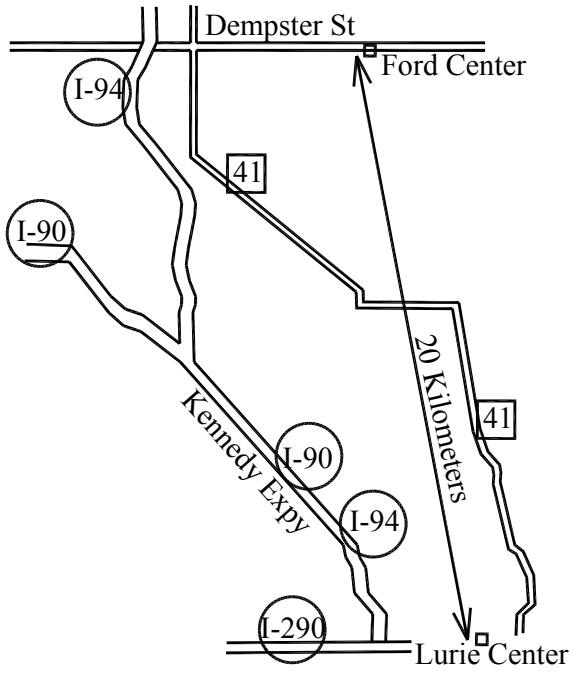

Figure 6-2 The geographic location of Lurie Center and Ford Center

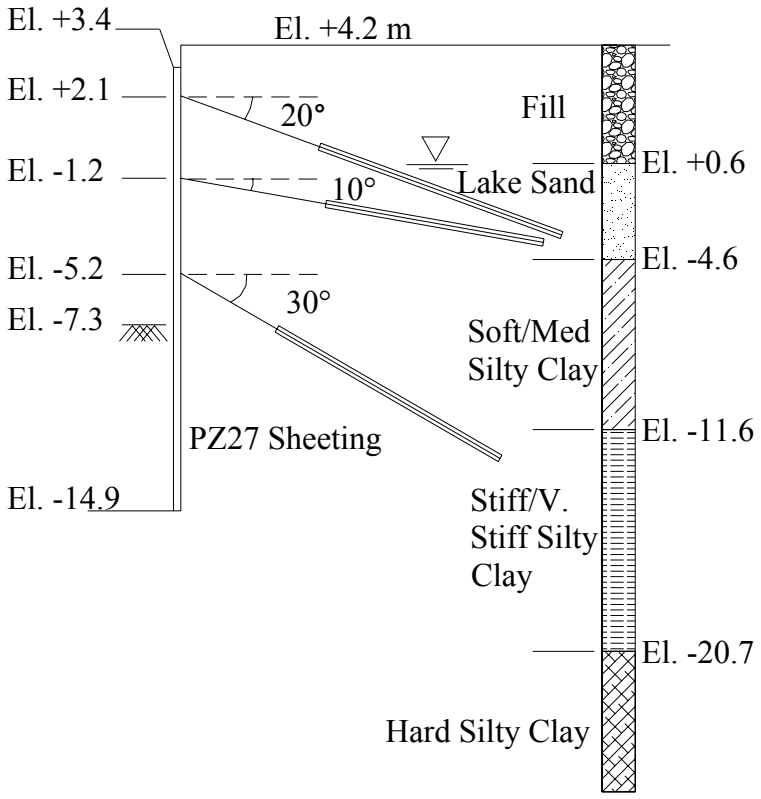

Figure 6-3 Cross section of the wall, Lurie Center excavation

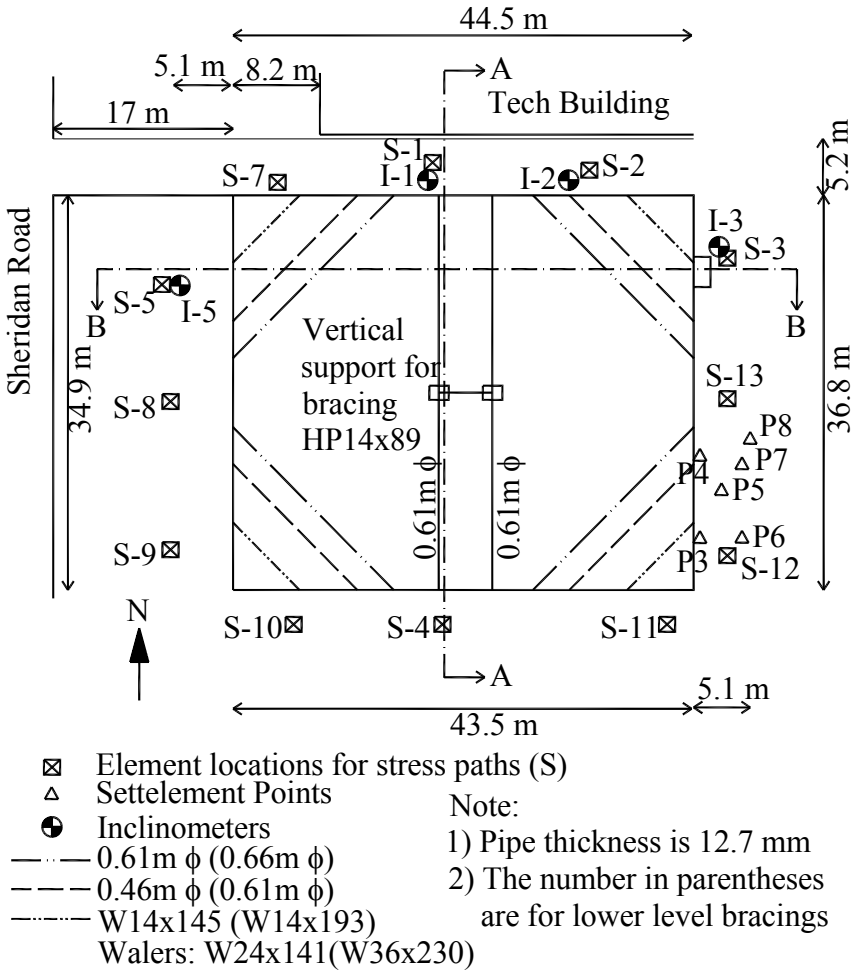

Figure 6-4 Plan view of Ford Center excavation, modified after Blackburn (2005)

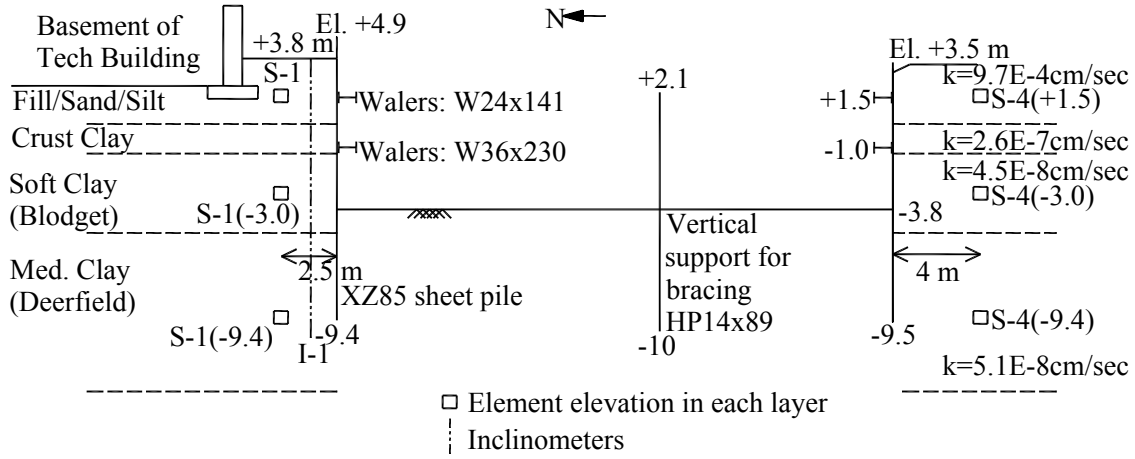

Cross section A-A

Figure 6-5 Eastward facing section, Ford Center excavation, modified after Blackburn (2005)

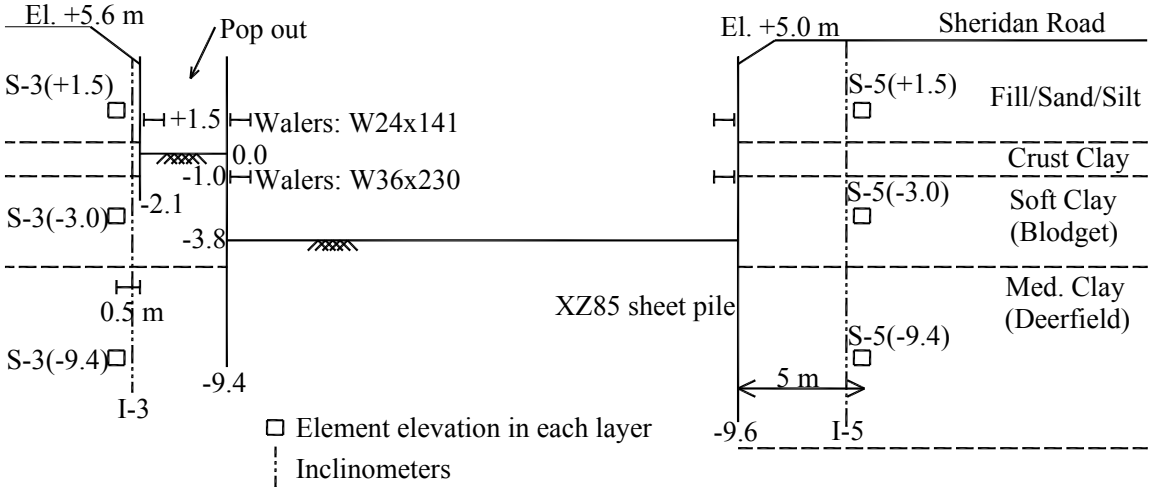

Cross section B-B

Figure 6-6 Southward facing section, Ford Center excavation, modified after Blackburn (2005)

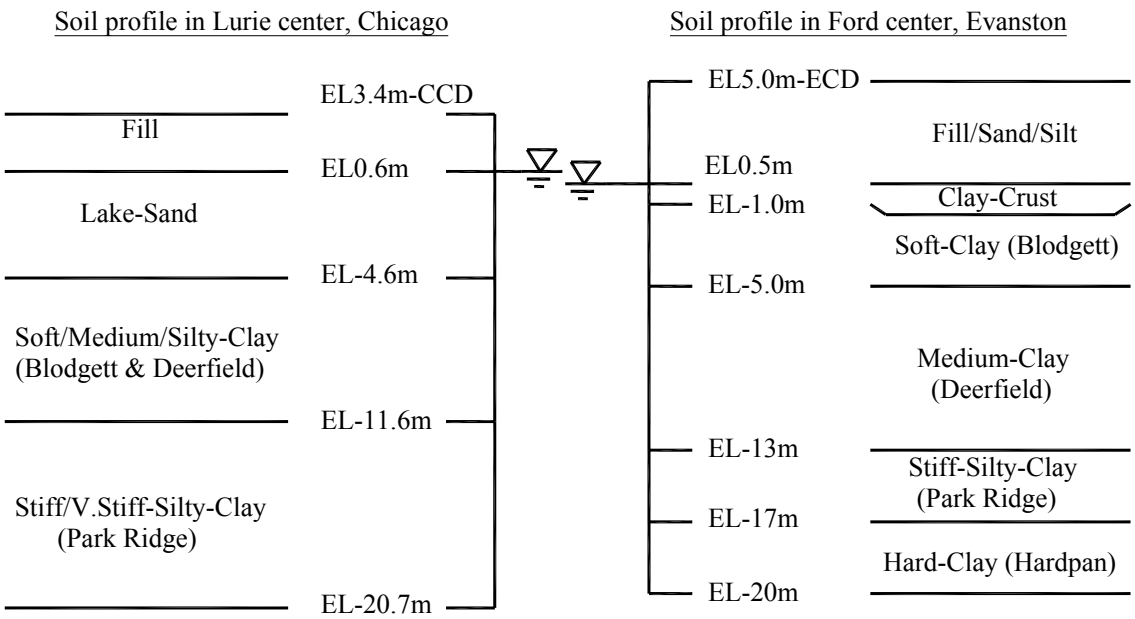

Figure 6-7 Soil profile of Lurie center in Chicago and Ford center in Evanston

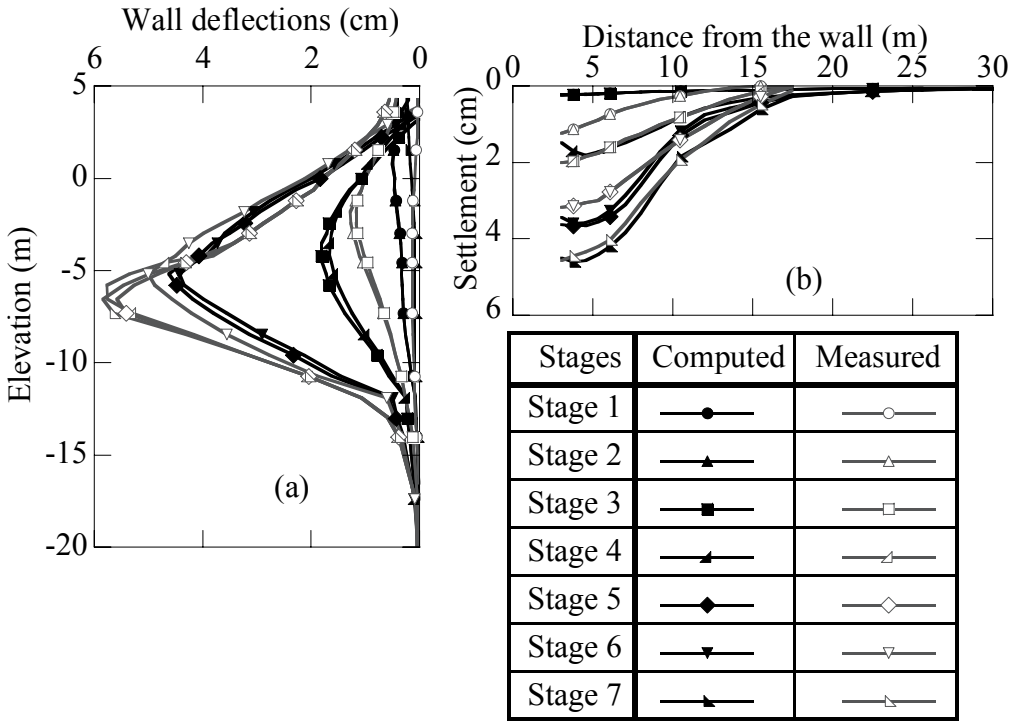

Figure 6-8 Computed and measured Lurie Center excavation response after SelfSim learning using inclinometers and surface settlements for (a) lateral wall deformations and (b) surface settlements, modified after Hashash et al.(2006)

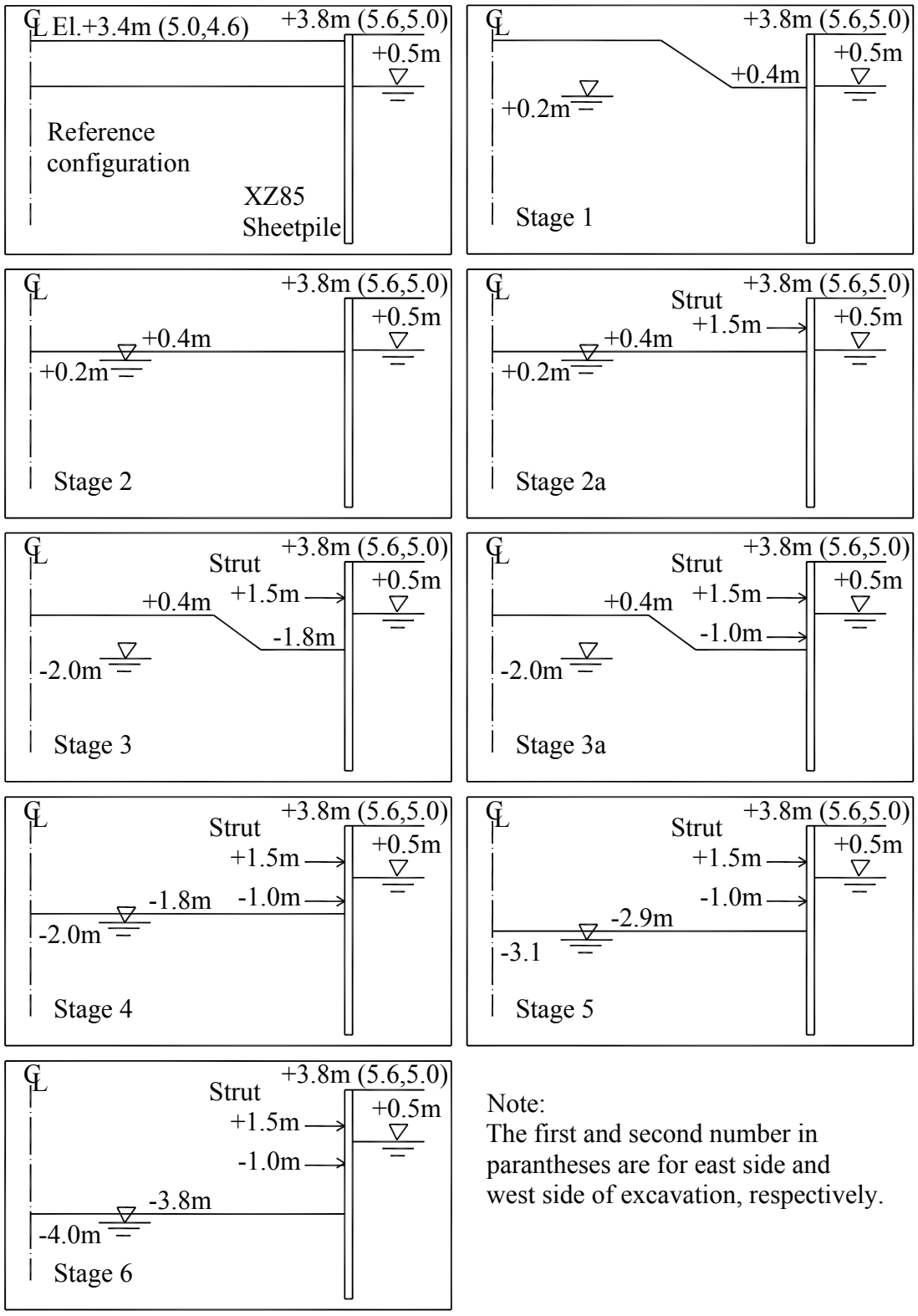

Figure 6-9 Construction sequence in 2D analysis for the north, east and west side, Ford Center excavation

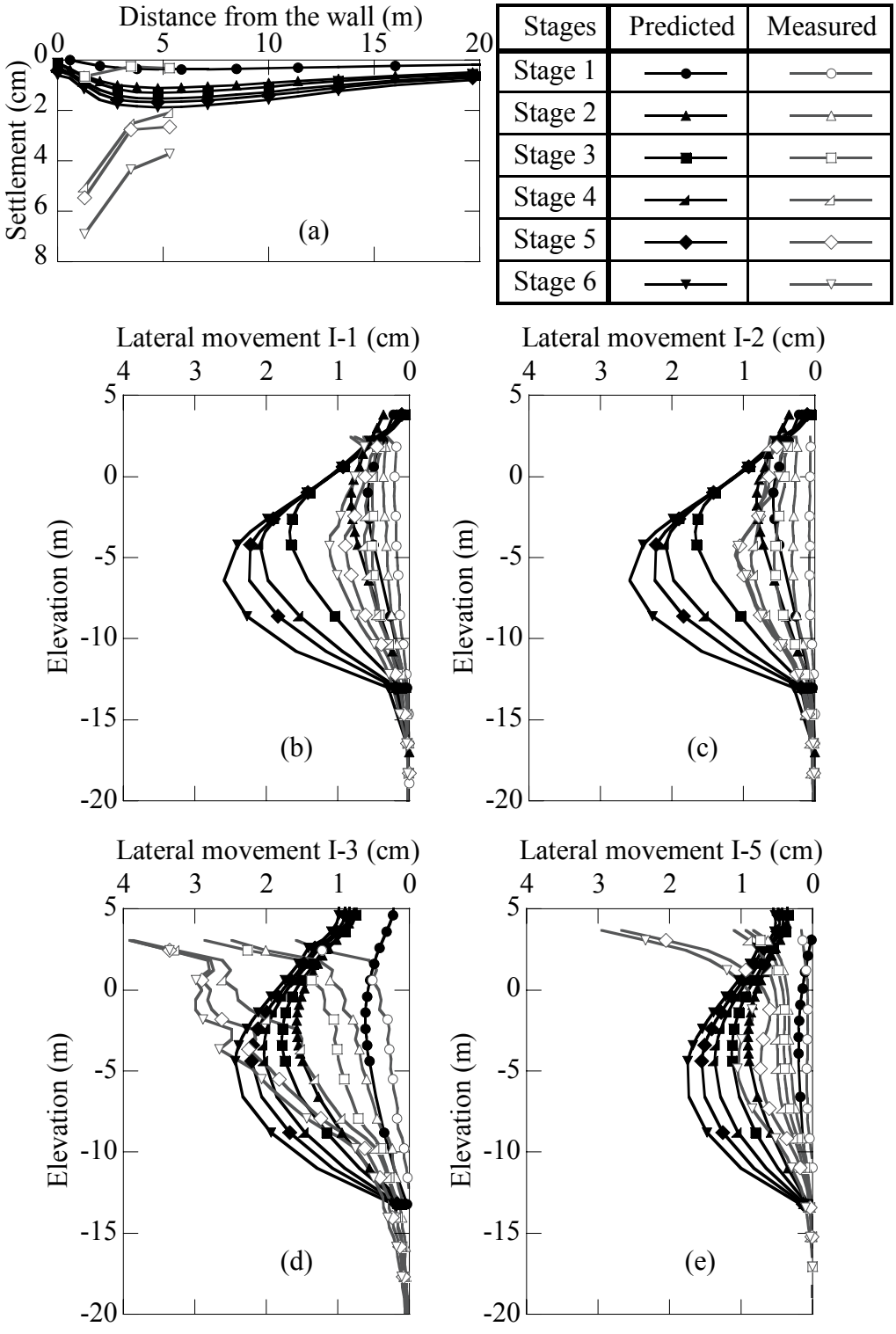

Figure 6-10 Predicted and measured Ford Center excavation response using the extracted model from Lurie center excavation in Chicago for a) surface settlements, b) lateral movements of I-1, c) lateral movements of I-2, d) lateral movements of I-3, and e) lateral movements of I-5

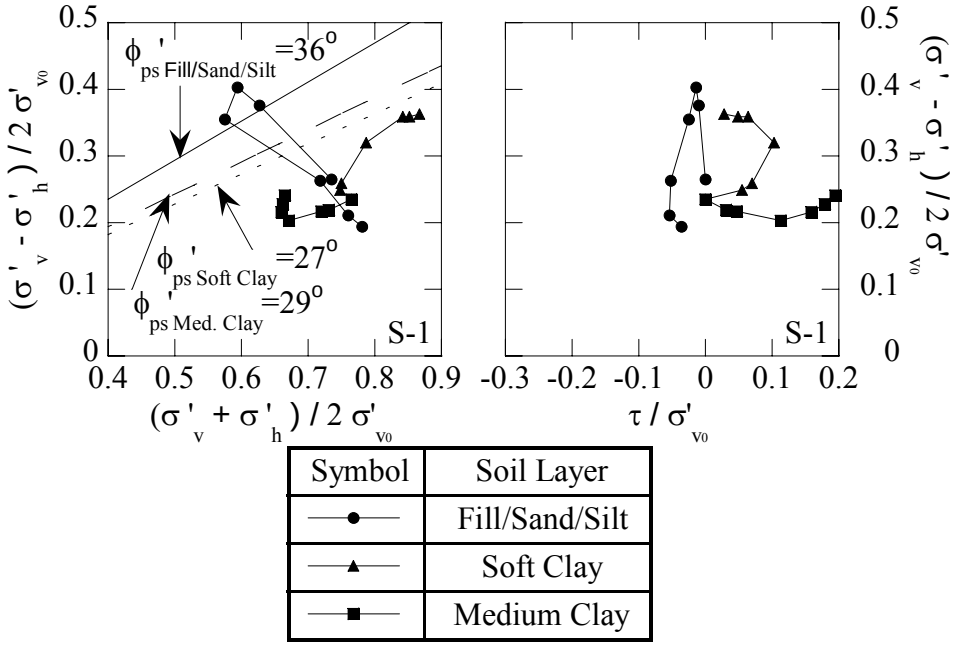

Figure 6-11 Normalized stress paths of (a) p'-q, and (b) τ-q for elements in middle of fill/sand/silt, soft clay, and medium clay layers for elements S-1 in the north side, Ford Center excavation, for locations see Figure 6-4

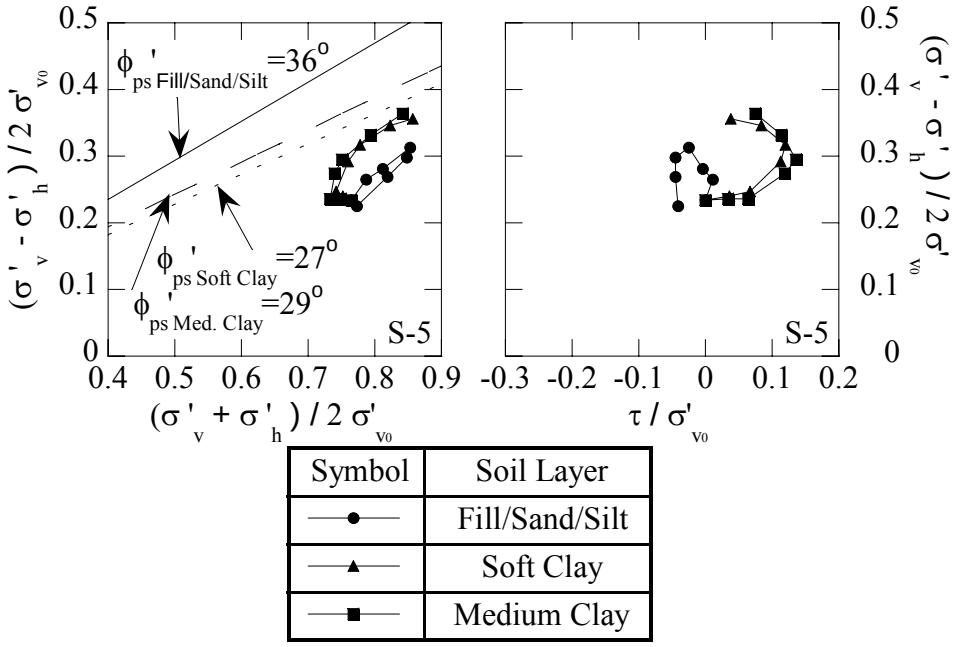

Symbol	Soil Layer
—●—	Fill/Sand/Silt
—▲—	Soft Clay
—■—	Medium Clay

Figure 6-12 Normalized stress paths of (a) p'-q, and (b) τ-q for elements in middle of fill/sand/silt, soft clay, and medium clay layers for elements S-5 in west side, Ford Center excavation, for locations see Figure 6-4

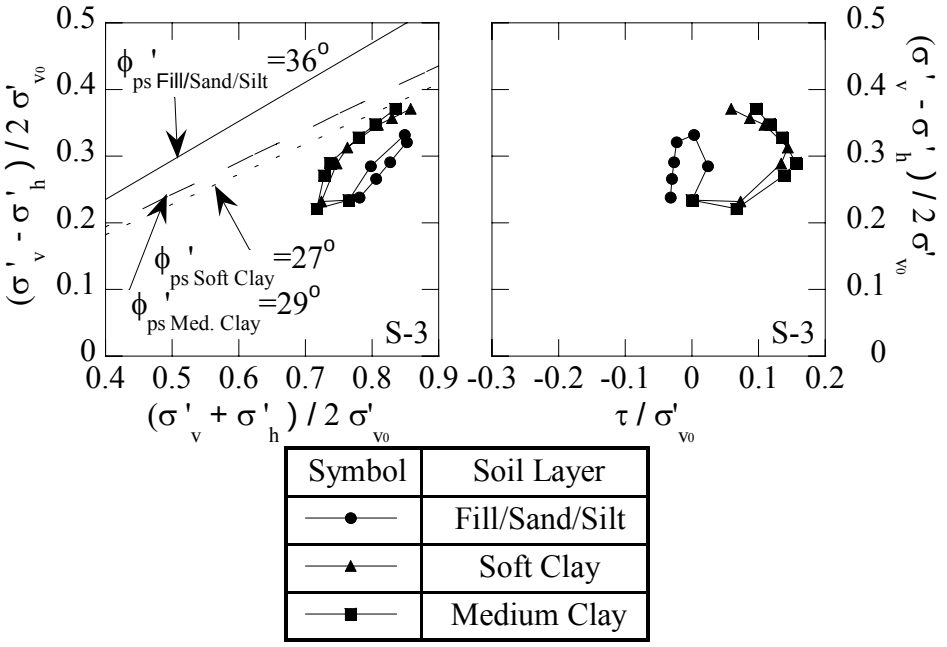

Figure 6-13 Normalized stress paths of (a) p'-q, and (b) τ-q for elements in middle of fill/sand/silt, soft clay, and medium clay layers for elements S-3 in east side, Ford Center excavation, for locations see Figure 6-4

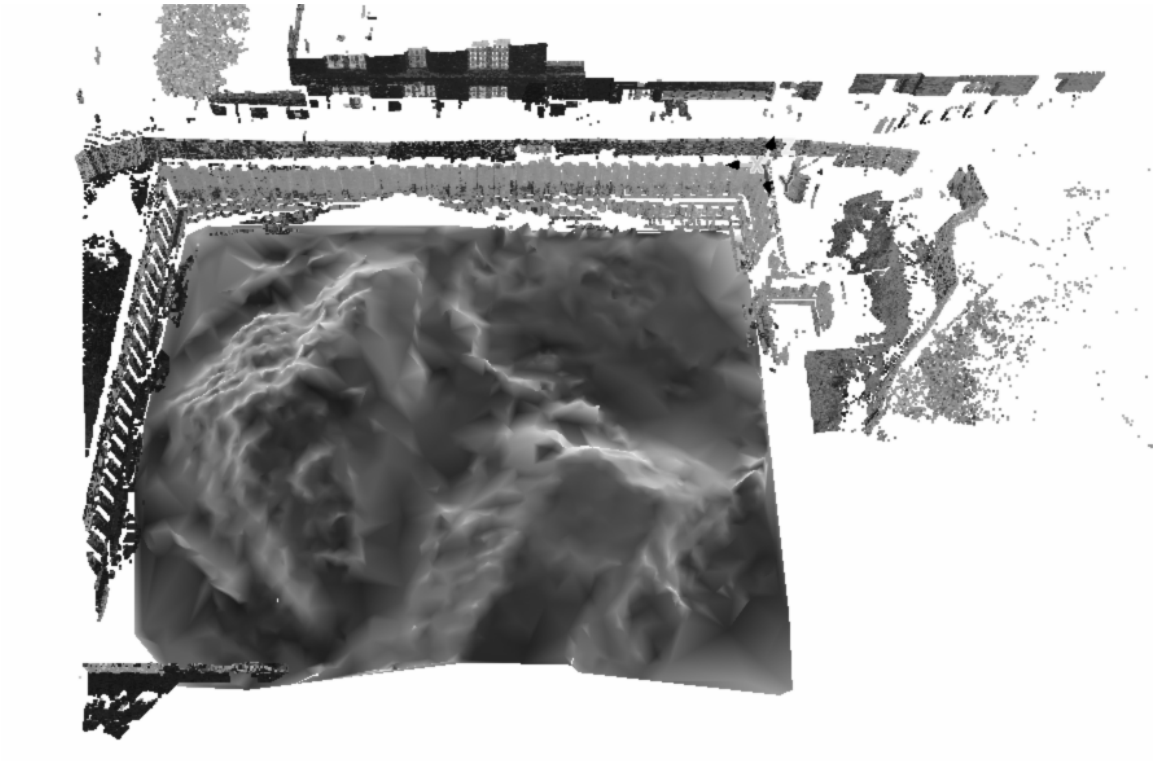

Figure 6-14. Laser scanned image of Ford Center excavation

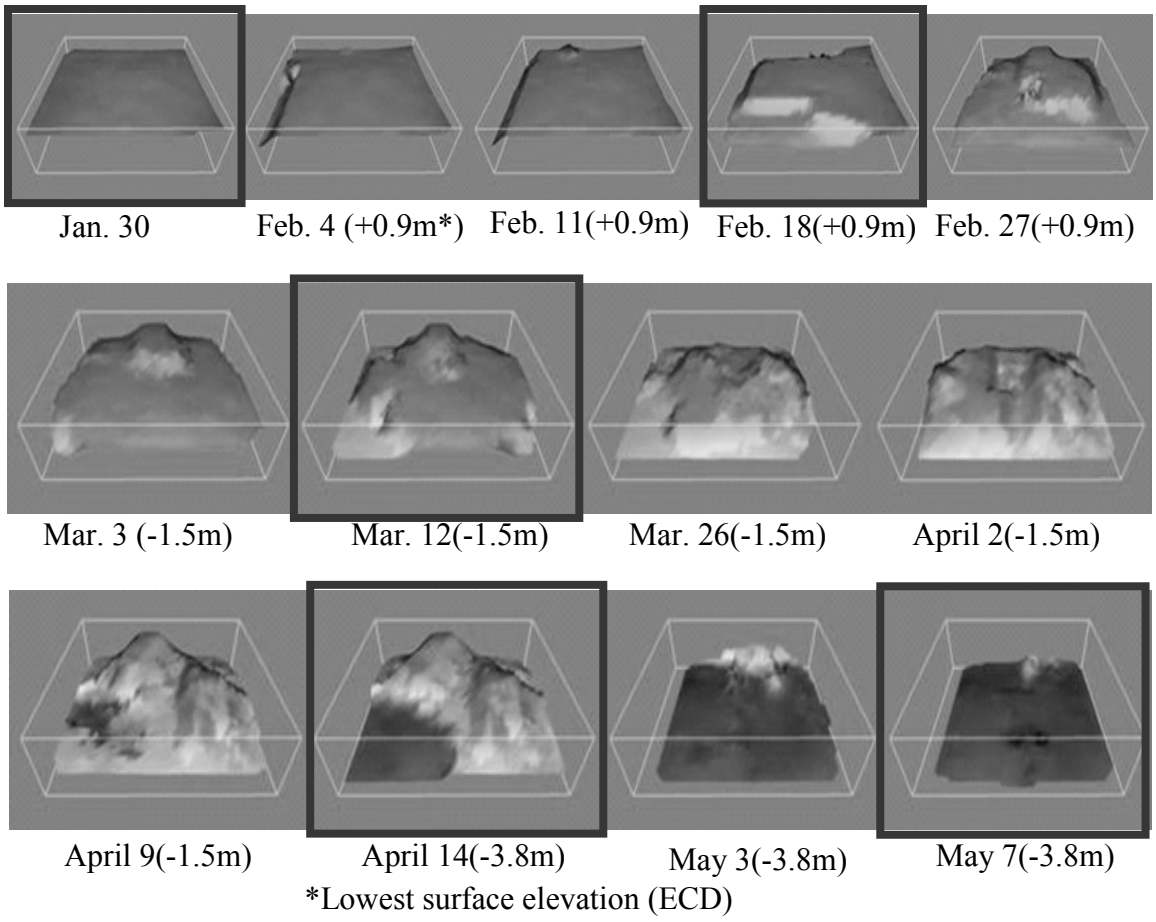

Figure 6-15 Scans of Ford Center excavation during construction

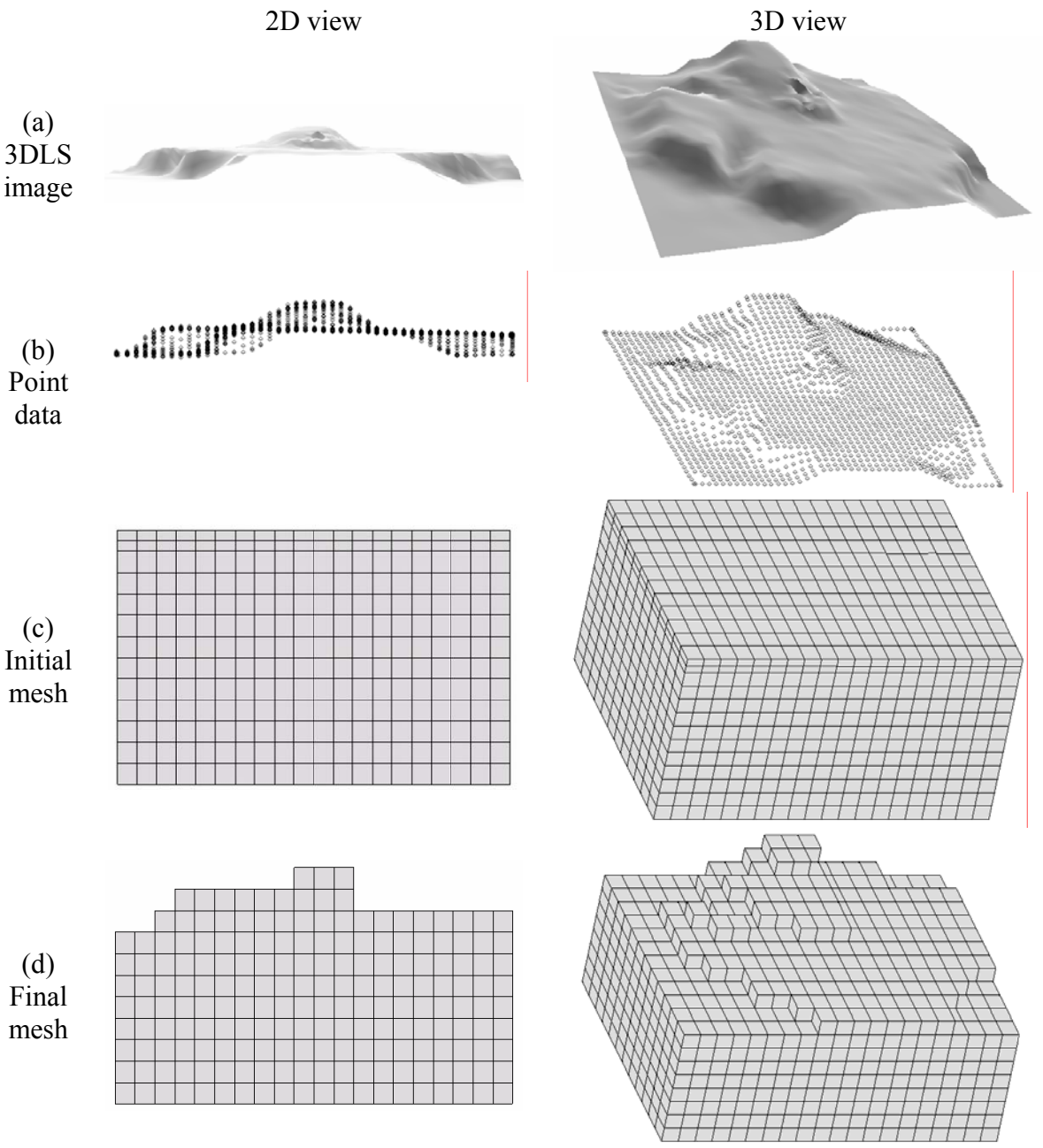

Figure 6-16. Procedure for generating 3D FE mesh from 3DLS image, Ford Center excavation

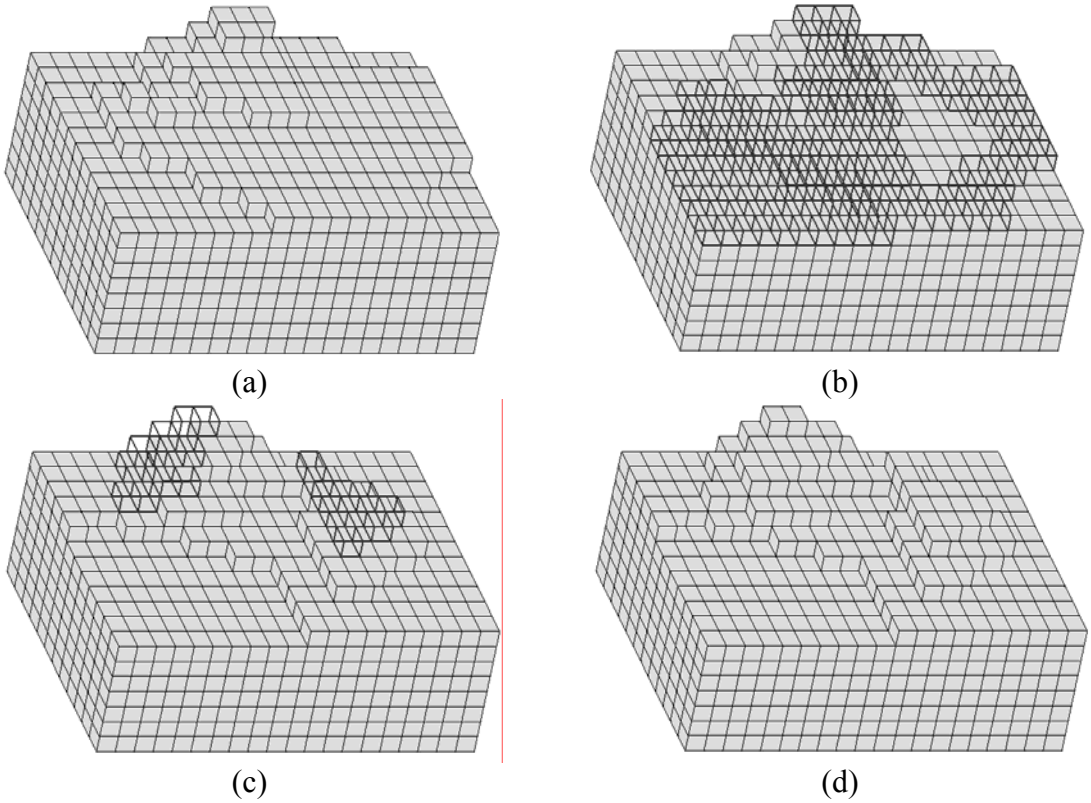

Figure 6-17. The procedure of generating excavation stages with add and remove options: (a) FE mesh for March 13th, (b) Elements deleted (bold line), (c)Elements added ((bold line), (d)FE mesh for April 14th

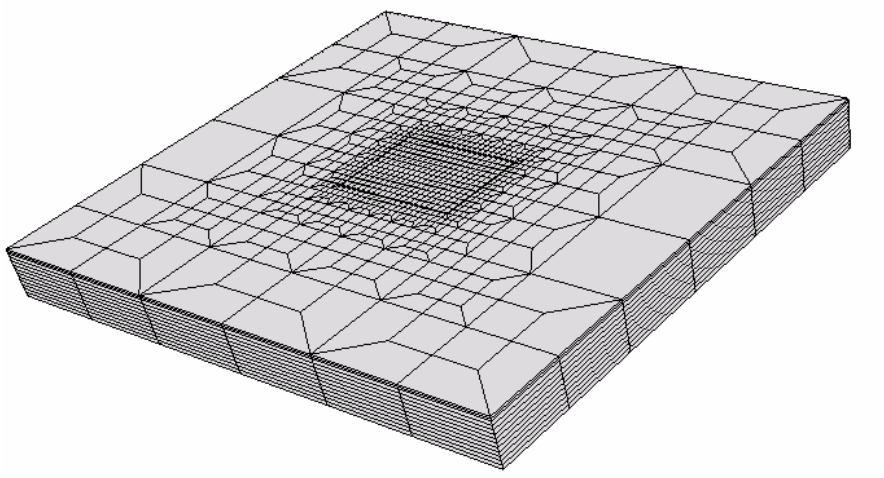

Figure 6-18. FE mesh of Ford Center

(a) Before excavation

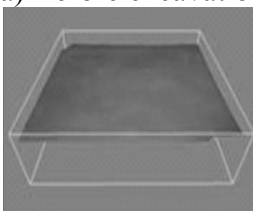

(b) February. 18th

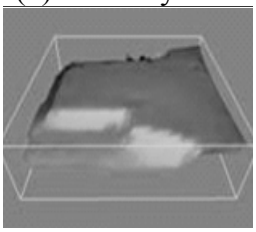

(c) March 12th

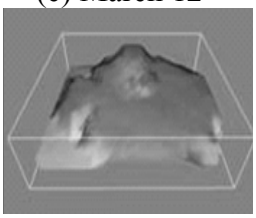

(d) April 14th

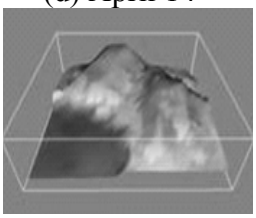

(e) May 7th

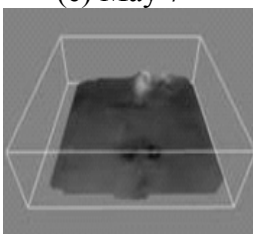

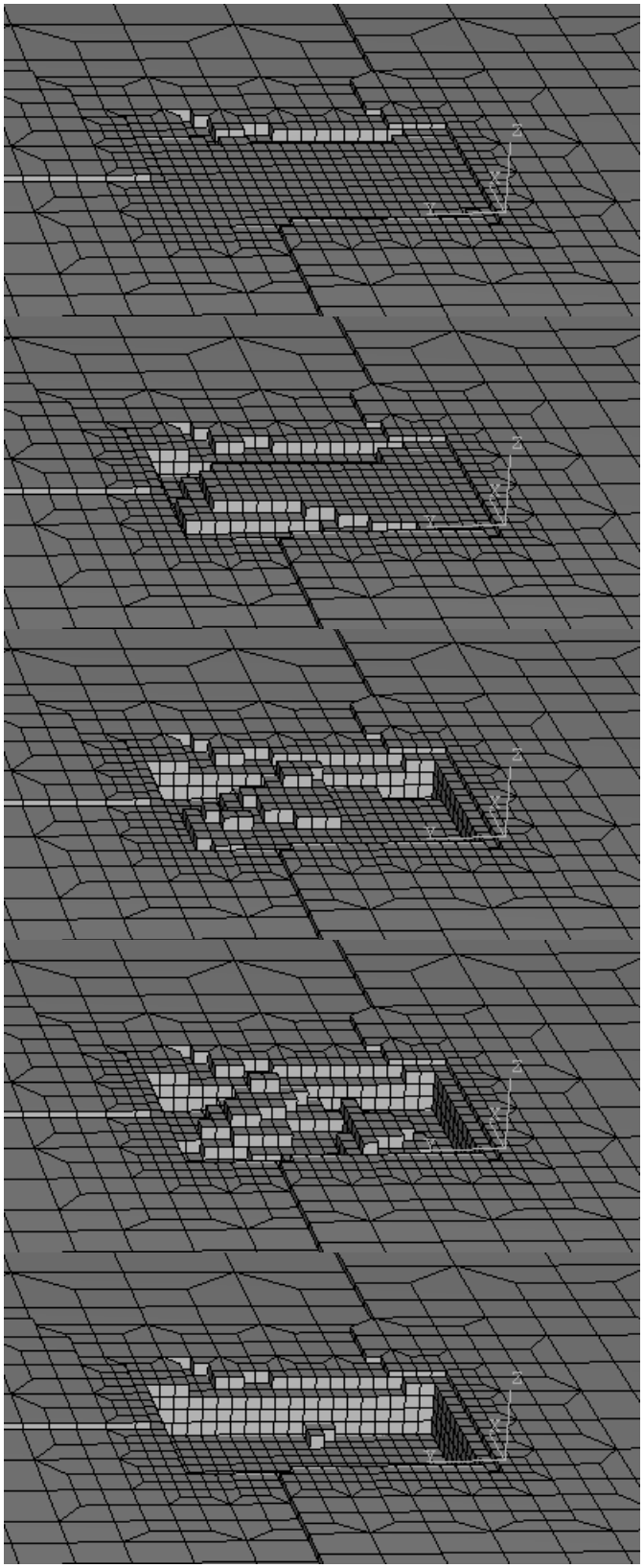

Figure 6-19. FEM mesh of five selected stages, Ford Center excavation

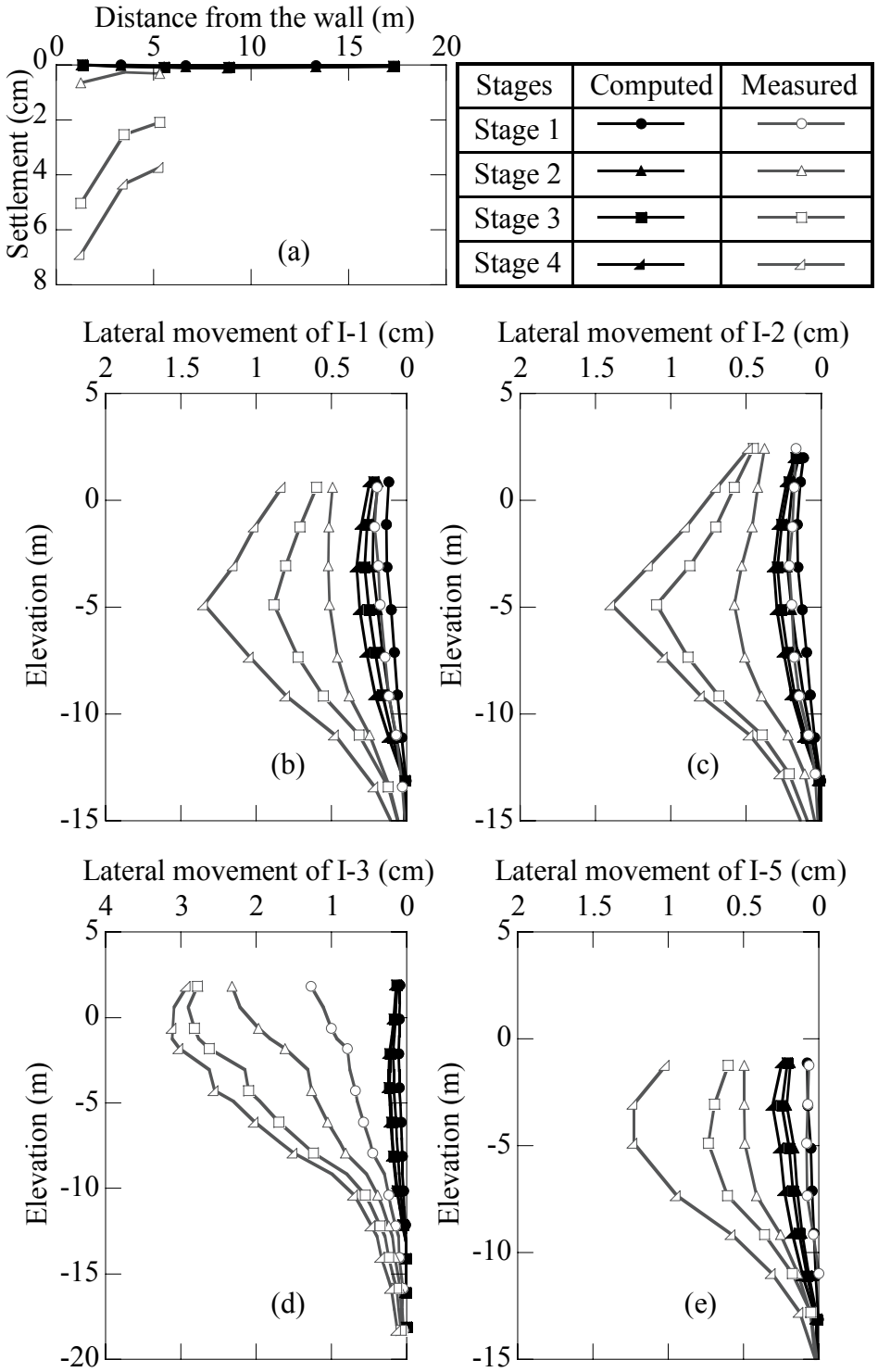

Figure 6-20 Computed and measured Ford Center excavation response prior to SelfSim learning in 3D simulation for a) surface settlements, b) lateral movements of I-1, c) lateral movements of I-2, d) lateral movements of I-3, and e) lateral movements of I-5

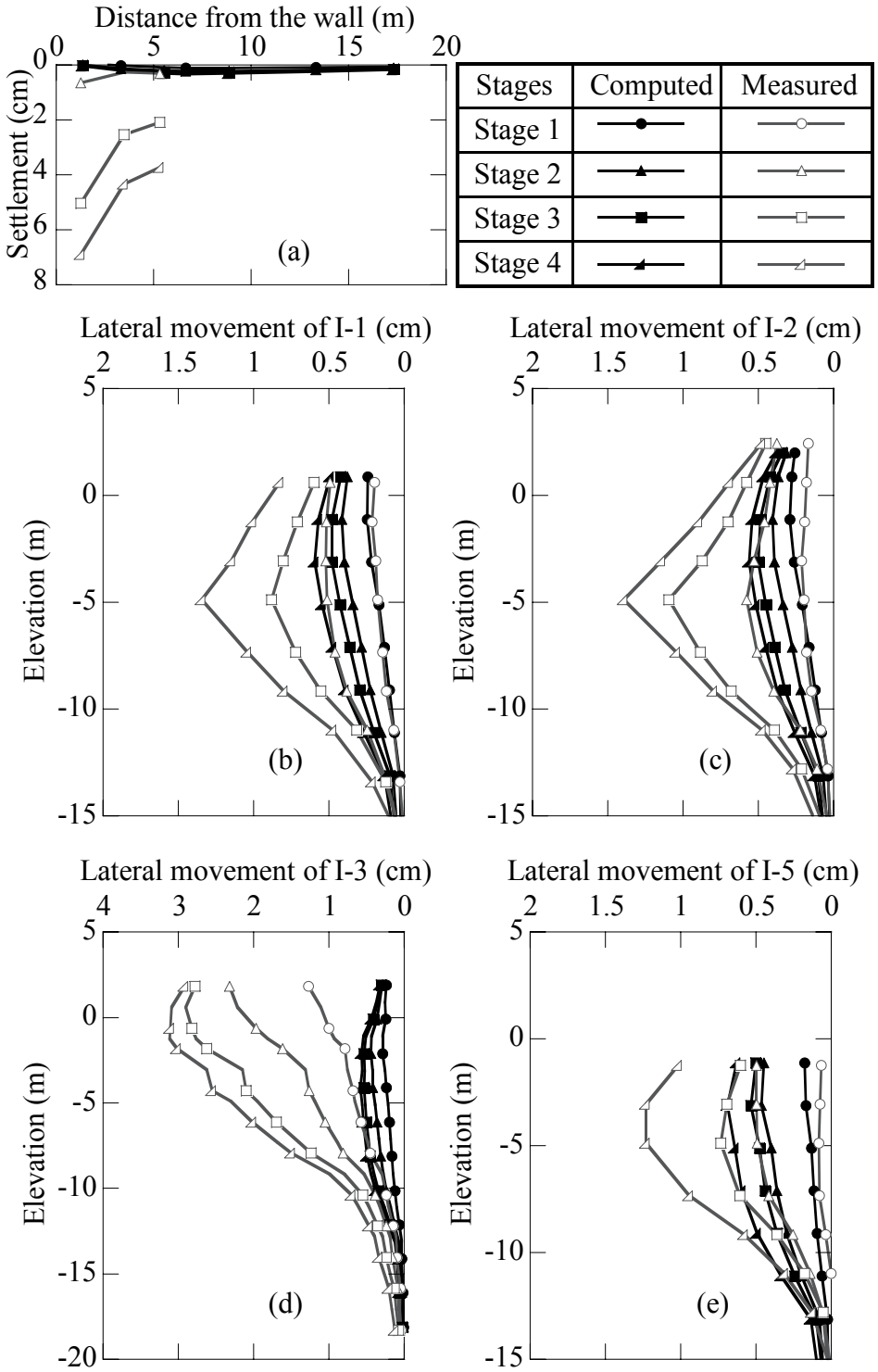

Figure 6-21 Computed and measured Ford Center excavation response after five passes of SelfSim learning using inclinometers I-5 only in 3D simulation for a) surface settlements, b) lateral movements of I-1, c) lateral movements of I-2, d) lateral movements of I-3, and e) lateral movements of I-5

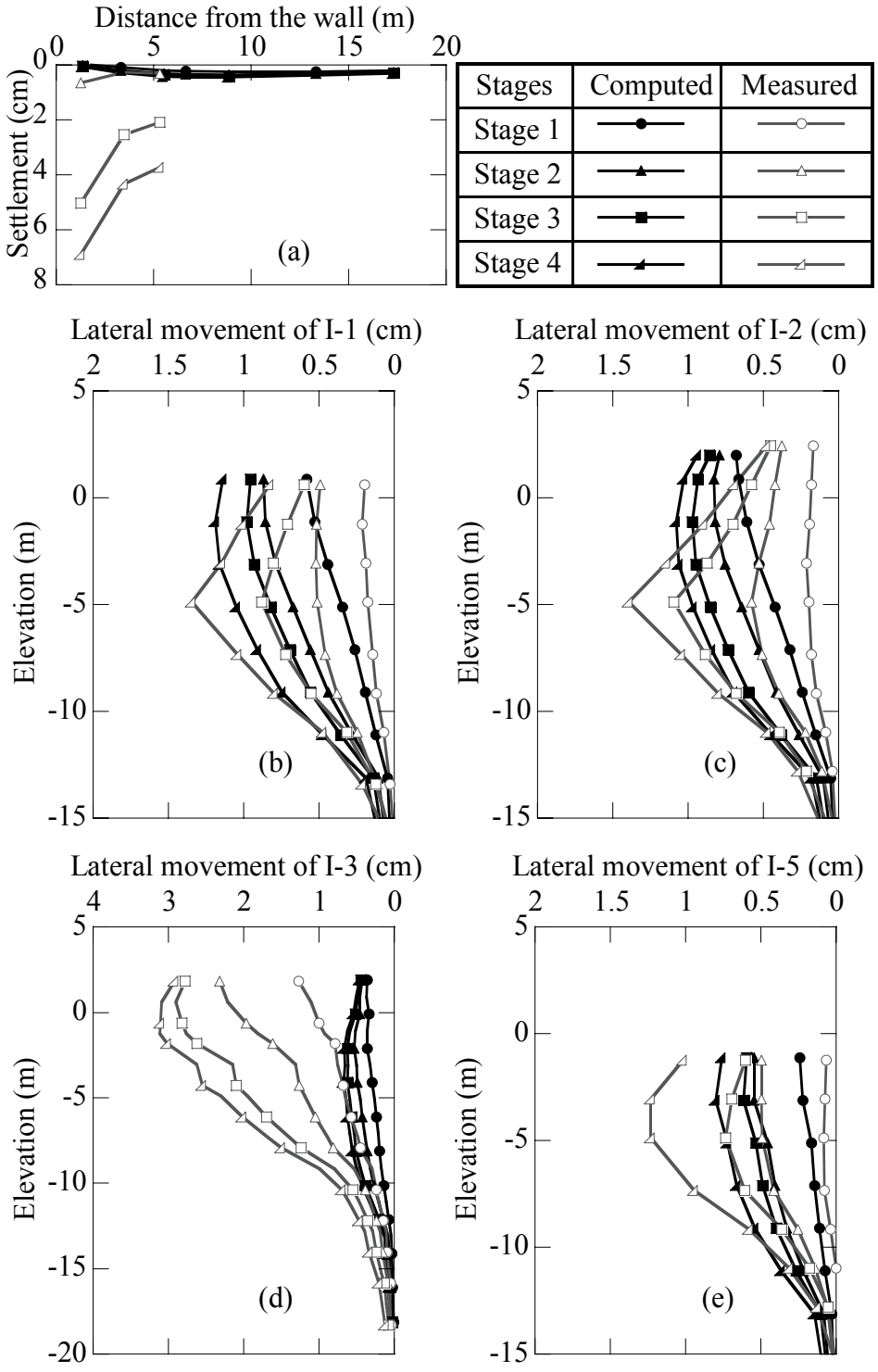

Figure 6-22 Computed and measured Ford Center excavation response after five passes of SelfSim learning using inclinometers I-5, and I-1 in 3D simulation for a) surface settlements, b) lateral movements of I-1, c) lateral movements of I-2, d) lateral movements of I-3, and e) lateral movements of I-5

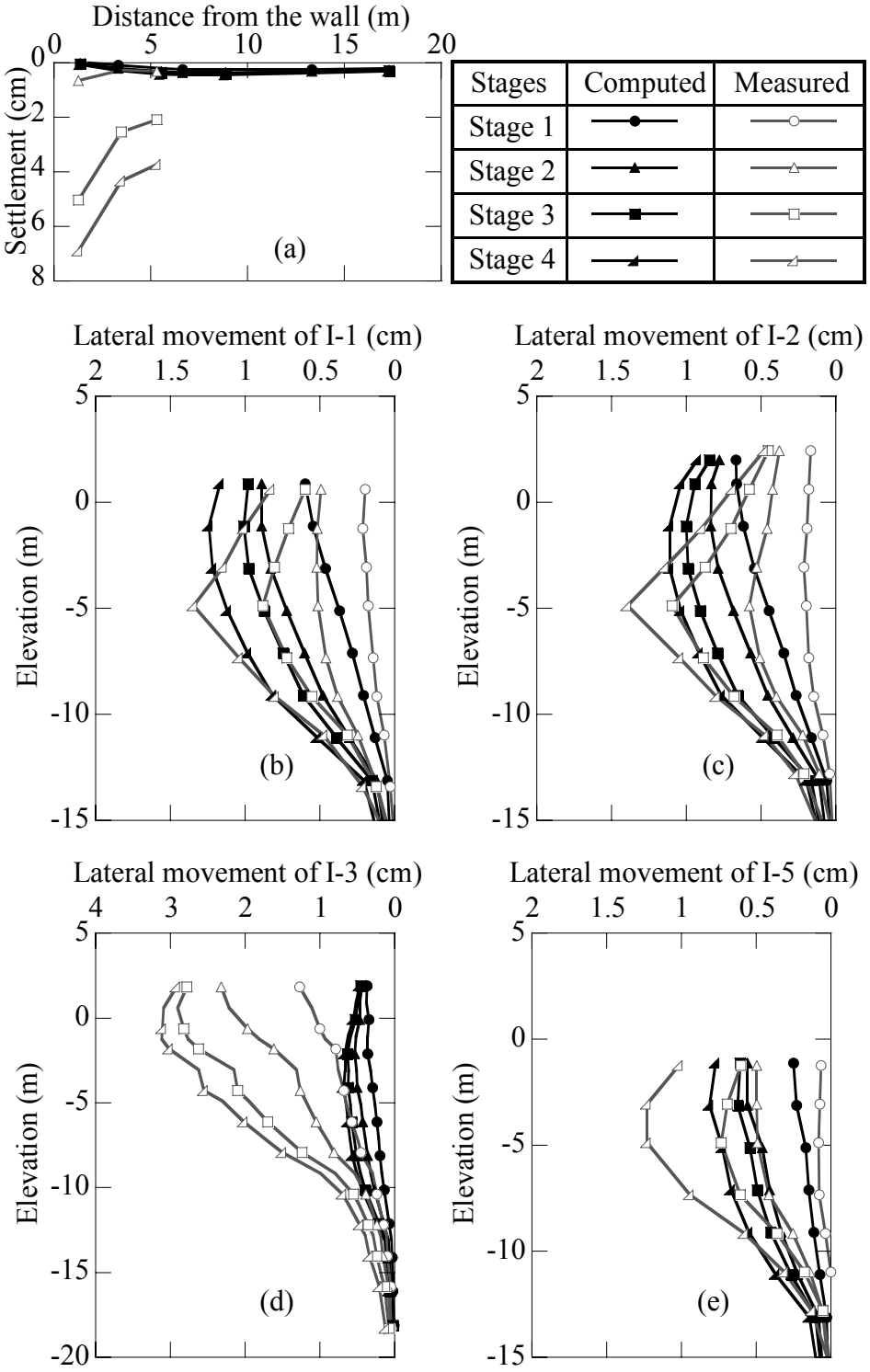

Figure 6-23 Computed and measured Ford Center excavation response after five passes of SelfSim learning using inclinometers I-5, I-1, and I-2 in 3D simulation for a) surface settlements, b) lateral movements of I-1, c) lateral movements of I-2, d) lateral movements of I-3, and e) lateral movements of I-5

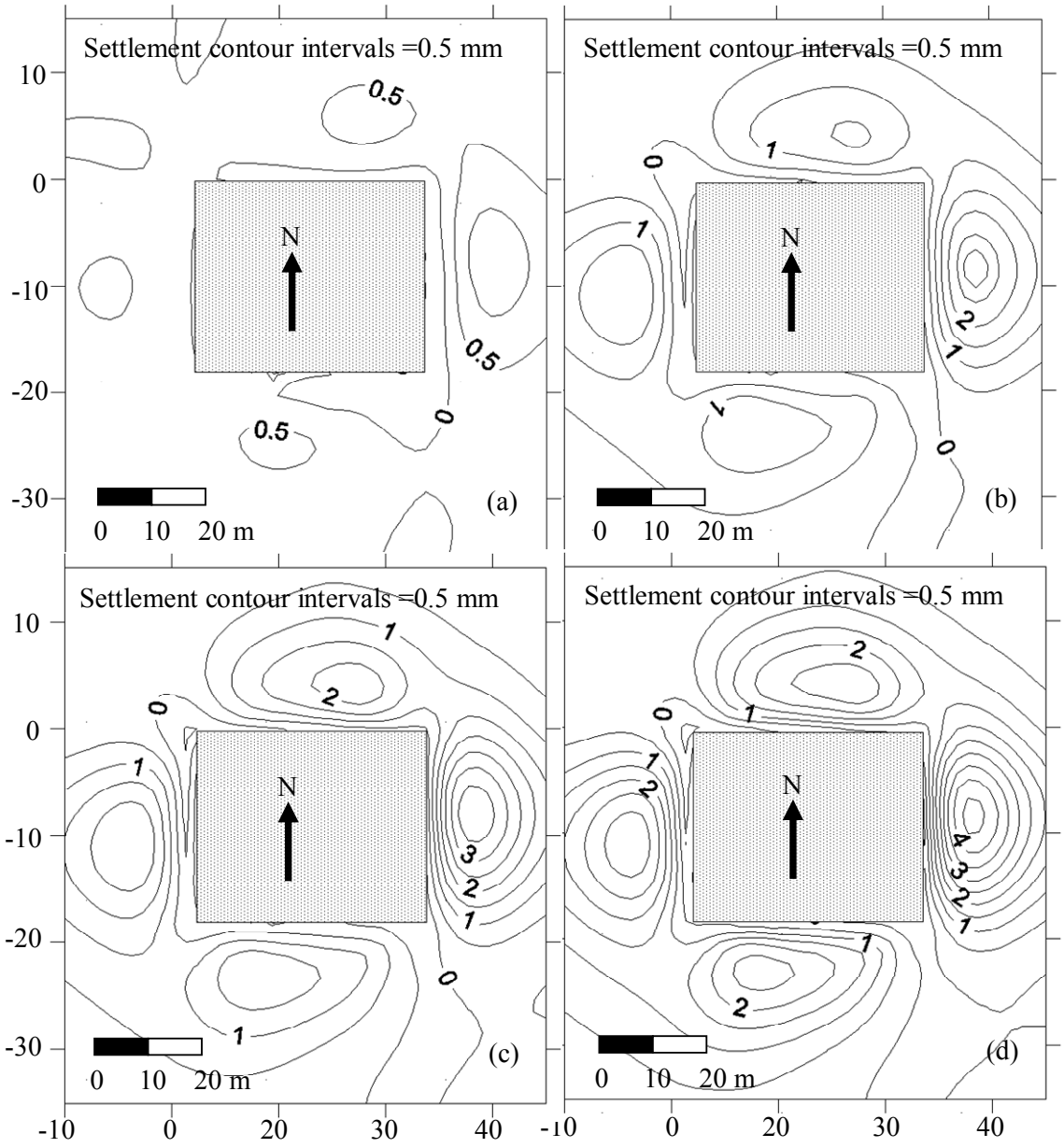

Figure 6-24 Surface settlement contours around Ford Center excavation site for a) stage 1, b) stage 2, c) stage 3, and d) stage 4

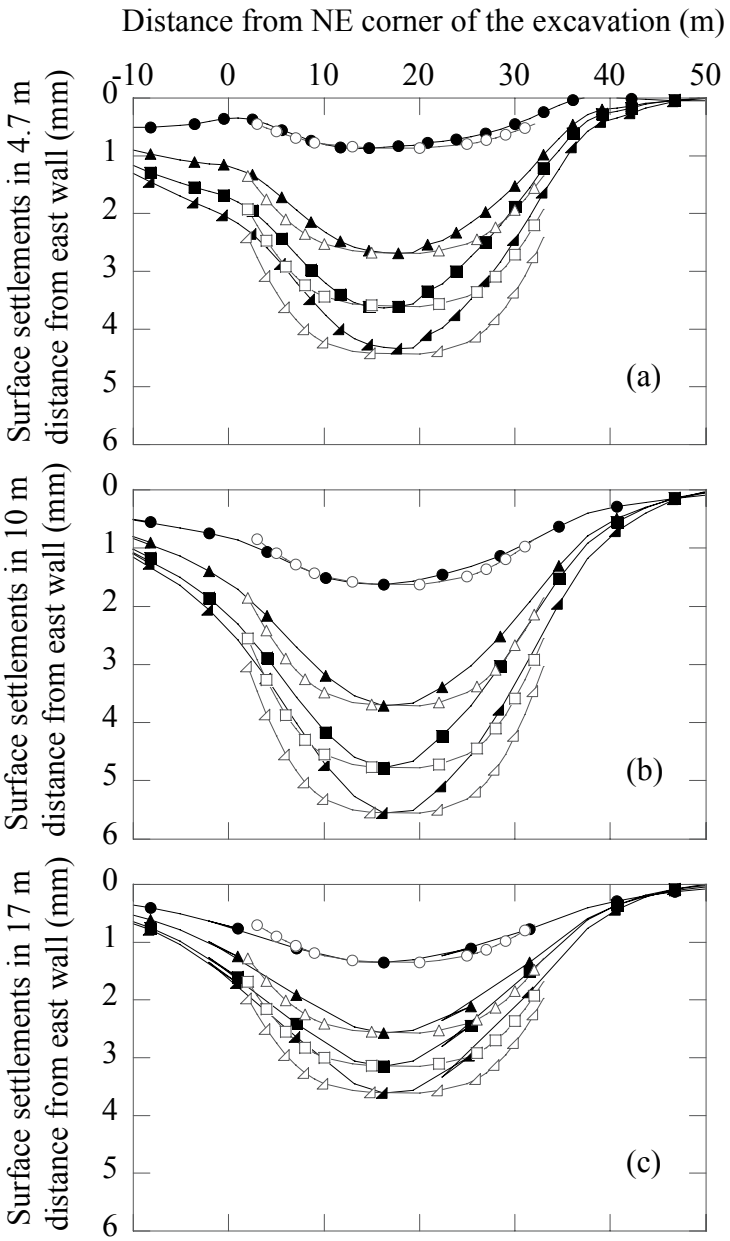

Figure 6-25 Surface settlement parallel to the east wall of the excavation, a) in 4.7 m distance from the wall, b) in 10 m distance from the wall, c) in 17 m distance from the wall, Ford Center excavation

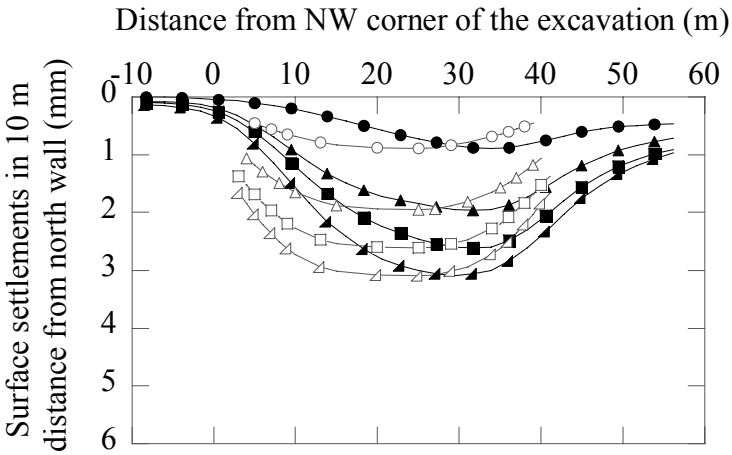

Figure 6-26 Surface settlement parallel to the north wall of the excavation in 10 m distance from the wall, , Ford Center excavation, (for legend see Figure 6-25)

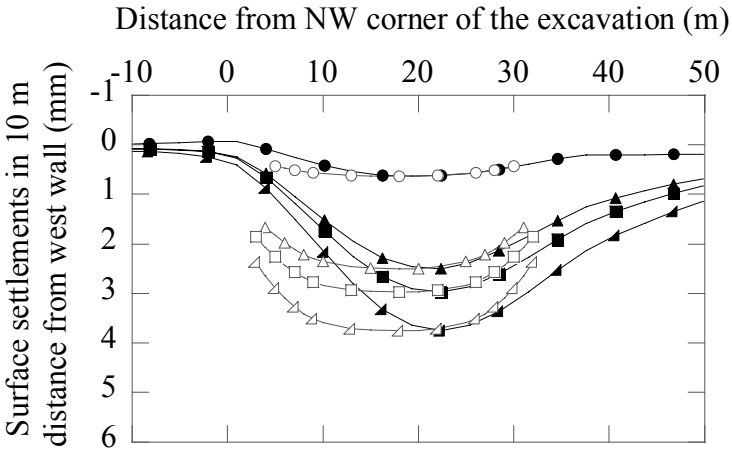

Figure 6-27 Surface settlement parallel to the west wall of the excavation in 10 m distance from the wall, , Ford Center excavation, (for legend see Figure 6-25)

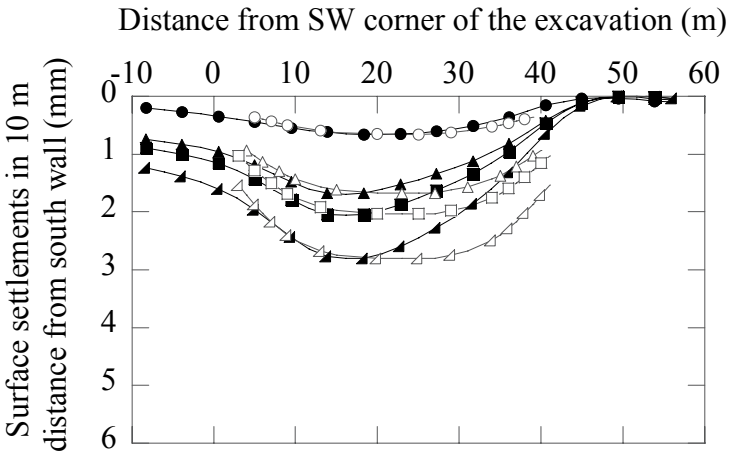

Figure 6-28 Surface settlement parallel to the south wall of the excavation in 10 m distance from the wall, , Ford Center excavation, (for legend see Figure 6-25)

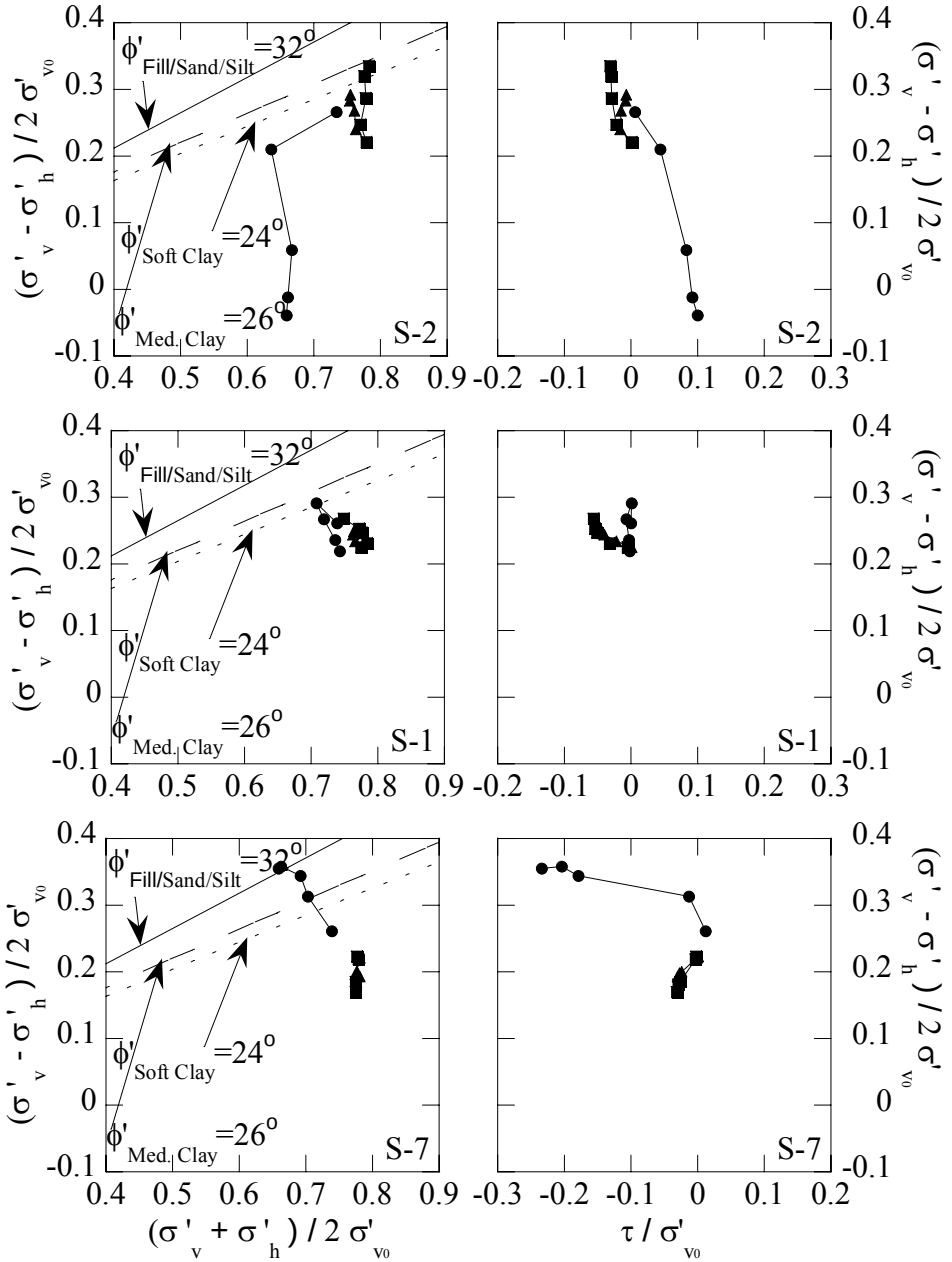

Figure 6-29 Normalized stress paths of (a) p'-q, and (b) τ-q for elements in middle of fill/sand/silt, soft clay, and medium clay layers for elements S-2, S-1, and S-7 in north side, Ford Center excavation, for locations see Figure 6-4

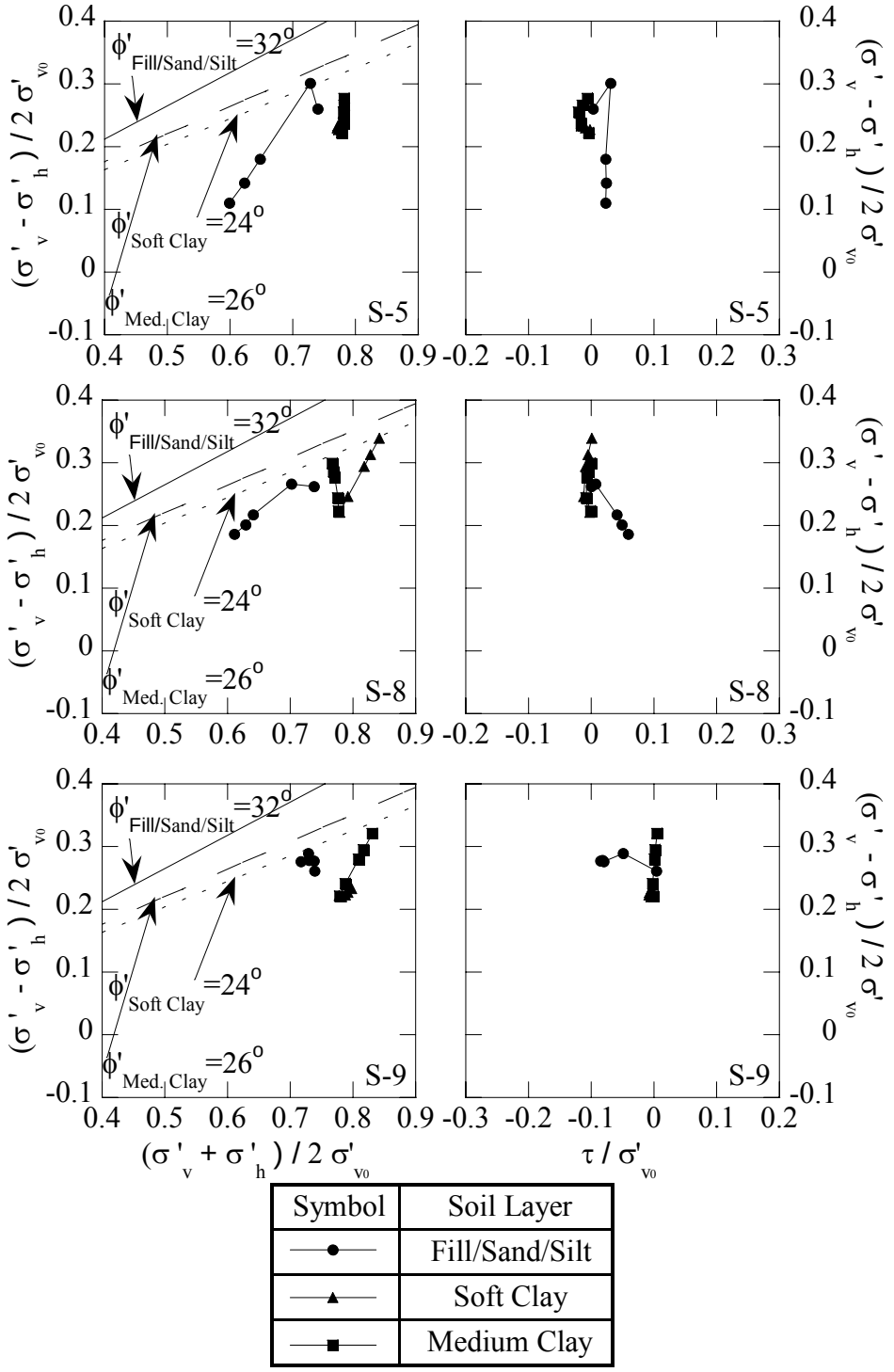

Figure 6-30 Normalized stress paths of (a) p'-q, and (b) τ-q for elements in middle of fill/sand/silt, soft clay, and medium clay layers for elements S-5, S-8, and S-9 in west side, Ford Center excavation, for locations see Figure 6-4

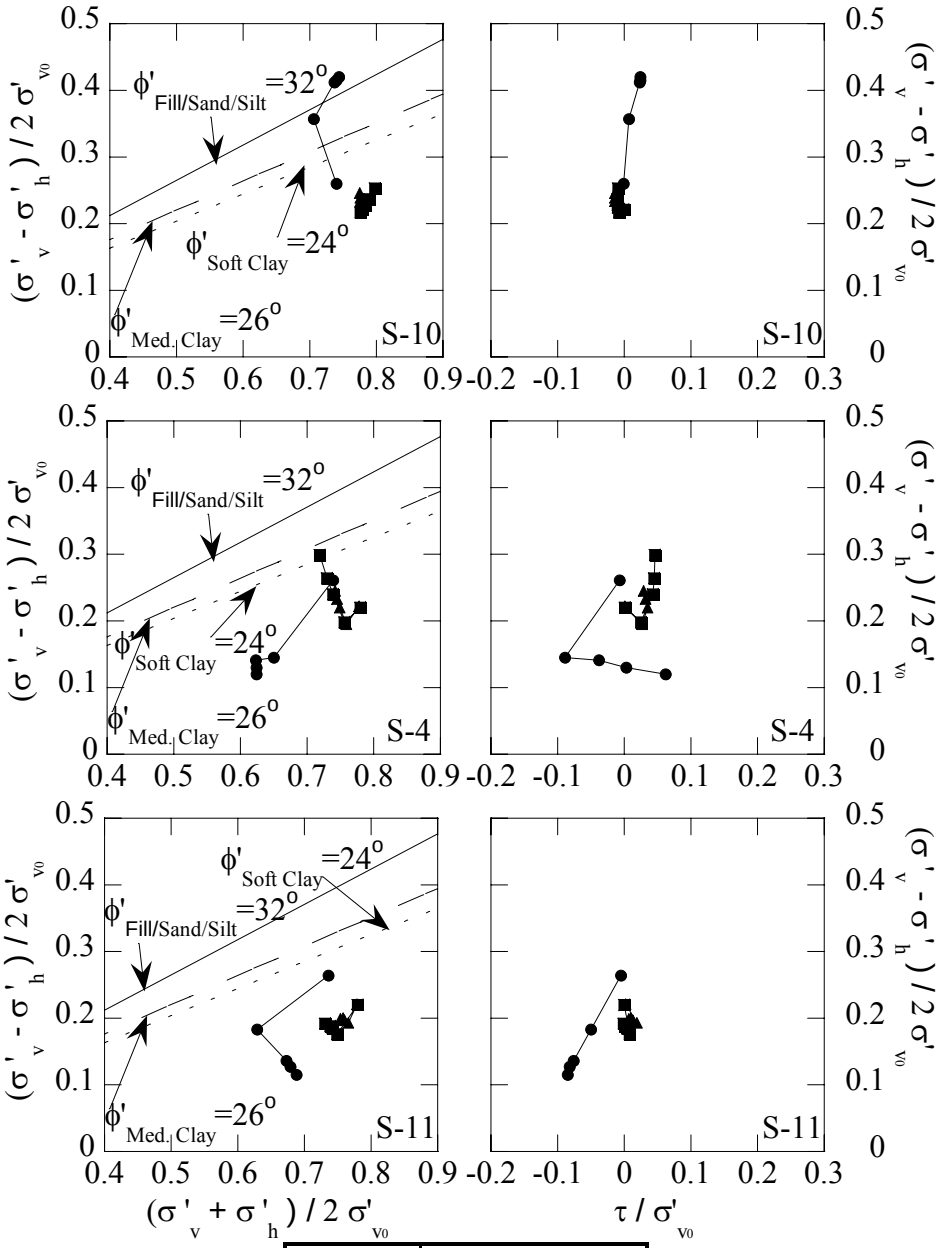

Figure 6-31 Normalized stress paths of (a) p'-q, and (b) τ-q for elements in middle of fill/sand/silt, soft clay, and medium clay layers for elements S-10, S-4, and S-11 in south side, Ford Center excavation, for locations see Figure 6-4

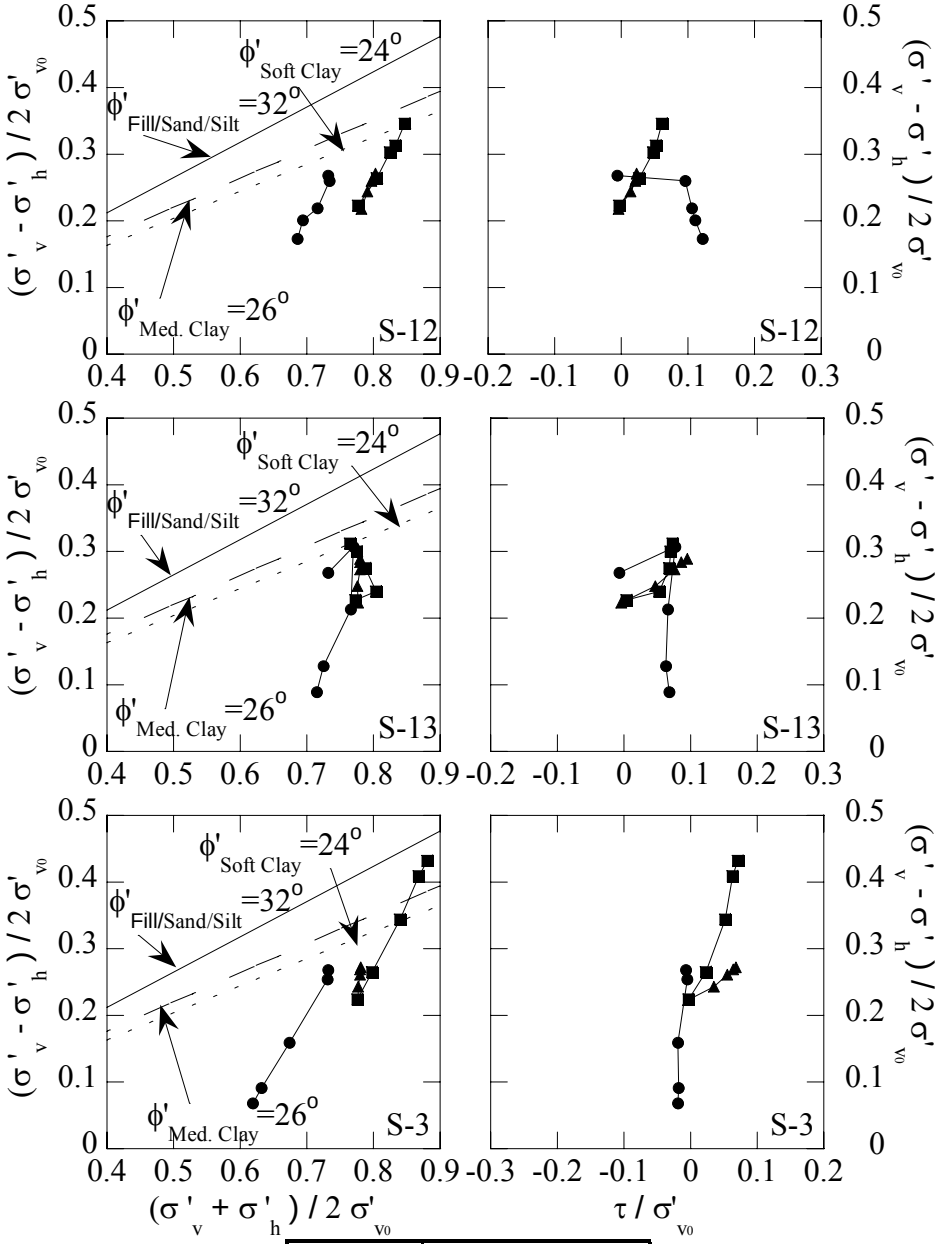

Figure 6-32 Normalized stress paths of (a) p'-q, and (b) τ-q for elements in middle of fill/sand/silt, soft clay, and medium clay layers for elements S-12, S-13, and S-3 in east side, Ford Center excavation, for locations see Figure 6-4

CHAPTER 7 CONCLUSIONS AND RECOMMENDATIONS FOR FUTURE RESEARCH

7.1. Summary and conclusions

In this study the potential capabilities of SelfSim were demonstrated using case studies of deep excavations. The proposed SelfSim framework utilizes a neural network material model and nonlinear finite element method. In SelfSim inverse analysis the measured excavation performance in forms of load and displacement boundary conditions is used to extract relevant soil behavior. The SelfSim framework allows numerical simulations of deep excavation to benefit from the continuous acquisition of data from instrumentation programs implemented to monitor the performance of the excavation and the surrounding ground. This framework provides a great opportunity to incorporate numerical simulations as an integral component in the application of the observational method in geotechnical engineering. The followings are the summary and conclusions of this study.

7.1.1. Comparison of optimization techniques using genetic algorithm and SelfSim learning in extracting the soil behavior-Lurie Center

Genetic algorithm and artificial neural Network algorithm are two useful methods for modeling excavations. Two methods are tested using measured data collected at the Lurie center case study in Chicago. Optimized parameters found from the GA approach and the learned constitutive responses from SelfSim formed the basis of simulations that could reasonably compute deformations observed during the excavation for the Lurie Center. Unlike GA analysis in which the soil model has to be preconstrained to specific model (in this study soil hardening model), SelfSim analysis does not have to be constrained to any predefined model. This capability allows SelfSim to capture the underlying soil behavior while it is learning about measurements at different construction stages. Optimization based on genetic algorithm could predict the inclinometer measurements and maximum surface settlements reasonably well. The stress paths results for this method show predominantly linear elastic behavior for clay layers, a feature of

the hardening soil model and the undrained simulation. On the other hand SelfSim is able to capture both lateral wall deformations and surfaces settlement profile. The stress paths from SelfSim analysis show a distinct nonlinearity of soil behavior for all clay and fill/sand layer. The SelfSim analysis shows that pattern of stress paths are far more complex than elastic behavior. This feature explains why the ANN model is able to compute settlement profile reasonably well.

7.1.2. The interplay between field measurements and soil behavior for capturing supported excavation response

The relationship between field instrumentation selection and the quality of learned excavation response facilitated by a unique inverse analysis framework, SelfSim, was explored. This study shows that integrating the proposed inverse analysis framework with a field instrumentation program for deep excavation can be used to supplement physical measurements and provide reliable estimates of deformations and loads elsewhere around the excavation. This finding can assist engineers on projects whereby cost and space constraints as well as damage to instruments during construction limit the number of available instrument measurements. The integration of the inverse analysis with the remaining measurements can help fill-in-the-gap otherwise unavailable information.

It is demonstrated that wall deformations and surface settlements provide essential information for learning of overall excavation behavior. An inclinometer placed within or in close proximity to the wall is essential. Additional inclinometers placed farther back from the wall provide supplementary information that can be used to complement prediction of surface settlements if that information becomes unavailable at certain excavation stages. The finding is confirmed using the TNEC excavation case study. This is a useful and practical finding as surface settlements point can be easily lost in a heavily trafficked urban environment.

It is shown that bracing loads and by analogy, tieback loads provide valuable information to extract soil behavior and enhance the overall quality of estimated ground response. Therefore, measurement of bracing loads is recommended.

Other instruments such as heave gauges, extensometers, and piezometers provide useful measurements in order to monitor construction and verify design assumptions;

though it appears in the simulated excavation study that they are less critical for overall learning of excavation behavior.

7.1.3. Case studies of prediction of excavation response using learned performance of similar excavations via inverse analysis

The field instrumentation measurements from several case studies are used to capture soil behavior from one section of a deep excavation and then use the developed soil model to predict the excavation performance in other sections of the same excavation or different excavation with similar soil stratigraphy.

It is demonstrated that the extracted soil behavior from two-level tieback section of the wall in Texas A&M case study in sandy soil could predict reasonably well the lateral deflections measured at the wall and in different locations behind the wall in one-level tieback section of the excavation.

It is shown that the extracted soil behavior from using wall deflections and surfaces settlements measurements in proximity to the Panel 27 of Yishan Road metro station in Shanghai could predict the excavation performance reasonably in other sections. Lateral wall deflections and surface settlements are predicted reasonably along the 335 m length of the station.

It is shown that the extracted soil behavior from TNEC excavation project can be used to predict the excavation response in Formosa case study in soft clays of Taipei. The lateral well deflections and surface settlements are predicted reasonably well in Formosa excavation. This study shows a successful implication of SelfSim framework whereby excavation performance can be predicted after learning from precedent. This finding is critically important as several case studies records are available in each urban area. The extracted soil behavior from those case studies "local experience" can be used in new excavation projects to assess excavation induced ground movements more accurately.

7.1.4. Ford Center excavation case study

The extracted soil models from Lurie Center excavation in downtown Chicago is used to predict excavation response in Ford Center excavation in Evanston, IL. The extracted soil models from Lurie Center overpredict excavation induced lateral deflections by approximately two orders of magnitude in Ford Center excavation.

Although the soil stratigraphy of the two sites is similar, elevated ground surface surrounding the Ford Center excavation imposes 3 dimensional effects in excavation performance. Three dimensional analysis of Ford Center excavation is inevitable task to capture excavation response in Ford Center. The new monitoring scheme, LIDAR scanning, of construction sequence of excavation sites are used and discussed. The development of 3D numerical modeling of SelfSim is explained. It is demonstrated that the computed lateral movements occurred during the excavation is improved via 3D SelfSim inverse analysis. The results show that it is critically important to have at least one inclinometer in each side of excavation to capture the soil behavior in 3D modeling. The predicted settlements profiles around the excavation site also show a significant 3D effect caused by elevated ground surface. The comparison of extracted soil behavior from 2D and 3D analysis demonstrate that the 2D analysis for Ford Center excavation can not represent the soil behavior.

7.2. Recommendations for future work

With the application of the SelfSim framework to extract material behavior from field measurements, there are a number of possibilities for future work. It is believed that the proposed SelfSim framework will make an important impact on the method of engineering analysis and design. The following represents some of the possibilities for future research within the framework of SelfSim:

7.2.1. Web-based database for field observations in deep excavations

SelfSim inverse analysis framework is a powerful tool that can change the current practice in design of deep excavations. The use of more case studies with diversified construction sequences, soil properties, and supporting systems improves the extracted model. The more information is provided, the more representative the extracted model would be. Therefore, a systematic complementary effort should be made to facilitate the access to more data in urban areas. There are currently numerous excavation case studies that are constructed in the dense populated cities that their information is not currently accessible for designers, engineers and researchers. Although, in last 30 years far-reaching progress has been made in development of emerging technologies, wireless

sensors, digital scanners and communication devices, geotechnical engineers have not fully benefit in their practice from those developments.

It is desirable to change the current practice of deep excavation designs by developing the following factors: 1) A web-based system should be designed to provide a template for collecting instruments measurements, geometry, site descriptions, etc. 2) The digital camera and laser scanners can be deployed before the start of excavation. 3) A wireless communication system can be set up to transfer the data collected by monitoring devices. 4) An Automated system should be designed to test and interpret the collected data to examine the data validity.

Should the aforementioned factors develop, a significant change and improvement is going to be observed in design, construction and monitoring of excavation sites.

7.2.2. Field data and construction records verification tool

There are lots of difficulties in interpreting the data collected from the field. Some of those demonstrated in Texas A&M and Shanghai case studies. These difficulties sometimes are due to incompatibility of the monitoring data and the recorded construction activities or the improper recording the monitoring devices. In either case the inconsistency between "cause and effect" imposes a pause for performing inverse analyses. Numerous case studies are reported in the literature; however they can not be used in inverse analyses studies. Therefore, it is critically important from the beginning of construction, the monitoring data is verified by the construction activity records in order to revise the monitoring scheme or to include the details of construction variation in the reports. For instance for excavations, it is needed to develop a software that field engineer quickly checks the validity of the collected monitoring data and construction sequence and to make sure the collected data logically makes sense.

7.2.3. The soil-wall interaction in numerical modeling

The interaction of the strut-wall-soil system in braced excavations is a complex phenomenon that has been studied extensively in the past. Careful assessment of the major change in stress and deformation influenced by soil-wall interaction is critically important. For instance soldier piles are often designed and analyzed as contiguous wall systems even though they are, in reality, not so. Nonetheless, designers have recognized

that the soldier pile retaining system is not only often more flexible than other systems but the stiffness of the system is non-uniform in that the piles are much stiffer than the timber lags. To the fact that the soldier piles and timber laggings have very different stiffness means that the interaction between the retaining system and the soil is three-dimensional (3D) in nature. Furthermore, supporting systems are commonly modeled as beam elements that have equivalent stiffness of the wall. Beam elements may not realistically represent the interaction between the supporting system and surrounding soil. More research and development is required to model soil-wall interaction.

7.2.4. Developing local experience database

The case studies in Taipei demonstrated that it is possible to learn from precedent case studies and predict performance of a new excavation in the same local. There are many construction case histories conducted in urban area that they have similar soil stratigraphy. The proposed inverse analysis approach can be used with available measurements from previous excavation case studies to develop numerical models with "local experience". This approach paves the way to develop area-specific soil models (e.g. San Francisco Bay Mud, Boston Blue Clay). Thenafter, the developed soil models can be used to provide acceptable predictions of excavation-induced ground deformations for new excavations constructed in these locals.

7.2.5. User interface development for SelfSim

The successful use of numerical softwares is dependent on their capability to handle broad range of problem; however having a user friendly interface is critically important. In the current format of SelfSim package for excavation application, a significant amount of time is spent for preparing the input files for SelfSim learning simulations, which is not affordable in practice. Indeed for 3D problems another program (e.g. Patran) is used to generate the mesh.

The interface should be designed to ask for the number of soil layers, geometry of the excavation, density of mesh, soil parameters, excavation sequence, instrument locations, raw measurements, NN structures for each soil layer, and SelfSim input

parameter from the user. Then the application of SelfSim would be much easier and more practical than its current format.

7.2.6. Hybrid constitutive models

The use of extracted constitutive models from SelfSim learning in predicting new excavations performances are appropriate as long as the stress-strain range of new excavations falls within the stress-strain range that was learned. In other words, SelfSim framework is not appropriate for extrapolation purposes. Therefore, it is desired to develop hybrid constitutive models in a framework that utilizes the extracted soil models from SelfSim learning within the learned stress-strain ranges and the suitable conventional models for outside of leaned stress-strain ranges. This will enhance the performance of simulations for the cases that the training dataset does not have sufficient information.

APPENDIX CENTRAL ARTERY/ TUNNEL PROJECT EXCAVATION INDUCED GROUND DEFORMATIONS

A.1 Introduction

A major concern for the development of urban excavations is the induced deformations in the surrounding soil and the subsequent impact on adjacent structures. Erroneous estimates of soil deformations prior to construction may result in either large construction costs due to excessive ground support or damage to the surrounding structures due to inadequate excavation support. Additional factors such as construction technique, soil type, and support system have significant influence on the predicted deformations. Therefore, new case histories add to our knowledgebase of precedent. Several studies (Peck 1969; Karlsurd 1986; Clough et al. 1989; Clough and O'Rourke 1990; Ou et al. 1993; Fernie and Suckling 1996; Wong et al. 1997; Long 2001; Moormann 2004; O'Rourke and McGinn 2006) compiled such case histories and developed empirical correlations for estimating ground deformations.

The Central Artery/Tunnel project is one of the largest and most complex highway construction projects ever undertaken in the US. The project encompasses 242 lane kilometers, of which half run underground in an 11.3 kilometers corridor as illustrated in Figure A-1. Excavations were extensively instrumented for construction monitoring and design verification purposes. These instrumented excavations provide a unique opportunity to observe ground response to excavation. The excavations are within typical soil profiles of Boston consisting of fill, clay, and glacial till. Instrumentation data from three construction contracts C11A1, C15A1, and C17A2, Figure A-1, are presented and summarized in this technical note.

A.2 Contracts C11A1, C15A1, C17A2

Contract C11A1

Contract C11A1 spans approximately 685 m, corresponding to a section of the CA/T I-93 Northbound alignment, Figure A-1. C11A1 extends between station CANB (THE CANBERRA HOSPITAL - A.C.T.) STA. 84+21, adjacent to the Wang Building on Kneeland Street, and station CANB STA. 106+70 located to the north of the Dewey

Square Tunnel Portal on Congress Street. The topography of the site is fairly level, with an average surface elevation (CA/T Datum) of 33.5 m. The depth of the excavations for the tunnels ranges from about 16.8 m to 33.5 m and the width of the excavations varies from about 17.7 m to 32.9 m.

Typical soil profile in this contract is shown in Figure A-2a. North of CANB Sta. 88, the sequence of stratification is fill and organic deposits at the top, underlain by Boston Blue Clay and glacial till over argillite bedrock. A detail description of subsurface conditions can be found in several published documents (H&A 1995; O'Rourke et al. 1997; O'Rourke and O'Donnell 1997; Lambrechts 1998; BSP 2006). The ground water table is approximately 1.5 m below the ground surface.

The excavation support walls with depth of 30.5 m consist of 0.9 m thick soldier piles and tremie concrete (SPTC) supported by 8 2-W30x173 or 2-W36x359 steel struts as cross-lot bracing at 2.1m to 3.6m spacing (Hashash et al. 2003). A typical excavation sequence begins by excavating to a level just below where the first struts are to be installed. Then walers are installed and struts jacked to about 50% of their design load. This process is repeated for the next strut level. A typical section along this contract is shown in Figure A-2b.

Contract C15A1

Contract C15A1 starts from STA 142 and ends at STA 155, Figure A-1. The excavation depth shown in Figure A-3a ranges from 18.3 m to 21.3 m with similar sequence of soil layers, and support system to C11A1, except the average vertical support spacing is 5.2 m (BSP 2006) Figure A-3b.

Contract C17A2

Contract C17A1 starts from STA 132 and ends at STA 142, Figure A-1. The soil profile consists of 6.1 m fill and organic deposits at the ground surface, clay and glacial deposits with variety in excavation depth on the bedrock shown in Figure A-4a. The excavation depth ranges from 13.7 m to 19.8 m. Figure A-4b shows, two middle walls in each section which separate west and east SPTC walls. The support system includes bracing with struts just at one elevation in addition to roof girders in every section and the spacing varies from 3.7 m to 7.6 m.

In all three contracts the support walls are embedded into the bedrock which limit the deformations due to excavation.

A.3 Lateral wall deformations

Maximum wall deflections versus excavation depth from the three contracts are shown in Figure A-5. The deflection measurements have an average trend line $\delta_{hm} / H = 0.07\%$ with $\delta_{hm} / H = 0.22\%$ as an upper limit for all measurements. This is significantly smaller than prior reported results (Clough and O'Rourke 1990) which provide $\delta_{hm} / H = 0.2\%$ as an average trend line and $\delta_{hm} / H = 0.5\%$ as an upper bound. The deflections in glacial till are less than those in clay even where the excavation depth is greater due to the greater stiffness of the till.

Although the thickness of clay layer in C11A1 is almost twice as the C17A2, the stiffer support system provided in C11A1 is effective in reducing deformations to levels comparable to those in C17A2. The embedment of the wall into the rock in addition to the system stiffness results in smaller deformations in all three contracts. The computed maximum wall deflections based on the model proposed by Kung et al. (2007) are plotted in this figure and are in general agreement with field measurements.

Figure A-6 plots the measured wall deflection ratios versus system stiffness and superimposed on the empirical chart proposed by Clough and O'Rourke (1990) which are routinely used in engineering practice. The hatched zones in this figure represent the ranges of calculated system stiffness and measured deformations for all excavations. The factor of safety against basal heave is estimated to be larger than 3. While there is general agreement between the field observations and the empirical chart, the measured deformations are very small and extend below the lowest curve (FS=3.0) shown in the chart.

A.4 Lateral deformations behind the wall

Figure A-7 is a plot of maximum lateral deflection ratio versus distance behind the wall obtained from inclinometers placed in the support wall and in the retained soil. An equation is proposed to represent a bound for all the data measured and it ranges from about 0.2% next to the wall to about 0.05% at a normalized distance of 1. Similar trend

was observed in the data provided by Koutsoftas et al. (2000). The data fall within the zone of high horizontal stiffness of Clough and O'Rourke (1990).

A.5 Surface settlement behind the wall

Figure A-8 plots maximum surface settlement versus excavation depth. The upper and average trend lines are $\delta_{vm} / H = 0.2\%$ and $\delta_{vm} / H = 0.05\%$, respectively. They are lower than the corresponding lines of Clough and O'Rourke (1990). The soil settlements behind the wall in C15A1 are less than in C17A2 at similar excavation depths because of greater stiffness provided by smaller vertical spacing of the struts. The computed maximum measured surface settlements are in the range that is computed by the model of Kung et al. (2007).

Figure A-9 plots maximum deformation versus distance behind the wall. The data shows that the maximum settlement for all the data is about 35 mm and that settlements extend as far as 100 m behind the wall, though the data is sparse beyond a distance of 60 m. Precision of measurements and construction activities near the settlement measurement locations may have some effect on measured settlements at distances far away from the excavation.

Figure A-10 shows the normalized settlements versus normalized distance behind the excavation. Both quantities are normalized with respect to excavation depth. Separate plots are shown for data corresponding to clay and till profiles. While most settlements are less than $\delta_{vm} / H = 0.02\%$, the normalized settlements extend to distances farther than the distance ratio of 2 to 3 suggested by earlier empirical envelopes. Data located at distances larger than D/H>4 correspond generally to excavation depths less than 12 m.

Figure A-11 plots the same data set, but now with settlements normalized by the corresponding maximum surface settlement. The measurements show that even for distances up to 4 to 5 times of excavation depth the settlements are on the order of 60% of maximum settlements. This behavior is especially pronounced for the contracts C11A1 and C17A2. The settlement data shows that the stiff support system combined with the influence of wall embedment in rock reduce the maximum settlement. Although the maximum settlement is now small, the settlement trough extends further than proposed in earlier studies. The measured data in this figure is compared with other proposed

empirical relations (Hsieh and Ou 1998; Kung et al. 2007). The CA/T measured data does not fit within the boundaries proposed in these studies.

Figure A-10 and Figure A-11 also show envelopes of the CA/T surface settlement data. The envelopes for the clay profiles reflect the lower settlement ratios but wider distribution of settlements behind the wall. For the clay profiles the envelopes reflect a limit on lateral extent of settlements to a distance ratio of 5. For the till profiles the envelopes reflect a limit on lateral extent of settlements to a normalized distance of 3. It is possible that these wider normalized settlement troughs are due to the relatively small deformations experienced by the soil. The soil response is likely to be more linear at smaller strains.

A.6 Conclusions

Measured deformations from three selected excavation contracts of Central Artery/Tunnel project show that it is possible to control deformations around an excavation to small levels. Increasing system stiffness and embedment of the wall into a stiff layer are key factors in limiting the deformations. Wall deflections are below $\delta_{hm} / H = 0.22\%$ and surface settlements are below $\delta_{vm} / H = 0.2\%$. Surface settlements, though small, extend to significant distance (up to 5x excavation depth) behind the support wall. Lateral deformations behind the wall reduce exponentially with distance from the wall. Both magnitude and distribution of surface settlements behind the wall are significantly less in till compared to clay.

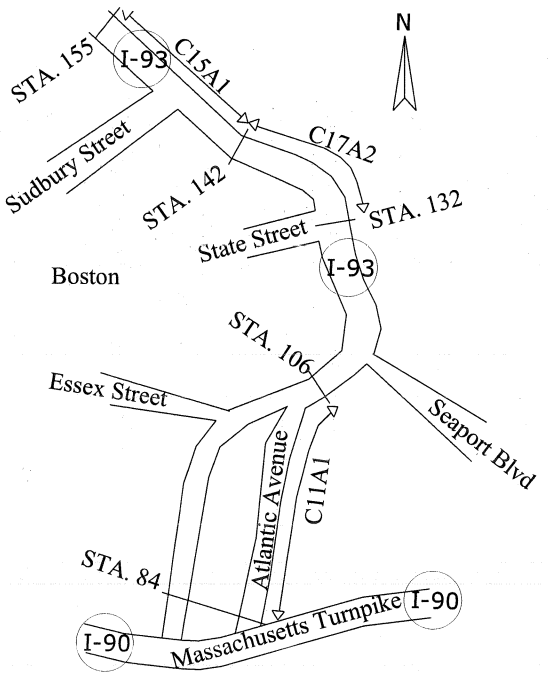

Figure A-1 Plan view of the Central Artery/Tunnel project C11A1, C17A2 and C15A1 construction contracts

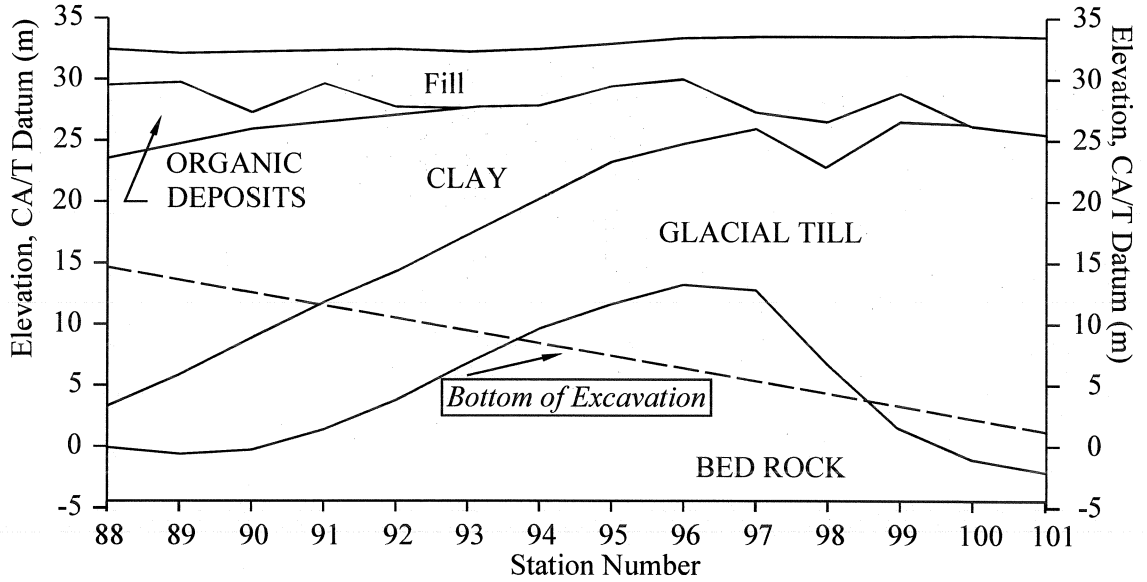

(a) Soil profile (STA 88 to STA 100)

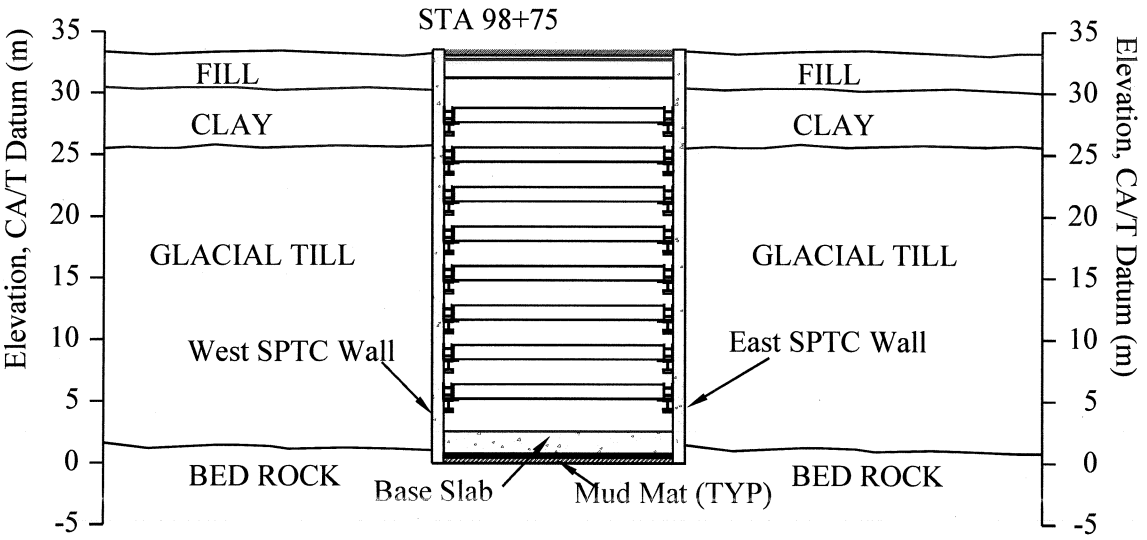

(b) Typical section of excavation bracing and support systems at STA98+75

Figure A-2 Contract C11A1 soil profile and section

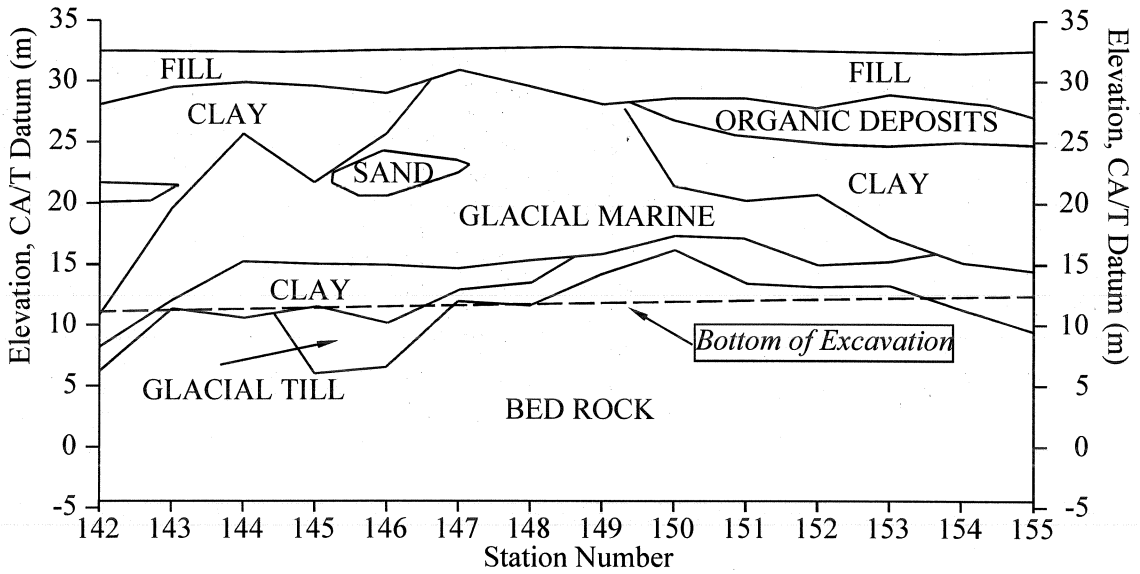

(a) Soil profile (STA 142 to STA 155)

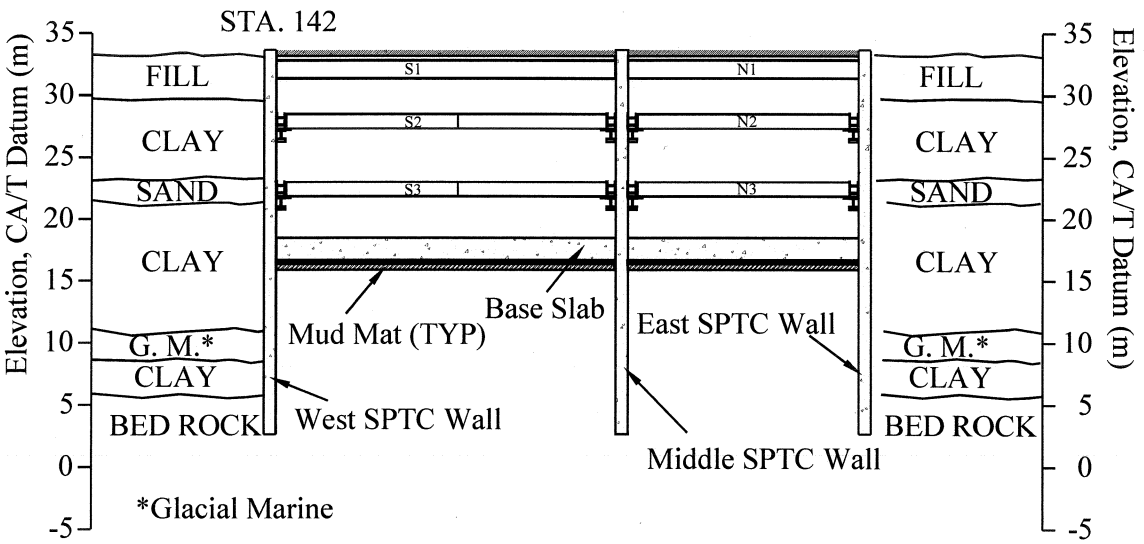

(b) Typical section of excavation bracing and support systems at STA142

Figure A-3 Contract C15A1 soil profile and section

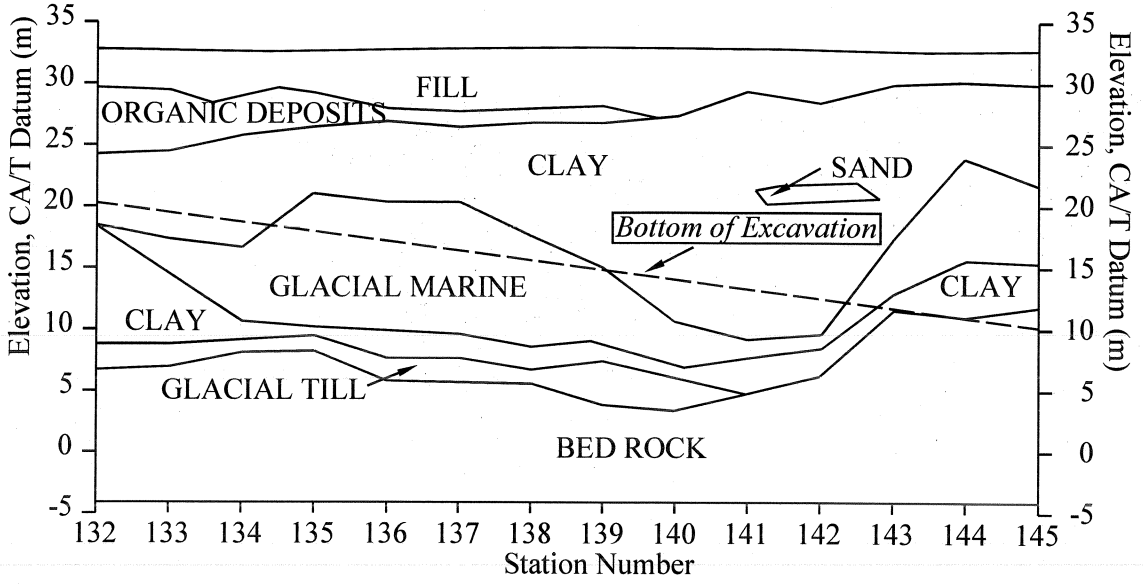

(a) Soil profile (STA 132 to STA 141)

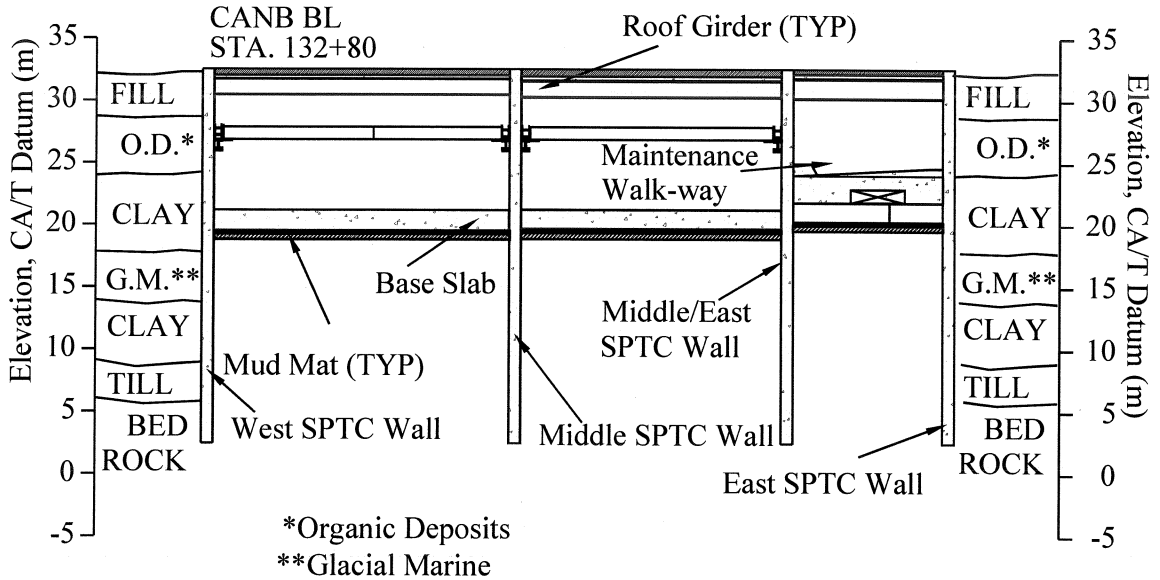

(b) Typical section of excavation bracing and support systems at STA 132+80

Figure A-4 Contract C17A2 soil profile and section

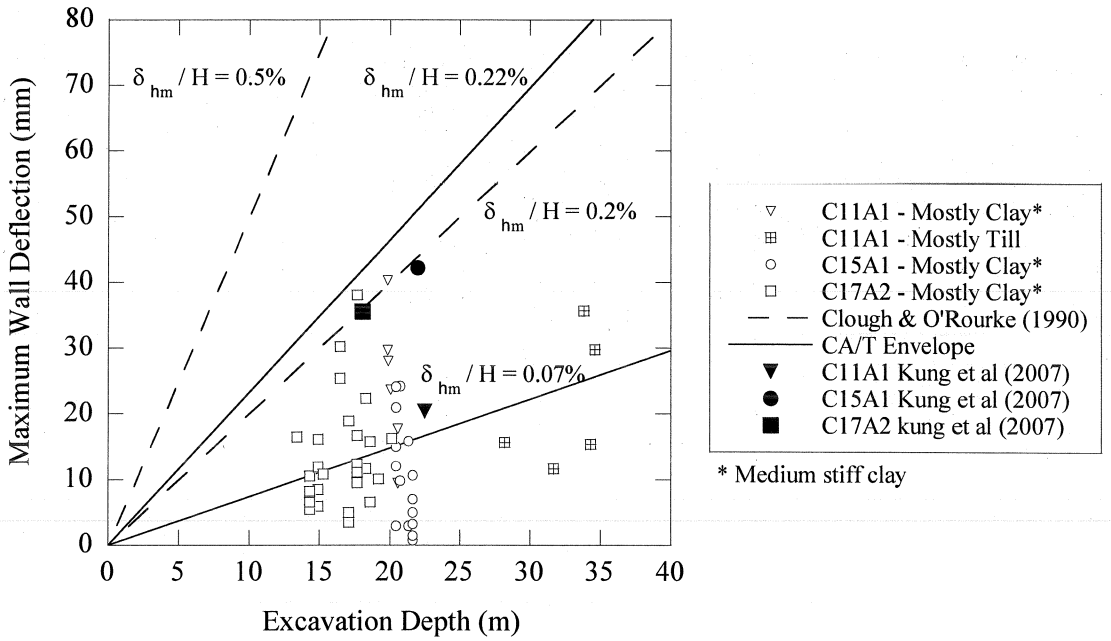

Figure A-5 Observed maximum lateral movements for in situ slurry walls

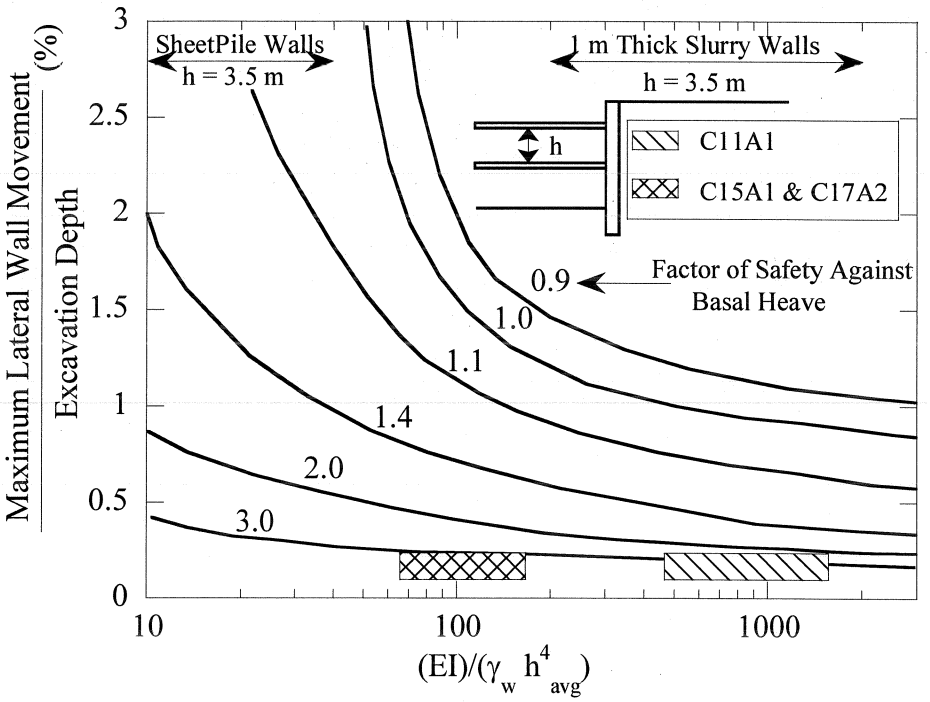

Figure A-6 Design curve to obtain maximum lateral movement for soft to medium clays, after modified after Clough et al. (1989)

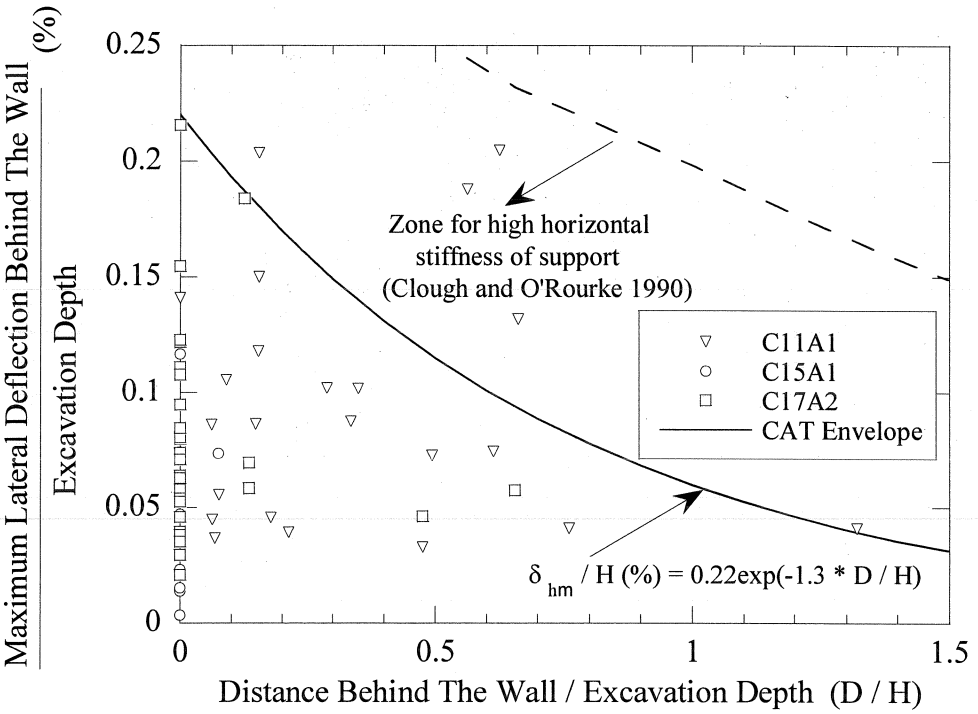

Figure A-7 Summary of maximum lateral deflection behind the wall versus distance from excavation both normalized to excavation depth (Linear scale)

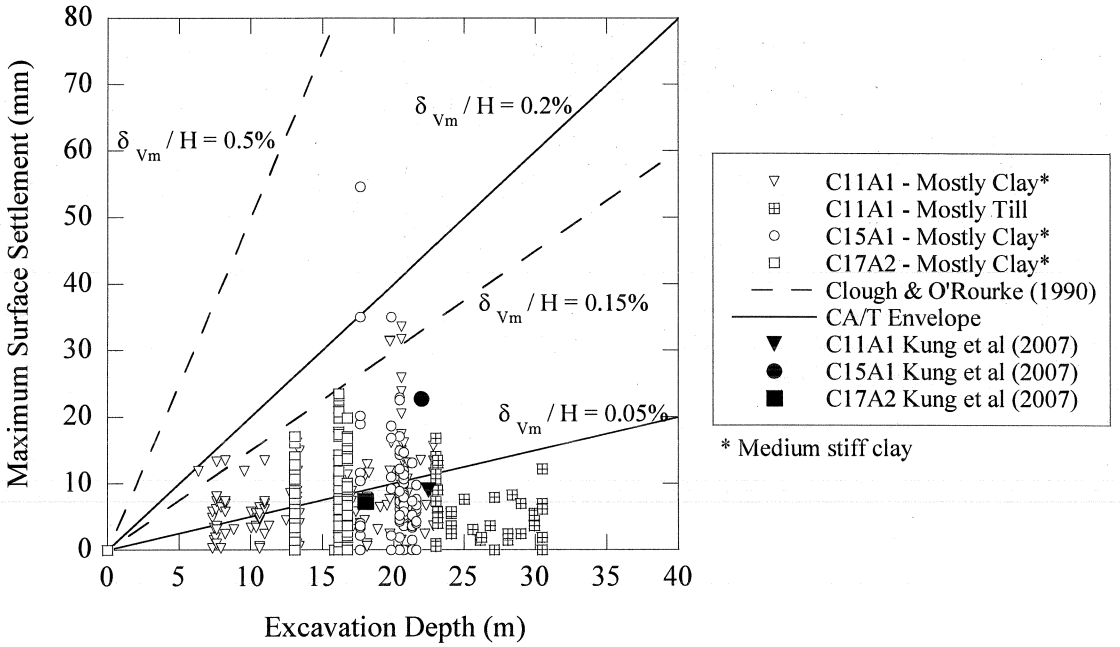

Figure A-8 Observed maximum soil settlement in the soil retained by insitu walls

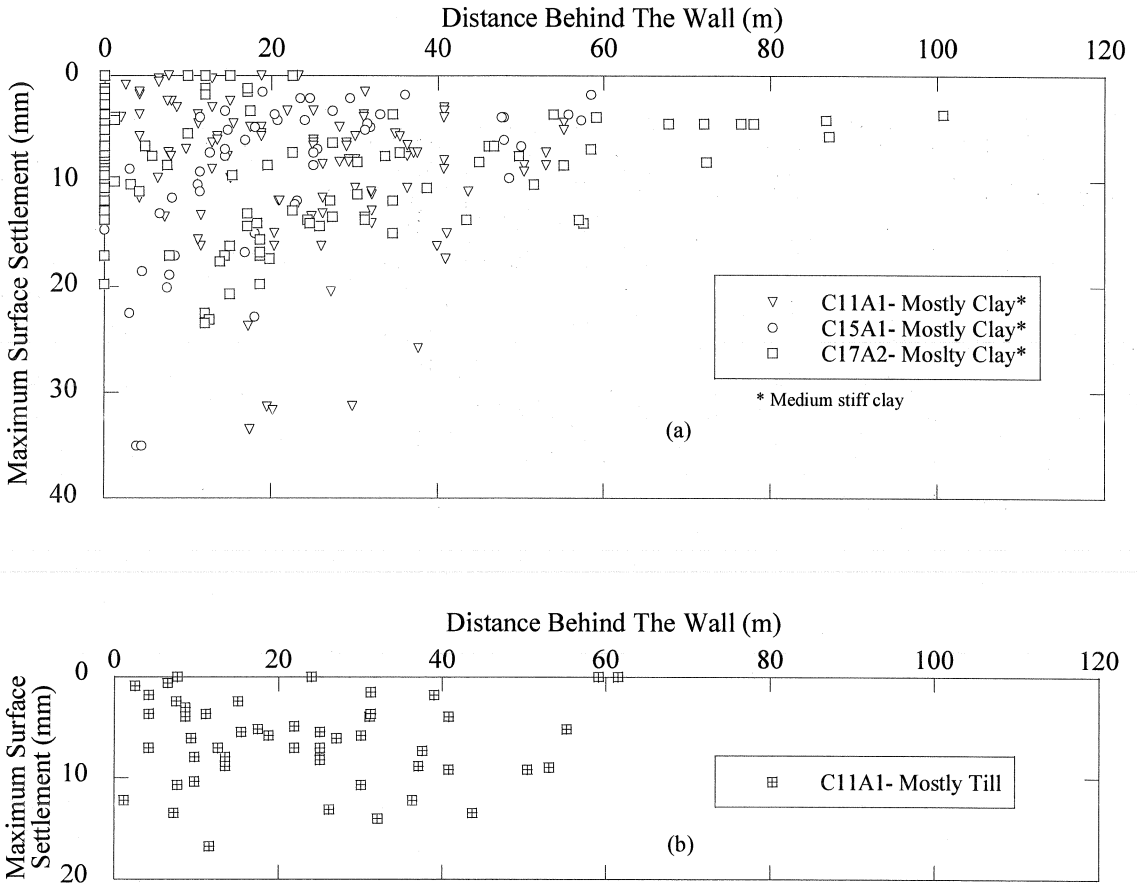

Figure A-9 Measured surface settlements versus distance behind the wall

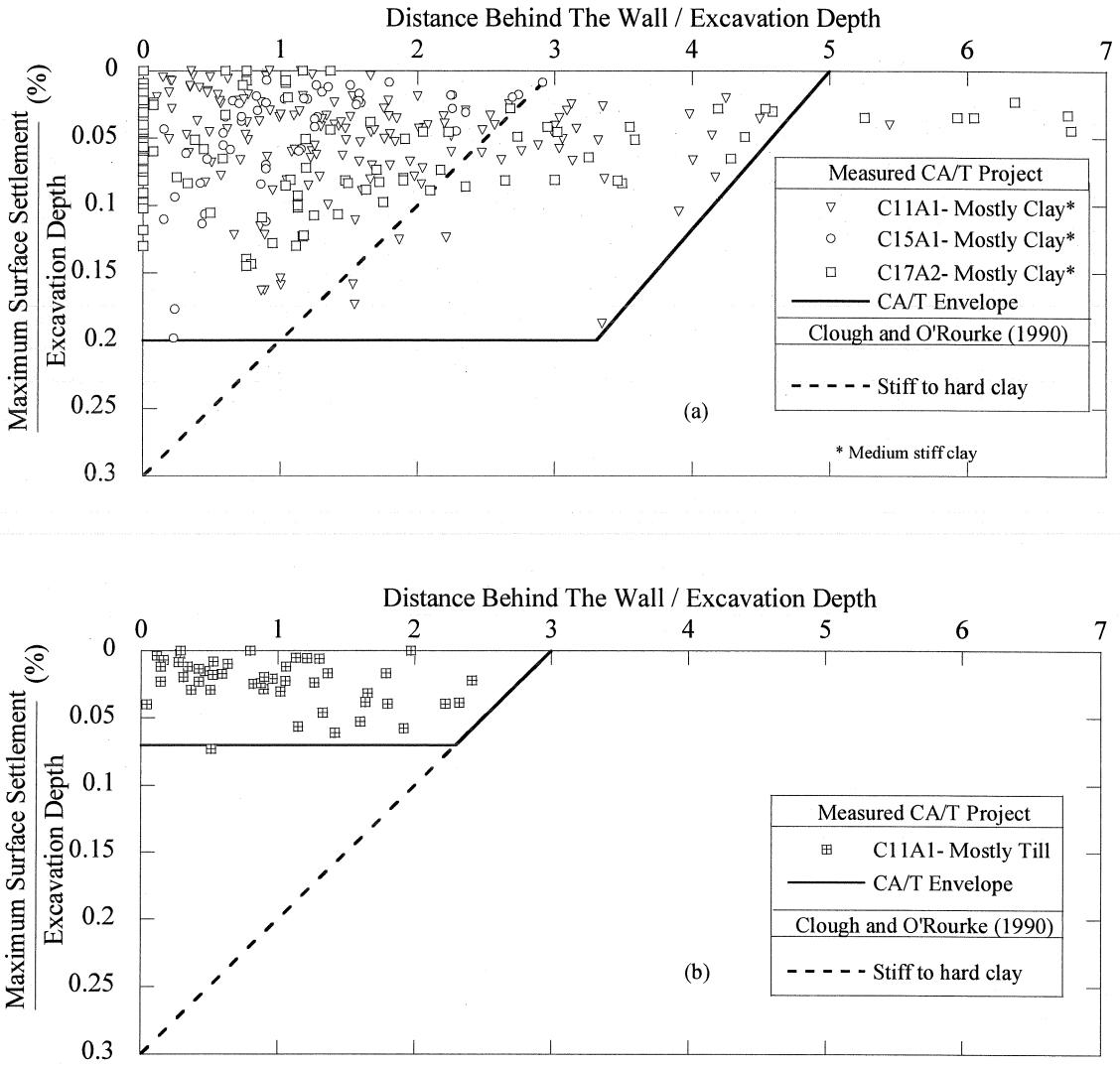

Figure A-10 Summary of measured surface settlement normalized to excavation depth

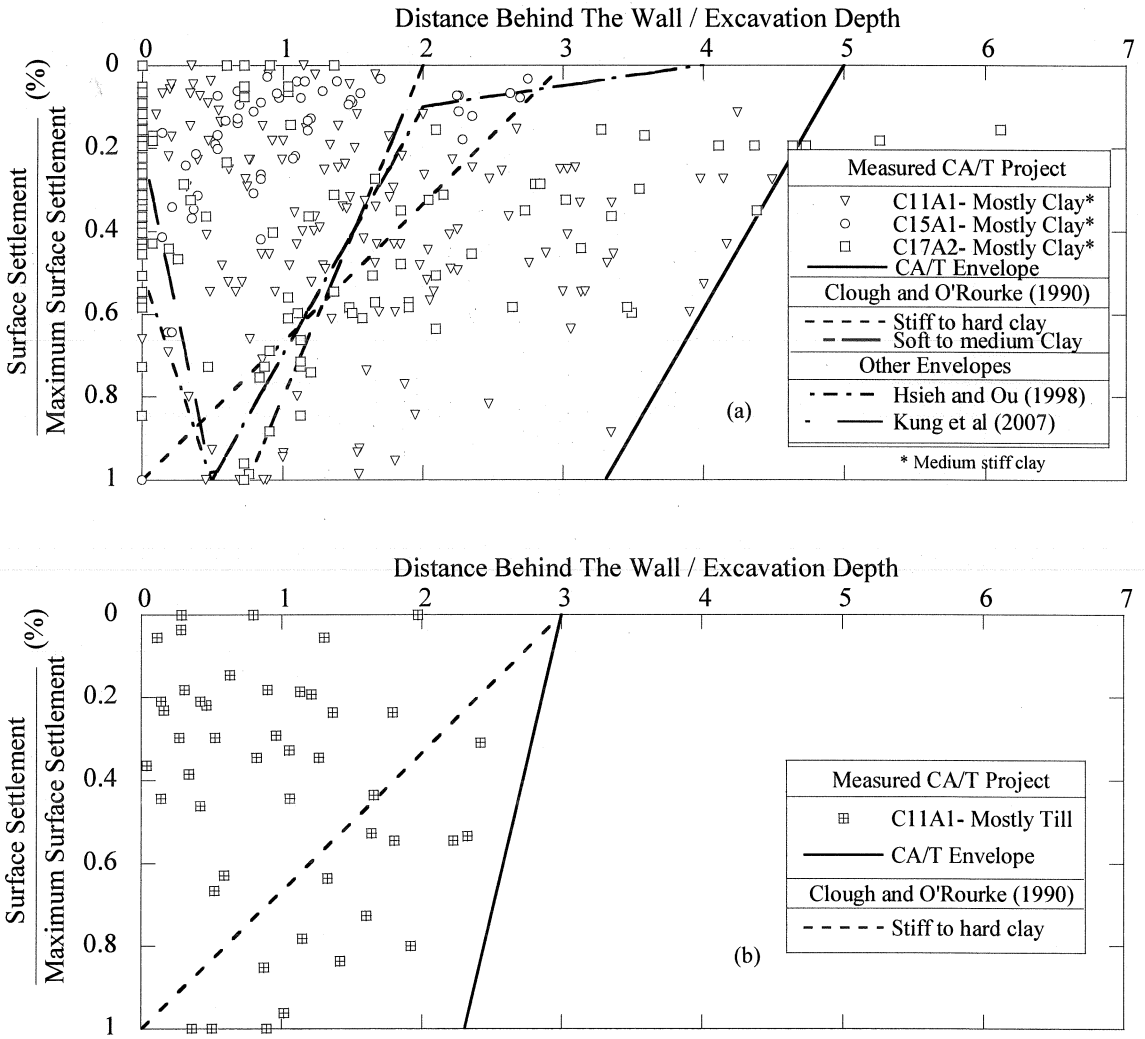

Figure A-11 Summary of measured surface settlements normalized to corresponding maximum surface settlement

REFERENCES

ABAQUS (2005). "ABAQUS/Standard, A General Purpose Finite Element Code". Pawtucket, RI, ABAQUS, Inc., formerly Hibbitt, Karlsson & Sorensen, Inc.

Anandarajah, A. and Agarwal, D. (1991). "Computer-Aided calibration of a soil plasticity model." *International Journal for Numerical and Analytical Methods in Geomechanics* 15(12): 835-856.

Arai, K., Ohta, H. and Kojima, K. (1986). "Application of back analysis to several test embankments on soft clay deposits." *Soil Foundation* 26(2): 60-72.

Benoit, J. and Lutenegger, J., Eds. (2000). "National geotechnical experimentation sites". *Geotechnical special publication No.93*.

Bishop, A. W. (1955). "The use of the slip circle in the stability analysis of slopes." *Geotechnique* 5(7-17).

Bjerrum, L. and Eide, O. (1956). "Stability of Strutted Excavations in Clay." *Geotechnique* 6: 32-48.

Blackburn, J. T. (2005). "Automated sensing and three-dimensional analysis of internally braced excavations", Northwestern University: 369.

Bland, J. M. and Altman, D. G. (1986). "Statistical methods for assessing agreement between two methods of clinical measurements." *Lancet*: 307-310.

Bland, J. M. and Altman, D. G. (1986). "Statistical methods for assessing agreement between two methos of clinical measurements." *Lancet*: 307-310.

Boscardin, M. D. and Cording, E. J. (1989). "Building response to excavation-induced settlement." *Journal of Geotechnical Engineering* 115(1): 1-21.

Bowles, J. E. (1996). "Foundation Analysis and Design".

Briaud, J. L. and Lim, Y. (1997). "Soil-nailed wall under piled bridge abutment: simulations and guidelines." *Journal of Geotechnical and Geoenvironmental Engineering* 123(11): 1043-1050.

Briaud, J. L. and Lim, Y. (1999). "Tieback walls in sand: numerical simulatio and design implications." *Journal of Geotechnical and Geoenvironmental Engineering* 125(2): 101-110.

Brinkgreve, R. B. J. (2003). "Plaxis v8."

BSP. (2006). "Boston subsurface project." 2006, from http://bostonsoil.atech.tufts.edu/.

Calvello, M. (2002). "Inverse analysis of a supported excavation through Chicago glacial clays". Evanston, IL, Northwestern University.

Calvello, M. and Finno, R. J. (2004). "Selecting parameters to optimize in model calibration by inverse analysis." *Computers and Geotechnics* 31(5): pp. 410-424.

Chung, C. K. and Finno, R. J. (1992). "Influence of depositional processes on the geotechnical parameters of Chicago glacial clay." *Engineering Geology* 32: 225-242.

Cividini, A. and Rossi, A. Z. (1983). "The Consolidation Problem Treated by a Consistent (Static) Finite Element Approach." *International Journal for Numerical and Analytical Methods in Geomechanics* 7: 435-455.

Clough, G. W. and Duncan, J. M. (1971). "Finite element analyses of retaining wall behavior." *Journal of the Soil Mechanics and Foundations Division* 97(SM12): 1657-1673.

Clough, G. W. and Mana, A. I. (1976). "Lessons Learned in Finite Element Analyses of Temporary Excavations in Soft Clay". *Second International Conference on Numerical Methods in Geomechanics*, Blacksburg, VA.

Clough, G. W. and O'Rourke, T. D. (1990). "Construction induced movements of insitu walls". Design and Performance of Earth Retaining Structures. New York, NY, ASCE: 439-470.

Clough, G. W., Smith, E. M. and Sweeney, B. P. (1989). "Movement control of excavation support systems by iterative design". Foundation Engineering Proceedings Congress. Evanston, IL, ASCE: 869-884.

Clough, G. W. and Tsui, Y. (1974). "Performance of tied-back walls in clay." *Journal of the Geotechnical Engineering Division* 100(GT12): 1259-1273.

Dunnicliff, J. (1996). "Geotechnical instrumentation for monitoring field performance", John Wiley and Sons.

Fernie, R. and Suckling, T. (1996). "Simplified approach for estimation of lateral movement of embedded walls in U.K. ground". *International Sym. Geo Aspects of Underground Construction: in Soft Ground*, City University, London.

Finno, R. J., Atmatzidis, D. K. and Perkins, S. B. (1989). "Observed performance of a deep excavation in clay." *Journal of Geotechnical Engineering* 115(8): 1045-1064.

Finno, R. J., Blackburn, J. T. and Roboski, J. F. (2007). "Three-dimensional effects for supported excavations in clay." *Journal of Geotechnical and Geoenvironmental Engineering* 133(1): 30-36.

Finno, R. J. and Calvello, M. (2005). "Supported excavations: Observational method and inverse modeling." *Journal of Geotechnical and Geoenvironmental Engineering* 131(7): 826-836.

Finno, R. J. and Harahap, I. S. (1991). "Finite element analyses of HDR-4 excavation." *Journal of Geotechnical Engineering* 117(10): 1590-1609.

Finno, R. J. and Roboski, J. F. (2005). "Three-dimensional responses of a tiedback excavation through clay." *Journal of Geotechnical and Geoenvironmental Engineering* 131(3): 272-283.

Fu, Q. (2007). "Interpretation of Soil Behavior from Laboratory Specimens Subjected to Non-uniform Loading Conditions". *Civil and Environmental Engineering*. Urbana, University of Illinois at Urbana-Champaign.

Fu, Q., Hashash, Y. M. A. and Ghaboussi, J. (2007). "Non-uniformity of stress states within a dense sand specimen.". *Geo-Denver 2007*, Denver, Co.

Fu, Q., Hashash, Y. M. A., Jung, S. and Ghaboussi, J. (2007). "Integration of laboratory testing and constitutive modeling of soils." *Computer and Geotechnics* 34(5): pp. 330-345.

Gens, A., Ledesma, A. and Alonso, E. E. (1996). "Estimation of parameters in geotechnical back analysis 2. Application to a tunnel excavation problem." *Computer and Geotechnics* 18(1): 29-46.

Ghaboussi, J., Pecknold, D. A., Zhang, M. and Haj-Ali, R. (1998). "Autoprogressive training of neural network constitutive models." *International Journal for Numerical Methods in Engineering* 42(1): 105-126.

Ghaboussi, J., Pecknold, D. A., Zhang, M. F. and Haj-Ali, R. M. (1998). "Autoprogressive training of neural network constitutive models." *International Journal for Numerical Methods in Engineering* 42(1): 105-126.

Ghaboussi, J. and Sidarta, D. E. (1998). "New Nested Adaptive Neural Networks (NANN) for Constitutive Modeling." *International Journal of Computers and Geotechnics* 22(1): 29-52.

Gioda, G. and Locatelli, L. (1999). "Back analysis of the measurements performed during the excavation of a shallow tunnel in sand." *International Journal for Numerical and Analytical Methods in Geomechanics* 23: 1407-1425.

Gioda, G. and Sakurai, S. (1987). "Back Analysis Procedures For the Interpretation of Field Measurements in Geomechanics." *International Journal for Numerical and Analytical Methods in Geomechanics* 11: 555-583.

Goh, A. T. C. (1996). "Pile Driving Records Reanalyzed Using Neural Networks." *Journal of Geotechnical Engineering* 122(6): 492-495.

Goldberg, D. E. (1989). "Genetic algorithms in search, optimization and machine learning." *Addison Wesley Publishing Company*.

H&A (1995). "Central artery (I-93)/Tunnel (I-90) project draft supplemental geotechnical data report, design section D009A, Boston, Massachusetts". *Report prepared for Massachusetts Department of Public Works*. Boston, Haley and Aldrich.

Haj-Ali, R., Pecknold, D. A., Ghaboussi, J. and Voyiadjis, G. Z. (2001). "Simulated micromechanical models usings artificials neural networks." *Journal of Engineering Mechanics-ASCE* 127(7): pp. 730-738.

Hashash, Y. M. A. (1992). "Analysis of deep excavations in clay". *Department of Civil and Environmental Engineering*. Cambridge, MA, Massachusetts Institute of Technology: 337 p.

Hashash, Y. M. A. (2007). "Extraction of material constitutive behavior from boundary measurements of forces and displacements". *Inverse Problems, Design and Optimization Symposium*, Miami, Florida, U.S.A.

Hashash, Y. M. A., Fu, Q., Ghaboussi, J., Lade, P. V. and Saucier, C. (2008). "Inverse analysis based interpretation of sand behavior from triaxial shear tests subjected to full end restraint." *Canadian Geotechnical Journal* in press.

Hashash, Y. M. A., Marulanda, C., Ghaboussi, J. and Jung, S. (2003). "Systematic update of a deep excavation model using field performance data." *Computers and Geotechnics* 30(6): 477-488.

Hashash, Y. M. A., Marulanda, C., Ghaboussi, J. and Jung, S. (2006). "Novel approach to integration of numerical modeling and field observations for deep excavations." *Journal of Geotechnical and Geoenvironmental Engineering* 132(8): 1019 - 1031.

Hashash, Y. M. A., Marulanda, C., Kershaw, K., E., C., Druss, D., Bobrow, D. and Das, P. (2003). "Temperature correction and strut loads in deep excavations for the Central Artery Project." *Journal of Geotechnical and Geoenvironmental Engineering* 129(6): pp. 495-505.

Hashash, Y. M. A., Osouli, A. and Marulanda, C. (2008). "Central Artery/ Tunnel Project Excavation Induced ground deformations." *ASCE Journal of Geotechnical and Geoenvironmental Engineering* 134(9): 1399-1406.

Hashash, Y. M. A. and Song, H. (2008). "The integration of numerical modeling and physical measurements through inverse analysis in geotechnical engineering." *Korean Journal Of Civil Engineering* 12(3): 165-176.

Hashash, Y. M. A. and Whittle, A. J. (1992). "Integration of Modified Cam Clay model in non-linear finite element analysis." *Computers and Geotechnics* 14(2): 59-83.

Hashash, Y. M. A. and Whittle, A. J. (1993). "Soil modeling and prediction of deep excavation behaviour".

Hashash, Y. M. A. and Whittle, A. J. (1996). "Ground movement prediction for deep excavations in soft clay." *Journal of Geotechnical Engineering* 122(6): 474-486.

Hashash, Y. M. A. and Whittle, A. J. (2002). "Mechanisms of load transfer and arching for braced excavations in clay." *Journal of Geotechnical and Geoenvironmental Engineering* 128(3): 187-197.

Honjo, Y., Wen_Tsung, L. and Guha, S. (1994). "Inverse analysis of an embankment on soft clay by estended Bayesian Method." *International Journal for Numerical and Analytical Methods in Geomechanics* 18: 709-734.

Hsi, J. P. and Small, J. C. (1993). "Application of a Fully Coupled Method to the Analysis of an Excavation." *Soils and Foundations* 33(4): 36-48.

Hsieh, P.-G. and Ou, C.-Y. (1998). "Shape of ground surface settlement profiles caused by excavation." *Canadian Geotechnical Journal* 35(6): 1004-1017.

Jan, J. C., Hung, S.-L., Chi, S. Y. and Chern, J. C. (2002). "Neural Network Forecast Model in Deep Excavation." *Journal of Computing in Civil Engineering* 16(1): 59-65.

Karlsurd, K. (1986). "Performance monitoring in deep supported excavations in soft clay". *4th Inetrnational Geo. Seminar, Field Instrumentation and In-situ Measurement*, Nanyang Technologocial Institute, Sigapore.

Kiefa, M. A. A. (1998). "General Regression Neural Networks for Driven Piles in Cohesionless Soils." *Journal of Geotechnical and Geoenvironmental Engineering* 124(12): 1177-1185.

Koutsoftas, D. C., Frobenius, P., Wu, C. L., Meyersohn, D. and Kulesza, R. (2000). "Deformations during cut-and-cover construction of Muni Metro Turnback project." *Journal of geotechnical and geoenvironmental engineering* 126(4): 344-359.

Kung, G. T. C., Juang, C. H., Hsiao, E. C. L. and Hashash, Y. M. A. (2007). "A simplified model for wall deflection and ground surface settlement caused by braced excavation in clays." *ASCE Journal of Geotechnical and Geoenvironmental Engineering.* 133(6): pp. 1-17.

Kung, G. T. C., Ou, C. Y. and Juang, C. H. (2009). "Modeling small-strain behavior of Taipei clays for finite element analysis of braced excavations." *Computers and Geotechnics* 36: 304-319.

Ladd, C. C. and Edgers, L. (1972). "Consolidated-undrained direct simple shear test on Boston Blue Clay". *Research report R72-82*, Department of Civil Engineering, MIT, Cambridge, MA.

Lambrechts, J. R. (1998). "Special Geotechnical Testing: Cetral Artery/Tunnel Project in Boston, MA". *Proceedings of Sessions of Geo-Congress 98*, Boston, MA.

Ledesma, A., Gens, A. and Alonso, E. (1996). "Estimation of parameters in geotechnical backanalysis. I - Maximum likelihood approach." *Compute Geotech* 18(1): 1-27.

Lee, F.-H., Yong, K.-Y., Quan, K. C. N. and Chee, K.-T. (1998). "Effect of Corners in Strutted Excavations: Field Monitoring and Case Histories." *Journal of Geotechnical Engineering* 124(4): 339-349.

Levasseur, S. (2007). "Analyse inverse en geotechnique: developement d'une methode base d'algorithmes genetiques". France, Universite Joseph Fourier, Grenoble.

Levasseur, S., Malecot, Y., Boulon, M. and Flavigny, E. (2008). "Soil parameter identification using a genetic algorithm." *International journal for numerical and analytical methods in geomechanics* 32(2): 189-213.

Levasseur, S., Malecot, Y., Boulon, M. and Flavigny, E. (2008 a). "Soil parameter identification using a genetic algorithm." *International Journal for numerical and analytical methods in geomechanics* 32(2): 189-213.

Levasseur, S., Malecot, Y., Boulon, M. and Flavigny, E. (2008b). "Inverse analysis in geotechnics based on a genetic algorithm 1. Method and developments using synthetic data." *International Journal for numerical and analytical methods in geomechanics* Submitted.

Levasseur, S., Malecot, Y., Boulon, M. and Flavigny, E. (2008c). "Inverse analysis in geotechnics based on a genetic algorithm. 2 Application to excavation problems and pressuremeter tests." *International Journal for numerical and analytical methods in geomechanics* Submitted.

Levasseur, S., Malecot, Y., Boulon, M. and Flavigny, E. (2009a). "Statistical inverse analysis based on genetic algorithm and principal component analysis: Method and developments using synthetic data." *International journal for numerical and analytical methods in geomechanics* Accepted.

Levasseur, S., Malecot, Y., Boulon, M. and Flavigny, E. (2009b). "Statistical inverse analysis based on genetic algorithm and principal component analysis: Application to excavation problems and pressuremeter tests." *International journal for numerical and analytical methods in geomechanics* Submitted.

Lin, L. (1989). "A concordance correlation coefficient to evaluate reproducibility." *Biometrics* 45: 255-268.

Liu, G. B., Ng, W. W. and Wang, Z. W. (2005). "Observed performance of a deep multistrutted excavation in Shanghai soft clays." *Journal of Geotechnical and Geoenvironmental Engineering* 131(8): 1004 -1013.

Long, M. (2001). "Database for retaining wall and ground movements due to deep excavations." *Journal of Geotechnical and Geoenvironmental Engineering* 127(3): 203-224.

Mana, A. I. and Clough, G. W. (1981). "Prediction of Movements For Braced Cuts in Clay." *Journal of Geotechnical Division* 107(GT6): 759-777.

Marulanda, C. (2005). "Integration of numerical modeling and field observations of deep excavations". *Civil and Environmental Engineering*. Urbana, University of Illinois at Urbana-Champaign: 269 p.

Marulanda, C. and Hashash, Y. M. A. (2007). "Relationship of inferred soil behavior to excavation instrumentation". *XIII Panamerican Conference on Soil Mechanic and Foundation Engineering*, Isla de Margarita, Venezuela.

Moormann, C. (2004). "Analysis of wall and ground movements due to deep excavations in soft soil based on a new worldwide database." *Soils and Foundations* 44(1): 87-98.

Moormann, C. and Katzenbach, R. (2002). "Three-dimensional effects of deep excavations with rectangular shape". *Proc. 2nd Int. Conf. Soil-Structure Interaction*, Zurich.

Morgenstern, N. R. and Eisenstein, Z. (1970). "Methods of Estimating Lateral Loads and Deformations". *Specialty Conference on Lateral Stresses in the Ground and the Design of Earth Retaining Structures*, ASCE.

Mueller, C. G. (2000). "Behavior of model scale tieback walls in sand". *Civil and Environmental Engineering*. Champaign-Urbana, University of Illinois.

Mueller, C. G., Long, J. H., Weatherby, D. E., Cording, E. J., Powers, W. F. and Briaud, J. L. (1998). "Summary report on permanent ground anchor walls, volume III: Model-scale wall tests and ground anchor ties", FHWA: 181.

Ng, C. W. W. and Lings, M. L. (1995). "Effects of Modeling Soil Nonlinearity and Wall Installation on Back-Analysis of Deep Excavation in Stiff Clay." *Journal of Geotechnical and Geoenvironmental Engineering* 121(10): 687-.

Ng, C. W. W., Lings, M. L., Simpson, B. and Nash, D. F. T. (1995). "An approximate analysis of the three-dimensional effects of diaphragm wall installation." *Geotechnique* 45(3): 497-507.

O'Rourke, T. D. (1981). "Ground Movements Caused By Braced Excavations." *Journal of the Geotechnical Engineering Division* 107(GT9): 1159-1178.

O'Rourke, T. D. (1992). "Base Stability and Ground Movement Prediction for Excavations in Soft Clay". *Earth Retaining Structures*, Cambridge, UK.

O'Rourke, T. D., Cording, E. J. and Boscardin, M. (1976). "The ground movements related to braced excavations and their influence on adjacent buildings". Champaign-Urbana, University of Illlinois: 137.

O'Rourke, T. D. and McGinn, A. J. (2006). "Lessons learned for ground movements and soil stabilization from the Boston Central Artery." *Journal of Geotechnical and Geoenvironmental Engineering* 132(8): 966-989.

O'Rourke, T. D., McGinn, A. J., Dewsnap, J. and Stewart, H. E. (1997). "Performance of excavations stabilized by deep soil mixining". *Report prepared for Bechtel/Parsons Brinckerhoff*. T. M. H. D. a. F. H. A. a. C. University. Ithaca, N. Y.

O'Rourke, T. D. and O'Donnell, C. J. (1997). "Deep rotational stability of tieback excavations in clay." *Journal of Geotechnical and Geoenvironmental Engineering* 123(6): 506-515.

Osouli, A. and Hashash, Y. M. A. (2008). "Learning of soil behavior from measured response of a full scale test wall in sandy soil". *6th International conference on case histories in geotechnical engineering*, Arlington, VA, August 11-16, 2008.

Ou, C.-Y., Chiou, D.-C. and Wu, T.-S. (1996). "Three-Dimensional Finite Element Analysis of Deep Excavations." *Journal of Geotechnical and Geoenvironmental Engineering* 122(5): 337-345.

Ou, C.-Y., Liao, J.-T. and Lin, H.-D. (1998). "Performance of diaphragm wall constructed using top-down method." *Journal of Geotechnical and geoenvironmental engineering* 124(9): 798-808.

Ou, C.-Y. and Shiau, B.-Y. (1998). "Analysis of the corner effect on excavation behaviors." *Canadian Geotechnical Journal* 35: 532-540.

Ou, C. and Wu, T. (1996). "Analysis of Deep Excavation with Column Type of Ground Improvement in Soft Clay." *Journal of Geotechnical and Geoenvironmental Engineering* 122(9): 709-.

Ou, C. Y., Chiou, D.-C. and Wu, T.-S. (1996). "Three-Dimensional Finite Element Analysis of Deep Excavations." *Journal of Geotechnical Engineering* 122(5): 337-345.

Ou, C. Y., Hsien, P. G. and Chiou, D. C. (1993). "Characteristics of ground surface settlement during excavation." *Canadian Geotechnical Journal* 30: 758-767.

Ou, C. Y., Shiau, B. Y. and Wang, I. W. (2000). "Three-dimensional deformation behavior of the Taipei National Enterprise Center (TNEC) excavation case history." *Can. Geotechnical Journal* 37: 438 - 448.

Ou, C. Y. and Tang, Y. G. (1994). "Soil parameter determination for deep excavation analysis by optimization." *Journal of the Chinise Institute of Engineers* 17(5): 671-688.

Ou, C. Y., Teng, F. C. and Wang, I. W. (2008). "Analysis and design of partial ground improvement in deep excavations." *Computers and Geotechnics* 35: 576-584.

Pal, S., Wathugala, G. W. and Kundu, S. (1996). "Calibration of a constitutive model using genetic algorithms." *Computers and Geotechnics* 19(4): 325-348.

Pande, G. N. and Shin, H. S. (2002). "Finite elements with artificial intelligence". *Eighth International Symposium on Numerical Models in Geomechanics - NUMOG VIII*, Italy, Balkema.

Peck, R. B. (1969). "Advantages and limitations of the observational method in applied soil mechanics." *Geotechnique* 19(1): 171-187.

Peck, R. B. (1969). "Deep excavations and tunneling in soft ground". *Seventh International Conference on Soil Mechanics and Foundation Engineering*, Mexico City, Sociedad Mexicana de Mecanica de Suelos, A.C., Mexico.

Pestana, J. M., Whittle, A. J. and Gens, A. (2002). "Evaluation of a constitutive model for clays and sands: part II - clay behaviour." *International Journal for Numerical and Analytical Methods in Geomechanics* 26(11): 1123-1146.

PLAXIS-B.V. (2002). "PLAXIS: Finite element Package for analysis of geotechnical structures". Delft, Netherland.

Poeter, E. P. and Hill, M. C. (1998). "Documentation of UCODE, a computer code for universal inverse modeling". *U.S. Geological survey water-resources investigations Rep. No. 98-4080, USGS.*

Potts, D. M. and Zdravkovic, L. (2001). "Finite Element Analysis in Geotechnical Engineering : Volume Two - Application". London, Thomas Telford.

Rechea, C., Levasseur, S. and Finno, R. J. (2008). "Inverse analysis techniques for parameter identification in simulation of excavation support systems." *Computers and Geotechnics* 35(3): 331-345.

Renders, J. M. (1994). "Algorithmes genetiques et reseaux de neurones." *Hermes*.

Roscoe, K. H. and Burland, J. B. (1968). "On the generalized stress-strain behaviour of "wet" clay". Engineering Plasticity. J. Heyman. Cambridge, England, Cambridge University Press: pp. 535-609.

Sakurai, A. and Takahashi, T. (1969). "Dynamic stresses of underground pipeline during earthquakes". *Fourth World Conference on Earthquake Engineering*.

Samarajiva, P., Macari, E. and Wathugala, W. (2005). "Genetic algorithms for the calibration of constitutive models of soils." *Int J Geomech* 5(3): 206-217.

Samarajiva, P., Macari, E. J. and Wathugala, W. (2005). "Genetic algorithms for the calibration of constitutive models of soils." *International Journal of Geomechanics* 5(3): 206-217.

Schanz, T., Vermeer, P. A. and Bonnier, P. G. (1999). "The hardening soil model - Formulation and verification". *Proceedings of the Plaxis symposium 'beyond 2000 in computational geotechnics'.*

Shin, H. S. and Pande, G. N. (2000). "On self-learning finite element codes based on monitored response of structures." *Computers and Geotechnics* 27(7): 161-178.

Sidarta, D. and Ghaboussi, J. (1998). "Modelling constitutive behavior of materials from non-uniform material tests." *Computers and Geotechnics* 22(1): 53-71.

Song, H., Osouli, A. and Hashash, Y. (2007). "Soil behavior and excavation instrumentation layout". *7th International symposium on field measurements in geomechanics FMGM 2007.*, Boston, MA.

Spencer, E. (1967). "A method of analysis of the stability of embankments assuming parallel interslice forces." *Geotechnique* 17(1): 11-26.

St-John, H. D. (1975). "Field and theoretical studies of the behaviour of ground around deep excavations in London Clay", Cambridge University.

Su, Y. Y., Hashash, Y. M. A. and Liu, L. Y. (2006). "Integration of construction as-built data with geotechnical monitoring of urban excavation." *Journal of Construction Engineering and Management* 132(12): pp. 1234-1241.

Tang, Y. and Kung, G. (2009). "Application of nonlinear optimization technique to back analyses of deep excavation." *Computers and Geotechnics* 36: 276-290.

Tarantola, A. (1987). "Inverse Problem Theory." Elsevier Science B. V.

Terzaghi, K. (1943). "Theoretical Soil Mechanics". New York, J. Wiley and Sons.

Terzaghi, K. and Peck, R. B. (1948). "Soil mechanics in engineering practice". New York, John Wiley & Sons.

Terzaghi, K., Peck, R. B. and Mesri, G. (1996). "Soil Mechanics in Engineering Practice". New York, Wiley.

Trofimenkov, J. G. (1974). "Penetration testing in USSR". E. Symp. Stockholm: Vol. I.

Tsai, C.-C. (2007). "Seismic Site Response and Interpretation of Dynamic Soil Behavior from Downhole Array Measurements". *Department of Civil and Environmental Engineering*. Urbana, University of Illinois at Urbana-Champaign.

Tsai, C.-C. and Hashash, Y. M. A. (2006). "A novel framework for extracting dynamic soil behavior from downhole array data". *Eigth National Conference on Earthquake Engineering*, San Francisco, CA.

Tsai, C.-C. and Hashash, Y. M. A. (2008). "A novel framework integrating downhole array data and site response analysis to extract dynamic soil behavior." *Soil Dynamics and Earthquake Engineering* 28(3): 181-197.

Tsai, C.-C. and Hashash, Y. M. A. (2009). "Learning of dynamic soil behavior from downhole arrays." *Journal of geotechincal and geoenvironmental engineering* in press.

Ukritchon, B., Whittle, A. and Sloan, S. (2003). "Undrained stability of braced excavations in clay." *Journal of Geotechnical and Geoenvironmental* 129(8): 738-755.

Wang, Z. W., Ng, C. W. W. and Liu, G. B. (2005). "Characteristics of wall deflections and ground surface settlements in Shanghai." *Can. Geotechnical Journal* 42: 1243 - 1254.

Weatherby, D. E., Chung, M., Kim, N.-K. and Briaud, J.-L. (1998). "Summary Report of Research on Permanent Ground Anchor Walls, Volume II: Full-Scale Wall Tests and a Soil-Structure Interaction Model". McLean, VA, Federal Highway Administration.

Whittle, A. J. (1987). "A Constitutive Model for Overconsolidated Clays with Application to the Cyclic Loading of Friction Piles". *Civil Engineering.* Cambridge, MA, MIT: 641.

Whittle, A. J. and Hashash, Y. M. A. (1994). "Soil modeling and prediction of deep excavation behavior". Pre-failure Deformation of Geomaterials. Shibuya, Mitachi and Miura, A.A. Balkema/Rotterdam: 589-594.

Whittle, A. J., Hashash, Y. M. A. and Whitman, R. V. (1993). "Analysis of deep excavation in Boston." *Journal of Geotechnical Engineering* 119(1): 69-90.

Whittle, A. J. and Kavvadas, M. J. (1994). "Formulation of MIT-E3 constitutive model for overconsolidated clays." *Journal of Geotechnical Engineering* 120(1): 173-198.

Wong, H. I., Poh, T. Y. and Chuah, H. L. (1997). "Performance of excavations for depresses expressway in Singapore." *Journal of Geotechnical and Geoenvironmental Engineering, ASCE* 123(7): 617-625.

Wong, I. H. (1970). "The Prediction of the Performance of Braced Excavations". *Civil Engineering.* Cambridge, MA, MIT.

Zdravkovic, L., Potts, D. M. and John, H. D. S. (2005). "Modelling of a 3D excavation in finite element analysis." *Geotechnique* 55(7): 497-513.

Zentar, R., Hicher, P. Y. and Moulin, G. (2001). "Identification of soil parameters by inverse analysis." *Computational Geotechnics* 28: 129-144.

Zentar, R., Hicher, P. Y. and Moulin, G. (2001). "Indentification of soil parameters by inverse analysis." *Computer and Geotechnics* 28: 129-144.

Zhang, M., Song, E. and Chen, Z. (1999). "Ground movement analysis of soil nailing construction by three-dimensional (3-D) finite element modeling (FEM)." *Computers and Geotechnics* 25: 191-204.

AUTHOR'S BIOGRAPHY

Abdolreza Osouli was born in Tehran in Iran on April 14, 1980. He graduated from Sharif University of Technology with a Bachelor of Science degree in Civil Engineering in June 2002. He received his Master of Science in Geotechnical Engineering from Sharif University of Technology in June 2004. He started his PhD program in Geotechnical Engineering division of University of Illinois at Urbana-Champaign in August 2004.